28 February 2008 | www.nature.com/nature | $10

THE INTERNATIONAL WEEKLY JOURNAL OF SCIENCE

nature

KILLER BLOW

Can a billion dollars defeat malaria?

STAR FORMATION
How massive stars get massive

MULTIPLE SCLEROSIS
Proteomic scan for drug targets

EVOLVING COOPERATION
Cheats that prosper

NATUREJOBS
Role models

$10.00US $12.99CAN
09
0 71486 03070 6

nature 451, 1029-1138 28 February 2008
www.nature.com/nature
no.7182 npg

Presenting!

Prestige Antibodies™

SIGMA Life Science

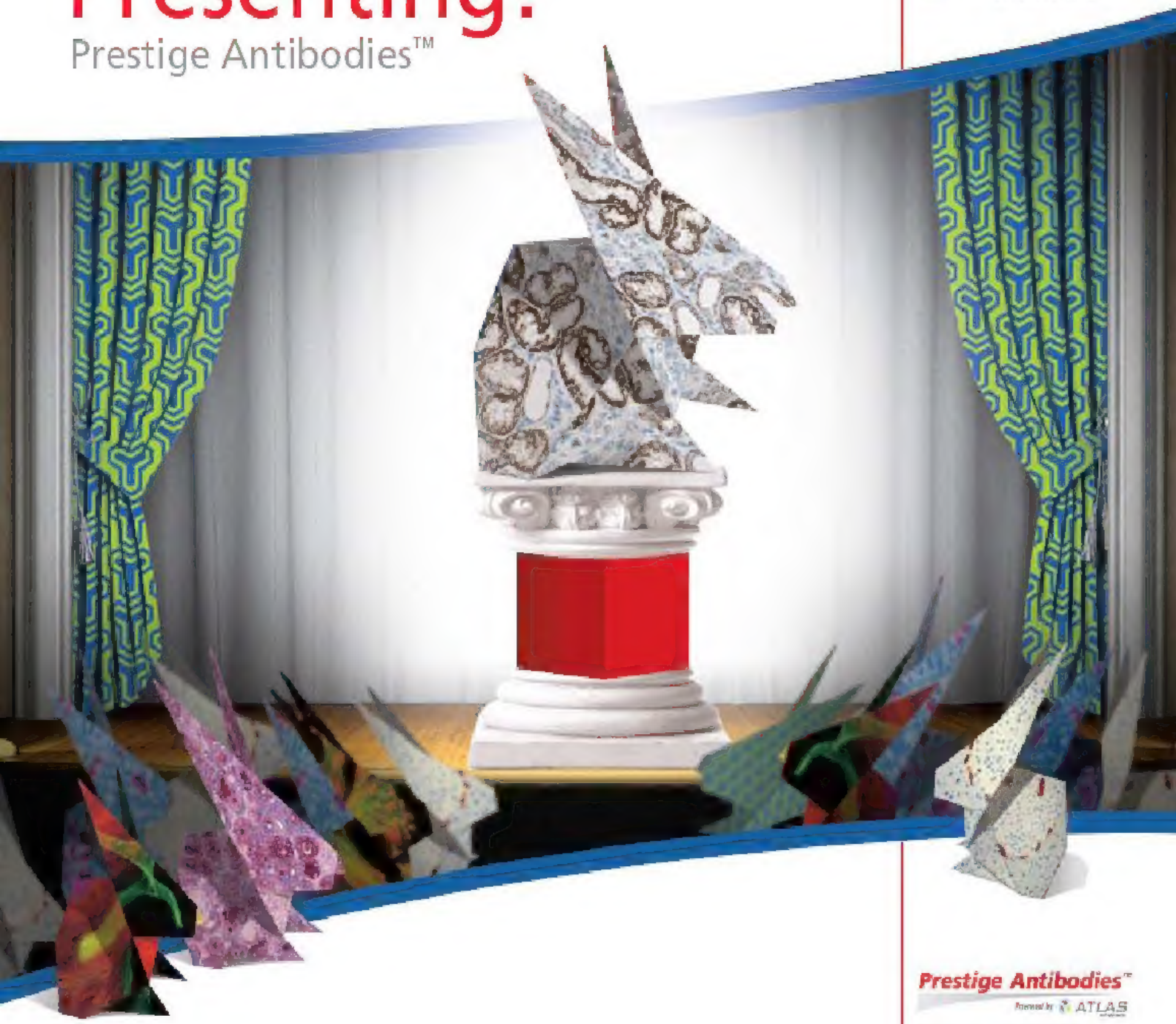

Antibodies that work, right out of the box!

The most highly characterized antibodies in the industry — **1,800 NEW** Prestige Antibodies™, Powered by Atlas Antibodies.

- Designed & validated by the Human Proteome Resource (HPR)
- Standardized in universal protocols
- Over 500 immunohistochemical images for every antibody
- Publicly available data on the web

Look even closer. Go to ***sigma.com/prestige*** for more information.

Our Innovation, Your Research — Shaping the Future of Life Science

Prestige Antibodies™
Powered by ATLAS

Anti-BID Cat No. HPA000722 on A-431 cells shown in green, nucleus in blue, microtubules in red and endoplasmic reticulum (ER) in yellow.

Just one of the over 500 IF, IHC and WB images available

myTetraCell.com
explore • share • connect

My Tetra Is...Versatile.

Transform the Mini-PROTEAN® Tetra cell to a Mini Trans-Blot® cell by simply swapping modules.

The Mini-PROTEAN Tetra system for one-dimensional vertical gel electrophoresis comprises a modular design to easily convert the electrophoresis cell into a blotting apparatus. The Mini-PROTEAN Tetra system can run as many as four SDS-PAGE gels simultaneously and is compatible with the Mini Trans-Blot module for gel transfer (one module can transfer two gels), eliminating the need for an extra blotting tank. Supported by Bio-Rad's 20 years of experience in gel electrophoresis and blotting, the Mini-PROTEAN Tetra system increases throughput, simplicity, and versatility in your experiments.

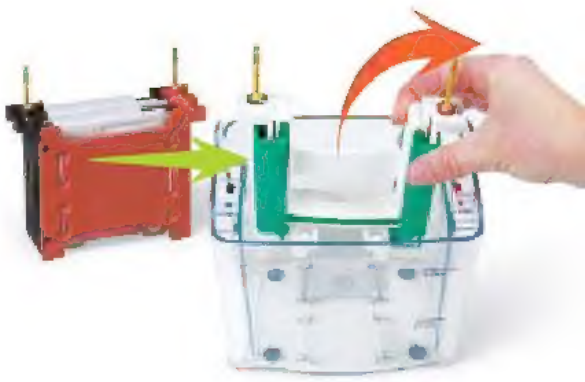

Interchangeable module system

With the Mini-PROTEAN Tetra system, you can:

- Convert the electrophoresis cell to a blotting apparatus
- Run up to 4 mini SDS-PAGE gels
- Use handcast or precast gels
- Be confident that the error-proof design ensures correct polarity and orientation

Explore, share, and connect at **myTetraCell.com**.

Winner takes all

Finnzymes' High Performance PCR – A Winning Combination Every Time

We have created an integrated solution that propels your PCR to unbeatable performance.

- ♠ **Speed** – Significantly faster than any other combination
- ♥ **Fidelity** – Superior accuracy over *Pfu* and *Taq* based systems
- ♣ **Yield** – Higher efficiency amplification results in more product
- ♦ **Specificity** – Reduced levels of primer-dimers and false-primed products

An integrated tripartite solution:

Phusion™ DNA Polymerases | Piko™ Thermal Cycler | UTW™ Vessels

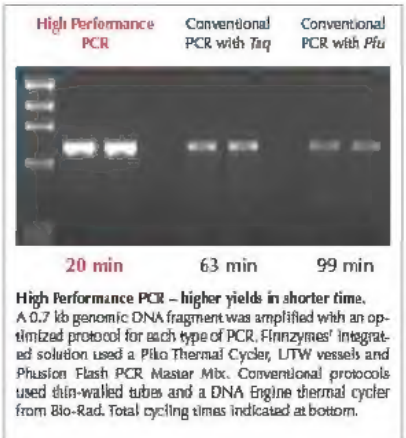

High Performance PCR – higher yields in shorter time. A 0.7 kb genomic DNA fragment was amplified with an optimized protocol for each type of PCR. Finnzymes' integrated solution used a Piko Thermal Cycler, UTW vessels and Phusion Flash PCR Master Mix. Conventional protocols used thin-walled tubes and a DNA Engine thermal cycler from Bio-Rad. Total cycling times indicated at bottom.

Find out more at www.highperformancepcr.com.

FINNZYMES
TOOLS FOR MOLECULAR BIOLOGY

Make Illumina part of your DNA.

The most comprehensive set of DNA analysis tools available.

Illumina's portfolio of DNA analysis products delivers industry-leading data quality at the lowest cost per study. Accelerate discovery by looking at DNA from every angle.

- **SNP genotyping** — Achieve significance with the industry's best genomic coverage and data quality.
- **CNV analysis** — Obtain the most comprehensive access to known and novel CNV regions.
- **DNA sequencing** — Sequence virtually anything at a fraction of the cost and time.
- **DNA methylation** — Get single CpG site resolution with high-multiplex standard or custom methylation panels.
- **ChIP-Seq** — Obtain genome-wide maps of DNA-protein interactions with unprecedented resolution, quality and cost.

Make us part of your DNA. Join the growing Illumina Community.

Find out how to make
Illumina part of your DNA:

www.illumina.com/DNA

illumina®

nature

Nature Publishing Group
The Macmillan Building,
4 Crinan St, London N1 9XW, UK
e-mail: nature@nature.com

NATURE

NATURE'S MISSION, 1869:
'The objective which it is proposed to attain by this periodical may be broadly stated as follows. It is intended, first, to place before the general public the grand results of scientific work and scientific discovery; and to urge the claims of science to move to a more general recognition in education and in daily life... Secondly, to aid scientific men [sic] themselves, by giving early information of all advances made in any branch of natural knowledge throughout the world, and by affording them an opportunity of discussing the various scientific questions which arise from time to time.'

Nature's mission statement was updated in 2000:
www.nature.com/nature/about
Submissions and Guide to Authors:
www.nature.com/nature/authors

Author and referee policies and services:
www.nature.com/authors

Nature® (ISSN 0028-0836) is published by Nature Publishing Group, a division of Macmillan Publishers Ltd (The Macmillan Building, 4 Crinan Street, London N1 9XW). Registered as a newspaper at the British Post Office.
North and South American orders to Nature, Subscription Dept, 342 Broadway PMB 301, New York NY 10013-3910, USA.
Other orders to Nature, Brunel Road, Basingstoke, Hants RG21 2XS, UK.

Identification code for Nature: 0028-0836/03
CPC PUB AGREEMENT #40032744.
In the US Nature (ISSN 0028-0836) is published weekly on Thursday, except the last week in December by Nature Publishing Group, 75 Varick St, 9th Fl, New York NY 10013-1917, USA. US Periodicals postage paid at New York NY, and additional mailing post offices.
US POSTMASTER: send address changes to Nature, Subscription Dept, 342 Broadway PMB 301, New York NY 10013-3910, USA.
Published in Japan by NPG Nature Asia-Pacific, Chiyoda Building, 2-37 Ichigayatamachi, Shinjuku-ku, Tokyo 162-0843, Japan.

npg
nature publishing group

EDITORIALS

RESEARCH HIGHLIGHTS

NEWS

NEWS FEATURES

MALARIA

CORRESPONDENCE

COMMENTARY

Order restored: trains and antelopes don't mix, p. **1034**.

Life in the fast lane: why is Silicon Valley special? Page **1054**.

BOOKS & ARTS

ESSAY

NEWS & VIEWS

NATUREJOBS

FUTURES

Same people. Same support. New possibilities.

If you work with proteins, you've relied on Pierce reagents. For gene silencing, you've depended on Dharmacon innovations. In cell culture, HyClone is likely a good friend. For PCR, ABgene has helped you along the way. And for high content screening, you've trusted Cellomics and BioImage.

Now these top names in life science are sold under the Thermo Scientific brand. You'll still find the same technical support and application expertise that you've come to expect. Only now, we can develop new ways to integrate technologies to accelerate and improve your results even further.

So yes, there's a new brand name – Thermo Scientific. But you can keep your trusted relationships and high level of service as we unite to help you pursue new possibilities.

Moving science forward

Learn more at www.thermo.com/LSR.

Part of Thermo Fisher Scientific

Thermo SCIENTIFIC

Glass act: dark metallic dendrites toughen the glass matrix in this composite that is one of the toughest materials known. Page **1085**, and see the Author Page overleaf.

NATURE ONLINE

ADVANCE ONLINE PUBLICATION

PUBLISHED ON 24 FEBRUARY 2008

Preserving cell shape under environmental stress
B Cook, R W Hardy, W B McConnaughey & C S Zuker
doi:10.1038/nature06603

Identification of a serotonin/glutamate receptor complex implicated in psychosis
J González-Maeso, R L Ang, T Yuen, P Chan, N V Weisstaub, J F López-Giménez, M Zhou, Y Okawa, L F Callado, G Milligan, J A Gingrich, M Filizola, J J Meana & S C Sealfon
doi:10.1038/nature06612

PUBLISHED ON 27 FEBRUARY 2008

SLAC1 is required for plant guard cell S-type anion channel function in stomatal signalling
T Vahisalu, H Kollist, Y-F Wang, N Nishimura, W-Y Chan, G Valerio, A Lamminmäki, M Brosché, H Moldau, R Desikan, J I Schroeder & J Kangasjärvi
doi:10.1038/nature06608

Dendritic cell PAR1–S1P3 signalling couples coagulation and inflammation
F Niessen, F Schaffner, C Furlan-Freguia, R Pawlinski, G Bhattacharjee, J Chun, C K Derian, P Andrade-Gordon, H Rosen & W Ruf
doi:10.1038/nature06663

CO_2 regulator SLAC1 and its homologues are essential for anion homeostasis in plant cells
J Negi, O Matsuda, T Nagasawa, Y Oba, H Takahashi, M Kawai-Yamada, H Uchimiya, M Hashimoto & K Iba
doi:10.1038/nature06720

UNC93B1 delivers nucleotide-sensing toll-like receptors to endolysosomes
Y-M Kim, M M Brinkmann, M-E Paquet & H L Ploegh
doi:10.1038/nature06726

The *Drosophila* pheromone cVA activates a sexually dimorphic neural circuit
S R Datta, M L Vasconcelos, V Ruta, S Luo, A Wong, E Demir, J Flores, K Balonze, B J Dickson & R Axel
doi:10.1038/nature06808

BRIEF COMMUNICATIONS ARISING

PUBLISHED ON 28 FEBRUARY 2008

Arising from 'Life-history trade-offs favour the evolution of animal personalities' by M Wolf *et al. Nature* **447**, 581–584 (2007).

Do animal personalities emerge?
F Massol & P-A Crochet
doi:10.1038/nature06743

Reply: M Wolf, G S van Doorn, O Leimar & F J Weissing
doi:10.1038/nature06744

PODCAST LATEST

On this week's podcast, the optimum strategy for a predator seeking widely dispersed prey, and the tricky question of what makes a few stars break the rules and become 'massive'.
www.nature.com/podcast
For the podcast archive (in mp3 format) and English transcripts of previous episodes, visit:
http://tinyurl.com/k62cvt

Enabling Technologies for Cancer Research

A Comprehensive Oncology Toolkit

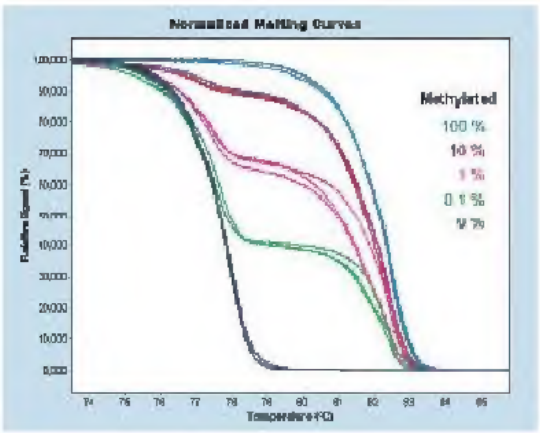

Analysis of tumor suppressor gene methylation with the LightCycler® 480 System. Mixtures of unmethylated and fully methylated genomic DNA were treated with bisulfite. A fragment of the MGMT tumor suppressor gene was then amplified and analyzed by high-resolution melting. This allowed semi-quantitative determination of the portion of methylated DNA contained in each case.

Data kindly provided by Tomasz K. Wojdacz and Alexander Dobrovic.

Drive your cancer research discoveries with Roche Applied Science's innovative, accurate, and versatile instruments and applications. We combine world-class technologies for real-time PCR, microarrays, and DNA sequencing to provide you with the most comprehensive cancer research toolkit available:

LightCycler® 480 Real-Time PCR System – Investigate genetic and epigenetic variation patterns with powerful real-time PCR applications, including high-resolution mutation screening, HRM methylation detection (Figure 1), and quantitative ChIP analysis.

NimbleGen® DNA Microarrays – Target and evaluate oncogenes and other regions of interest with long oligos at high resolution (2.1 million probes).

Genome Sequencer FLX System – Identify rare (<1%) cancer-associated somatic mutations at the molecular level from heterogeneous tissue samples.

Discover... Analyze... Validate.
Visit ***www.roche-applied-science.com*** for more information or to find a local representative.

Roche Diagnostics GmbH
Roche Applied Science
68298 Mannheim, Germany

Roche

THIS ISSUE

FINAL CHAPTER The report by Robert Woodward and William Doering of the total synthesis of quinine in 1944 caused a sensation: it was hoped that the process could be scaled up as part of the battle against malaria. But it was the start of a long-running controversy over what they — and a 1918 paper that they referenced — had really achieved. As Philip Ball reports in News and Views, a paper just published in *Angewandte Chemie* has validated the 1918 work — and therefore Woodward and Doering's too — once and perhaps for all. [News & Views p. 1065]

DÉJÀ VU Counterfeiting of pharmaceuticals is a growing problem, with even cancer, AIDS and diabetes treatments being faked. Globalization and the Internet are contributory factors. But few things are new, and the current epidemic of fakery has echoes with a previous era. That crisis was resolved by the development of an ordered international marketplace based on enforceable patents — the very structure threatened by today's fakes. [Essay p. 1058]

NIGHT VISION The Eise Eisinga Planetarium in Franeker, The Netherlands, is the oldest functioning planetarium in the world. Built between 1774 and 1781 to prove a point — that a particular alignment in the Solar System would not prompt the end of the

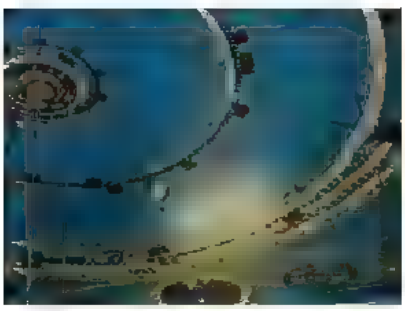

COMBI HOMMEMA

world — it has remained open to visitors ever since. It's the latest in our 'Hidden treasures' series. Alison Abbott describes the visitor experience, and answers the question: how many Solar System planets were known then? [Books & Arts p. 1057]

CHINA STORY Stalactites, stalagmites and the many other forms of mineral deposits found in caves are a mainstay of climate studies, recording oxygen isotope ratios in limestone laid down over time. That pattern links to the water temperature of ancient oceans, and thus to climate. A new oxygen isotope record from Sanbao Cave, central China, tells the story of the region's climate stretching back 200,000 years, filling gaps in the record of a particularly important climate event, the East Asian monsoon. [Letter p. 1090; News & Views p. 1061]

COVER GRAPHIC BY DAVID PARKINS

After being starved of funds for many years, the efforts of the Gates Foundation and others have raised the stakes in the war against malaria, still a major killer, especially in Africa. This week's *Nature* looks at the prospects for progress. There is still no vaccine. Brendan Maher explains why, and reports on the push to develop one. [News Feature p. 1042] Zambia is one of the hardest hit countries and in 2005 launched a plan to cut malaria incidence by 75% by 2008. Michael Hopkin reports on the work of the Malaria Institute at Macha, a centre of excellence established to bolster the national effort and to export expertise to other countries. [News Feature p. 1047] In a Commentary, epidemiologist Mark Grabowsky stresses the importance of spending the 'new money' in the right way — on surveillance networks for example. [Commentary p. 1051] Martin Kemp browses the notebooks of Ronald Ross, and finds more than 'just' the discovery linking malaria and the mosquito. [Books & Arts p. 1056] See also the Editorial [page 1030] and the online malaria special on http://www.nature.com/news/specials/malaria/index.html.

Massive stars: tipping point

Massive stars are rarities because the collapsing gas clouds in which stars form tend to cool efficiently, so that the temperature is fairly even across the cloud. This favours fragmentation into stars of around the mass of the Sun or smaller. Occasionally fragmentation stops short, producing a massive star hundreds of times larger than the Sun. The mystery is, what are the conditions that stop fragmentation. Mark Krumholz and Christopher McKee now show that it is a question of how concentrated the gas is. In regions of high concentration, the energy released when a few small stars form heats the remaining gas up to a point where it can no longer break up. Instead it collapses monolithically to produce larger stars. [Letter p. 1082; www.nature.com/podcast]

Multiple sclerosis targets

A large-scale proteomic analysis of tissue samples from multiple sclerosis (MS) lesions from different stages of the disease has identified proteins peculiar to brain lesions associated with different disease stages. Several new potential therapeutic targets were found. Two proteins in particular showed signs of damage during the chronic active period of the disease. One, called tissue factor, is involved in the initiation of blood clotting and the other, protein C inhibitor, in anti-inflammatory pathways. Administration of activated protein C or the anticoagulant hirudin slowed disease progression in a mouse model of multiple sclerosis, suggesting that the coagulation cascade has a previously unsuspected role in MS pathogenesis. [Article p. 1076]

Cheating but cleverly

The evolution of cooperation is central to the transition by organisms from unicellular to multicellular states. Mutant cells that 'cheat' by benefiting from the cooperation of others but offering nothing in return are seen to undermine cooperation. This view is questioned by a new study of the social amoeba *Dictyostelium discoideum*. A genome-wide scan reveals more than 100 mutations that allow cheating. Many of these cheaters were of an unusual and clever type; they facultatively cheat others while cooperating amongst themselves and developing normally. These findings challenge the idea that cheaters threaten the existence of cooperation: facultative cheaters dominate this system, yet they can spread through a population leaving cooperation intact. [Letter p. 1107]

Garbage in, all sorts out

Until recently, autophagy, or cellular self-digestion, was thought of primarily as part of the cell's garbage disposal system. Now it is know to be involved in cellular protein and organelle degradation during development as well as during adaptations to changing environmental conditions. Many intriguing questions remain to be answered about this process. For example, how can this one pathway be involved in cytoprotection as well as cell death? What is the connection between autophagy and human disease or ageing? In a review, Mizushima *et al.* consider recent progress in the field. [Review Article p. 1069]

Microsoft® HealthVault™

Be Well Fund

It's time to bring healthcare into the Internet Age.

Let's do it *together*.

Announcing the $3,000,000 Microsoft® HealthVault™ Be Well Fund.

The Microsoft HealthVault application platform has the potential to revolutionize traditional healthcare, and may enable fundamentally new and innovative scenarios that have not yet been imagined.

The purpose of the HealthVault Be Well Fund is to stimulate the development of these new, yet-to-be imagined Web applications that will help people live longer, healthier lives.

Microsoft is calling on research and academic institutions to join us in the search for new, innovative health applications in the areas of social applications, primary prevention, secondary prevention, acute care, and juvenile disease management.

For more information on how your institution can submit a proposal to the HealthVault Be Well Fund, visit **www.healthvault.com/fund**.

Microsoft

A perfect match

Bulk metallic glasses (BMGs) are a new class of engineering materials attracting significant technological interest. Many of these metals exhibit high strength and resist fracture, but they tend to lack tensile ductility and fail in an apparently brittle manner under a mechanical load. BMG–matrix composites, in which isolated dendrites stabilize the glass against catastrophic failure, overcome some of these weaknesses. Hofmann *et al.* take this approach a stage further by producing 'designed composites' with optimized mechanical properties by the matching of key fundamental mechanical and microstructural length scales. The resulting titanium–zirconium-based composites demonstrate high ductility and fracture toughness comparable with the toughest titanium and steel alloys. [Letter p. 1085, Author Page]

A Lévy walk on the wild side

Little is known about what controls predator movement patterns, and hence their distribution in the natural environment because in most cases they are logistically difficult to study. This lack of knowledge hinders progress in making realistic predictions about how these important species will respond to environmental change. Now an electronic tagging study of over a million movement displacements of individual marine predators — including basking sharks, sea turtles and penguins — has provided the data needed to analyse predator search patterns. What emerges is in line with the 'Lévy-walk' model, the predicted optimal strategy for a predator with little prior knowledge of prey distribution. Simulations suggest that the foraging predators adopt a random walk characterized by many short steps and rare long steps, maximizing encounter rates in natural-like prey fields. [Letter p. 1098; www.nature.com/podcast]

Growing apart

Many species that are palatable to predators evolve to resemble unpalatable poisonous species that possess warning coloration. These 'batesian mimics' profit by looking like the dangerous model, and theory predicts that mimics should not occur in areas where their model is absent because predators there would not be under selection to avoid the dangerous species or a look-alike. Yet, in seeming contradiction of this theory, the geographical distributions of many mimics extend far beyond that of their models. The non-venomous scarlet kingsnake is one example, sometimes found hundreds of kilometres outside the range of its model, the venomous eastern coral snake. George Harper and David Pfennig have found an explanation for this apparent paradox that leaves the basis of the theory intact. Initially the harmless mimics

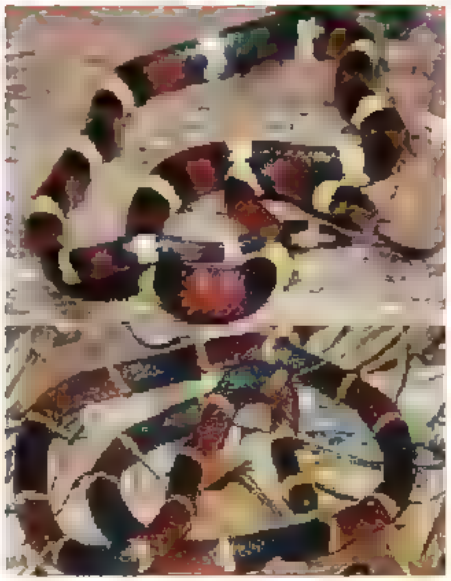

W VAN DEVENDER

Spot the difference: Mimic (top) and mimicked

occur where coral snakes are absent because of dispersal by male kingsnakes from regions where both snakes are present. Genetic analysis shows that once separated from the coral snakes, natural selection promotes the evolution of kingsnakes that look less like their model. [Letter p. 1103]

Resistance in *BRCA2* cancers

The platinum chemotherapeutics such as cisplatin and carboplatin are in clinical use in patients with *BRCA2* mutated ovarian cancer. The initial response is generally good but most ovarian carcinomas ultimately become resistant to therapy. Two papers in this issue have identified a possible cause of this resistance as further mutation of the *BRCA2* gene. Mutations in *BRCA2* are associated with familial breast and ovarian cancer. Loss of BRCA2 function impairs DNA repair by homologous recombination and renders cells particular sensitive to cisplatin and also to PARP (poly (ADP-ribose) polymerase) inhibitors. The secondary 'resistance' mutations act by restoring the wild-type *BRCA2* reading frame. [Letters pp. 1111, 1116; News & Views p. 1066]

The opposite of sex

Certain plant species produce seeds that are genetically identical by an asexual process called apomixis — a botanical equivalent to the parthenogenesis found in some animals. The first step in apomixis is 'apomeiosis', the formation of genetically identical female gametes. Now a study of the model sexual plant *Arabidopsis* shows that alteration of a single gene can bring about apomeiosis, resembling an early stage in the evolution of apomixis. This finding is important for understanding the basic mechanisms of plant reproduction and also has important implications for plant breeding because the development of crop plants capable of apomixis would be highly desirable for producing high yielding hybrid seeds. [Letter p. 1121, News & Views p. 1063]

LightCycler®
10 years
inspiring real-time PCR

www.roche-applied-science.com

LightCycler® Real-Time PCR Systems

Unleash the Potential of Real-Time PCR

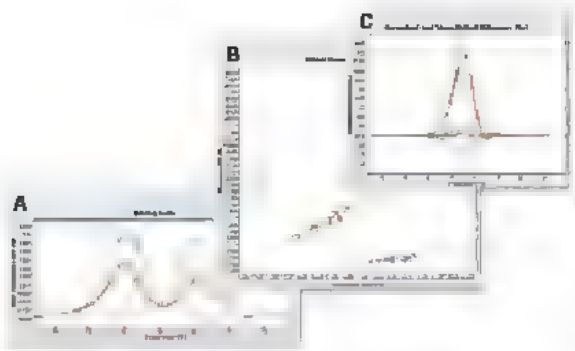

Figure 1: Confidently detect genetic variation with the powerful combination of LightCycler® 480 System analysis modules for:

A. Melting Curve Analysis
B. Endpoint Genotyping
C. High Resolution Melting

The introduction of the LightCycler® Instrument in 1998 launched a new era in real-time PCR, inspiring novel applications and discovery. The versatile **LightCycler® 480 System** continues this tradition, unleashing the potential of real-time PCR through expanded analysis capabilities with the power to meet evolving research demands.

Efficiently analyze genes with High Resolution Melting: Apply this publication-proven method to investigate SNPs, degree of methylation, and RNA editing.

Detect genetic variation with confidence: Use a powerful combination of three robust and convenient analysis methods to obtain comprehensive results (Figure 1).

Rapidly analyze gene expression data: Choose from a broad range of basic and advanced quantification methods to meet your research needs.

Explore the possibilities of Real-Time PCR.
Visit **www.lightcycler480.com** to learn more about the LightCycler® 480 System and register for updates about special events celebrating the 10th Anniversary of the LightCycler® System.

Roche Diagnostics
Roche Applied Science
Indianapolis, Indiana

Roche

Abstractions

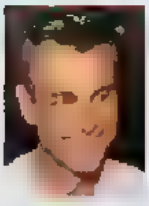

LAST AUTHOR

Cooperation is a key driver in the evolution of multicellular organisms as well as societies. Molecular biologist Gad Shaulsky at Baylor College of Medicine in Houston, Texas, teamed up with evolutionary biologists to find 'cheater' mutations — those that enable some strains to benefit from the cooperation of others — in the social amoeba *Dictyostelium discoideum*, an organism that alternates between a unicellular and a multicellular form (see page 1107). They found cheater mutations in more than 100 genes. Shaulsky tells *Nature* that even cooperative species sometimes cheat to survive.

Your early work was on cancer — how did you get into the social dynamics of amoeba?

While working on the tumour-suppressor gene *p53* as a student, I became interested in communication between cells. I was curious to know why some cells risk foregoing their own survival to become part of a multicellular structure. To answer this question, I needed a social organism that can form chimaeras — organisms that combine DNA from two or more genetically distinct individuals. In conditions of starvation, multicellular chimaeras of the normally unicellular *Dictyostelium* form, in which spores (live cells) and stalk cells (dead) arise from genetically equitable mixtures of two or more strains.

How did the work on cheating come about?

In 2000, before we collaborated, two of our co-authors at Rice University discovered that one *Dictyostelium* strain makes more than its fair share of spores within chimaeras — in other words, it cheats. Rice is only across the street from Baylor, but we didn't team up until later that year, when we were all at a meeting in Scotland. We decided to search for cheater mutations and, to our surprise, found more than 100 genes involved in cheating — which suggests frequent opportunities for cheating in natural populations.

Is this subterfuge unique to amoebae?

No. The large number of genes we discovered indicates a long evolutionary history of social competition.

Can *Dictyostelium* shed more light on sociality?

Yes. Of the organisms whose genomes have been sequenced, there are no other social eukaryotes that are also amenable to genetic modification. Evolutionary biology is a field with many robust theories, and we want to test them at the molecular level. The molecular details of these mechanisms almost certainly differ between species, but the concepts will probably be the same. We think *Dictyostelium* will become the *E. coli* of social evolution for the coming decade. ■

MAKING THE PAPER

Douglas Hofmann

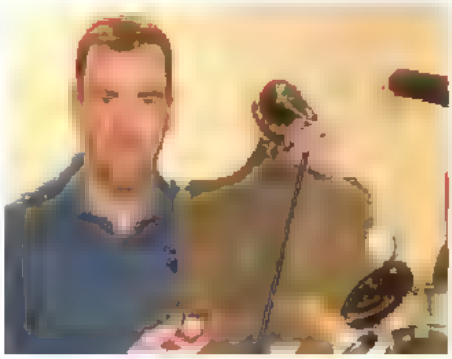

Large, branched crystals make metallic glasses less brittle.

Despite what parents may tell their children, watching television is not always a waste of time. For Douglas Hofmann, it led to a graduate project helping to produce a new class of metal alloys that are more resistant than other types to fracture under stress.

In 2003, Hofmann saw William Johnson, a professor of materials science at the California Institute of Technology (Caltech) in Pasadena, on a televised history programme. Johnson talked about his invention of bulk metallic glasses — an unusual group of metal alloys. Typically, these are about twice the strength of similar metals as a result of their amorphous microstructure; traditional metal alloys consist of crystalline matrices of atoms.

Intrigued by the topic, Hofmann, who had been searching for a materials engineering programme, enrolled as a graduate student at Caltech, with Johnson as his adviser. There, he learned that metallic glasses do have a weakness: when overloaded, they fracture without warning. Unlike their crystalline counterparts, metallic glasses don't show any signs of breaking under stress — a property known as ductility. "Ductility is important for structural things, such as bridges," says Hofmann. "You want to see signs that they will buckle or break."

On the basis of previous research by several groups, Hofmann and his colleagues knew that to make metallic glass ductile they would need to add 'dendrites' — branched crystalline particles that form in a liquid. Through a series of metal 'bending' experiments, they discovered that, to make the metallic glass less brittle, the crystalline particles had to be softer than the metallic glass — like adding bits of rubber to plastic — and of a fairly large size. "Once we figured these two things out, actually making the composite was the next step," says Hofmann.

This took the researchers into uncharted territory. "We had no idea how to make the particles sufficiently large for ductility," says Hofmann. But, as it turned out, their first attempt was successful. "I took a shot in the dark and it worked," Hofmann says.

He admits that fortune smiled on their efforts. He decided to use an induction coil — an instrument that heats over a lower range of temperatures and provides better temperature control than other instruments typically used to melt metals in alloy production.

In a subsequent analysis of the technique, Hofmann learned that when the metal–glass composites are heated in the temperature range above the melting point of glass and below that of the dendrites, two phases form. The metallic glass becomes a liquid with little crystalline particles floating in it. When this 'slush' is cooled, the crystalline particles grow larger. "It was a lucky choice," says Hofmann, "but now that we look at the thermodynamics, it seems so obvious" (see page 1085).

The technique, which Hofmann has dubbed "slushy processing", resulted in a final glassy composite with large coarsened dendrites, providing the microstructure needed for ductility.

Now that the researchers understand the process needed to impart ductility to metallic glass, they want to refine it further. Eventually, Hofmann would like to create bulk metallic glass composites that are both lighter and cheaper — made using iron, for example, rather than titanium or zirconium. And, if he succeeds, perhaps he'll find himself on television. ■

FROM THE BLOGOSPHERE

One of *Nature Medicine*'s peer reviewers recently told the editors that it is unreasonable of the journal to seek advice from more than three reviewers for a paper, because it places an undue burden on authors.

Juan-Carlos Lopez, the journal's chief editor, explains on the blog 'Spoonful of medicine' (http://blogs.nature.com/nm/spoonful/2008/02/strength_in_numbers.html) that this practice, which is not undertaken lightly, is often necessary. One reason for this is that one of the referees may be someone who has not reviewed for the journal before, who may turn out to be either too tough or the opposite — what editors call "wet".

Second, many submissions to *Nature Medicine* are multidisciplinary studies. In some cases, the editor will need one reviewer with expertise on animal experiments, another to advise on potential relevance to human disease, and others who are knowledgeable in the various disciplines and technologies involved.

Third, editors don't ask authors to address every point each referee raises. So, as Lopez says, "two referees times two does not necessarily equal four sets of comments"! ■

Visit Nautilus for regular news relevant to *Nature* authors ▸ http://blogs.nature.com/nautilus and see Peer-to-Peer for news for peer reviewers and about peer review ▸ http://blogs.nature.com/peer-to-peer.

nature

Vol 451 | Issue no. 7182 | 28 February 2008 **www.nature.com/nature**

EDITORIAL

LONDON nature@nature.com
The Macmillan Building, 4 Crinan Street, London N1 9XW
Tel: +44 (0)20 7833 4000 Fax: +44 (0)20 7843 4596/7
EDITOR-IN-CHIEF: Philip Campbell
PUBLISHING EXECUTIVE EDITOR: Maxine Clarke
EDITORIALS: Philip Campbell, M Mitchell Waldrop
NEWS/FEATURES/ONLINE NEWS: Oliver Morton, Geoff Brumfiel, Daniel Cressey, Michael Hopkin, Nicola Jones, Anna Petherick, Katharine Sanderson, Sarah Tomlin, Gaia Vince
BOOKS & ARTS/CORRESPONDENCE & ESSAYS/COMMENTARIES: Sara Abdulla, Joanne Baker, Lucy Odling-Smee, Sarah Tomlin
NEWS AND VIEWS: Tim Lincoln, Andrew Mitchinson, Sadaf Shadan, Richard Webb
PHYSICAL, CHEMICAL AND EARTH SCIENCES: Karl Ziemelis, Rosamund Daw, Joshua Finkelstein, Magdalena Helmer, Juliane Mössinger, Karen Southwell, John VanDecar, Liesbeth Venema
BIOLOGICAL SCIENCES: Ritu Dhand, Lesley Anson, Tanguy Chouard, Henry Gee, Marie-Thérèse Heemels, Rory Howlett, Claudia Lupp, Barbara Marte, Deepa Nath, Ursula Weiss **INSIGHTS/REVIEWS/PROGRESS:** Lesley Anson
SUBEDITORS: Colin Sullivan, Sarah Archibald, Anne Blewett, Catherine Cassidy, Davina Dadley-Moore, Isobel Flanagan, Paul Fletcher Jenny Gillion, Dinah Loon, David Price, Chris Simms, Anna York
EDITORIAL PRODUCTION: James McQuat, Alison Hopkins, Marta Rusin, Charles Wenz, Lauren Wethmar
MANUFACTURING PRODUCTION: Jenny Henderson, Stewart Fraser, Susan Gray, Jocelyn Hilton, Yvonne Strong
ART AND DESIGN: Martin Harrison, Wesley Fernandes, Madeline Hutchinson, Barbara Izdebska, Paul Jackman, Fern McNulty, Nik Spencer
ADMINISTRATION: Pauline Haslam, Karen Jones, Helen Anthony, Jayne Henderson, Aimee Knight, Alison McGill, Jenny Meyer, Alison Muskett, Nichola O'Brien, Naomi Thornhill, Holly Welham
PRESS OFFICE: Ruth Francis, Katherine Anderson, Rachel Twinn

WASHINGTON DC nature@naturedc.com
968 National Press Building, 529 14th St NW, Washington DC 20045-1938
Tel: +1 202 737 2355 Fax +1 202 628 1609
EDITORIAL: Eric Hand, Gene Russo Leslie Sage, Jeff Tollefson, M Mitchell Waldrop, Alexandra Witze **ADMINISTRATION:** Katie McGoldrick, Kenneth Simpson

NEW YORK nature@natureny.com
75 Varick St, 9th Floor, New York, NY 10013-1917
Tel: +1 212 726 9200 Fax: +1 212 696 9006
EXECUTIVE EDITOR: Linda Miller
EDITORIAL: I-han Chou, Chris Gunter, Kalyani Narasimhan, Helen Pearson

BOSTON nature@boston.nature.com
25 First Street, Suite 104, Cambridge, MA 02141
Tel: +1 617 475 9275 Fax: +1 617 494 4960
EDITORIAL: Angela Eggleston, Joshua Finkelstein, Heidi Ledford **ADMINISTRATION:** Eric Schwartz

SAN FRANCISCO nature@naturesf.com
225 Bush Street, Suite 1453, San Francisco, CA 94104
Tel: +1 415 403 9027 Fax: +1 415 781 3805
EDITORIAL: Erika Check Hayden, Natalie DeWitt, Alex Ecclestone
ADMINISTRATION: Jessica Kolman

SAN DIEGO r.dalton@naturesf.com
3525 Del Mar Heights Road, PMB No 462, San Diego, CA 92130
Tel: +1 858 755 6670 Fax +1 858 755 8779
EDITORIAL: Rex Dalton

MUNICH a.abbott@nature.com
Josephspitalstrasse 15, D-80331 München
Tel: +49 89 549057-13 Fax: +49 89 549057-20
EDITORIAL: Alison Abbott, Quirin Schiermeier

PARIS d.butler@nature.com
2 rue Moreau Vincent, 37270 Veretz Tel +33 2 47 35 72 15
EDITORIAL: Declan Butler

TOKYO editnature@natureasia.com
Chiyoda Building 5-6th Floor, 2-37 Ichigaya Tamachi, Shinjuku-ku, Tokyo 162-0843
Tel: +81 3 3267 8751 Fax: +81 3 3267 8754
EDITORIAL: David Cyranoski, Mika Nakano, Akemi Tanaka

CONTRIBUTING CORRESPONDENTS
AUSTRALASIA: Carina Dennis Tel: +61 2 9404 8255
INDIA: K. S. Jayaraman Tel: +91 80 26966579
ISRAEL: Haim Watzman Tel: +972 2 6714077
SOUTH AFRICA: Michael Cherry Tel: +27 21 886 4194
WASHINGTON DC: Meredith Wadman Tel: +1 202 626 2514
MISSOURI: Emma Marris Tel: +1 573 256 0611

NATURE ONLINE

www.nature.com/nature

CHIEF TECHNOLOGY OFFICER: Howard Ratner **PUBLISHING DIRECTOR, NATURE.COM:** Timo Hannay
WEB PRODUCTION/DESIGN: Jeremy Macdonald, Glennis McGregor, Alexander Thurrell
WEB PRODUCTION TECHNOLOGIES: Heather Rankin **APPLICATION DEVELOPMENT:** Peter Hausel
NATURE PODCAST: Adam Rutherford, Kern Smith, Sara Abdulla

PUBLISHING

LONDON feedback@nature.com
The Macmillan Building, 4 Crinan Street, London N1 9XW
Tel: +44 (0)20 7833 4000 Fax: +44 (0)20 7843 4596/7
MANAGING DIRECTOR: Steven Inchcoombe
PUBLISHER: Steven Inchcoombe
ASSISTANT PUBLISHER: Samia Mantoura
PUBLISHING ASSISTANT: Claudia Banks

TOKYO feedback@natureasia.com
Chiyoda Building 5-6th Floor, 2-37 Ichigaya Tamachi, Shinjuku-ku, Tokyo, 162-0843
Tel +81 3 3267 8751 Fax +81 3 3267 8754
PUBLISHING DIRECTOR — ASIA-PACIFIC: David Swinbanks
ASSOCIATE DIRECTOR — ASIA-PACIFIC: Antoine E Bocquet

DISPLAY ADVERTISING

MANAGEMENT: John Michael

NORTH AMERICA display@natureny.com
NEW ENGLAND: Sheila Reardon Tel +1 617 494 4900 Fax +1 617 494 4960
NEW YORK/MID-ATLANTIC/SOUTHEAST: Jim Breault Tel: +1 212 726 9334 Fax +1 212 696 9481
MIDWEST: Mike Rossi Tel: +1 212 726 9255 Fax, +1 212 696 9481
WEST COAST SOUTH: George Lui Tel: +1 415 781 3804 Fax: +1 415 781 3805
WEST COAST NORTH: Bruce Shaver Tel: +1 415 781 6422 Fax +1 415 781 3805

EUROPE/REST OF WORLD display@nature.com
GERMANY/SWITZERLAND/AUSTRIA/OTHER EUROPE: Sabine Hugi-Fürst
Tel +41 52 761 3386 Fax. +41 52 761 3419
UK/IRELAND/FRANCE/BELGIUM: Jeremy Batts
Tel +44 (0)20 7843 4959 Fax: +44 (0)20 7843 4749
SCANDINAVIA/THE NETHERLANDS/ITALY/SPAIN/PORTUGAL/ISRAEL/ICELAND Graham Combe
Tel. +44 (0)20 7843 4914 Fax. +44 (0)20 7843 4749

ASIA-PACIFIC display@natureasia.com
JAPAN: Kate Yoneyama, Ken Mikami
Tel. +81 3 3267 8765 Fax. +81 3 3267 8746
GREATER CHINA/SINGAPORE: Gloria To
Tel +852 2811 7191 Fax: +852 2811 0743

SPONSORSHIP

EUROPE/NORTH AMERICA e.green@nature.com
NATURE BUSINESS DEVELOPMENT EXECUTIVE: Emma Green
Tel +44 (0)20 7833 4000 Fax +44 (0)20 7843 4749

NATUREJOBS

naturejobs@nature.com

Please refer to panel at the start of the *NatureJobs* section at the back of the issue.

MARKETING & SUBSCRIPTIONS

USA/CANADA/LATIN AMERICA subscriptions@natureny.com
Nature Publishing Group, 75 Varick St, 9th Floor, New York, NY 10013-1917
Tel: (USA/Canada) +1 866 363 7860; (outside USA/Canada) +1 212 726 9365
MARKETING: Sara Girard **FULFILMENT:** Karen Marshall

JAPAN/CHINA/KOREA subscriptions@natureasia.com
Chiyoda Building 5-6th Floor, 2-37 Ichigaya Tamachi, Shinjuku-ku, Tokyo, 162-0843
Tel: +81 3 3267 8751 Fax: +81 3 3267 8746
MARKETING/PRODUCTION: Keiko Ikeda, Takeshi Murakami

EUROPE/REST OF WORLD subscriptions@nature.com
Nature Publishing Group, Subscriptions, Brunel Road, Basingstoke, Hants RG21 6XS, UK
Tel: +44 (0)1256 329242 Fax +44 (0)1256 812358
MARKETING: Katy Dunningham, Elena Woodstock

INDIA npgindia@nature.com
Nature Publishing Group, 3A, 4th Floor, DLF Corporate Park, Gurgaon 122002
Tel. +91 124 2881053/54 Fax +91 124 2881052
HEAD OF BUSINESS DEVELOPMENT, INDIA: Jaishree Srinivasan **MARKETING:** Harpal Singh Gill

Annual subscriptions (including post and packing)

INSTITUTIONAL/CORPORATE RATE:	$2,730
PERSONAL RATE:	$199
STUDENT RATE:	$99
POSTDOC RATE:	$119

Printed in USA. Individual rates available only to subscribers paying by personal check or credit card. Orders for student/postdoc subscriptions must be accompanied by a copy of student ID. Rates apply to USA, Canada, Mexico/Central & South America
Add 7% GST tax in Canada (Canadian GST number 140911595).
BACK ISSUES: US$ 20.00

SITE LICENSES, FULFILMENT & CUSTOMER SERVICES

feedback@nature.com
SITE LICENSES: npg.nature.com/librarians
FULFILMENT: Dominic Pettit
CUSTOMER SERVICE: Gerald Coppin

nature MILESTONES

Nature Milestones in Spin

Nature Publishing Group is pleased to announce the publication of *Nature Milestones in Spin*.

A presentation from *Nature Physics*, this supplement focuses on the concept of 'spin' — the idea that elementary particles possess intrinsic angular momentum. The history of spin is a rich one, having an impact on chemistry and biology, and culminating in ground-breaking technologies, such as 'spintronics'.

Nature Milestones in Spin tells the story through a series of 'milestones' marking the significant developments through the twentieth century to the present day.

Read the entire content of the supplement free online for 6 months, download the digital edition or order your free print copy

www.nature.com/milestones/spin

Produced with support from Organic Spintronics

nature publishing group npg

Real Time PCR with Perfect Results

SYBR® Green

SYBR® *Premix Ex Taq*™

SYBR® *Premix Ex Taq*™ (Perfect Real Time) delivers exceptional real time PCR results quickly and easily.

- **Easy-to-Use:** convenient premix formula.
- **Less Optimization:** great for first screens.
- **Versatile:** use on any real-time PCR instrument.
- **Low C_T Values:** high sensitivity with detection of as few as 10 copies.
- **Precise Quantification:** 2-fold difference can be accurately detected.
- **Fast:** works with high speed qPCR instruments.

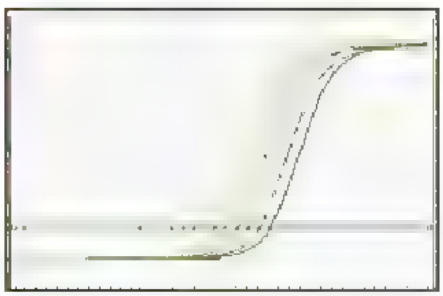

Accurate detection of 2-fold difference, using SYBR® *Premix Ex Taq*™ with an Applied Biosystems 7500 Real Time System

Also Available in a Premix for TaqMan® Probe Detection

TaKaRa

Visit our Website Today!
www.takara-bio.com

Japan:
Takara Bio Inc.
+81 77 543 7247
www.takara-bio.com

USA:
Takara Bio USA*
888-251-6618
www.takarabiousa.com

Europe:
Takara Bio Europe S.A.S.
+33 1 3904 6880
www.takara-bio.eu

China:
Takara Biotechnology (Dalian) Co., Ltd.
+86 411 8764 1681
www.takara.com.cn

Korea:
Takara Korea Biomedical Inc.
+82 2 2081 2525
www.takara.co.kr

nature

www.nature.com/nature

Vol 451 | Issue no. 7182 | 28 February 2008

A new Silver Age?

The Spanish government has doubled research spending in four years. The next government must create the legal structures to ensure that this money is wisely spent.

Spain's ruling Socialist Party came to power in 2004 vowing to reinvigorate its nation's turgid, bureaucracy-ridden research enterprise, and proceeded to make impressive progress towards that goal — not least by doubling the government's funding for science. But money is not everything. The next government, due to be elected on 9 March, will face the much harder challenge of modernizing the organization and management of Spanish science, so that the higher budgets can be spent more effectively.

Central to the reform effort is the Spanish National Research Council (CSIC), which has had a turbulent history as the government's leading research agency. The council was created in 1907 as the JAE, the Council for the Extension of Studies and Scientific Research, to promote science and foster links with European culture in general. The JAE operated a humming campus that hosted most of Spain's budding intellectuals at some stage in their creative lives, and helped to nurture Spain's 'Silver Age'. This period in the early twentieth century saw Salvador Dalí paint his surrealist masterpieces, Luis Buñuel make avant-garde films, Federico García Lorca write sublime poetry, and Santiago Ramón y Cajal push the boundaries of neuroanatomy — work for which he won the 1906 Nobel prize.

The Silver Age was brought to an abrupt end in the mid-1930s by the Spanish Civil War. What followed, under the nearly four-decade dictatorship of Francisco Franco, can only be described as an intellectual dark age. Many of Spain's best scientists were driven into exile. Those that remained found themselves isolated. And the JAE, taken over by Franco and renamed the CSIC, had its intellectual ambitions drastically pared down.

The agency — and Spanish science in general — has struggled to recover ever since. For nearly 30 years after Franco's death in 1975, successive democratic governments introduced only the most hesitant reforms and budget increases. The CSIC grew to encompass 116 institutes and more than 150 research groups in universities. But it remained a stodgy bureaucracy in which buying a small item of equipment could take months and recruiting a scientist could take more than a year.

Fresh impetus

Hoping to improve matters, the current Socialist government came into office promising to double research funding; to turn the CSIC into an independent agency; and to create a separate, independent granting agency. The government fulfilled the first of these promises, more than doubling the research budget to over €8 billion (US$11.8 billion). Spain's spending on research now exceeds 1.1% of its gross domestic product — still well below the European Union average of 1.8%, but a major improvement over the level of 0.4% at the end of Franco's dictatorship. If it wins a second term, the socialist party plans to boost this figure to 2% by 2011.

But the outgoing government has not done so well on the other two promises. It has laid the legal foundations for the much-needed granting agency, but the agency has yet to appear; the handful of competitive granting programmes that currently exist are offered by individual ministries, mostly earmarked for particular themes. And the promised liberation of the CSIC is still incomplete. The council was spun out of the science ministry to become an independent agency last December. But the heavy political representation on its executive board leaves scientists wondering how 'independent' it will actually be. The board is now drafting the by-laws of the CSIC agency, which will define exactly how it will operate.

Of particular concern to scientists is whether these rules will reform Spain's inflexible system of academic recruitment, which remains the biggest obstacle to efficiency. University professors and CSIC scientists alike are civil servants with total job security. As a result, hiring at any level is desperately slow, the hiring of foreigners is difficult, and it is almost impossible to offer anyone a competitive package of salary and research money.

> "Spain's pockets of scientific excellence show that it is capable of entering a new Silver Age."

Cutting through the red tape

This seemingly intractable problem has forced research administrators to devise ingenious work-arounds. The health ministry, for example, has created autonomous public-research institutes outside the standard system. One, the National Cancer Research Centre in Madrid, has built itself up into an internationally renowned centre just ten years after its founding. And although the CSIC's own institutes are still locked into conditions dictated by the science ministry, one of them, the National Centre for Biotechnology in Madrid, has managed to create its own 'pseudo-tenure-track' programme. It allows young scientists with their own research grants to move into space in its new start-up incubator building, which is not yet fully rented out.

The CSIC itself has done a good job over the past few years preparing itself for its new era as an agency. It has evaluated all of its institutes, closed three as a result, and merged many more to consolidate and focus research efforts. The real question is whether government officials, wary of what they see as losing control, will give it the freer rein it needs to realize its potential. Yes, the CSIC must operate under normal systems of accountability. But its new by-laws must allow it to offer proper career paths to its young scientists, and attractive packages to more senior scientists. If the bureaucrats don't ease up on their top-down control, the CSIC will be lost to mediocrity. The best scientists will go to the new autonomous institutes, which treat them better.

If the CSIC agency is allowed to develop appropriately, and an independent granting agency is created, then Spain will be well on its way to European norms. Spain's pockets of scientific excellence — reflected in its success in winning many of the first highly competitive European Research Council grants — show that the country is capable of entering a new Silver Age. If only its government will let it. ■

Lone Star vs creationism

The battle against anti-scientific literalism continues. Next stop Texas.

The creation–evolution debate in the United States is ever-changing: any given week might bring good news for science advocates in some states, but bad news in others. At the moment, the good news is coming from Florida, which on 19 February voted to adopt new science standards that significantly strengthen the role of evolution in the state's biology curriculum (see page 1041).

But the next round of news will undoubtedly come from Texas, where a state agency faces a decision whose ramifications could resonate across the United States for years to come. The Texas Higher Education Coordinating Board is considering an application by the Institute for Creation Research (ICR) to grant online master's degrees in science education. And an advisory panel to the board has recommended that Texas should accept the application.

The ICR accepts the Bible as literal truth on all topics. According to its website, the palaeoclimatology class covers "climates before and after the Genesis Flood". Anatomy lab includes "limited discussion of embryology and accompanying histology, specifically in regards to evolutionary theory and its alternative — the creation of fully functional major groups of animals".

For most of its existence the ICR was ensconced in the San Diego area, but in 2007 it relocated to Dallas, in an apparent move to expand its national reach. California may have been glad to see it go; the state had been battling the ICR over accreditation since 1981, when, under a sympathetic official, the institute first got the go-ahead to offer degrees. But in Texas the ICR must win approval from the state board to continue setting up its graduate programmes before seeking permanent accreditation.

The decision falls to the nine-member higher-education board. It had been expected to vote on the issue in January, but instead asked the ICR for more information — about the research done by its faculty members, about how an online course would teach experimental science, and about why its curriculum is so different from other degree-granting institutions in science education. A vote is expected at the board's 24 April meeting.

High-powered scientists in Texas are already weighing in, asking board commissioner Raymund Paredes to deny accreditation. And there are signs that the board is listening. In a response to Nobel laureate Steven Weinberg, Paredes wrote that "our primary criterion will be how the proposed program will contribute to preparing high school students to do rigorous science in higher education". One can only hope such rational approaches will outweigh the primary ICR reaction, which has been to send out a call for prayer.

Scientists in Texas and the rest of the country must continue to make it clear to Paredes why the board should deny accreditation to this organization. The ICR has managed to con its way into the California educational system for decades. Texas must not succumb as well. ■

Time to take control

With money now flowing in, the fight against malaria must shift from advocacy to getting results.

"The billion-dollar malaria effort is flying blind," declares Mark Grabowsky in a Commentary on page 1051 of this issue. And given that Grabowsky is malaria coordinator of the Global Fund to Fight AIDS, Tuberculosis and Malaria, which disburses almost half the US$1 billion spent annually on malaria control, we might do well to listen.

Grabowsky argues that, above all, malaria control requires data: to assess the present situation, to target control measures and to evaluate their effectiveness. He also says that an adequate surveillance programme would cost as little as $10 million a year. Yet that money has not been forthcoming; malaria managers still lack even the most rudimentary information (see *Nature* doi:10.1038/news.2008.621; 2008).

The surveillance problem is symptomatic of a wider failure in basic project management. The 'international' malaria effort is actually a hotch-potch of fragmented, country-level projects funded by multiple donors, with little regional and international coordination. Such leadership would normally be provided by the World Health Organization (WHO), as it has done to great effect in the fight against measles and polio. But the WHO-led Roll Back Malaria initiative is mired in bureaucracy and anything but effective (see *Nature* **430**, 935; 2004).

That management problem, in turn, reflects a still deeper issue: the agencies involved in the malaria fight, including the WHO, have for too long been driven largely by advocacy. It's true that advocacy was a supreme need a decade ago, when malaria control was off the radar and gathering a mere $100 million a year. But that mindset has persisted even as the funding has multiplied tenfold.

Take the good news spin put on recent studies showing that bed nets and drugs cut the malaria burden by as much as half in Zanzibar, Ethiopia and Rwanda. That sounds dramatic. But it's hardly unexpected, as the low malaria transmission rates in these countries make the disease comparatively easy to control. And in the meantime, silence surrounds the lack of a single win in high-transmission areas such as the Democratic Republic of the Congo or Nigeria, which account for half the malaria mortality in Africa.

Yes, on-the-ground conditions are difficult, as is reported in Zambia, the flagship of international efforts (see page 1047). But the international malaria effort is still geared towards maintaining donor support instead of getting teams into the field gathering data and delivering basic items such as bed nets. That's why almost no country is near to meeting Roll Back Malaria's target of having 80% coverage with bed nets and drugs by 2010; why malaria is still killing more than 1 million people every year; and why the global control effort is way off track to meet the internationally agreed goal of halving malaria deaths by 2010.

Such goals are undeniably ambitious. But they are a spur to action — and in line with what the WHO has already achieved with measles and polio. What the malaria effort urgently needs now is leadership, and a shift from spin to substance and results. ■

RESEARCH HIGHLIGHTS

STEM CELLS

Insulin from scratch

Nature Biotechnol. doi:10.1038/nbt1393 (2008)

Researchers have used human embryonic stem cells to generate insulin-producing pancreatic cells that respond to glucose and protect against a diabetes-like condition in mice. The approach may one day be useful for treating diabetics.

Previous attempts had yielded pancreatic cells that did not respond to glucose. But Emmanuel Baetge and his co-workers at Novocell in San Diego, California, adjusted their protocol to select cells at an earlier stage of differentiation. When those pancreatic cells were grafted into mice, the cells began producing insulin within 30 days of the transplant.

Both fasting and glucose intake triggered insulin production by the transplanted cells. The cells also protected mice from diabetes caused by a toxin that selectively kills mouse insulin-producing cells.

ENTOMOLOGY

Metal mouth

Naturwissenschaften doi:10.1007/s00114-008-0346-3 (2008)

The termites of the subfamily Kalotermitidae have mandibles that are harder than those found among any of their kin, according to Bronwen Cribb at the University of Queensland in Brisbane, Australia, and her colleagues.

The secret to their hardness seems to be the substantial amount of zinc in the wood that termites eat, which the Kalotermitidae alone concentrate along the edges of their mandibles (pictured below). The researchers analysed the elemental composition of different termite species' mandibles and applied scratch tests along the mandible edges to determine just how hard they were. Previous work found that zinc reinforcement made mandibles up to 20% harder.

Most termites eat damp or moistened wood, whereas the Kalotermitidae specialize in consuming dry wood, which is tougher to chew through and is probably what drove the evolution of their extra hard bite.

B. W. CRIBB

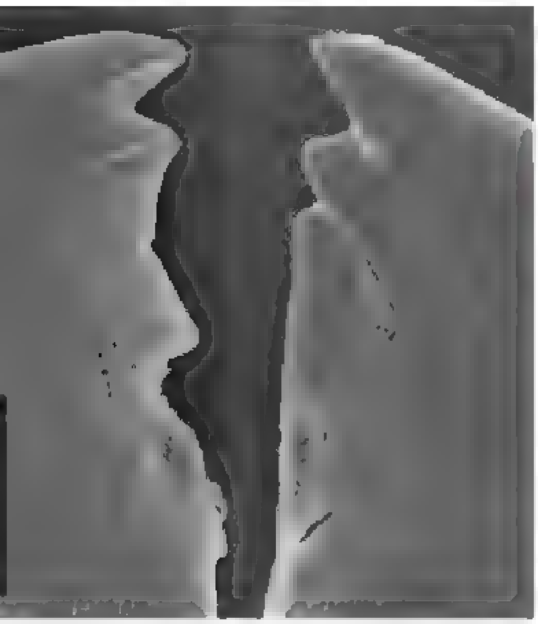

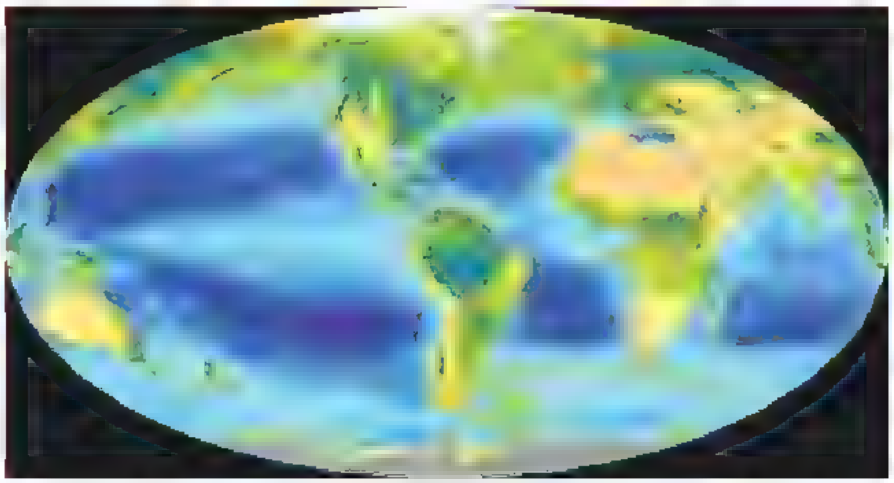

NASA

Hue and die

Geophys. Res. Lett. 35, L03618 (2008)

The ocean's colour from space is determined by the density of its photosynthetic life, allowing researchers to track changes in sea life over time across extensive areas.

Jeffrey Polovina of the US National Oceanic and Atmospheric Administration's Pacific Islands Fisheries Science Center in Honolulu, Hawaii, and his co-workers looked at the colour of the least biologically productive reaches of the ocean, known as the subtropical gyres, from 1998 to 2006. They found that the most desert-like areas (darkest blue in this false-colour map) are expanding — hand in hand with rising sea surface temperature due to global climate change. Warmer waters see less vertical mixing and therefore reduced movement of nutrients from the depths to the sunlit surface.

The work provides an update on analyses done with the same data set but over fewer years, and startles with its dire conclusions. waters containing 0.07 milligrams or less of chlorophyll per cubic metre have expanded by 6.6 million square kilometres, that is, by about 15%, in nine years. This is a much faster rate than expected from climate models.

SEMICONDUCTORS

Under the wave

Phys. Rev. Lett. 100, 073602 (2008)

In the semiconductor business, the smaller the circuit that can be etched onto a microchip, the more profit a company is likely to see. The wavelength of light used to etch the chips is one of the main constraints on miniaturization.

Muhammad Suhail Zubairy at Texas A&M University's campus in Doha, Qatar, and his colleagues have found a way — in theory at least — to make smaller features.

The team's calculations show that multiple lasers can be beamed onto a surface in a way that creates quantum interference. This interference could, in turn, be used to create sub-wavelength patterns on a chip.

GENETICS

Smoking in black and white

Hum. Mol. Genet. doi:10.1093/hmg/ddn044 (2008)

Why is kicking the habit so hard for some? A protein involved in directing neuronal wiring looks increasingly like a culprit. Ming Li at the University of Virginia in Charlottesville and his colleagues analysed 21 points of frequent variation in the gene encoding neurexin 1 in smokers of varying levels of addiction.

Their findings confirm previous gene-association studies linking neurexin 1 to susceptibility to nicotine dependence. They further suggest that the same gene associates with dependence in Americans of both European and African descent, but in different ways. Different regions of the gene link to smoking for blacks and whites.

Neurexins are cell-adhesion molecules that may help form and maintain neuronal synapses. Another neurexin, neurexin 3, has previously been linked to alcohol addiction.

NEUROLOGY

Diabetes lessens learning

Nature Neurosci. doi:10.1038/nn2055 (2008)

A stress-related steroid may damage regions of the brain responsible for memory in animals with diabetes.

Mark Mattson and his colleagues at the National Institute on Aging in Baltimore, Maryland, found that both rats modelling type 1 diabetes and mice modelling type 2 diabetes formed fewer new neurons in the hippocampus and experienced more difficulty learning than normal rodents.

Both rodent models also had higher levels of corticosterone. Humans with diabetes sometimes have higher levels of a related steroid called cortisol. Lowering corticosterone in diabetic rodents restored their capacity for learning, and later administration of high levels of corticosterone to these rodents reinstated the learning deficits. Taken together, the results suggest that corticosterone may cause cognitive impairment in diabetes.

MATERIALS

Gecko glue

Proc. Natl Acad. Sci. USA 105, 2307–2312 (2008)

Inspired by geckos' feet, researchers have developed and tested *in vivo* a biodegradable tape that may one day be used as a replacement for sutures. The tape is made from a thin polymer film, etched with a forest of nanoscale, cone-shaped projections similar to the tiny bristles that cover the hairs on the pads of geckos' toes.

Geckos' feet bind to surfaces owing to simple intermolecular forces between the surface and these bristles. But the tape, developed by Robert Langer of the Massachusetts Institute of Technology in Boston, Jeffrey Karp of Harvard Medical School and a large team, depends on an extra layer of stickiness from a coating of sugar that assists with bonding.

Gecko-modelled adhesives have been developed in the past, but the researchers say this is the first to show compatibility in living tissue.

OPTICS

Hidden source

Phys. Rev. Lett. 100, 063904 (2008)

If a spherical 'invisibility cloak' could hide physical objects, as recently proposed, it could also hide electromagnetic fields, according to Hongsheng Chen and his co-workers at Zhejiang University in Hangzhou, China.

The shield uses metamaterials, which interact with light in unusual ways, to divert electromagnetic waves around the inside of the shielded space. The principle has been demonstrated experimentally at microwave frequencies, but it wasn't clear whether it would work for cloaking 'active' devices such as electronic circuits, which produce electromagnetic fields that could leak out of the shield and undermine the invisibility.

Chen and colleagues calculate that such fields create electric and magnetic fields at the inner surface of a spherical shield, which, in turn, reflect any waves broadcast from an active object inside and prevent them from escaping.

K. PRUDIC

EVOLUTION

Back into hiding

Proc. R. Soc. B doi:10.1098/rspb.2007.1766 (2008)

Many species, especially insects, protect themselves from predators by mimicking the bright warning markings of other, better-defended creatures. A study of butterflies confirms one theory about this phenomenon — that when the noxious model species disappears the mimic does not necessarily vanish with it, but can revert to a less-conspicuous outfit.

Kathleen Prudic and Jeffrey Oliver at the University of Arizona in Tucson compiled an evolutionary family tree of North American admiral butterflies, a subspecies of which mimics the wing patterns of the toxic black pipevine swallowtail butterfly (mimic pictured above). One subspecies of *Limenitis arthemis* is descended from such mimics, but displays the camouflage patterns of its ancestors (pictured, inset), suggesting that it has re-evolved its disguise.

JOURNAL CLUB

Eric J. Nestler
University of Texas Southwestern Medical Center, Dallas

A psychiatrist talks about finding answers that add up across all levels.

Often when we study the brain and behaviour, we fail to tie molecular events to higher-order changes in composition, to shifts in the organ's circuitry, or all the way up to changes in actions or broad mental abilities. Many scientific fields suffer from this problem of scale, but the recent explosion in techniques available for molecular biology and quantitative behavioural analysis has given neurobiology the potential to bridge many conceptual gaps.

An excellent example is a study carried out by Roberto Malinow of Cold Spring Harbor Laboratory, New York, and his colleagues (H. Hu *et al. Cell* 131, 160–173; 2007). They elucidated a molecular mechanism by which emotional stress and arousal promote long-term memory formation. In doing so, they brought together two well-characterized phenomena: that noradrenaline stimulates memory formation in the brain's hippocampus, and that the trafficking of a type of glutamate receptor is important for a form of plasticity in the same brain region.

Malinow's team shows that, by stimulating noradrenaline release in the hippocampus, emotional stress leads to phosphorylation of glutamate receptors. This boosts the incorporation of these receptors at the synapse — the junction between nerve cells — which, in turn, enhances synaptic function and improves memory formation. Crucially, mice with a mutation that prevents phosphorylation of the relevant part of the glutamate receptor do not show noradrenaline-mediated memory enhancement.

Impressively, this study begins with a clinically important phenomenon — memory enhancement by emotional stress — and establishes a detailed biological pathway that underlies a behavioural endpoint in an animal model. Studies such as this are what the field needs.

Discuss this paper at **http://blogs.nature.com/nature/journalclub**

NEWS

Animal-rights activists invade Europe

A rash of vandalism, intimidation and arson across continental Europe in 2008 is evidence of a worrying new wave of animal-rights extremism being exported from Britain, experts say

In early January, threats led to a Dutch developer withdrawing from a new, €60 million (about US$89 million) biomedical research park in Venray, the Netherlands. A month later, Hasselt University's Biomedical Research Institute in Diepenbeek, Belgium, was set on fire. And in Barcelona in Spain, vandals targeted the offices of biomedical-research firm Novartis.

The pattern "is quite clear-cut", according to Simon Festing, director of the Research Defence Society, a London-based group representing medical researchers. Festing says that he believes new, more stringent enforcement in the United Kingdom has led many extremists to move their activities overseas. "Activists are not finding it easy here," he says. "So they're just going across to Europe"

Over the past year, the United Kingdom has cracked down on animal-rights activists who break the law. Last May, police carried out Operation Achilles that led to charges against 16 activists. A trial involving several of them is expected to begin later this year.

Novartis's Barcelona offices have been attacked.

E. DE MATEO

Neither Interpol nor Europol, which coordinates European police activities, have firm statistics on extremist acts, but anecdotal evidence suggests that Britain's tougher law enforcement has led to a rise in activities on the continent. "It's been going on for years, but it's become worse," says Robert Janssen, the managing director of the Netherlands' biotechnology industry association NIABA in Leidschendam. Janssen estimates that Dutch researchers and institutions have received more than 200 threats in the past year.

It has come as a shock to some in the scientific community. "We've never had problems before," says Piet Stinissen, director of the Biomedical Research Institute at Hasselt University. On 1 February, the Institute was set ablaze, causing around €100,000 in damages. The fire was believed to be caused by the Animal Liberation Front, an extremist group. Stinissen, who has been at the University since 1994, says that he cannot remember a single previous incident of extremism.

Andrew Jackson, deputy head of security at Novartis in Basel, Switzerland, says that industry is also being affected. On 9 February, Novartis's offices in Barcelona were vandalized during a protest, and Jackson says that there has been an overall increase in both legal demonstrations and illegal acts. "We've had to increase the security of some of our facilities in Europe," he says. Novartis says that incidents outside the United States and United Kingdom rose by nearly 50% last year to 97. There have been 15 events so far this year.

Jackson believes that the protests and criminal acts are being fuelled in part by British activists travelling abroad. "There is a perception that EU law enforcement has something

Acclaimed photo was faked

An award-winning photograph of a herd of endangered Tibetan antelopes apparently undisturbed by a passing train on the controversial Qinghai–Tibet railway has been exposed as a fake. The image was widely hailed in China as a symbol of harmonious co-existence between man and nature and strong testimony against any adverse effect of the new railway on the animals.

Photographer Liu Wei-qiang admitted the fabrication last week after comments on the Chinese online photography forum Without Fear questioned the picture's authenticity. Liu was promptly dismissed from the *Daqing Evening News*, based in Harbin, Heilongjiang province, where he was the deputy director of its photography department. The newspaper has also issued a public statement apologizing for the incident and announcing the resignation of its chief editor.

"The train was real, and so were the antelopes," said Liu in a posting on the photography forum. "But the magic moment just didn't happen even after I had waited for two weeks." Therefore, he decided to merge together one picture of a passing train with another of the migrating animals "to raise the public awareness of antelope protection". The merged picture was published by more than 200 media outlets around the world and won Liu a bronze medal in the 2006 Most Influential News Photos of the Year competition, sponsored by CCTV, China's state television.

Yang Xin, president of Green River, a non-governmental environmental organization based in Chengdu, Sichuan province, met Liu on the Tibetan plateau in 2006. He says that he was surprised by the photographer's luck in seeing the train and animals passing on the same spot. "It is probably a one-in-a-thousand opportunity," he said.

"The truth is probably the opposite of what the picture was trying to claim," says Su Jian-ping, a zoologist at the Northwest Institute of Plateau Biology, Chinese Academy of Sciences, in Xining, Qinghai province. Su is sceptical of the government's claim that the railway has no impact on the antelopes' migration patterns. The antelopes are shy creatures and particularly prone to disturbances, he says, having spent years on the plateau studying their behaviour. There is no such a thing as "harmonious co-existence" between the train and antelopes, he adds. "You just don't see them together."

The 'photo' was actually a merger of two images.

Yang describes Liu's behaviour as "totally inexcusable", and says that it has tainted the field of wildlife conservation. "Liu fabricated and supplied the image the government badly wanted to see, which may not have reflected the reality."

of a soft touch," he says. Jackson says that he has noticed a correlation between availability of budget flights to Basel and extremist activity. "It makes for a fun weekend," he notes wryly

But not everyone agrees that the British crackdown is behind increased activity elsewhere in Europe. Activists do occasionally go abroad to protest, says Amanda Richards, a spokesperson for SPEAK, an animal-rights group based in Northampton, UK, which has led a campaign against a primate laboratory at Oxford University (*Nature* 438, 716; 2005). But she believes that the rise in Europe is due primarily to rising awareness on the continent. "It's mainly people in the countries themselves," she says. SPEAK has been contacted by several individuals and groups in Europe who want to organize events against animal testing, she adds.

Janssen says that in the Netherlands at least, the government now appears to be taking animal-rights extremism more seriously. On 12 February, the Dutch parliament passed a motion to support the use of animal testing and condemning extremist acts. Janssen says that he hopes the motion will be followed by more rigorous law-enforcement. ■

Geoff Brumfiel

The incident is not the first faked image to be used in the environmental arena. Last October, the Shanxi Forestry Department publicized two photographs of a South China tiger in the wild, which caused much excitement as the species had been considered functionally extinct. According to the verdicts of six experts in forensics and image verification, the pictures were fake, probably taken of a cardboard tiger planted in the woods. The farmer claiming to have taken the snaps stands by their authenticity, and the local government is yet to release the report of its own investigation.

"These are hardly isolated incidences," say Qiu Ren-zong, an ethicist at the Institute of Philosophy, Chinese Academy of Social Sciences, in Beijing. "China suffers from a serious lack of accountability with rampant fraud and corruption in its political, economic and academic life." Real transparency and an effective check-and-balance system must be put in place if China is to move forward, he says. ■

Jane Qiu

Revamp for NIH grants

Scientists applying to the US National Institutes of Health (NIH) for grants could be accelerated through the painful peer-review process under recommendations proposed on 21 February aimed at overhauling the decades-old system.

Currently, a grant proposal can take 18 months to pass through the system, waiting in line behind older applications, most of which must go back and forth to the applicants for rewrites and amendments before approval. The new proposals aim to change this, at least for the best grants, by eliminating what they call the 'special status' of amended applications that often sees them funded before promising first-time proposals.

"It's a system that rewards persistence over brilliance sometimes. And we really want to change that," says NIH director Elias Zerhouni, whose advisory committee was presented with a 78-page draft report of recommendations.

Applicants would also no longer have to respond to reviewers' comments as part of their second or third attempts with the same application. Nor would reviewers considering amended applications any longer see previous reviewers' comments. That way, they "will not be biased in any way by any prior review", says Lawrence Tabak, director of the NIH's dental institute who co-chaired the two advisory panels charged with reviewing the system.

The panels — an internal working group of senior NIH officials and another of external scientists — were asked last June to come up with recommendations to ensure that the $29.3-billion agency funds "the best science, by the best scientists, with the least administrative burden".

Other recommendations include substantially shortening the 25-page applications by minimizing the preliminary data and methodological detail required. They say that the NIH should consider reviewing early-career investigators in a separate pool against each other, rather than throwing them up against established veterans. And they advise that the poorest-quality applications (not just early-career ones) should be bluntly coded NRR — "not recommended for resubmission".

In a bid to share finite riches, but one that seems bound to stir controversy among superstar grantees, the panels would like to see the NIH require principal investigators to commit at least 20% of their time to work on any single grant that is funded. For the vast majority of grantees, who receive one or two grants, that should be possible; for the 783 grantees awarded four or more grants, it will clearly have consequences.

Several scientists not involved in the process say they are pleased with the scope and broad-mindedness of the recommendations. "The focus on making the system work better is exactly right," says David Korn, chief scientific officer of the Association of American Medical Colleges and a former dean of the Stanford University School of Medicine. "And it's really terrific that the NIH has decided to go at it very explicitly and very boldly."

"It was pretty obvious that this was going to be a serious effort at improving the system, and I think they've come through," says Katherine Wilson, a cell biologist at the Johns Hopkins University School of Medicine in Baltimore, Maryland, who testified to the external panel last summer on behalf of the American Society for Cell Biology.

Wilson did some back-of-the-envelope sums based on NIH numbers in the draft report (see graph). If every grantee with four or more NIH grants was reduced to holding two grants, she calculates, "that boosts the number of available grants by 1,852 — that's 5%. It's the difference between the current grim situation and making the system work again."

Others contend that the recommendations, however enterprising, will not improve a situation that has seen NIH funding essentially frozen since 2003. Zerhouni will now consider the report and plans to assemble an implementation team in the next two months. ■

Meredith Wadman

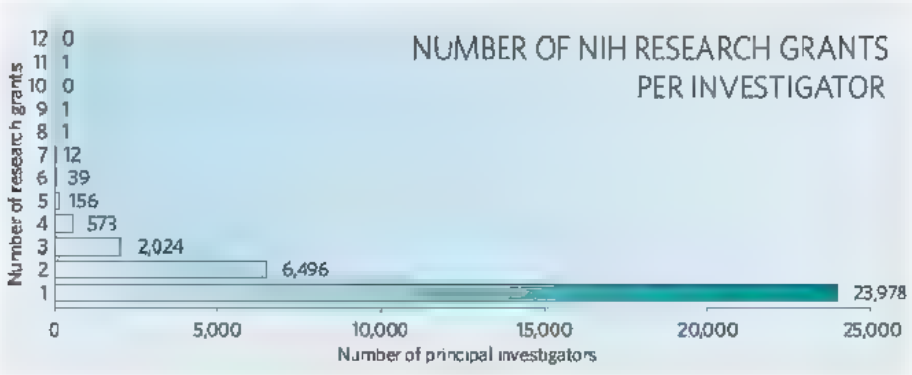

Q&A

The aftermath of independence

The formerly Serbian province of Kosovo unilaterally declared its independence on 17 February. Some 10,000 Serbian students and academics live in enclaves in the ethnically divided city of Kosovska Mitrovica in the north of the new country dominated by Kosovar Albanians. Endocrinologist **Aleksandar Jovanovic**, vice-rector for science and international relations at the University of Mitrovica, discusses recent events.

What is the University of Mitrovica's set-up?
We were the University of Priština, but during the war in 1999 the university was split, and the main Serbian part was re-established in Mitrovica in 2001 [where it goes by the protracted name of the University of Priština in Kosovska Mitrovica]. The university is licensed by the United Nations Mission in Kosovo and funded by the Serbian government, at a cost of around €10 million (US$14.8 million) per year, which is spent mostly on salaries. We have around 10,000 students and 700–800 professors, who are paid a 100% 'Kosovo bonus' to work and teach here. The university has ten departments including faculties for science, medicine, engineering, economics and agriculture.

How did you react to the declaration of independence?
It is our clear wish to stay with Serbia. There is no way that professors or students here would teach, or get taught, in a Kosovar-Albanian-led educational system. It just wouldn't work. We have very different traditions, and we haven't had any contact with the Kosovar Albanian academic community for years. Unfortunately, there are broader political interests that are currently a higher priority than university affairs.

What are your main concerns?
In an independent Kosovo we're expecting all kinds of difficulties. Luckily, Serbia says it will continue to support our work. We need to remain a Serbian institution, otherwise this university will just cease to exist. We cannot survive without Serbian support. At the moment our main concern is security. There haven't been major clashes since March 2004, when there were attacks on the Serbian communities in Kosovo. The unilateral declaration of Kosovo's independence means that there is potential for violent conflict once more. Political rhetoric is up, anything can happen.

Students are leading the protests in Mitrovica against Kosovar independence. Is the university term being interrupted?
We're midway through the spring term and we're doing our best to carry on teaching. Student protests began on 18 February, the day after the declaration of independence, and have been going on every day since. But lectures are taking place as usual. There are courses until noon, then the students — between 3,000 and 5,000 each day — take to the streets until 3 p.m., and then everybody comes back for the afternoon classes. We must keep up the work, or we will pay the price later. When we allowed protesting students to proceed to the next term without any exams in 1996, it took several years to return to academic order.

Has there been violence?
The student protests have mostly been peaceful. There was one incident on Saturday [23 February] when some radicals tried to provoke police, throwing bottles and fake bombs. We don't know whether there were any students involved, though.

Why is the university so important for the Serbs in Kosovo?
It is vital for the Serbian enclaves in northern Kosovo. It is the only strong economic factor in a region where just 8% of the economy is private sector. Without the university, the 100,000-strong Serbian minority would further evaporate. We need the students, and we hope that many will stay here after graduation and help keep the economy alive.

Is any scientific research now going on at the university?
We're mostly just teaching. There are 46 small scientific projects, many of which were started before we moved from Priština in 1999. We have a collaboration in material sciences with Queen's University in Ontario, Canada, and we have partnerships with universities in Serbia, Macedonia, Greece and Bosnia. We're also hoping to launch a collaboration with the University of Grenoble in France. Health and environmental issues related to the mining activities in the region could be a priority for future research activities.

What difficulties do you face?
We're working under chaotic conditions. The biggest problem is that our infrastructure is devastated and that our labs are very poorly equipped. There is a lack of everything, from lighting, to computers, to chemicals. Part of our equipment, such as computers and lab tools, are locked in Priština. We have been trying to get it back or be reimbursed, but so far without success.

Is there any contact between Serbian and ethnic Albanian scientists in Kosovo?
There hasn't been any cooperation between the universities of Priština and Mitrovica since the Serbian community had to leave Priština in 1999. I hope that in the future we will collaborate with Albanian-language scientists and academics again. ■

Interview by Quirin Schiermeier

Neglected diseases get vaccine research boost

Swiss pharmaceutical giant Novartis has opened a non-profit research institute in northern Italy to develop vaccines for neglected diseases prevalent in the developing world.

The new Novartis Vaccines Institute for Global Health is based in Siena, the home of Novartis Vaccines and Diagnostics. It will be managed independently of the commercial vaccine company and will have its own team, focusing initially on diarrhoeal diseases that have been overlooked by the major research funders. "Diarrhoeal diseases cause more deaths per year among children under five than malaria and AIDS together," says Rino Rappuoli, global head of vaccine research at Novartis, who has been the force behind the venture.

"Diarrhoeal diseases cause more deaths in children under five than malaria and AIDS together."

Rappuoli has spent his entire career in vaccine research, joining the Sclavo Institute in Siena 30 years ago, and seeing it through its takeover by Chiron in 1992 and then by Novartis two years ago. "I've had to develop vaccines for the rich world, where our customers are — but I knew how easily our technology and knowledge could be applied to vaccines for the poor world," he says.

The new institute will be headed by Allan Saul, who led the malaria vaccine programme at the US National Institute of Allergy and Infectious Diseases before moving to Novartis last year. The plan is to develop a polyvalent vaccine (effective against more than one strain) for three forms of *Salmonella* infection and a polyvalent vaccine for *Shigella* and ETEC (enterotoxigenic *Escherichia coli*). Over the next few years, other diseases will be targeted.

Choosing the diseases to focus on was tricky, Saul says. "We started with a list of 57 and whittled it down to a short list of five — all diarrhoeal diseases — where we thought we could get the best return on investment: these diseases kill millions each year, and we can build on existing basic research."

The institute complements the Novartis Institute for Tropical Diseases, another non-profit organization founded five years ago in Singapore to develop drugs for diseases such as malaria, tuberculosis and dengue fever. The vaccine institute hopes to recruit up to 20 scientists by 2009, and eventually to have around 80 staff working on four programmes. Novartis will pay the institute's staff and running costs, but most of its project money will have to be sought from other sources, such as the Bill & Melinda Gates Foundation. ■

Alison Abbott

SNAPSHOT

'Doomsday vault' opens

M. TEFRE/GLOBAL CROP DIVERSITY TRUST

The glittering entrance to the Svalbard Global Seed Vault leads into a 100-metre tunnel dug in the side of a cave at Longyearbyen, a remote Arctic archipelago in Norway. Its first batch of seeds was accepted on 26 February — the initial stage in a plan to provide a repository holding back-up copies of seeds representing almost every food crop in existence.

At its launch, Jacques Diouf, head of the United Nations Food and Agriculture Organization, described the project as "one of the most significant acts in the preservation of humanity". ■

Michael Hopkin

J. MCDONALD/CORBIS

ON THE RECORD

"We are not recommending you import alligators into California. That would not be a good idea."

Zoologist Gordon Rodda from the US Geological Survey in Colorado pours cold water on a tactic to prevent a feared invasion of Burmese pythons in San Francisco.

SCORECARD

The Galapagos
Ecuador's president Rafael Correa has pledged to stamp out the use of fossil fuels on the Galapagos Islands by 2015, starting with a huge wind farm that will halve their diesel requirements.

The Amazon
Ecologists say that the 60-metre-wide protected rainforest corridors flanking many of the Amazon's rivers are too narrow to conserve biodiversity. They are calling for government action to raise the minimum width to 400 metres.

OVERHYPED

Gravity lamp
The inventor of a gravity-powered lamp — Clay Moulton from Virginia Polytechnic Institute in Blacksburg — has been forced to admit that his device would be too weak to power current light-emitting diodes.

ROBOT NEWS

Java Justine
A coffee-making robot has been developed by Italian (of course) scientists. Sceptics who argue that coffee machines already have the automated-coffee-making market sewn up should note that the robot, called Justine, can also tidy clothes off the floor.

Sources: EurekAlert, Conserv. Biol., San Francisco Chronicle, Virginia Tech News, Spiegel

SIDELINES

Iran refuses to cooperate with atomic agency

The International Atomic Energy Agency (IAEA) last week completed a long-awaited report that was expected to wrap up its investigation of Iran's nuclear programme. But the report has failed to make progress on the two major sticking points.

According to sources close to the inquiry, the IAEA is keen to close the Iran file, but on two conditions. One is that Iran comes clean on any past weapons work. The other is that it agrees to the 'additional protocol' to the IAEA safeguards agreement, which gave extra powers to the IAEA in 1997, such as short-notice inspections of any site the agency wants to visit. This would give the IAEA greater confidence in being able to detect any clandestine facilities and operations.

Iran has not ratified the additional protocol, and although it voluntarily allowed broader inspection access from May 2004, it stopped doing so in January 2006. According to the report, released on 22 February, Iran has recently opened some sites to the IAEA, but the agency's director-general Mohamed ElBaradei says that this is "not, in my view, sufficient". He adds that the additional protocol is "key for us to start being able to build progress in providing assurance that Iran's past and current programmes are exclusively for peaceful purposes".

But Iran is playing hardball. It told the agency that it would comply with the additional protocol only "if the nuclear file [on Iran's nuclear capabilities] is returned from the security council to the IAEA". Iran has also refused to comply with repeated calls by the United Nations Security Council — backed up with economic and political sanctions — to halt its uranium enrichment (see *Nature* **451**, 750–751; 2008).

"Iran is playing hardball."

On the question of past suspect activities, the IAEA report says that it considers several to be "no longer outstanding". These include work on polonium-210 and the Gchine uranium mine, which the military was suspected of being involved in running. The report adds, however, that for each issue cleared, it was still seeking "corroboration of its findings and to verify this issue as part of its verification of the completeness of Iran's declarations".

But on the major item of allegations of direct nuclear weapons work, the report says that the IAEA "still awaits" adequate responses from Iran. These include details about the 'Green Salt' project, named after the common name of uranium tetrafluoride (UF_4), a key intermediate in the production of uranium hexafluoride (UF_6) for enrichment. It was part of an illicit project that the US Central Intelligence Agency says was described in a laptop computer it obtained in Iran, and that also described a possible clandestine processing plant and military connections, including tests related to nuclear weapons and missiles.

In a meeting with Iran from 3 to 5 February, the IAEA confronted it with new intelligence information relating to high-voltage detonators and an "explosive testing arrangement that involved the use of a 400-metre shaft and a firing capability remote from the shaft by a distance of 10 kilometres". The report says that the IAEA believed both "would be relevant to nuclear weapon R&D". Iran says the intelligence documents are fabricated. ■

Declan Butler

First chapter of book of life goes live

The ambitious Encyclopedia of Life project published its first web pages on Earth's biological diversity on 26 February — one species per page.

Born of a 2003 essay by biologist Edward O. Wilson and formally announced in May 2007, the website (http://eol.org) aims to create an extensive, expert-created page for each of Earth's 1.8 million named species (see *Nature* 449, 23; 2007). Many of the world's foremost natural-history institutions are participating.

Most of the 1 million pages set up so far are placeholders with minimal information. Around 30,000 of them are fuller, thanks to pre-existing online databases that have agreed to share their data, including the Solanaceae Source website, FishBase and AmphibiaWeb. And 24 'exemplar pages', which are rich in information and multimedia content, show how the pages will eventually look.

The project has no new funding beyond that announced last year: US$2.5 million from the Alfred P. Sloan Foundation in New York and $50 million from the John D. and Catherine T. MacArthur Foundation in Chicago, Illinois. More will be needed if the project is to meet its goal of a full page for every species by 2017.

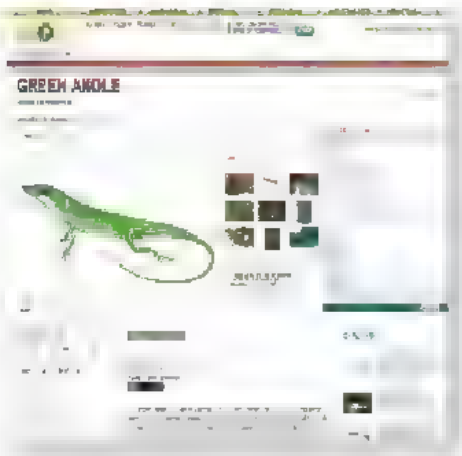

A sample page from the Encyclopedia of Life.

Executive director James Edwards says the project's biggest challenge is "providing incentives for the scientific community to participate". He is working on ways to make the pages similar to conventional publications so that academics will be credited for their input. Each page will have its own digital object identifier, and publications that cite the pages will be able to be tracked. Citations of the pages will contribute to the author's publication record.

Edwards admits that money could be problematic. "Another challenge further down the road will be to implement a financial model that will assure long-term sustainability," he says.

In the past, critics have noted that because the costs of maintaining and updating vast online databases never end, the projects tend to peter out when the funders lose interest. Sustaining their excitement about the encyclopedia for a full decade will be difficult.

The first batch of pages was officially launched this week at the TED (Technology, Entertainment, Design) conference in Monterey, California. ■

Emma Marris

A. GAROFALO/REUTERS

Seeking succulence: the goal of maximizing the taste of beef is furthered by a hand-held device.

Meat meter measures marbled muscles

Japanese researchers have developed a device to objectively assess the deliciousness of meat — an important concern for a nation that is especially demanding about the quality of its beef.

Japan's Wagyu beef is prized for its marbled fat, which gives the meat its particular flavour, succulence and tenderness. But marbling is not the whole story, says Masakazu Irie, an expert in animal husbandry at the University of Miyazaki. Meat doesn't necessarily get tastier as marbling increases. "If the fat is hard, with a high melting point, it can be like eating a candle," he says. But not all soft fat is good either — fat high in linoleic acid is soft and still unpleasant, Irie notes.

> "If the fat is hard, with a high melting point, it can be like eating a candle."

Irie and his colleagues have come up with a hand held, portable device that measures the concentration of oleic acid in the meat. This monounsaturated fat, they say, is a reliable indicator of tastiness. A fibre-optic probe directs near-infrared light into the meat, and the light bounces off the fat with a signature dependent on the type of fat and its concentration. The result can be read within seconds and doesn't damage the meat.

But Carol Christensen, a former taste researcher at the Monell Chemical Senses Center in Philadelphia, Pennsylvania, says that Irie's device is unlikely to be able to replace the tongue. "Food manufacturers want to replace human sensory panels with metrics, but I think it is just a pipedream," she says. "There's a lot going on in your mouth."

Irie plans to use the device in another project led by Tadashi Kawamura at the National Livestock Breeding Center in Fukushima. Kawamura is trying to establish a system for rating beef based on its chemical properties. He has a panel of more than 10 trained beef tasters who are judging sensory characteristics, such as how tender, fatty and juicy the meat is. These data will then be matched with chemical data on the concentration of some 20 components in beef, including oleic acid and inosinic acid, which enhances umami, the taste associated with monosodium glutamate.

Kawamura hopes that supermarkets and restaurants might some day offer steaks with a standardized ranking, perhaps on a scale of 1–5, for qualities such as juiciness and fattiness. ■

David Cyranoski

English grants under review

Proposals to radically alter the way English universities are funded could mean that young researchers lose out, academic groups warned last week.

In 2009, a system of 'metrics' will be rolled out to replace the Research Assessment Exercise (RAE) peer-review system in England — the first country to apply metrics to funding on this scale. The new Research Excellence Framework will allocate its £1 billion (US$2 billion) a year funding to departments mainly on the basis of citations, rather than RAE grade. It is an attempt by the Higher Education Funding Council for England (HEFCE) to make the process fairer and the applications process easier.

But academic groups are worried that the new system might discriminate against researchers who have not yet had time to build up many citations. "Obviously you don't want a system that penalizes people at the start of their careers or people who take career breaks," says Steve Smith, chair of the 1994 Group, an advocacy group that represents a number of high-profile UK universities. "It does worry me."

A consultation on the new metrics, which closed this month, reveals that academic groups are not entirely against it, but they do have some concerns. Policy experts are uneasy about a wholesale move away from peer review and concerned that the metrics system will not correctly assess the merits of some disciplines, be very costly for institutions initially and may discourage interdisciplinary research. Last year, the HEFCE was warned by its own audit committee that "a number of technical areas require further work if the new system is to have credibility".

"The RAE undoubtedly had flaws, and it was revised continually to address them," says Bahram Bekhradnia, director of the UK Higher Education Policy Institute. "But it was probably better than anything that is likely to appear."

However the HEFCE, which is now analysing the responses to the consultation, defends the new system and thinks that the university sector is now broadly behind the proposals. ■

Daniel Cressey

Strict ordering slashes tarmac time

A physicist says he has solved a problem that costs airlines millions every year: what is the quickest way to get passengers aboard an aircraft? Boarding is a serious issue for airlines, particularly those operating short flights that run several times a day, yet boarding times have steadily increased for decades.

No wonder. Jason Steffen of the Fermilab in Batavia, Illinois, who has come up with the ideal boarding sequence, says the method used by many airlines is almost the worst.

Steffen shifted his attention from the search for exotic new particles after becoming frustrated with the long waiting lines at departure gates. He used a computational technique called the Monte Carlo algorithm — which is widely used to investigate how atoms and molecules arrange themselves — to simulate how passengers move around a gridded space on an aircraft.

In its simplest form, the algorithm searches the arrangements generated by random shuffling of the components for the lowest-energy equilibrium states. A molecule, for example, is moved at random and the system's total energy is recalculated. If the new energy is lower, the probability that the change is accepted depends on the amount of improvement.

The method was applied to aircraft boarding by admitting passengers on board at random, each with a specified seat number, and looking for the sequences that filled the plane quickest. He assumed that the biggest cause of delay is aisle-blocking by people stowing their luggage before sitting down, and that each passenger takes a random amount of time to do this (J. H. Steffen preprint at http://arxiv.org/abs/0802.0733; 2008).

Steffen characterized each sequence in terms of the difference in seat number for successively boarding passengers. He assumed that each passenger needed at least one free space either in front of or behind them to stow their luggage. The best distributions turned out to be those in which the highest fraction of passengers had an empty row separating them from those admitted before and after them, ensuring that there was enough stowing room between successive individuals. In other words, what matters is not the absolute seat positions in the sequence, but where those seats are relative to each other.

The sequence of boarding from back to the front of the aircraft, used widely by airlines, turns out to be very inefficient — little better, in fact, than the worst case, boarding from front to back.

The optimal boarding sequence requires that each passenger be given a specific queueing position. A compromise would be to board in several groups with all members of each group having seats in widely separated rows. Another efficient option is to board window seats first.

These block strategies can more than halve the boarding time compared with the worst-case patterns. But Steffen says that the strictly ordered optimal sequence does so much better — reducing boarding time by a factor of 7 for a 240-seat, 40 row aircraft, relative to conventional back-to-front loading — that it is likely to remain the best even if several passengers board out of order, whether because they are in a family group, or simply defiant or confused.

Computer simulations and mathematical models have often been used before to try to optimize aircraft boarding schemes. But Steffen says that his strategy outperforms all those currently in use. ■

Philip Ball

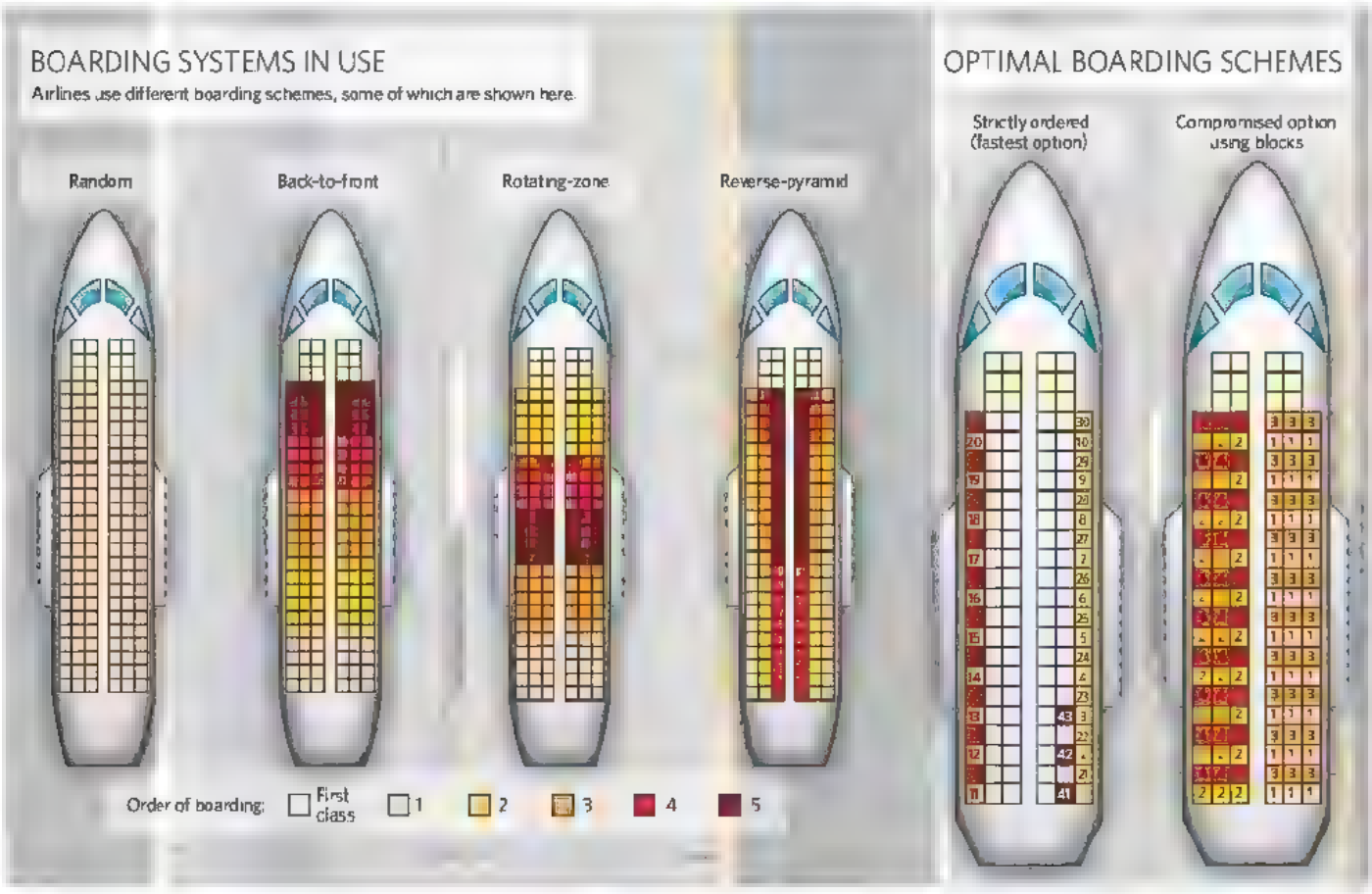

UCLA wins restraining order against activists

The University of California, Los Angeles, (UCLA) succeeded last week in getting a temporary restraining order against five vociferous animal-rights activists, as well as organizations such as the Animal Liberation Front, who have claimed responsibility for various property crimes and threats against researchers.

The ruling stipulates that the activists must stay farther than 15 metres from researchers and remove the scientists' addresses from their websites. UCLA spokesman Phil Hampton called the ruling "a clear victory in the continuing process of UCLA protecting its researchers". The university will seek permanent restraining orders in a hearing on 12 March.

"They are trying to mix above-ground protestors that never do anything illegal in with the Anima. Liberation Front and the underground organizations that have flooded homes and broken windows," says Jerry Vlasak, press officer for the North American Animal Liberation Press Office. "The two groups are completely separate; they don't know who each other are."

Indonesia relents over bird-flu sample release

Indonesia has resumed sending samples of the H5N1 bird-flu virus to the World Health Organization (WHO) after refusing to share samples for more than a year (see *Nature* 450, 1137; 2007). The US Centers for Disease Control and Prevention in Atlanta, Georgia, a WHO flu collaborating centre, has received a batch of samples from two patients — a woman who died earlier this month, and a girl hospitalized after her mother died of the disease.

The move is seen as an encouraging step towards ending a dispute in which Indonesia has argued that it is unfair that it should share samples without having access to affordable vaccines developed by countries using its samples. It wants a material transfer agreement to protect its rights over the samples.

The latest samples were sent under a draft agreement that allows the WHO to use them for research, but bans their commercial use without Indonesia's consent, says one source close to the negotiation.

F. LIS NAWATI/AP

Health officials test birds at an Indonesian market.

Grey wolf no longer in danger, says US government

Calling its wolf programme a "remarkable conservation success story", the US Fish and Wildlife Service last week announced plans to remove grey wolves (*Canis lupus*) in the northern Rocky Mountains from the federal list of endangered species.

The decision comes 13 years after the first of 66 Canadian wolves were released in Yellowstone National Park and central Idaho. Some 1,500 wolves, with at least 100 breeding pairs, now live in Wyoming, Montana and Idaho.

These states will use hunting to manage the wolf population, which could set up a prolonged battle between the ranchers and hunters who support the plan, and environmentalists who fear that wolf hunts could once again reduce the population to perilous levels.

All three states have pledged to maintain at least 150 wolves and 15 breeding pairs, although preliminary population targets are between 900 and 1,250 wolves, according to the agency. Environmental groups plan to challenge the decision in court.

MIKE LANE/FLPA

Biosafety lapses cost Texas A&M $1 million

Texas A&M University in College Station has agreed to pay a $1-million fine for lapses in biosafety procedures. The failures resulted in lab workers becoming exposed to several deadly pathogens, including the organisms that cause brucellosis and Q fever.

The US Centers for Disease Control and Prevention (CDC) in Atlanta, Georgia, shut down all biodefence-related research at the university last June, after the violations came to light. A&M officials say they have since stepped up safety procedures and training for lab workers. The university had suggested it deserved a $10,000 fine.

CDC officials will visit the university in March, and if the labs pass the inspection, biodefence research could resume shortly afterwards.

US missile destroys toxic tank on spy satellite

The United States has successfully destroyed an errant spy satellite, the Pentagon says.

The US National Reconnaissance Office lost contact with the satellite shortly after its launch in December 2006. The satellite contained 450 kilograms of toxic hydrazine propellant. "There was a reasonable chance that this hydrazine, if it fell in a populated area, would affect people," General James Cartwright, head of US Strategic Command, told reporters.

On 21 February, the USS *Lake Erie* fired a modified Standard Missile 3 — normally used as part of the US missile-defence system — to strike the satellite as it passed 247 kilometres over the Pacific Ocean. Four days later, Pentagon officials confirmed that the missile had successfully destroyed the fuel tank.

Critics say that the shot was meant to demonstrate US anti-satellite capabilities to China, which conducted its own test in 2007. Cartwright denies that charge.

Florida adopts teaching of evolution in its schools

The state of Florida can now officially teach evolution in its schools, following a 19 February vote.

The state's board of education voted 4–3 to include "the scientific theory of evolution" in its teaching standards. Evolution had not previously been mentioned by name in the biology-curriculum standards.

But the phrase "the scientific theory of" was added at the last minute, in order to garner enough votes to pass. One board member had proposed adding an amendment that would allow teachers to opt for exploring criticisms of evolution, but the amendment failed to go anywhere.

Still, science-education experts praised the standards change as a major step forward.

THE END OF THE BEGINNING

After decades of work, a pioneering malaria vaccine may soon reach the final phase of clinical trials. In the first of two features on efforts against malaria, **Brendan Maher** reports on a vaccine that is far from perfect — but which may provide new direction and save thousands of lives.

In 1987 Rip Ballou taped an ice-cream carton to his arm. The young US Army doctor was doing his bit for science; inside the carton five hungry mosquitoes set about doing theirs. It's an uncomfortable situation, Ballou remembers with a grimace, to have a bunch of the insects "just whaling away on your arm", all the more so when you know that they have been carefully infected with malaria parasites, and soon you will be too.

Ballou and five colleagues at Walter Reed Army Institute of Research (WRAIR) in Silver Spring Maryland were testing a vaccine candidate, FSV-1. They'd first been injected with it a year earlier; now it was time for any immunity they might have developed as a result to be 'challenged'. Nine days after the mosquitoes had their meals, the first unvaccinated control tested positive for parasites and was given drugs to clear his system. The second control and three vaccinated volunteers followed suit in short order, apparently no more resistant.

On the eleventh day another of the six volunteers fell ill — the tremors struck Stephen Hoffman, a WRAIR colleague in the Navy as he was giving a lecture in San Diego. On the twelfth day, while at a party, Ballou started to feel out of sorts. Not sure if it was the home-brewed beer he'd been drinking or parasites ravaging his red blood cells, he had his wife drive home. Soon he was cycling between chills and fevers and experiencing headaches of unprecedented intensity. "I have never been so sick in my life," he says. "It gave me an extremely healthy respect for this disease." Five of them had succumbed.

But the sixth vaccinee, Daniel Gordon, was still healthy more than four weeks later. For the first time a simple vaccine had protected someone from malaria*.

That first glimmer of hope grew into an extensive collaboration between WRAIR and the drug company GlaxoSmithKline (GSK) that has turned a descendant of the FSV-1 vaccine, the oddly named RTS,S, into the world's 'most advanced' malaria vaccine. Most advanced means that phase III clinical trials, the final step before licensing the drug, could start by this September. If they go well the vaccine could be licensed and in use by 2011.

To get this far speaks of determination, imagination and perseverance — qualities Ballou and his colleagues, like so many researchers into tropical medicine, show in abundance. It also speaks of something rarer in the field: a lot of money. All told, GSK and partners will have spent upwards of US$500 million by the end of the next set of trials. "We were convinced that if we develop the malaria vaccine it will be hard for society to refuse to pay for it," explains Jean Stéphenne, president and general manager of GSK Biologicals, the unit that works on the vaccine at its facility in Rixensart, Belgium.

And in recent years this conviction has begun to look warranted. Private donors and governments are funnelling hundreds of millions of dollars into projects such as the GAVI Alliance, which provides access to immunizations in the developing world; there is increasing pressure for countries to promise 'advanced market commitment', the setting aside of funds today to buy vaccines when they become available tomorrow.

"I have never been so sick in my life. It gave me an extremely healthy respect for this disease."
— Rip Ballou

But if RTS,S is the first vaccine to be so bought, it will still fall short of the traditional goals for vaccines. It has improved since its meagre one-in-six showing in that first 1987 challenge, but not that much. RTS,S will offer at best partial protection, maybe 30%, against infection; some indicators predict it might diminish levels of severe malaria by as much as 50%. That may be enough to give infants and small children a better chance of surviving the scourge while they're most vulnerable. But it is a long way from the last word.

Military origins

Malaria research has long been of interest to armies and navies fighting wars in hot wet climes. It was while embroiled in Vietnam that the US military began funding work at New York University on irradiated parasites, which turned out both to be non infectious and to provide immunity in lab animals. The work culminated in a landmark 1973 paper describing long-lasting protective immunity in humans inoculated with irradiated sporozoites[2] — the form of the parasite that travels from the insects' salivary gland to the victim's liver.

Irradiated sporozoites were not, however, seen as a practical way forward, because their production required live mosquitoes and the use of human blood (Hoffman is now revisiting that conclusion at Sanaria, a company that he has founded in Rockville, Maryland). Instead, researchers looked for what it was about the sporozoites that gave protection, and how the new technologies of genetic engineering might mass produce it.

In the early 1980s antibodies against the sporozoites were used by researchers at the National Institutes of Health and WRAIR to identify the 'circumsporozoite' protein (CSP) and clone the relevant gene[3]. Working with WRAIR, the labs of what was then SmithKline Beckman in Philadelphia, Pennsylvania, zeroed in on a repeating pattern in the protein that seemed to be a major target of antibodies. This fragment, grown from genes cloned into bacteria, went on to become the main ingredient in FSV-1.

In the coming years, Ballou and the SmithKline researchers in Philadelphia tested several variations on the theme. But SmithKline had been moving most of its vaccine development efforts to Rixensart, where they had recently acquired a small but dynamic laboratory, Recherche et Industrie Thérapeutiques. Joe Cohen, who took over the project in Rixensart at the same time as Ballou and his colleagues were infecting themselves, had new plans for the CSP.

Faced with turning the repeating fragment from the protein into a real vaccine, Cohen decided to use lessons that the company had learned from its successful development of a recombinant hepatitis B vaccine, Engerix-B. That vaccine consisted of a surface antigen protein from hepatitis grown in yeast; at high enough concentrations that protein spontaneously forms virus-like particles that have a greater effect on the antibody making parts of the immune system than loose proteins could. Fusing the repeat region from the CSP to the hepatitis surface antigen protein, Cohen hoped, would make similar particles festooned with the CSP fragments and thus able to provoke the production of antibodies targeted at the sporozoites.

Given a widespread suspicion that antibodies wouldn't be enough to elicit immunity, Cohen

P. COLL. NS/WRAIR

went on to add a fragment from the tail end of the CSP that was thought likely to interest the other arm of the immune system — the arm that prompts T cells to attack infected cells. The resultant "double whammy", as Cohen calls it, was a gene for a protein containing the antibody-inducing repeat (R), the portion recognized by T cell white blood cells (T) and the hepatitis B surface antigen (S).

With all these additions, though, the surface antigen protein lost its knack for self assembly. Through a lot of fine tuning, Cohen finally hit on a way to regain it: one part RTS to four parts plain old S. RTS,S was born.

The vaccine factory

Cohen has shaggy grey hair and an endearing politeness. When showing visitors around the Rixensart facilities where RTS,S was developed, he holds the door for all those he has in tow, necessitating an awkward dance as he takes up the lead again.

Although Ballou and others wax eloquent about the part he played in inventing RTS,S (the patent is in his name), Cohen shrugs the praise off, insisting it was a team effort. But the pride with which he opens a nondescript door in a nondescript building on GSK's Rixensart campus and ushers visitors into the production facilities is unmistakeable. Knee-high windows along one side of a long hallway look out over a fermentation room where yeast colonies from Petri dishes are scaled up to fill 1,600-litre vats, tended by technicians clad in clean-room paper suits. Through a second set of windows opposite, more technicians tend the bank of computers that monitor fermentation. They're in testing now, but Cohen says that once running at regular capacity, this facility could produce tens of millions of RTS,S doses per year. Already, there is more than enough capacity to provide the doses needed for the 16,000 infants he and his colleagues want to recruit into the imminent phase III trials, which will take place across 10 research sites in 7 African countries.

It's just one indication of how quickly the project is moving. Twenty kilometres away, in Brussels, investigators from all over Africa are arriving at a moderately swanky Sheraton right near the Grand Place — people such as Salim Abdulla of Tanzania, who oversees the Ifakara Health Research and Development Centre, a research study site in Bagamoyo, and currently chairs the Clinical Trials Partnership Committee, the formal group of study-site leaders that meets once a year. His cackling laugh rings out repeatedly despite the 30 hours he spent travelling here and the knowledge that the next two days will be intense. High on the agenda is how the different study sites that might take part in phase III trials define severe malaria, a measure

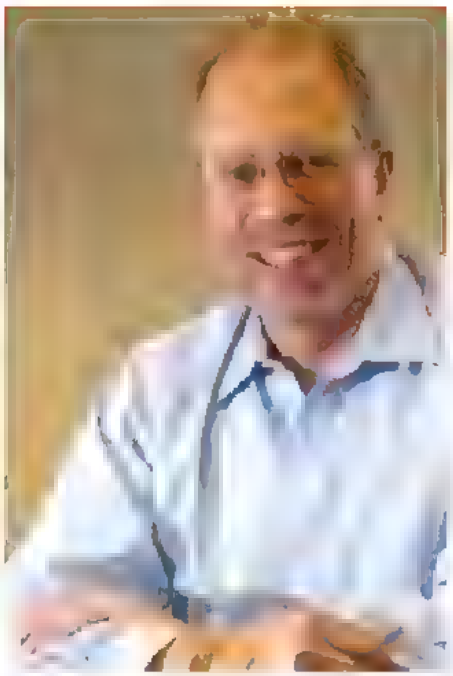

Rip Ballou giving himself malaria in 1987 (above), and today (right), with the vaccine that failed to protect him in a lucite block on his desk.

that has been difficult to standardize. "They go to the same school but they don't agree," Abdulla says. In the lobby, talk centres on the state of affairs at the two sites in Kenya, where violence has been spreading after a disputed election.

Getting from a well designed virus-like particle to international politics and hundred million-dollar trials was a demanding business. The first requirement was to find a way to get the biggest immunological bang possible for the RTS,S buck — which is to say choosing the right adjuvants. Adjuvants are, in the oft-quoted words of Yale immunologist Charles Janeway, the vaccine makers' "dirty little secret". Ranging from inorganic chemicals such as aluminium hydroxide to fragments of bacterial cell wall, adjuvants boost the immune system's response to the vaccine they accompany, although only recently have researchers begun to understand why. In the 1980s one of the arguments that Stéphenne used to convince SmithKline to invest heavily in Rixensart was that more sophisticated adjuvant formulations would lift hard-to-develop vaccines to the next level of efficacy. The malaria effort, aiming at something no other vaccine had ever achieved — immunity against a complex parasite — was in part an adjuvant stalking horse.

In 1990 the first human challenge trials of RTS,S showed that adjuvants were crucial; with one adjuvant preparation the vaccine was worthless, but with another it protected two out of eight subjects — with a hint of the sought-after T-cell response. "People were excited," says Gray Heppner, a major in Ballou's department at the time. Heppner, now a colonel at WRAIR, has an encyclopaedic knowledge of the army's malaria programmes and an enthusiasm for sharing that knowledge.

Heppner cooked up a protocol to look for responses in Rhesus macaques, and once the difficulties of assessing the monkeys' responses to skin tests in a dimly lit monkey house were sorted out, he had a winner — an oil in-water emulsion with monophosphoryl lipid A (MPL) and QS21, an extract from the Chilean soapbark tree *Quillaja saponaria*. In 1996 the first human trial with this 'AS02' adjuvant provided protection for an impressive six-out-of-seven individuals[4]. "That was a huge a-ha moment for us," says Ballou.

As with much of the celebration around RTS,S, though, there was sombre dénouement. Six months after the first challenge, five volunteers who had been protected by RTS,S/AS02 took up their ice-cream containers again. This time all but one fell ill[5]. This pattern has, in general, held ever since; the vaccine's protection falls off quite steeply with time.

> "I knew there and then that this was going to be a vaccine against malaria."
> — Joe Cohen

Nevertheless, the results were deemed good enough to take into the field. In the summer of 1998, 250 men in the Gambia received three doses of either RTS,S/AS02 or a rabies vaccine and were followed up for 15 weeks. The unblinding, in which the differences — if any — between control and test group are revealed, took place the next year in Rixensart. These unblindings are long-drawn-out processes. Statisticians who know what the data show describe every aspect of the study — compliance rates, randomization, adverse events, immunogenicity and more — to the researchers who actually carried out the work but, because of the blinded structure of the study, didn't know what was going on. Sitting in the audience, Ballou was anxious.

The results were difficult to interpret. During the surveillance period 81 of 131 men who had been given the RTS,S/AS02 vaccine exhibited measurable levels of parasite in their blood. In the control group 80 out of 119 tested positive[6]. That's 62% against 67%, which is not much of a margin. "People really felt that this was way too low to be important," says Heppner. "But Dr Ballou said 'Wait a minute. Look, it works well for the first portion of the trial'" Indeed, during the first nine weeks of surveillance, the vaccine posted an impressive 70% efficacy, but that had tailed off to zero in the remaining six weeks. "It took some additional investigation and analysis by the statistician there to put that into context of what was happening," says Ballou. They were dealing with adults of different ages, many of whom had had malaria many times over and had a certain level of natural immunity to the disease. Further confounding things was that as individuals became infected, the pool of people from whom cases could be measured was shrinking.

Booster benefit

SmithKline, WRAIR and their collaborators in the Gambia quickly made a decision to follow up with a booster dose for a portion of the men the next summer. That follow-up provided strong signals that the vaccine was acting in two ways; it was protecting against infection, and it was also weakening the symptoms in cases where the infection nevertheless took hold. SmithKline decided that a vaccine that could protect people in these ways when they were most vulnerable could save lives. And the most vulnerable are the young: children under five are thought to account for 75% of malaria mortality in Africa.

So SmithKline decided to step down the age of the next trial participants to infancy; if it hadn't, Ballou says, the project would have died. But the company felt that at this stage, it needed help: Ballou remembers Stéphenne telling him and Cohen that to move forward they would need a partner with more money. Ballou wrote a proposal to the William H. Gates Foundation asking for $25 million to help assume some of the risk that SmithKline was taking. In the end the Gates foundation gave $50 million to establish the Malaria Vaccination Initiative (MVI) through PATH, a non-profit organization based in Seattle, Washington. Ballou was asked to lead it, but instead took a job with Washington DC biotechnology

firm MedImmune working on other vaccines, and Regina Rabinovitch, who had managed a network of vaccine initiatives at the National Institutes of Health, became the leader

With MVI on board, what was by now GSK began to collaborate with Pedro Alonso, a researcher at Barcelona Centre for International Health Research in Spain, who had developed a field research site in Sau de de Manhiça, Mozambique, in 1996. In addition to building health and research facilities, making such a site ready requires outreach to thousands of people in surrounding communities, training staff and developing reliable logistics, such as the 'cold chains' required to keep vaccines viable on their way to recipients. Alonsos site would be the setting for the biggest RTS,S trial so far, a study called Malaria 026 that eventually enrolled an unprecedented 2,022 children between the ages of 1 and 5 to test RTS,S/AS02. Melinda Moree, who succeeded Rabinovitch at the head of MVI, says that the study's tremendous scale was undertaken to make it definitive It would make or break RTS,S.

When Ballou rejoined the effort in 2003, having left MedImmune to join the GSK team in Rixensart, Malaria 026 was just ramping up and the mood, he says, was very positive. The unblinding was held in Maputo, the capital of Mozambique, on 9 August. For Ballou, Cohen and other veterans, the lengthy ritual was a gratifying one. In one cohort of 1,600 children, infection in the vaccine group was 37% lower. What's more, the vaccine seemed to reduce severe malaria infections by 65% (although that number would come down with further follow-up data)[7]. Cohen says that the news left "A moment of silence that is very difficult to describe ... I knew there and then that this was going to be a vaccine against malaria."

If the investigators were elated, MVI policy-makers were a little less so. "We had sort of our go criteria and our no-go criteria. Then there was this whole area called the grey zone. We were hoping the results wouldn't be in the grey zone," says Moree. But they were. "So there was some amount of disappointment." Even so, Moree put more Gates Foundation money into the MVI project for further trials. "I'd make that call again without hesitation," she says.

Several smaller phase II studies ensued, including Malaria 038, a Manhiça trial looking at safety and efficacy in infants vaccinated at 10 weeks, 14 weeks, and 18 weeks of age. Its results were published in October 2007. The vaccine was safe and seemed again to have effi cacy on the order of 65% in the first 3 months and 35% in the first 6 (ref. 8). Across the continent, operations have expanded to encompass several more research sites, all in preparation for the big show, a clinical phase III trial enrolling 16,000 children. MVI has $107 million earmarked for the phase III trials, says Barbara Savarese, a senior programme director there, and intends "to spend every dime of it". The investment is on a par with practically any modern vaccine initiative, says Ballou (who is in the process of moving again, this time to the Gates Foundation).

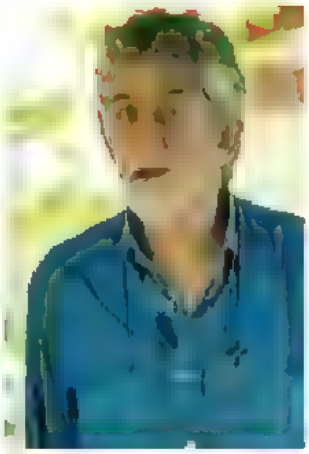

Joe Cohen tailored the genes necessary for the RTS,S vaccine.

© CAH ... /GLAXOSMITHK... NE BIO...OGICA...S

But doubts persist. In a commentary that accompanied Malaria 038's results in *The Lancet*, Judith Epstein of the US Military Malaria Vaccine Program took issue with the degree to which the RTS,S trials rely on what is known as time-to-event analysis rather than the overall number of cases in the two groups[9]. Although such analysis is appropriate, she says, on its own it may not communicate the whole picture to the people who would ultimately use the vaccine. Hoffman is more critical. "It's not as if it's inappropriate to evaluate a vaccine based on this time-to-event analysis. But the point is, what's the biological meaning of that type of an analysis, and the answer is, we don t know." Without knowing what exactly is going on, how can researchers explain to potential vaccinees what they should expect?

> "A vaccine with 50% efficacy against severe malaria gives us a chance to save 1,000 to 1,500 lives daily."
> — Christian Loucq

Better than nothing

Dyann Wirth of the Harvard School of Public Health, who is considering a collaboration with RTS,S trial investigators, offers an explanation of what might be going on that draws on analogy to a previous intervention. "The sporozoite vaccine is like the effect of the bed net. It doesn't completely eliminate infection but it does reduce the onset of disease. And the interpretation of that could be that fewer sporozoites get through and establish infection." It is possible that these infecting sporozoites are, in a way, extending the work of the

SOME MALARIA VACCINES IN RECENT OR CURRENT DEVELOPMENT

Stage of infection targeted	Vaccine	Antigen	Phase	Location	Developer
Pre-erythrocytic (targets sporozoite cells, or the liver cells they infect)	RTS,S with AS01/AS02	Circumsporozoite protein (CSP)	Ib/IIb	Multiple African sites	GlaxoSmithKline
	Fowlpox (FP) 9/modified vaccina virus Ankara (MVA), ME-TRAP	Multi-epitope thrombospondin-related adhesive protein (ME-TRAP)	IIb	Kenya	University of Oxford
	Simian adenovirus/MVA	ME TRAP	Ia/Ib	United Kingdom	University of Oxford
	Liver-stage antigen (LSA) 1/AS02	LSA-1	Ia/IIa	United States	Walter Reed Army Institute of Research (WRAIR)
	Human adenovirus serotype 35 (AdHu35)	CSP	Ia	United States	Crucell
Blood stage (targets merozoite cells that infect human erythrocytes)	Falciparum malaria protein (FMP) 1/AS02	$MSP1_{42}$	Ib/IIb	Kenya/Mali	WRAIR
	Apical membrane antigen (AMA) 1/AS02	AMA1	Ia/IIa	United States	WRAIR
	Merozoite surface protein (MSP) 1_{42}/Alum bi-allelic	MSP1	Ia	United States	National Institutes of Health (NIH)
	AMA1 C1/Alum + CpG	AMA	Ia/Ib	United States/Mali	NIH
	$pfAMA1\text{-}FVO_{[25\text{-}545]}$	AMA1	Ia/Ib	Netherlands/Mali	Biomedical Primate Research Centre
	GMZ2	Glutamate-rich protein/MSP3	Ia	Germany	Statens Serum Institute
	PfCP2.9	$AMA1/MSP1_{19}$	Ia	China	Shanghai Wanxing
	MSP3-Long synthetic peptide	MSP3	Ib	Tanzania	Pasteur Institute
Multi-stage (targets multiple stages of the parasite)	FP9/MVA polyprotein	Six antigens	IIa	United Kingdom	University of Oxford
	PEV3a	AMA1/CSP	IIa	United Kingdom	Pevion
	Adenovirus 5	AMA1/CSP	I/IIa	United States	US Navy

A...V S H...

vaccine. A child may be inoculated with sporozoites by hungry mosquitoes dozens of times. If the vaccine means fewer of those inoculations lead to disease, even for a little while, the children may be able to build more of their own natural immunity before the vaccine's effects dissipate. They'll still get malaria — but not as debilitatingly

This line of argument offers some grounds for optimism. Clinical trials of insecticide-treated sleeping nets in the 1980s and 1990s posted modest, sometimes conflicting reductions in clinical malaria. But some areas with expanded programmes have now reported 50% or better reductions in child mortality (see page 1047). Malaria control is already a multi-factorial undertaking, with spraying, drugs and bed nets playing what seem often to be reinforcing roles. Even a partially effective vaccine could be another useful component to the strategy. It could even, conceivably, be the one that tips it over onto a trajectory leading to the eradication of the disease — the Gates Foundation's long-term goal.

The Malaria Vaccine Technology Roadmap put together in 2006 by a group from the malaria-vaccine community shows how partially effective vaccines are now playing a part in thinking on the disease. The group's goal for 2025 was a vaccine that provided four years of protection from clinical disease to 80% of users — the sort of target that traditional vaccines aim for, although not a very stringent one. But as a nearer-term goal it saw real advantages in a vaccine offering 50% protection from severe disease for a year. If indications of RTS,S's efficacy against severe malaria hold up, it might deliver that, which would be no small thing. "If tomorrow we can propose a vaccine in Africa that is going to have 50% efficacy against severe malaria," says Christian Loucq, the current director of the MVI, "we have a chance to save 1,000 to 1,500 lives daily."

Adrian Hill at the University of Oxford's Jenner Institute, UK, isn't impressed, though. He is concerned with the reporting from Alonso's group on a second cohort in the Malaria 026 trial. In a 400 subject cohort at a second site with much higher transmission rates, the proportion protected at the end of 6 months seems to be just 11%. Moreover, the data showed no difference in clinical malaria. The investigators on the study maintain that clinical malaria was not a primary endpoint for that part of the study, which was designed to measure the time to the first infection. But Hill still wonders how a phase III roll out will look: "Will it be like cohort 1 or cohort 2?"

Hill's doubts about the vaccine bolster a more general frustration with what he sees as GSK's go-it alone approach, "unconnected to the other 12 or 15 groups developing vaccines". (see table, page 1045) He and others want different vaccines to be combined with RTS,S in Phase II testing, suspecting efficacy might be greatly enhanced. Heppner, for example, says that results of studies he and his colleagues have carried out on macaques indicate that combining an adenovirus-based vaccine made by the Netherlands biotech company CruCell with RTS,S would offer much better effects[10]: "My hope is that a way can be found to evaluate this clinically just as we've done for earlier improvements of RTS,S." Ballou says that although progress in studying this combination has been stalled for "various business reasons", several collaborative efforts continue.

J.-M. MAAS/DARBY COMMUNICATIONS

Salim Abdulla wants new vaccines to be able to build on the advances of RTS,S.

Going it alone

Although mixed phase II trials are possible at some time, there's every likelihood that Phase IIIs of RTS,S on its own will go forward later this year. GSK is already looking beyond them to potential sales. It has made extensive inroads with government agencies and organizations that may purchase the vaccine for the developing world as those concerned attempt to assess the demand and the price per dose. (An interesting wrinkle here is that RTS,S, being very similar in molecular terms to the hepatitis B vaccine, provides immunity against that, too — a facet that some health officials say makes it more attractive.) GSK doesn't expect to turn huge profits. It can't. But getting a return on the investment will make it sustainable, potentially leading to better products. Bill Gates recently singled out the company's collaborative efforts as a model example of "creative capitalism"

Meanwhile, the partnership has been building infrastructure and good will in Africa. At the meeting of site investigators in Brussels, there was a buzz of excitement about the coming trials. Abdulla is one of the many African doctors who will be seeing the RTS,S project through to its completion, some 25 years after Ballou first had a carton of mosquitoes taped to his arm. Abdulla projects a chipper but world-weary wisdom. His laugh comes easily when describing the maddening attitudes of some local politicians or when he is asked how many times he has had malaria himself and realizes he doesn't know — in the dozens at least. He doesn't worry about the results of phase III. And he doesn't worry that mothers in Africa will feel a false sense of security about their vaccinated children, as Epstein's article suggested[9]. They're more savvy than that. They know that all the various approaches are only partially effective, and that progress means using the right combination.

With luck, Phase III trials will show that RTS,S might be part of that combination. What matters most to Abdulla, though, is that even if it isn't, the infrastructure for research is maintained, so that if after all its hard work GSK has to pull out, there is still a trials pipeline down which future candidates may flow. Whatever the phase IIIs of RTS,S show, there will be volunteers such as Ballou taping ice-cream cartons of mosquitoes to their arms for years to come in the expectation of a short, sharp introduction to one of the world's worst killers. And there will be researchers such as Abdulla, for whom repeated infection is a way of life, eager to take the fruits of those volunteers' labours. Creating a lasting link between them may offer as much lasting benefit as any single vaccine. ■

Brendan Maher is a features editor at *Nature*.

1. Ballou, W. R. *et al. Lancet* **8545**, 1277–1281 (1987)
2. Clyde, D. F., Most, H., McCarthy, V. C. & Vanderberg, J. P. *Am. J. Med. Sci.* **266**, 169–177 (1973)
3. Dame, J. B. *et al. Science* **225**, 593–599 (1984)
4. Stoute, J. A. *et al. N. Engl. J. Med.* **336**, 86–91 (1997)
5. Stoute, J. A. *et al. J. Infect. Dis.* **178**, 1139–1144 (1998)
6. Bojang, K. A. *et al. Lancet* **358**, 1927–1934 (2001)
7. Alonso, P. L. *et al. Lancet* **364**, 1411–1420 (2004)
8. Aponte, J. J. *et al. Lancet* **370**, 1543–1551 (2007)
9. Epstein, J. E. *Lancet* **370**, 1523–1524 (2007)
10. Stewart, V. A. *et al. Infect. Immun.* **75**, 2283–2290 (2007)

See Editorial, page 1030, and online at www.nature.com/news/specials/malaria/index.html.

You think Taq is hot? This is pure

Phire™

Phire™ Hot Start DNA Polymerase – speed and specificity for PCR

Finnzymes' novel PCR enzyme outperforms every *Taq*-based hot start polymerase on the market. Phire DNA Polymerase is an ideal solution for routine and high throughput PCR applications.

Short protocols: Amplify 3 times faster than with hot start *Taq*
Specific products. Unique hot start technology with zero-time reactivation
High yields: Efficient PCR results in more product

For more information visit **www.finnzymes.com**
To receive a sample please contact your local distributor

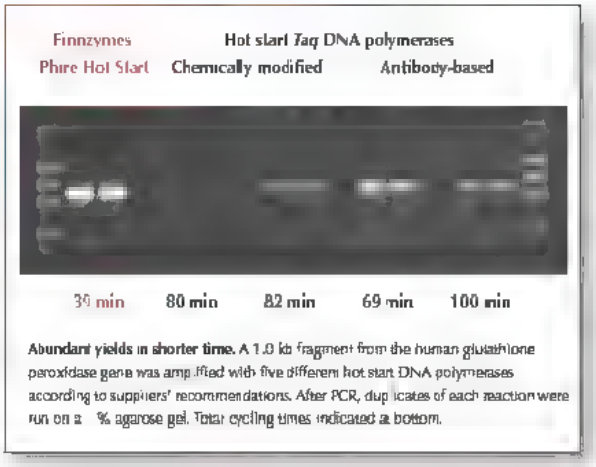

Abundant yields in shorter time. A 1.0 kb fragment from the human glutathione peroxidase gene was amplified with five different hot start DNA polymerases according to suppliers' recommendations. After PCR, duplicates of each reaction were run on a % agarose gel. Total cycling times indicated at bottom.

NEW ENGLAND BioLabs Inc.
the leader in enzyme technology

Distributed in the US and Canada by New England Biolabs.
Other countries visit www.finnzymes.com.

Phire is a trademark of Finnzymes Oy.

FINNZYMES
TOOLS FOR MOLECULAR BIOLOGY

Suck it and see: Zambian researchers capture the mosquitoes that prey on them.

THE BIG PUSH

Zambia, with help from partners around the world, is stepping up its battle against malaria. **Michael Hopkin** reports from the rural front line.

It's not long after dark on a starry night, and three SUVs are bumping along a dirt track in a remote corner of southern Zambia. Inside the vehicles is a troop of more than a dozen men, most dressed in green overalls that bear more than a passing resemblance to army fatigues. Their mission is mundane, even boring: they will spend the entire night sitting still — up to 12 straight hours punctuated only by the odd insect bite. They say that the boredom really begins to kick in at around 02:00.

But for all the tedium, the mosquito 'hunters' mission is vitally important. The insects they catch will provide information about exactly when and where people receive bites that transmit the malaria parasite and help researchers to compile a genetic catalogue of the local mosquito population. This is the front line of the battle with malaria.

Zambia sees nearly four million cases of malaria diagnosed each year, and some 50,000 deaths, mostly among children. Two years ago, its Ministry of Health embarked on an ambitious plan to cut the incidence of malaria by 75%. As a result, the country is now a destination for a significant fraction of the estimated US$3.6 billion pledged to fight malaria worldwide by a host of sources, including the World Bank, the Global Fund to Fight AIDS, Tuberculosis and Malaria and the Bill & Melinda Gates Foundation. Bill Gates has described the Zambian initiative as an "inspiring example of a nationally coordinated effort".

Last October, Gates and his wife called for the malaria parasite to be sent the same way as the smallpox virus, which remains the only pathogen that humans have ever successfully removed from the natural world. Few have dared to suggest that malaria, which still kills a million people every year, could be totally wiped out — most efforts focus on control rather than eradication. But although the Gates admit that the goal will take "multiple decades" to reach, they believe it can be done. And Zambia is seen by many as one of the places where the winning formula might be devised.

It is a long way from the world of megabucks philanthropy to the grassroots work that will make inroads against the disease (see page 1051). And people do not always agree on how best to fight the battle. Some researchers in Zambia share the Gates's absolutist attitude, others argue that it needs to be tempered with a little more pragmatism and a lot more data.

As the mosquito-catchers at their nightly vigil will testify, collecting malaria data is tedious work. The researchers, from the Malaria Institute at Macha (MIAM), some four hours' drive from the Zambian capital Lusaka, spend hours catching mosquitoes because it's the best way to learn about how malaria spreads.

M. HOPKIN

Captive audience

The technique is called 'human landing capture', and involves sitting with sleeves and trouser-legs rolled up, waiting for a mosquito to bite. The researchers work in pairs — as one is bitten, his partner uses a plastic tube to suck up the mosquito and collect it for study. They do their fieldwork in real dwellings, one pair sitting inside and another outside, to sample both indoor and outdoor biters. The team is currently calibrating a set of mosquito-attracting light traps that will eventually do the same job with less manpower.

Researchers at MIAM are also preparing a bid to wipe out malaria from a 1,000-square-kilometre swath of countryside around Macha, as

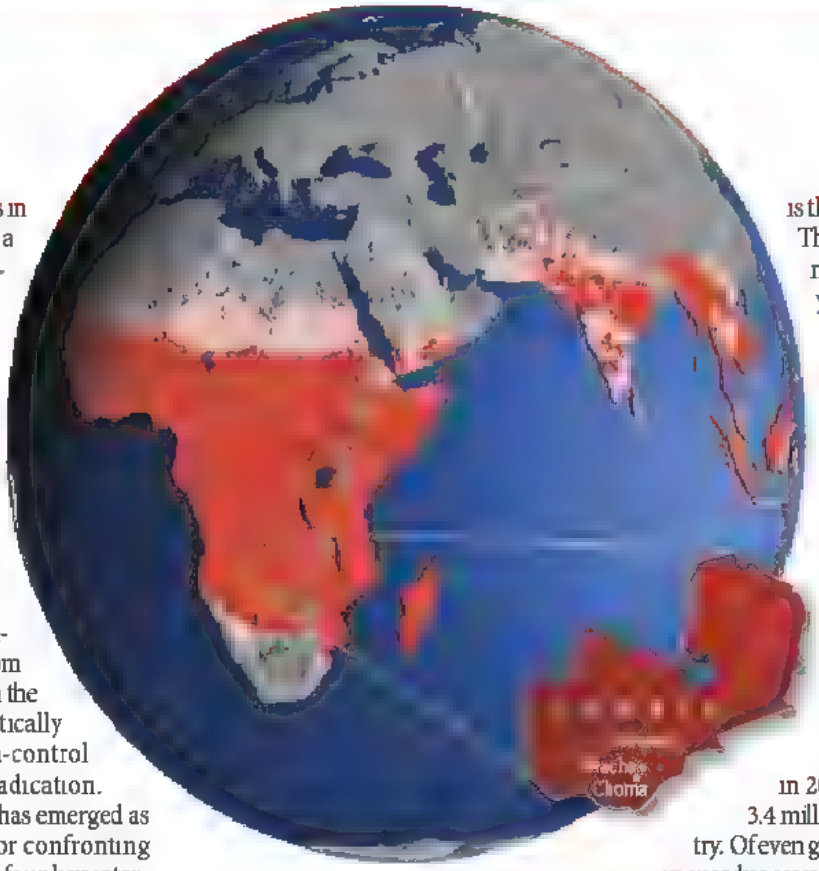

In areas where malaria affects fewer than 1 person per 10,000 per year (pink, population 1 billion), the disease is more amenable to control than in areas where transmission rates are higher (red, population 1.4 billion), such as Zambia.

C. A. GUERRA ET AL., *PLOS MED* 5, E38 (2008); WWW.MAP.OX.AC.UK

a proof of principle. The plan is in its infancy, but will probably be a 'shock-and-awe' campaign consisting of several interventions. "We'll be using techniques we know work — we'll throw everything at it," says Sungano Mharakurwa, MIAM's scientific director. "If it works in that area, we would want to go for the district and then the national level. On ethical grounds, people won't want to wait."

The methodology they envision is not that different from the nationwide plan, although the government is more pragmatically focusing on a set of malaria-control targets, rather than total eradication. The national strategy, which has emerged as the favoured combination for confronting malaria in Africa, focuses on four key interventions, each of which has a coverage target: getting insecticide-treated bed nets to 80% of the population; treating 80% of acute malaria cases with a new generation of drugs called artemisinin-based combination therapies (ACTs) within 24 hours; the routine provision of an alternative malaria drug combination, sulphadoxine and pyrimethamine, to pregnant women to protect unborn children; and indoor spraying of pesticide in 85% of households in 15 urban districts. The global community has set itself a goal of halving the number of malaria deaths by 2010 using similar interventions.

Slow but sure

So far, Zambia's progress has been slower than it had hoped. The initial time-frame for cutting malaria by 75% set a 2008 deadline, but this has been put back to 2011. To date, the Zambian government claims that the number of people dying from malaria has dropped by 10% since its project began in earnest in 2006. Yet a preliminary report[1] for four African countries compiled by the World Health Organization (WHO) offers hope of greater progress to come. Clinical data for Zambia collected between November and December 2007 show that, since 2000, malaria incidence in children under five — the age group at greatest risk — has declined by 29%, mortality has fallen by 33%.

Two other countries covered by the WHO report, Ethiopia and Rwanda, achieved even greater reductions in childhood deaths from malaria, at 51% and 66%, respectively. Unlike Zambia, these two countries have high-altitude terrain that limits mosquito breeding, but they managed to achieve these cuts even though they had not met their coverage targets for any of the interventions.

The WHO data, based on hospital admissions, are the first nationwide update on Zambia's malaria situation since a 2006 government survey[2] of some 3,000 of the nation's more than 2 million households. Mark Grabowsky, who helped to compile the WHO figures, says that Zambia and its partner organizations need to spend more resources on monitoring the progress of its programme — getting up-to-date information on incidence and mortality to decide which interventions should receive the most effort. "There is no surveillance system in place that allows these decisions to be made." He says that most big health projects, such as the international drive to stamp out polio, have conventionally put aside at least 10% of their funds for surveillance.

"Malaria is a difficult disease to measure well"

John Miller, a monitoring and evaluation specialist with the Malaria Control and Evaluation Partnership in Africa (MACEPA), admits that although there is fairly strong evidence of a downward trend in malaria, the exact figures are hard to compile, not least because some of its symptoms can also be caused by other diseases. "Malaria is a difficult disease to measure well — it is a disease of poverty, it is a rural disease. Understanding how much is there is difficult," Miller says. The Gates foundation is planning another survey for this year, and aims to do one every two years to monitor progress, says David Brandling-Bennett, a US-based senior programme officer with the foundation.

The 2006 survey revealed some useful information on interventions that has guided MACEPA's activities. For example, the report showed that only 50% of the population owned any sort of bed net, and barely 20% of children slept under an insecticide-treated net. So in 2007, the project handed out 3.4 million bed nets across the country. Of even greater concern is the shortfall in speedy access to ACTs. The survey showed that only 13% of children with acute malaria received the drugs within 24 hours. But Miller says that "not all interventions can be scaled up at the same pace. Delivery of antimalarial treatments through the public-health sector by its very nature requires many broader health systems to function well." Zambia is still ahead of many other countries in providing such drugs and infrastructure. "A lot has happened since 2006," says Miller.

Death traps

Back in Macha, MIAM's mosquito-trappers are collecting the sort of valuable information that could help to delay the emergence of resistance to malaria drugs — something that is essential if malaria control or eradication efforts are to succeed. Earlier attempts at malaria eradication in the 1960s failed because the effectiveness of the best available drugs, such as chloroquine, was severely hampered by the emergence of resistant strains of malaria. Today, chloroquine is almost useless in sub-Saharan Africa.

Mharakurwa believes that detailed monitoring of the malaria parasite in the field is key to preserving the effectiveness of newer drugs. "Drugs are getting more and more expensive, so we want to get it right," he says. And his field data, although only preliminary, illustrate how the complex biology of the malaria parasite can affect the emergence of resistance.

The researchers who study the emergence of resistance in Zambia's main malaria parasite, *Plasmodium falciparum*, have only a limited

understanding of how resistance spreads. Based on his research at Macha, Mharakurwa thinks that spraying buildings with long-lasting pesticides to help keep mosquitoes at bay helps reduce drug resistance. Samples of the parasite taken from local infected people showed that almost all were resistant to sulphadoxine–pyrimethamine, which is a drug combination still widely used. But the *P. falciparum* population living in mosquitoes was different: in areas where houses were sprayed, only 10% were resistant to the drug.

Furthermore, Mharakurwa thinks that spraying reduces resistance through subtle effects linked to the complex life cycle of *P. falciparum*. His data suggest that although drug-resistant parasites have a competitive edge when living in humans, this advantage may come at a cost of poorer performance inside the mosquito's body. And this population effect could be narrowed still further by spraying, which reduces mosquito numbers and so increases the competition among the parasites.

Spraying is a key component of the government's malaria plan, but it has not been rolled out nationwide. Unlike drug distribution, which can piggyback on existing health infrastructure, spraying requires additional government coordination and training of personnel to scale up effectively. As a rural area, Macha is not currently included in the spraying programme, which focuses on the one-third of the population in the most urbanized districts. But Mharakurwa is keen to introduce it there.

After years of controversy over the side effects of the pesticides used, the WHO finally endorsed spraying as an effective way to fight malaria in September 2006. But some still see drug use or bed nets as the dominant strategies to be pursued. And the latest WHO data from Ethiopia and Rwanda could support this view. Both countries achieved dramatic drops in malaria deaths by relying on mass distribution of bed nets and ACTs with little if any documented spraying. Nevertheless, Mharakurwa insists that spraying is a proven weapon and that "we should attack malaria with all the weapons that we have to hand". "It depends where you are and what goals are feasible," he says, "one size does not fit all. However, if we want to eventually eliminate the problem of malaria, which many believe is realistic in southern Africa, then spraying is one tool that we know works."

If his bid to eradicate malaria in the 1,000-square kilometre patch works, it will earn Macha a reputation as a test bed for dealing with malaria in remote rural areas, where the poorest, and hardest hit by malaria, live. As with the national plans, MIAM will need to collect careful data on malaria prevention, treatment, cases and deaths to bolster their case.

"It's not easy," says James Phiri, Macha's environmental health technician, a vocal advocate of spraying and the man in charge of handing out bed nets to the local community. "Right now I estimate that we have 4,000 nets, against a population of 20,000." Popular stories about bed nets being used for fishing or even as wedding dresses suggest that some people at a local level are yet to be fully convinced of the benefits of malaria programmes.

> "We should attack malaria with all the weapons that we have to hand."
> – Sungano Mharakurwa

Double jeopardy

Next door to MIAM is the local hospital, which despite being two hours' drive from the nearest paved road not only deals with malaria but also offers a twice-weekly HIV clinic — a reminder that no health problem, no matter how pressing, can ever be viewed in isolation in Africa. The facility also illustrates the often-fragmented nature of healthcare in the developing world. The hospital pharmacy has a healthy stock of ACTs, including Coartem (artemether and lumefantrine), the Novartis-owned drug currently viewed as the best available treatment. But logistics are a constant headache — the only transport link is a bumpy, waterlogged dirt road to Choma, the district's main town.

"Last year, we ran out of Coartem and saw a real, real increase [in illness]," says the hospital's clinical officer Onaty Hanyuma. Another problem is that, in the absence of nationally coordinated health records (Macha's hospital still uses cards to record patients' details), it can be difficult to keep track of case numbers at all. Hanyuma is reserving judgement on figures for 2008 until after the peak malaria months of April and May, by which time several months of rains will have bolstered the mosquito population. During those times, Hanyuma says, he typically sees around 30 new cases of acute malaria a day. He thinks that cases "have gone down a bit" since the government programme got under way, but he cannot provide more details than that.

The experts at MACEPA are fervently hoping that the lessons learned in Zambia can be transferred to other parts of sub-Saharan Africa. But critics point out that Zambia is at the southern end of malaria's distribution, and the problem is more entrenched elsewhere. They also suggest that strategies against *Anopheles arabiensis*, the main mosquito carrier in Zambia, may not work in more northerly regions, where the disease is transmitted by other mosquitoes.

In the meantime, donors are determined to press ahead with a continent-wide boost in the scale of malaria programmes. A branch of MACEPA called the Learning Community, based in Lusaka, is aiming to spread Zambia's expertise to several countries, including Ethiopia, Tanzania, Malawi and Zimbabwe. And household assessments are planned by the governments of more than 40 countries in Africa. "We are confident that these are the same strategies that will work in a Tanzania or a Zimbabwe, for example," says Judith Robb-McCord, who runs the Learning Community. "They may have a different spin in terms of their adaptation in particular countries, but we're relying on the theory that practices that work here will work in other countries." ■

S. HENRY/REUTERS

Spraying homes with pesticides could help tackle the problem of malaria drug resistance.

Michael Hopkin is a senior reporter with *Nature*.

1. WHO Global Malaria Program Surveillance, Monitoring and Evaluation on *Impact of Long-Lasting insecticidal-treated nets (LLINs) and artemisinin-based combination therapies (ACTs) measured using surveillance data, in four African countries* (WHO, Geneva, 2008)
2. *MACEPA Technical Brief 1. Zambia 2006 National Malaria Indicator Survey* (MACEPA, 2007)

See Editorial, page 1030, and online at www.nature.com/news/specials/malaria/index.html.

Political debate: science will be the loser

SIR — David Goldston appropriately demolishes the idea of a US presidential candidate debate on science, in his Column 'A debatable proposition' (*Nature* **451**, 621, 2008). It's hard to imagine anything worse for the cause of science than to subject it to the sort of high-profile demagogic posturing now reserved for immigration, medical care, social security, the economic downturn and the war in Iraq. Science continues to enjoy a protected and privileged status in American politics, in no small part because of its absence from the national political stage — a fact that many science promoters stubbornly refuse to understand.

Daniel Sarewitz
Consortium for Science, Policy and Outcomes, Arizona State University, Tempe, Arizona 85287, USA

Political debate: it is a risk, but one that's worth taking

SIR — David Goldston in his Column 'A debatable proposition' (*Nature* **451**, 621; 2008) questions the wisdom of a presidential debate on science and raises several issues that explain his scepticism. I am in favour of such a debate, but I urge the organizers of the petition calling for this, at www.Sciencedebate2008.com, to give thoughtful consideration to Goldston's points.

I believe the debate is important for several reasons. It will improve the public's understanding of the host of challenges faced by the new president, and by the rest of us in the United States, in areas such as health and medicine, energy and climate change, economic competitiveness and jobs, clean air and water, security, natural (and unnatural) disasters and many others. These will require the new knowledge and tools that stem from research and innovation, coupled with wise policy choices. The American people should expect their future president to understand and be able to articulate this coupling and how it relates to his or her priorities. And the candidates should see this as an opportunity to show the voters what visionary leadership in the twenty-first century is all about.

In framing the debate and developing specific questions for the candidates, the organizers should bear in mind some of the pitfalls that Goldston mentions. For example, understanding climate change and its probable impact on the planet and its people is a matter for science. But the challenge goes far beyond science and technology, even though taking steps to lessen the negative consequences will require scientific understanding and technology. It will involve political trade-offs that we in the science community might not want the public to associate with science. So there is a risk in holding such a debate. However, in my opinion, the risk is well worth taking.

Neal Lane
Department of Physics and Astronomy and James A. Baker III Institute for Public Policy, Rice University, Mail Stop 108, Box 1892, Houston, Texas 77251-1892, USA

Government subsidized by academia on conservation

SIR — Your Editorial 'The great divide' (*Nature* **450**, 135–136; 2007) argues that conservation biologists should be more involved in conservation practice. Subsequent Correspondence (*Nature* **451**, 127; 2008) suggests that this should be an integral part of the process in promotion and tenure of academic conservation biologists. In my view, this is frankly unrealistic.

Of course academic studies should inform practice, but this does not mean that academics should be practitioners. The suggestion that the value of a conservation biologist should be measured by what would have happened had that person not carried out their work, despite being almost impossible to evaluate, runs into the same problems as placing a value on any conservation activity. Should a UK institution, for example, promote a tropical rainforest conservation biologist over a colleague who studies British moorland, or one who works on tiger conservation?

Academic research should be relevant to practice, but not practice-led. If we need to chase science that can be put into practice to demonstrate our effectiveness, conservation biology as a discipline will never move from being a reactionary science to dealing with issues of biodiversity conservation in a pro-active manner. The fact is that universities have long been subsidizing efforts in the practice of nature conservation that should be made by governments and non-governmental organizations.

The divide is one of personnel. Positions are needed for academically able and well informed practising conservationists within governmental agencies. In Britain, this has not been the case since the Nature Conservancy split from the Natural Environment Research Council in 1973. The efforts of those academics pushing for evidence-based conservation are an important step in the right direction, but a step that should have been taken by the government long ago.

Philip Wheeler
Centre for Environmental and Marine Sciences, University of Hull, Scarborough Campus, Filey Road, Scarborough YO11 3AZ, UK

Celebrations for Darwin downplay Wallace's role

SIR — We agree with Kevin Padian ('Darwin's enduring legacy' *Nature* **451**, 632–634; 2008) that next year's Darwin anniversaries — the 200th anniversary of his birth and 150th anniversary of *On the Origin of Species* — should be celebrated enthusiastically. But few seem to be aware that this year marks the 150th anniversary of one of the greatest discoveries in the history of science: the theory of evolution by natural selection. Although this idea is often credited solely to Charles Darwin, it was independently discovered by naturalist Alfred Russel Wallace 150 years ago this month, while he was suffering from fever on the Indonesian island of Halmahera. Wallace sent Darwin an essay detailing the theory, which was published, together with two short excerpts from Darwin's unpublished writings on the subject, by the Linnean Society of London in August 1858.

Widespread preparations for the Darwin celebrations are now being made by the University of Cambridge and the Natural History Museum, among many others (see http://darwin-online.org.uk/2009.html and a Darwin walk at http://tinyurl.com/ysofwn). But to our knowledge, very little is being planned to celebrate the 150th anniversary of the discovery of natural selection. This contrasts with the lavish series of events and exhibitions that took place 50 years ago to celebrate the centenary of the discovery. The Linnean Society will host a modest event to commemorate the pre-publication reading on 1 July 1858 of Darwin and Wallace's seminal papers. Information is available from the Alfred Russel Wallace Memorial Fund (founded by G. W. B.) at www.wallacefund.info/2008-events.

This lack of interest in the 2008 anniversary is indicative of how Wallace's achievements have been overshadowed by Darwin's since Wallace's death in 1913, a process certainly not helped by the Darwin 'industry' of recent decades. During his lifetime, Wallace received plenty of recognition from his contemporaries for his part in the discovery, as indicated by the many honours bestowed on him. These include the Darwin–Wallace and Linnean Gold Medals (Linnean Society); the Copley, Darwin and Royal Medals (Royal Society), and the Order of Merit. Isn't it perhaps time for the current darwinocentric view of the history of biology to be revised?

George W. Beccaloni, Vincent S. Smith
Entomology Department, The Natural History Museum, Cromwell Road, London SW7 5BD, UK

Contributions to this page may be sent to correspondence@nature.com. See Guide to Authors at http://tinyurl.com/373jsv.

COMMENTARY

M. HALLAHAN/SUM TOMOK HEMICA/POLYSET NET

The billion-dollar malaria moment

For years the global malaria effort has been asking for more resources. Now the field needs to figure out a systematic strategy for spending the money effectively, says **Mark Grabowsky**.

Several years ago, I was explaining the value of a measles-vaccination campaign to a doctor at a paediatric hospital in northern Uganda, where, at that time, measles was endemic. The proposed campaign would control the disease and potentially enable the hospital to close the measles ward. The doctor responded that if there was also a campaign that controlled malaria he could "close the entire hospital".

There is still no vaccine for malaria, but Uganda has adequate resources — as do many other countries — for a national campaign of several malaria interventions, including insecticide-treated bed nets and effective drugs. The challenge is to scale-up those services. Just as high levels of vaccination coverage led to closing Ugandan polio and measles wards, rapid scale-up of prevention measures could end the malaria crisis in Africa. Slashing malaria cases and deaths would also free up vital resources for other diseases that have had too little attention for too long.

This vision is in stark contrast to the experience of recent decades, which have seen flagging global efforts and rising mortality from malaria. For a disease that still kills a million people a year, uses almost half of the clinic services in Africa, and reduces economic growth by up to 1%, controlling malaria may be the most important challenge in global public health.

But hope is arriving in Africa. The malaria crisis is starting to yield to new tools and strategies made possible by a substantial increase in resources over the past ten years — from less than US$100 million to about $1 billion this year. With most resources coming from a few donors, such as the Global Fund to Fight AIDS, Tuberculosis and Malaria, the World Bank and the President's Malaria Initiative, the current global goal — coordinated by the Roll Back Malaria (RBM) Partnership — is to halve the number of malaria deaths by 2010. However, these donors rely on a country-led process of planning and goal setting, and many nations' plans are not yet sufficiently ambitious in scope, intensity or timeliness to reach the 2010 target. Adequate funding for malaria control is an important first step, but unprecedented coordination, planning and operational support will be required to achieve the goals.

"The current global plan is to halve the number of malaria deaths by 2010."

Recent progress has come from applying four interventions: sleeping under insecticide-treated bed nets, spraying houses with insecticides, preventive treatment for pregnant women, and timely treatment of the sick with effective drugs. The RBM target is to reach 80% coverage with each of these interventions by 2010. Within one year of scaling up these interventions in 2006, malaria hospital admissions of children fell by more than about 60% at selected facilities in Ethiopia[1], Rwanda[2], Zanzibar[2] and on the coast of Kenya[3]. Achieving the overall targets for Africa by 2010 is a huge challenge, and scaling-up drug treatment is particularly daunting, but the widespread use of bed nets should reduce case numbers and ease the demand for drugs.

In response to this initial progress, the leading public-health agencies attending the Bill and Melinda Gates Foundation malaria forum in Seattle last year boldly endorsed eliminating malaria as a public health and economic problem. Bill and Melinda Gates went further and called for malaria eradication. But achieving eradication is a decades-long project that will require new tools, including an effective vaccine (see page 1042).

Integrated prevention

The malaria community can learn a great deal from the scaling up of vaccination programmes for polio and measles. Ten years ago, about half a million children died of measles annually in Africa and many countries were endemic for polio. Since then, hundreds of millions of doses of vaccines have been delivered, and cases and deaths for both diseases have fallen by more than 90%. Despite the lack of a malaria vaccine, these successes can serve as an important model and inspiration for rapid scale-up.

M. HALLAHAN/SUMITOMO CHEMICAL/OLYSET NET

Bed nets are a key weapon against malaria.

Taking advantage of the existing delivery systems for childhood vaccination is the most efficient method for rapidly scaling up malaria prevention. Measles vaccination campaigns occur every three years in most African countries. During these week-long campaigns, children under five years of age are vaccinated — these are the same children that need insecticide-treated bed nets. Giving out free bed nets to children and their caretakers when they attend the measles campaigns achieves rapid, high and equitable bed-net coverage at low cost[4]. These integrated campaigns are now the most common method for providing bed nets to Africans, with more than 40 million delivered over the past two years. During one week in December 2007 in Mali, more than 2.1 million nets were delivered along with measles vaccination, vitamin A and deworming medicine.

Even though periodic mass campaigns can rapidly achieve high coverage, because children are born every day, there is a need for ongoing bed net distribution between campaigns. This can happen when a mother brings a child to a clinic for routine vaccination[5]. There are twenty countries in sub-Saharan Africa where infants have at least four vaccination visits to the health centre in the first year of life. But these visits are rarely used for malaria prevention. In Nigeria, where vaccination coverage of measles is close to 70%, bed-net coverage is less than 10%. If these vaccination visits were used to give out bed nets, coverage would eventually rise to near target levels.

There are also opportunities for malaria prevention when pregnant women come to a clinic for pre-natal care. Countries need to adopt these proven and efficient approaches to integrated delivery. This requires national malaria-control programmes to coordinate more with their colleagues involved in other health programmes.

The challenge of treatment

Malaria prevention can build on these existing strategies, provided that countries and donors pull together. But of the four 2010 targets, achieving 80% rates of drug treatment is the greatest challenge. The difference in the ability to deliver prevention and treatment is illustrated in Sierra Leone. In 2006, in eight districts supported by the Global Fund, bed-net delivery was integrated into existing prevention services, and drugs and diagnostic kits were supplied to health centres.

After one year, 80% of children and 60% of pregnant women in Sierra Leone slept under a bed net. Virtually every clinic had adequate stocks of the recommended drugs for malaria treatment. However, only 4% of the children with malaria symptoms received appropriate treatment in a timely fashion (within one to two days of fever onset).

Malaria is a disease of poverty. Three-quarters of the population in rural Africa lives in extreme poverty, as defined by the family only having the income to buy enough food to ward off starvation. Free services at health facilities do not remove other barriers to reaching a clinic, such as transportation, or taking time away from work, growing food or fetching water. Integrating treatment into clinic-based services, even if low-cost or free, will fail to reach many of the poorest. Improved access will require new approaches that are not clinic-based.

One proposal is to subsidize drugs at private pharmacies[6]. In theory, patients will benefit from local access to such shops and the presumed effects of private-sector competition to lower prices. Better consumer education, such as placing recommended prices on product labels, may also improve access. But recent findings suggest that this may still not be enough to reach those with other barriers to access, particularly children in poor families.

> "Without high-quality surveillance, the billion-dollar malaria effort is flying blind."

Evidence from pilot projects in Africa shows that new drugs can be effectively delivered to rural children within 48 hours of fever onset through either community-based volunteers or home-treatment kits[7]. But can such approaches achieve the ambitious 2010 targets? One example of success is in Ho District in Ghana where community workers — usually farmers and teachers selected by the community — were able to correctly deliver drugs to 75% of sick children[7]. But whether resource-poor government services can support civil efforts in malaria care is unproven. Partnering with community based groups such as the Red Cross may be the key to large-scale implementation. The Global Fund, therefore, encourages governments and civil society to submit coordinated but separate applications so they do not compete for resources.

As countries pursue the 80% coverage targets, data are needed to relate coverage to the more important goal of halving deaths caused by malaria. In areas of moderate transmission — such as the Kenyan coast — even modest bed net coverage may be able to reduce mortality by 50%. In areas of intense transmission, that may not be enough. The only way to routinely relate coverage to impact is through systematic disease surveillance. Routine and standardized monitoring is essential for a business-like approach to decision-making, but no such systematic surveillance data exists for malaria.

Monitoring is essential to protect our tools. Resistance to the pesticide DDT and the drug chloroquine contributed to abandoning malaria eradication in the 1960s. Today's efforts also depend on two molecules: pyrethroids to treat bed nets and artemisinin for treatment. Resistance is widespread for the former and emerging for the latter. Moreover, more money for drugs invites counterfeits, as seen in Asia and now in Africa. Achieving the malaria-control goals, or elimination, risks failure if detection and response to resistance remain inadequate.

Secret weapon

In many ways, disease surveillance has been the secret weapon for polio and measles control, powering funding and informing decisions. An example is the regional monthly newsletter of measles cases. It allows countries, donors and planners to systematically monitor progress towards goals.

Without ongoing high-quality data it will be impossible to monitor progress and focus efforts on elimination or eradication. There are technical challenges to improving malaria surveillance, including the need to move away from presumptive to laboratory diagnosis. But most of these challenges can be resolved with adequate investment, training and management.

As the global community scales up malaria control, it must ensure that all countries have adequate monitoring systems in place. Nonetheless, a country based approach by itself is neither technically nor financially appropriate. There must also be regional laboratory networks that support country efforts, apply standardized monitoring techniques, rapidly share findings and manage coordinated responses. This is particularly essential for monitoring drug quality. It would cost about $10 million annually to get useful, monthly, surveillance data and to support regional monitoring, laboratory and surveillance networks. Without it the billion-dollar malaria effort is flying blind. ■

Mark Grabowsky is at the Global Fund to Fight AIDS, Tuberculosis and Malaria, 8 Chemin de Blandonnet, 1214 Vernier, Geneva, Switzerland

1. http://www.who.int/malaria/docs/ReportGFImpactMalaria.pdf
2. Bhattarai, A. *et al. PLoS Med.* **4**, e309 (2007)
3. Okiro, E. A. *et al. Malar. J.* **6**, 151 (2007)
4. Grabowsky, M. *et al. Bull. World Health Organ.* **83**, 195–201 (2005)
5. Grabowsky, M., Nobiya, T. & Selanikio, J. *Trop. Med. Int. Health* **12**, 815–822 (2007)
6. Institute of Medicine of the National Academies Board on Global Health *Saving Lives, Buying Time. Economics of Malaria Drugs in an Age of Resistance* (Natl Acad. Press, Washington DC, 2004)
7. Ajay, I. O. *et al. Malar. J.* **7**, 6 (2008)

See Editorial, page 1030, and online at www.nature.com/news/specials/malaria/index.html.

BOOKS & ARTS

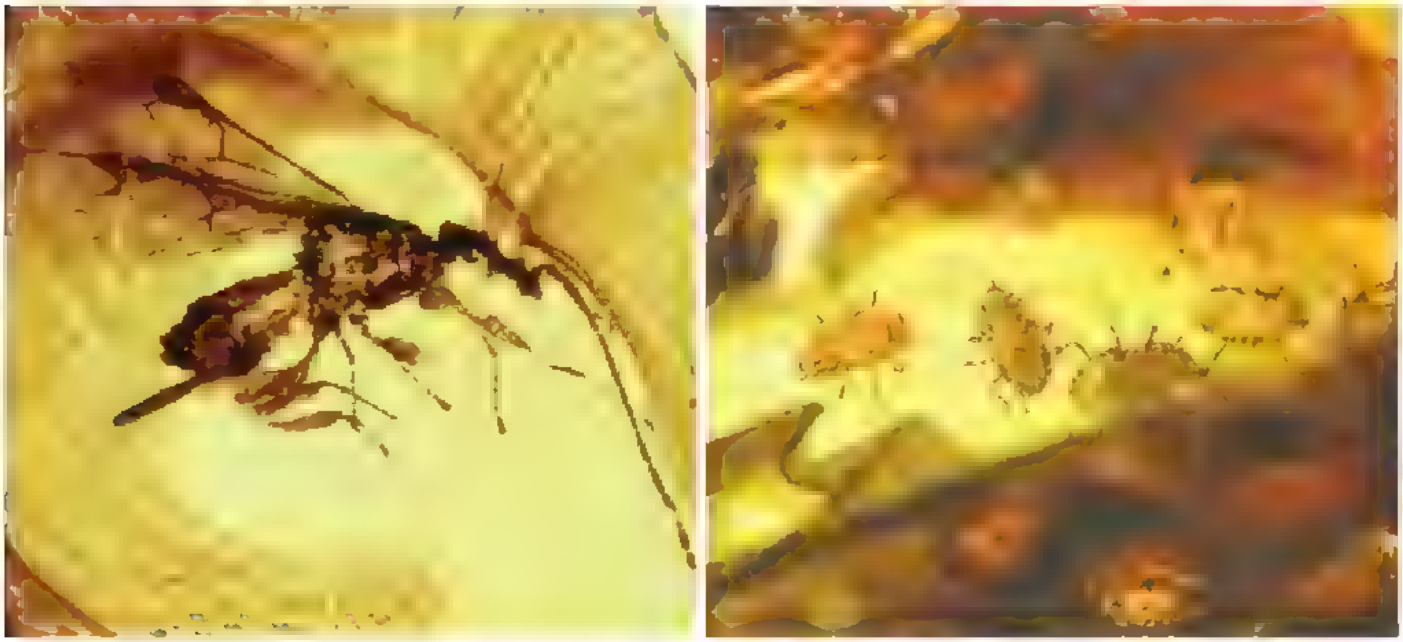

ROYAL TYRRELL MUS., POINAR AMBER COLLECTION/OREGON STATE UNIV

Pest friends in the Cretaceous

Fossils preserved in amber hint at surprising links between dinosaurs and their insect contemporaries.

What Bugged the Dinosaurs? Insects, Disease, and Death in the Cretaceous
by George Poinar Jr and Roberta Poinar
Princeton University Press: 2008. 296 pp
$29.95, £17.95

Karen Chin

Dinosaurs are usually portrayed as the pristine masters of the Cretaceous. George and Roberta Poinar's new book presents a different view — dinosaurs besieged by swarms of insects; dinosaurs with oozing, infected bites; dinosaurs weakened by parasite-induced illnesses.

What Bugged the Dinosaurs? draws on the Poinars' many studies of fossils in amber to show how dinosaurs interacted with their more abundant invertebrate contemporaries. Amber preserves a serendipitous selection of soft bodied or lightly skeletonized organisms that were small enough to be mired in tree resin (pictured). The Poinars focus on exquisitely preserved fossil organisms from three key deposits: 135 million- to 130-million-year-old Lower Cretaceous Lebanese amber; 105-million- to 97-million-year-old Middle Cretaceous Burmese amber, and 79-million- to 77-million-year-old Upper Cretaceous Canadian amber.

Many of these fossils are insects, the most diverse group of multicellular organisms on Earth. Familiar creatures such as biting midges, aphids and black flies were common in the Cretaceous alongside bizarre specimens with odd features as well as less charismatic invertebrates, such as ticks and nematodes.

The authors make the case for regular contact between numerous different invertebrates and dinosaurs. Bloodsuckers, scavengers, dung-eaters and parasites would have been particularly interested in the resources in and emanating from the dinosaurs' large bodies. Such opportunists would then have been ideal vectors for diseases. Just as close relationships between vectors and pathogens are common today — for example, diseases such as anthrax, malaria and plague can all be transmitted by insects — so dinosaurs might have contracted diseases.

In a few cases the evidence for interactions is strengthened by rare fossils such as insect borings in bone and dung beetle burrows in fossil faeces. Most striking are the blood- and pathogen filled sand fly guts that support the spectre of bloodsucking insects dining on dinosaurs.

Other relationships can be predicted by considering the body structure of Cretaceous organisms together with the behaviour of their modern relatives. The often surprising and complex examples of interactions between modern organisms (such as lizards, which can acquire parasitic stomach worms by eating infected ants) expand our perceptions of how ancient ecosystems may have been structured. The authors create vivid images of the Cretaceous in which dinosaurs browsing in lush forests disturbed plant-eating insects and were, in turn, set upon by hordes of biting insects.

Reconstructing ancient ecosystems is an ambitious undertaking. We scarcely understand the intricacies of modern ones, much less those for which we have spotty fossil evidence. Limiting palaeontological studies to simple lists of fossil organisms diminishes our ability to comprehend the complex interrelationships of past ecosystems. Integrative approaches such as those in *What Bugged the Dinosaurs?* help us build up more sophisticated visions of the past.

But terrestrial life on Earth has evolved since the Cretaceous, and some ecological interactions may have changed as well. Thus, as new fossil evidence helps fill in our picture, we should be on the lookout for patterns in resource utilization that are different from today's. After all, the dinosaur-dependent insects that survived the Cretaceous/Tertiary mass extinction certainly had to adjust to life without the big guys.

To paraphrase John Donne, no dinosaur is an island. Although vertebrate palaeontologists acknowledge the ubiquity and abundance of insects, we are often vertebrate chauvinists. This book reminds us to consider the profound influence of insects and other invertebrates. We have much to learn about and from them. ■

Karen Chin is an assistant professor of geological sciences and curator of palaeontology at the Museum of Natural History, University of Colorado, UCB 265, Boulder, Colorado 80309, USA.

EXHIBITION

Shots of Silicon Valley

Fred Turner

In the mid-1990s, as the Internet entered our daily lives, a chorus of pundits sang out that the laws of the material world were giving way to those of information. This was especially true in the semi-arid flatlands running south from San Francisco. In the popular imagination, Silicon Valley became a place to turn knowledge into bits and to leave behind the hulking, filthy factories of the industrial era.

Last year the San Francisco Museum of Modern Art commissioned the Italian photographer Gabriele Basilico to profile Silicon Valley. The record he made reminds us that for all the intellectual power unleashed here, the Valley remains a place. Its landscape is shaped by its history, and especially by a series of cultural collisions. Mexican day labourers, Asian coders, Air Force officers and former hippies have added to the Valley's physical character while sustaining its entrepreneurial ethos.

Basilico trained as an architect, and his pictures rarely include people. Yet they invite viewers to read the everyday lives of local citizens from the evidence they leave behind. In Silicon Valley, Basilico works his way up and down the area's two main freeways, pausing only occasionally to pay homage to the glossy headquarters of high-tech firms such as Apple and Google. More often, he takes his camera to a nearby hilltop and snaps panoramas of condominiums, parking lots and the sinewy tarmac of the freeways themselves.

These still images repay meditation. One depicts an abandoned 1930s blimp hangar at NASA's Moffett Airfield in Mountain View. Grass has cracked the pavement around it and toxins leach from its shell. Even without the airmen who staffed it, the hangar reminds us of the military's presence and role in the Valley's growth.

Basilico also turns his lens on the Victorian houses of San Francisco, making wide-angled colour views of the city's parks and skyline. To anyone more than 40 years old, and especially a Californian, these images recall the countercultural revolution that found its legs in Haight-Ashbury. Even now, the 1960s still supply the rhetoric of individual independence and creativity that rings throughout Silicon Valley. More than a few software engineers still sport the long hair and libertarian values of the Summer of Love.

Ironically, this is also where Basilico's method breaks down. His focus on the large-scale elements of the region's infrastructure inadvertently privileges those who have had the power to build companies, highways and cathedrals. There is another Silicon Valley, one of pollutants lurking beneath the land and parents working in multiple minimum-wage jobs. Only one image here points to that Valley: a photograph of a nineteenth-century Catholic church in San Jose. Compared with the post-modern blandness of snap-to-grid office parks, the church looks strangely ornate.

It is a sturdy reminder that for more than a century, the Valley has depended on migrant labour for everything from agriculture to light manufacturing, restaurant work to software coding. The Valley's cosmopolitan puzzle includes service personnel from Vietnam and the Philippines and engineers from India and China. It is tempting to imagine these mobilized workers as packets of information, shuttling across the landscape as if the laws of matter really had been repealed. These photographs remind us they haven't. Silicon Valley's success continues to depend on its infrastructure — material and cultural. ■

Fred Turner is an assistant professor of communication in the Department of Communication at Stanford University, Stanford, California 94305-2050, USA. He is the author of *From Counterculture to Cyberculture: Stewart Brand, the Whole Earth Network, and the Rise of Digital Utopianism.*

Gabriele Basilico: From San Francisco to Silicon Valley **is at the San Francisco Museum of Modern Art until 15 June (www.sfmoma.org).**

Fly image wins photo prize

Joanne Baker

This image of a live *Drosophila* larva in a water droplet has won the photographic competition that forms part of celebrations marking the 200th anniversary of the Royal Netherlands Academy of Arts and Sciences (KNAW). Winner Robert Markus, of the Biological Research Center of the Hungarian Academy of Sciences in Szeged, received the award at a ceremony on 25 February in Amsterdam.

The jury was chaired by KNAW president Frits van Oostrom, and included Dutch scientists and journalists as well as *Nature*'s editor-in-chief Philip Campbell. It selected *Hemocyte Compartments of the* Drosophila *Larva (*In Vivo *—* Live Drosophila *Larva in a Drop of Water)* as the best portrayal of the 'magic of science', the bicentenary's theme.

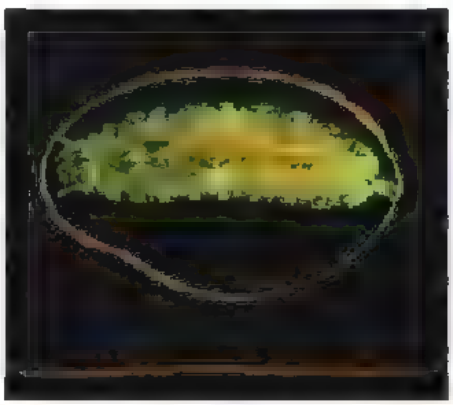

Markus took his photograph to show how blood cells affect the fruitfly's immune system. "By identifying blood-cell-specific genes, we can generate transgenic *Drosophila* strains in which the blood cells express green fluorescent protein, so that they are visualized *in vivo*, making *in vivo* research possible on the immune system," he explained.

KNAW's bicentenary celebrations (www.knaw200.nl) include talks, exhibitions and guided tours of the academy's Trippenhuis Building headquarters. They also feature a mass experiment on human 'waves' propagating through a crowd of soccer fans in Rotterdam's Kuip Stadium (the team FC Feyenoord celebrates its 100th anniversary in 2008) and a tour bus taking science to schools. ■

Joanne Baker is *Nature*'s Books & Arts editor.

Biopiracy started with a bounce

The Thief at the End of the World: Rubber, Power, and the Seeds of Empire
by Joe Jackson
Viking: 2008. 432 pp. $27.95

Michael A. Gollin

Some people call it the original act of 'biopiracy.' In 1876, Henry Wickham, a self-trained rubber tapper under contract to the Royal Botanic Gardens at Kew in London collected 70,000 highly perishable *Hevea* rubber seeds from Santarém in Brazil. Wickham rushed them on a steam ship to Kew, where the seeds were immediately germinated and sent to the British colonies in India. The resulting plantations broke the Amazon rubber monopoly and dominated the rapidly growing market until Japan seized the plantations in the Second World War, and synthetic rubber was invented.

The Thief at the End of the World chronicles the life of the audacious Wickham, who fled the London cholera epidemics to become a tropical adventurer and planter. Joe Jackson's strong investigative and story-telling skills conjure up the colour and characters of Wickham's meandering path through the British colonies and beyond. Wickham encountered natural threats — malaria, parasites, injuries and floods. And he faced human difficulties — slave traders, murderous jungle barons, cannibal tribes, financial ruin and the deaths of family members whom he convinced to join him in his quixotic quests. Somehow he bounced back every time to cultivate his public image until he was knighted soon before his death in 1928.

Kew's leaders pioneered public–private partnerships between collectors, government botanists and the colonial plantations. But they held Wickham, a freelancer, in contempt. They expected him to fail in his contract to deliver even 1,000 viable seeds for £10 (US$20), and were shocked by his success, in view of numerous failures by established collectors. Wickham apparently succeeded because of his years working as a planter and rubber tapper alongside locals. Kew honoured its financial commitment to Wickham, yet denied him any recognition, and foolishly rejected his offer to help cultivate rubber in Asia, delaying the plantation effort by two decades. This insider–outsider dichotomy echoes today in the broader politics and rivalries of scientific research and funding by governments, philanthropies and businesses.

Wickham's life spanned the Rubber Age. With Goodyear's invention of vulcanization as a way to make rubber harder and more durable, rubber became a billion-dollar product essential for the revolutionary innovations of the day: steam-engine gaskets in ships and trains, telegraph wire insulators, bicycle and then automobile tyres, and military equipment including First World War gas masks. Fifty years after the adventurer left Santarém with rubber seeds, Henry Ford invested US$20 million in a rubber plantation in the same region. Ford's colossal, well intentioned failure underscores the enormous challenges that Wickham, Kew and the British plantations overcame. Like oil today, and perhaps biofuels in the future, rubber called for risk and failure, led to boom-and-bust cycles, and had far-reaching impacts on technology, geopolitics and the environment.

Rubber had far-reaching impacts on technology, geopolitics and the environment.

In calling Wickham a "thief", Jackson oversimplifies a complex event at a transitional time in world history. Brazilian officials later vilified Wickham, but it seems he broke no laws. Wickham said he told Brazilian officials that what he was taking were "exceedingly delicate botanical specimens specially designated for delivery to Her Britannic Majesty's own Royal Gardens of Kew". Jackson describes this as bluff and aggressive, but not a lie. The rule of law was weak then: slavery was still legal in Brazil, brutality was widespread, and 'take what you can' was a guiding principle.

Today, Wickham's acts would be illegal. Biodiversity prospectors must obtain informed consent before removing biological materials. Under the 1992 Convention on Biological Diversity, many countries have passed laws that require scientists to obtain collecting permits, and to share any resulting benefits with locals. Brazil put in place strict and cumbersome permitting laws, and even amended its patent law to require inventors to disclose any Brazilian genetic material used in making their inventions. In 2007, a Brazilian court jailed a Dutch biologist for keeping primates in a rehabilitation facility, stalling further research.

So modern collectors face strict scrutiny, but with perseverance they can reach sustainable collaborative arrangements such as those used to produce the malaria medicine artemisinin from Chinese wormwood using newer synthetic-biology techniques. Hopefully such collaboration will help biodiversity prospecting yield another bounty as great as Wickham's rubber seeds — this time with the benefits more broadly shared. ■

Michael Gollin is a patent attorney focused on intellectual property management in the life sciences at Venable LLP, 575 7th Street, NW, Washington, DC 2004, USA. He is author of *Driving Innovation: Intellectual Property Strategies for a Dynamic World*.

SCIENCE MUSEUM/SSPL

Many rubber trees derive from seeds Henry Wickham took from Brazil.

A feverish imagination

Poems, plays and novels punctuated the life of Ronald Ross.

Martin Kemp

There was more to Ronald Ross (1857–1932) than his Nobel Prize for discovering the role of the *Anopheles* mosquito in the transmission of malaria. Ross's *Memoirs* paint a picture of a driven man, intolerant of petty-minded administrators, whose inner life was coloured by a vivid literary and artistic imagination.

Ross' father had thwarted his initial ambitions to become an artist. Subsequently, a series of deeply felt poems, plays and novels punctuated his working life as a doctor specializing in tropical medicine. An admirer of the full-blooded romanticism of Lord Byron and Alfred Lord Tennyson, and a friend of John Masefield (the later poet laureate), Ross was also drawn at an early age to Johann Wolfgang von Goethe's *Faust*, as a skilled drawing in his teenage sketchbook from 1872 testifies.

Much of the sketchbook is occupied by accomplished landscape drawings and watercolours made on the Isle of Wight, perhaps with the assistance of a camera lucida. An annotation in the sketchbook records the source of Ross's drawing of Faust as Moritz Retzsch's 27 illustrations of Goethe's tragedy, first published in Britain in 1820. However, this is true only in a generic sense, because Ross's drawing does not correspond directly to any of the Retzsch prints but seems to be his own imaginative variation on the theme. Faust sits brooding in a landscape, while an owl, a symbol of night, hovers nearby. The demeanour of Faust manifests the devilish melancholy that traditionally afflicts those who strive towards the ultimate and the unattainable.

Ross's *Memoirs*, in the period leading up to his discovery, oscillate between hope and despair. Posted in Secunderabad, India, he had himself contracted malaria in April 1897. The monsoon was slow to break. The heat became stifling and the insects intolerable. Working in isolation with feverish intensity, he painstakingly dissected mosquitoes fed on his malaria-infected patients. His research was running into a dead end: "failure followed failure". He drafted impassioned lines for his running poetic composition *In Exile*:

> What ails the solitude?
> Is this the Judgement Day?
> The sky is as red as blood
> The very Rocks decay.

Then, the sudden breakthrough. He dissected mosquito no. 38 without much expectation that it would be different. He observed "some large cells with pigment" in its stomach, no less than nine of them. The note (pictured) is triple underlined. Below some characteristically rapid graphic notations of the kind that punctuate his notes and letters, he records the tell-tale pigments. "The outline of the cells is generally thick, but in the smaller ones sometimes delicate." These were the malaria cells in the mosquito's stomach for which he had been desperately searching. The tone of *In Exile* transforms:

> This day designing God
> Hath put into my hand a
> Wondrous thing. And God
> Be praised. At his command,
>
> I have found thy secret deeds
> Oh million-murdering Death.

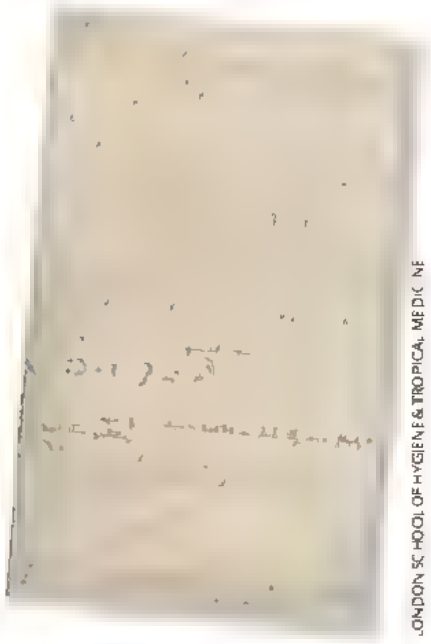

LONDON SCHOOL OF HYGIENE & TROPICAL MEDICINE

> I know this little thing
> A myriad of men will save.
> O Death. Where is thy sting?
> Thy victory, O Grave.

Faust was driven by Mephistopheles, Ross by God. They were well matched in the intensity of their quests. By September, Ross had drafted his urgent official report from India. His regular correspondent and fellow researcher Patrick Manson safeguarded Ross's priority claim by ensuring that his friend's discovery was presented forthwith to the British Medical Association. Two years later Ross was installed in the Liverpool School of Tropical Medicine. The Nobel prize followed in 1902, in the face of formidable competition from Ivan Pavlov, and a knighthood in 1911. Ross was not simply a doctor who wrote poetry; his science and art manifest the imaginative fire that governed his creative life in all its aspects. ■

Martin Kemp is research professor in the history of art at the University of Oxford, Oxford OX1 1PT, UK.

LONDON SCHOOL OF HYGIENE & TROPICAL MEDICINE

Ronald Ross's drawing of Goethe's Faust

Hidden treasures: Eise Eisinga Planetarium

The world's oldest functioning planetarium was built by an eighteenth-century wool-comber in the Netherlands. **Alison Abbot** reports, in the second of her monthly series on small museums.

Early in 1774, a Dutch preacher and amateur astronomer, Eelco Alta, scared his compatriots out of their wits by predicting that the world would end on 8 May. His scientific arguments seemed plausible and terrifying. Astronomers in Dresden had just calculated that there would be a rare conjunction of four planets and our Moon on that day. Alta believed that the celestial bodies would crash, hurling Earth into the Sun.

Fortunately the Low Countries were also home to a smarter amateur astronomer, Eise Eisinga. The wool-comber, only 30 years old at the time, decided that the locals of his native town Franeker in Friesland needed to see for themselves why such a catastrophe could never happen. To the consternation of his wife, Eisinga built a planetarium into his living-room ceiling. It took seven years. He carved its extraordinarily intricate clockwork elements from oak, and individually forged each of the 10,000 nails for the gearing teeth. The immense workings, with more than 60 wheels, lie in the roof space above the living-room with its inbuilt cupboard bed. They still drive what is now the world's oldest functioning planetarium — and without doubt the most charming.

Just one pendulum propels the six planets that were known at the time along their concentric orbits around a painted Sun at the centre of the ceiling. The planets are wooden balls suspended on metal pins that move imperceptibly, completing one circumlocution per real-time orbit. So Mercury takes 88 days, while the outermost Saturn takes 29 years and 164 days. Uranus was discovered in 1781, just as Eisinga's work was complete — which is just as well because it would have busted the perfect $1:10^{12}$ scale of the planetarium that fitted Eisinga's living-room so neatly.

The pendulum is also the pacemaker for other dials on the ceiling and walls that indicate, with near-perfect accuracy, the date, weekday and hour, as well as lunar phenomena such as phase and rising and setting times. It is powered by weights that must be raised by hand at defined times, the heaviest every five days, the lightest every six months.

When Eisinga sketched out his plans, he calculated on the basis of a metre-long pendulum that would swing at 60 strokes per minute. Only when he set about the physical work did he realize that the attic space was not quite high enough. His long-suffering wife put her foot down when he raised the possibility of cutting a hole directly above the bed so the pendulum could swing freely. Seeing no room for negotiation, he re-calculated the entire gearing system on the basis of a faster-swinging 75-centimetre pendulum.

© HOMMEMAYROVA, EISE EISINGA PLANETARIUM

One pendulum propels the six planets known in the 1770s around the Sun at the centre of the ceiling.

Eisinga was a man of artistic skills too. His painting and gilding are decorative and informative. True orbits are elliptical, not circular, so Eisinga has marked the points where each planet is closest, or farthest away from, the Sun. And since the planets lie close to, but not within, the ecliptic plane, he indicates in white circles of varying thickness around each orbit the orientation of each planet at any time. The ceiling-sky is divided into the signs of the zodiac to indicate the sky segment. All this information allows the planetarium user to pinpoint exactly the position of each planet in the night sky outside.

A visitor making the 125-kilometre drive across the dykes from Amsterdam may wonder: how did something so sophisticated spring up in such a remote, watery landscape?

Now just another pretty medieval town, Franeker in the seventeenth and eighteenth centuries was a thriving university city. The university was founded by Prince Maurits in 1585, during the Netherlands 80-year war with the Spanish Empire, as a reward for the town's political support. When Franeker remained politically neutral during the violent revolutionary movement in the 1790s, it set the seeds of its own decline. Franeker's decline went into freefall after Napoleon closed the university in 1811.

Happily, the planetarium, whose guestbook was first signed in 1781, has never closed to visitors — even when politics and violence forced them to enter through the back door. ■

Alison Abbott is *Nature*'s Senior European Correspondent.

The Eise Eisinga Planetarium is open Tuesday to Saturday 10:00–17:00 and Sunday 13:00–17:00. It is also open Monday afternoons during the summer. http://tinyurl.com/2ykck4

When authorship met authenticity

As counterfeit drugs abound, **Adrian Johns** recalls how medical patenting was created in the seventeenth century to secure trust across growing international trade networks by quashing fakes.

Adrian Johns

Pharmaceutical counterfeiting is on the rise. In 2005, the Organisation for Economic Co-operation and Development, based in Paris, reported the emergence of fakes of even specialized medicines for the most chronic and serious conditions such as cancer, AIDS, diabetes and Alzheimer's disease, as well as ubiquitous antibiotics and weight-loss pills. Widely distributed in Africa and the developing world, such counterfeits have become increasingly common in Europe and North America with the growth of Internet pharmacies.

Counterfeit drugs can be dangerous. They may have the wrong ingredients, or the right ones in the wrong concentrations. More than 100 Panamanians were killed in 2007 by copycat cough syrup. Fake anti-malarials led to the death of a renowned conservation biologist in Cambodia in 1999 (*Nature* 434, 132–136, 2005). Individual patients cannot generally tell whether a drug is fake or not, even if they are aware of the possibility. On a community level, counterfeits can make it difficult to test if a drug actually works, or, by under-dosing, generate increased microbial resistance to genuine drugs (M. D. Green *J. Postgrad. Med.* 52, 288–290; 2006).

Pharmaceutical counterfeiting is an unwelcome by-product of globalization, and demands a commensurately global response. For example, concern has become so acute that, in May 2005, the World Health Organization created a Rapid Alert System for combatting counterfeit drugs, modelled on those for epidemics such as bird flu. And in November 2006 the organization established IMPACT (the International Medical Products Anti-Counterfeiting Taskforce) to seek global solutions.

Yet in some senses globalization is actually returning us to what was the historical norm. For most of human history there was fear of adulteration, rather than confidence in its absence. Ancient authorities such as Dioscorides, Theophrastus and Galen warned of the risks of ill prepared medicines. In the days of William Harvey and Isaac Newton, physicians were accustomed to warning against apothecaries' deceptions. Leading members of London's Royal College of Physicians believed that anyone who trusted "Apothecaries, and common Chymists" was placing their life in the hands of "as great cheats as are now Extant in the World." And in the Enlightenment a new generation of experts warned that the pharmaceutical marketplace was, in the words of botanist J. E. Gilibert, "anarchic".

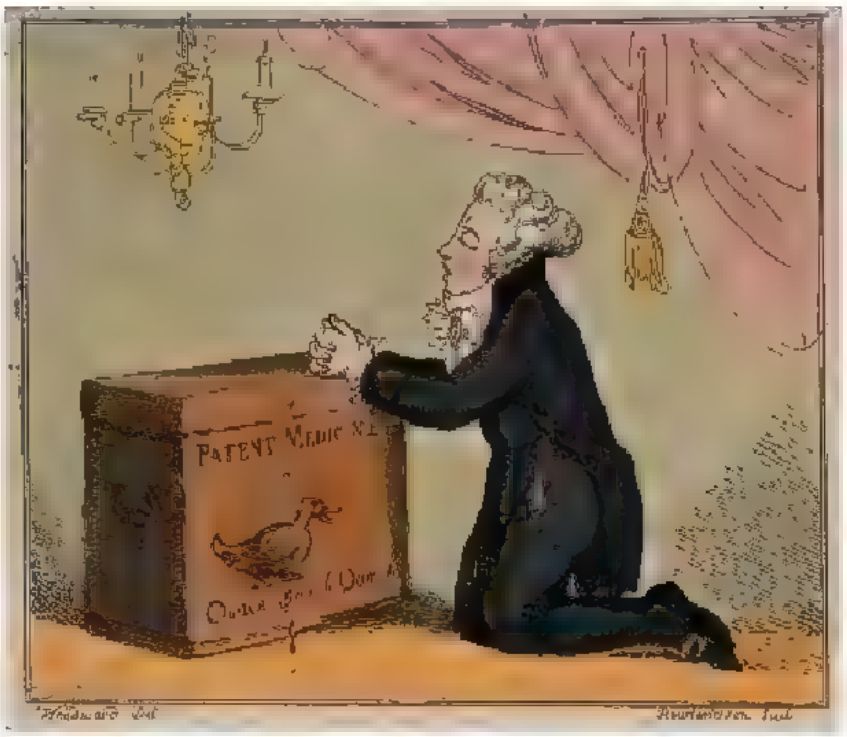

WELLCOME LIBRARY, LONDON

By the nineteenth century the pharmaceutical marketplace was less anarchic than before.

It was in this fraught setting that the basis for modern medical patenting was laid, complete with the debates that still dog the issue.

Log books

Various solutions were tried. Pharmacopoeias — official books listing recognized medicinal substances — had long existed. In 1618 the Royal College of Physicians issued the first national one, largely to police the pharmaceutical marketplace. It did not work. Pharmacopoeias were easy to pirate and to misuse. In 1690 Robert Boyle tried a different tack. He suggested in *Medicina Hydrostatica* that measuring specific gravities with a precision balance could reveal counterfeits. The proposal did not catch on. Neither rules nor technology did much to stop the flourishing of what French pharmacist A. P. Favre later called "pharmaceutical piracy."

Meanwhile France, England and the Netherlands were competing to establish global trading empires. Such international commerce depended on trust at a distance. Remote merchants, doctors and patients had to be confident in the authenticity of the goods being shipped. If medicines were untrustworthy even in London or Paris, what could the burgeoning empires do?

The answer proved to lie not in a regulatory code, nor in a machine, but in the assertion of authorship. It was an extension of the idea that one would trust a drug if one has seen the person who ground it up and handed it over. This solution drew on practices that had been developed to establish experimental science itself as the new universal learning.

At the Royal Society of London, founded in the early 1660s, experimenters had developed authorship and publication protocols to secure and protect discoverers and inventors. They sought to manage priority disputes, and to encourage participants to communicate new discoveries.

For example, the Society had established a register in which contributions were logged as they arrived, with dates and detailed descriptions. Inventions could be locked away in the Society's repository, and mathematical theorems lodged in code to safeguard them. The idea was to establish the Society as a 'bank' for what we now call science, to which contributors from continental Europe and the colonies could trust their reputations. In 1665 the Society also launched the first scientific journal, the *Philosophical Transactions*, as a public counterpart to this system. Experimental

philosophy became a self-perpetuating international endeavour. Its protocols became mainstays of the scientific enterprise itself.

Privileged few

Patents were different. Invented in the middle ages, a patent or 'privilege' was a legal document, issued by the king, extending state control over some economic goods such as steel, gunpowder or soap. Patents had long been controversial tools for rewarding favoured courtiers and tradesmen. In 1624, the English Parliament sought to limit them by passing the Statute of Monopolies, which ratified the use of patents only in cases of new inventions. This became the origin of all later intellectual-property law in the English-speaking world.

In practice, to obtain a patent for a new device was labyrinthine, expensive and uncertain. There was no such thing as a patents system in Britain until the mid nineteenth century, long after it had been created in the United States and, in a very different way, in France. There were isolated examples of patents on medical devices such as baths and distillation techniques. And some substances such as guaiac (imported from the New World and reputedly effective against syphilis) were privileged. But nobody seems to have sought a patent on a new pharmaceutical substance as such.

This makes it all the more interesting that the man who introduced pharmaceutical patenting to the English-speaking world was also responsible for maintaining the nascent protocols of experimental science. In effect, he created the modern alliance between authorship and authenticity in pharmaceuticals.

Grew knew

That man was Nehemiah Grew (1641–1712). Grew was a physician and advocate of, in his words, the anatomy and physiology of plants. Grew owed his reputation and livelihood to the Royal Society's authorship and publication system, which had secured his early botanical researches against potential rivals on the continent. He became Secretary of the Society in 1677, and for a few years took over the management of its all important international correspondence network and the *Philosophical Transactions*. Then Grew saw a chance to make his fortune. He began to manufacture and sell a "bitter purging salt" with the medicinal virtues of the spa water at Epsom, to which London's fashionable elite were then thronging. He hired an 'operator' (loosely, a foreman) named Thomas Trammel and set up a factory to mass-produce 'Epsom salts'.

Almost immediately Grew faced competition. A pair of brothers, Francis and George Moult, apothecaries both, set up their own Epsom-salts plant, and an extraordinary feud ensued. At its height, it implicated the public authority of the Royal Society and the Royal College of Physicians. Grew's camp called their rivals' salt a counterfeit. The Moults countered they stood for freedom of knowledge and accused Grew of being a monopolist. Grew's side responded that the competing salt was not just fake, but poisonous. It had already killed its first victim, they charged, an unfortunate Irish bishop.

First Grew tried to use the Royal Society's protocols to defend his enterprise. He appealed to its log of his own claim to priority. The Moults were unrepentant.

His next move was momentous. In 1698 he obtained a patent on his manufacturing technique from the royal court at Whitehall. It was not the first privilege on a medicine, but it does seem to have been the first on the basis of a medicine being an invention. Grew then transferred the patent to a friend and fellow physician Josiah Peter, who published a book mounting a vigorous defence of the inventor's right — and of the very principle of pharmaceutical patenting.

Confidence trick

Peter's defence, *Truth in opposition to ignorant and malicious falshood* [sic], is perhaps the single most important forgotten document in the history of 'intellectual property' in pharmaceuticals. Circulated in 1701, it advanced the first public argument for such property. Its rationale was precisely the phenomenon of trust that is now once again under such strain. It claimed, in short, that medical patenting must be created in order to secure confidence in the authenticity of medicines across international trade networks. Empires could be built on it.

Peter argued that Grew's salts could become a valuable commodity, and an economic asset to the British realm. This could only happen, he urged, if the preparation could be trusted abroad, as well as at home. A patent, Peter proposed, was the way to secure that trust. With a patent inhibiting imitators, the salts would benefit from trust at a distance, and a major new international business would surely come into being. Without one, "counterfeit salts" would jeopardize trade by destroying the reputations of any merchants who dealt in them.

Peter lost his fight over Epsom salts. The Moults continued to make and sell their copycat product. But a major step had been taken. Pharmaceutical patents began to increase soon after. The next one in England arrived in 1711, and more followed in a steady and growing stream. After the American Revolution, when the newly independent United States quickly established a legal machinery for issuing and policing patents, the practice expanded rapidly there too.

A national and international medicinal marketplace arose. The rules melded authorship and authenticity to secure both. They were premised neither on a Lockean philosophy of property (title being created by the application of labour) nor on a principle of Romantic genius (title deriving from the emanation of some uniquely individual creativity) — the two alternatives that we tend to invoke. Instead, those rules originated in the quest to establish genuineness. So it was that the alignment between trust and trade became foundational to the modern patenting regime in pharmaceuticals.

Today this alignment is once more cast into doubt. Again we face the problem of guaranteeing the identity of pills and powders across trade networks that extend far beyond national policing regimes. The dangers are real, and much greater than in pre-industrial Europe. Nonetheless, Grew's misfortune is worth recalling for two reasons. First, that the very idea of pharmaceuticals as authorial properties arose from a need to connect trade, empire and trust across global distances. Second, that the principle of medical authorship reflected the practical conventions from which modern science itself emerged.

> "If medicines were untrustworthy even in London or Paris, what could the burgeoning empires do?"

In other words, the forceful return of counterfeits spotlights tensions that are implicit in science and trade from their origins in the early modern period. What came into existence then was a medical marketplace for which patents provided principal ground-rules. They did not eliminate counterfeiting, of course, and patented drugs were never the only ones counterfeited, as remains the case today. Yet with authenticity brought into alignment with authorship by patenting, a system arose in which trust could persist at a distance — and both the trade and science of medicines could become global. The credibility of this system itself could only endure with constant policing. That too remains true today. The question for us is this: will the challenge of counterfeiting in a truly global economy force the protocols of scientific authorship and authenticity to change just as fundamentally all over again? ■

Adrian Johns is professor of history at the University of Chicago, 1126 East 59th Street Chicago, Illinois 60637, USA. His new book *Piracy* will be published by the University of Chicago Press.


MEDICAL NEWS
World's last AIDS patient now disease-free
Today, in labs all over the world, researchers are working around the clock to develop vaccines and other therapeutics against HIV. Soon all the components of a cure will be found. And after that, who knows? Maybe a complete victory over AIDS. When that day comes, we want to have played a small part in it. To learn more about the part scientists like you are playing in discoveries now, visit promega.com/today
©2007 Promega Corporation
TODAY COULD BE THE DAY.
Promega

NEWS & VIEWS

PANORAMIC IMAGES/GETTY IMAGES

Spa deposit — speleothems such as these examples in an Arkansas cave, can be reliable, long-term climate indicators.

PALAEOCLIMATE

The rhythm of the rains

Jonathan Overpeck and Julia Cole

Deposits in a Chinese cave tell the story of the region's climate stretching back more than 200,000 years, well past the last interglacial warm period — an invaluable resource for understanding the Asian monsoon.

In the quest to understand past climate change, and thus to anticipate future trends, records from cave deposits — speleothems — are increasingly taking centre stage. On page 1090 of this issue, Wang *et al.*[1] present a virtuoso study: a 224,000-year chronicle of the past variability of the East Asian monsoon, recorded in the oxygen isotope ratios of stalagmites built up from the floor of the Sanbao Cave in eastern central China. This is the latest in a series of records[2–7] from Chinese caves that has illuminated the workings of the East Asian monsoon, over timescales ranging from thousands of years to tens of millennia. Much remains to be understood, but the significance of this work extends well beyond the caves and the monsoon that feeds them. It provides yet more backing for a once-daring hypothesis: that wobbles in Earth's passage around the Sun are a prime mover of long-term monsoon variation.

As Earth moves around the Sun, its orbital eccentricity (the deviation of its path from a perfect circle) and its obliquity (the tilt of its rotational axis) vary slowly over time. The axis of its rotation also wobbles like that of a spinning-top, a phenomenon known as precession. These effects combine to induce a 23,000-year quasi-periodicity in the distribution of incoming solar radiation (insolation). At different stages of this slow precessional cycle, insolation at a particular place on Earth's surface may be strongest during winter, summer, or somewhere in between.

In 1981, John Kutzbach recognized[8] that the changing seasonal contrast in insolation might have a significant effect on the Asian monsoon, which is driven by different rates of seasonal heating over the continents and the oceans. By taking the values for the amount of radiation hitting Earth 9,000 years ago — when the Northern Hemisphere was closer to the Sun in summer than it is today, and the influence of glacial ice from the preceding ice age had all but disappeared — and plugging them into a climate model, he calculated that the Asian monsoon circulation must have been more intense at that time than it is today. That result matched observations that rainfall was greater in many areas of the tropics between 10,000 and 5,000 years ago. Various data sets have since been used to establish the details of this relationship over many precessional cycles.

Compared with other stalwart proxies of palaeoclimatology — records from tree-rings, sediments, ice cores, corals and the like — speleothems are relative newcomers. Like many proxies, they record the ratios of different oxygen isotopes in material laid down over time. These ratios are sensitively linked to the composition of precipitation, and thus to the prevailing climate. There are valuable examples of speleothem records from most continents, from mid-latitudes into the tropics, but few regions have proved to be as fertile as eastern China. Among the exciting records stored here are several from the Dongge Cave that span the Holocene, the interglacial period from 11,550 years ago to the present[3,6]. These complementary records elegantly confirm the orbital theory of monsoon variability, but also reveal decade- to century-scale variability that differs between geological formations (Fig. 1, overleaf).

Speleothems work best when there are consistent conduits for moisture to work its way through soil and rock into a relatively closed cave where, drip by drip, it contributes to the build-up of stalagmites. As carbon dioxide is lost from this dripwater, calcium carbonate ($CaCO_3$) precipitates. Many factors, including evaporation in soil and the nature of the cave environment, can change the oxygen isotope composition of the water after it leaves the atmosphere[9,10], interfering with the primary climatic signal. The robustness of a speleothem as a climate record thus depends on a large signal-to-noise ratio and on replication and/or calibration to identify clear climate signals.

Wang and colleagues' Sanbao Cave record[1] shows that essential aspects of past monsoon variability can be replicated not just within a single cave, but also between widely spaced caves in the same region: the monsoon signal

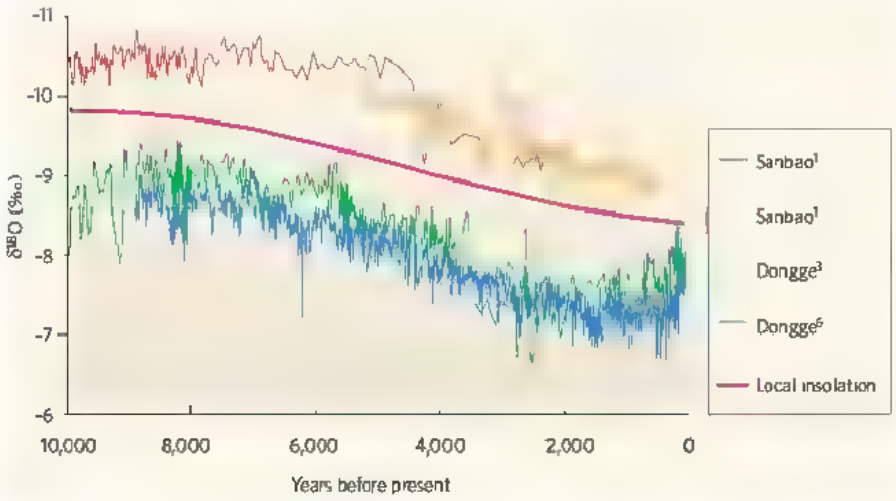

Figure 1 | Cave records. A comparison of oxygen isotope ratios (expressed as $\delta^{18}O$) from Sanbao[1] (two records) and Dongge[3,5] caves in eastern China over the Holocene period yields clear trends in agreement with millennial-scale decline in insolation[16] (in July at 30° N, pink line), caused by variations in Earth's orbit. The mean values are offset between the two caves owing to differences in elevation and temperature[1]. Century scale variance is not always consistent among the records, highlighting the need for replication to isolate climate signals that are uniform over whole regions.

swamps non-climatic and local noise over the long timescales of orbital change. What emerges is a record of monsoon variation unprecedented in its detail and chronology stretching back 224,000 years. The primacy of orbital precession in driving the monsoon with a quasi-periodic beat of approximately 23,000 years is nicely revealed, as are details of millennial monsoon variability that show the influence of changed ocean circulation in the North Atlantic during glacial periods.

These results bring into sharp relief the true power of speleothems: the ability to date their records precisely. This is made possible by measuring the growth of the isotope thorium-230 from the slow radioactive decay of uranium, which is incorporated in trace amounts in the speleothem deposits. This method works for samples hundreds of thousands of years old, far beyond the limit of about 50,000 years that radiocarbon dating allows. Until now, the best well-dated, high-resolution records of climate variability from the Northern Hemisphere have been those from the long cores extracted from the remote Greenland ice cap. These justly famous records extend back only into the last interglacial period, less than 125,000 years ago, and uncertainties in the models used to date the cores remain above the precision possible with uranium–thorium dating[11].

The Sanbao Cave record reveals that there is more to monsoon variability than a simple linear response to precessional climate effects. Precession unsurprisingly controls the largest changes in amplitude in the Asian monsoon, by altering the supply of latent heat from the Southern Hemisphere or the amount of heating over the adjacent, 5,000-metre-high Tibetan Plateau, or possibly both[8,12,13]. But the maximum-insolation peak during the last interglacial seems to have produced a weaker monsoon than smaller insolation maxima during the glacial period that preceded it. The monsoon response is also far less uniformly sinusoidal than the precession-induced variation in insolation, making it hard to judge the true nature of the phasing between the two effects. Work to unravel these mysteries will have to tap a variety of proxy sources and elaborate on the mechanisms linking monsoon variability to broader climate variability[14,15].

The smaller amplitude, higher-frequency variations of the monsoon that occurred during both glacial and interglacial periods are even more of a challenge here, the discrepancies between individual Sanbao records, just as with the Dongge data, indicate that details may be clouded by the smaller apparent signal-to-noise ratio (Fig. 1). Is the problem related to noise associated with cave processes? Or is it simply that smaller changes in climate forcing yield a monsoon response that varies more from place to place than is supposed? The answer will come from continuing to build up a network of data from different proxy sources, such as speleothems and lake and marine sediments, that covers the most recent glacial cycle, and especially the past 10,000 years.

The foremost goal is, of course, to anticipate how the Asian monsoon might change in the future. One thing seems certain: the monsoon is sensitive to climate changes, and if the future brings a sufficiently large net increase in summer heating of the Tibetan Plateau, its response could be large and relatively homogeneous. That could be good for those living in the shadow of the monsoon who need more rainfall. But a stronger monsoon would be hard on those in parts of south and east Asia already plagued by summer flooding. As sea levels rise along with monsoon floodwaters, the low-lying

50 & 100 YEARS AGO

50 YEARS AGO

Charles Dupin, a French mathematician and naval engineer visiting Britain in 1816, was much struck by two brothers who worked in a bakehouse which they had equipped with portable gas-lights. In the intervals of baking bread these two made a steam engine which they used in turn to make "des machines et des instruments de physique". Their uncle (who apparently owned the bakehouse) was neither amused nor interested; according to Dupin, "il préfère de beaucoup la boulangerie et la pâtisserie à la gazométrie et l'astronomie". These baking brothers, who symbolized for Dupin the incubation of technological zeal in Britain, were neither an isolated nor a new phenomenon.. The steam-intellect societies had begun.

From *Nature* 1 March 1958.

100 YEARS AGO

Alcohol and the Human Body—The importance of the alcohol question to the well-being of the race can scarcely be exaggerated, and in many respects this book will be very useful, but it is questionable whether the authors do not go too far in ascribing to alcohol ill effects only .. surely there is a consensus of opinion that the moderate use of good, well-matured spirit or wine is frequently beneficial in some disease conditions .. The experiments quoted, in which even weak solutions of alcohol are shown to be protoplasmic poisons, are hardly convincing as to the deleterious action of alcohol on the organism as a whole, for are not distilled water, 3 per cent salt solution, and beef-tea similarly protoplasmic poisons? A good deal is made of the supposed disastrous effect of alcohol on the nervous system, and it is stated that alcohol is accountable for 20 per cent of the cases under care in our asylums .. [but] in an American inquiry into the subject, total abstinence was found to be more frequently an antecedent of insanity than was intemperance.

From *Nature* 27 February 1908.

areas draining monsoon Asia could be especially at risk.

Jonathan Overpeck and Julia Cole are in the Departments of Geosciences and Atmospheric Sciences, University of Arizona, Tucson, Arizona 85721, USA.
e-mail: jto@u.arizona.edu

1. Wang, Y. et al. *Nature* **451**, 1090–1093 (2008).
2. Cheng, H. et al. *Geology* **34**, 217–220 (2006).
3. Dykoski, C. A. et al. *Earth Planet. Sci. Lett.* **233**, 71–86 (2005).
4. Kelly, M. J. et al. *Palaeogeogr. Palaeoclim. Palaeoecol.* **236**, 20–38 (2006).
5. Wang, Y. J. et al. *Science* **294**, 2345–2348 (2001).
6. Wang, Y. et al. *Science* **308**, 854–857 (2005).
7. Yuan, D. et al. *Science* **304**, 575–578 (2004).
8. Kutzbach, J. E. *Science* **214**, 59–61 (1981).
9. McDermott, F. *Quat. Sci. Rev.* **23**, 901–918 (2004).
10. Mickler, P. J., Stern, L. A. & Banner, J. L. *Geol. Soc. Am. Bull.* **118**, 65–81 (2006).
11. Andersen, K. K. et al. *Nature* **431**, 147–151 (2004).
12. Clemens, S. & Prell, W. *Mar. Geol.* **201**, 35–51 (2003).
13. Ruddiman, W. F. *Quat. Sci. Rev.* **25**, 657–658 (2006).
14. Goswami, B. N., Madhusoodanan, M. S., Neema, C. P. & Sengupta, D. *Geophys. Res. Lett.* **33**, doi:10.1029/2005GL024803 (2006).
15. Barnett, T. P., Dümenil, L., Schiese, U. & Roeckner, E. *Science* **239**, 504–507 (1988).
16. Berger, A. L. *J. Atmos. Sci.* **35**, 2632–2637 (1978).

BIOTECHNOLOGY

A hold on plant meiosis

Peter J. van Dijk

The process of meiosis involves genetic shuffling that dilutes the desirable traits of sexually reproducing crops. Identification of a mutation in which shuffling does not occur is a step forward for plant breeders.

Some plants can reproduce clonally through their seeds, resulting in offspring that are genetically identical to the mother plant. This unusual breeding system is called apomixis, and is known from more than 400 wild species, including dandelions, blackberries and various grasses. It does not occur in the major crops, which reproduce sexually. But it would greatly boost the efficiency of plant breeding if apomixis could be introduced into them.

On page 1121 of this issue, Siddiqi and colleagues[1] report on a mutation in the model plant *Arabidopsis* that promotes an essential element of apomixis — the omission of meiotic recombination and reduction. This is the exchange between parental chromosomes and the halving of the chromosome number that occurs during meiosis, the double cell-division that produces four haploid (n) gametes or spores from a single diploid ($2n$) precursor.

Crop domestication and improvement are based on the selection of superior plants for crossing. This enriches the gene pool with favourable genes. When a trait is controlled by many genes, each having a small effect, improvement is slow. There will still be wide genetic variation, with some individuals being much better than the rest. These outstanding genotypes are the winning tickets of the meiotic recombination lottery. Yet these gene combinations will be destroyed again by recombination in the next round of sexual reproduction.

The clearest example of the destructive effect of meiosis on favourable gene combinations comes from the self-fertilization of the first-generation offspring (F_1 hybrids; Fig. 1). F_1 hybrid cultivars of many crops are grown because their yield is superior to that of the parental inbred lines; this is a phenomenon known as heterosis, or hybrid vigour. But self-fertilization of the F_1 offspring and its descendants causes a progressive decline of the heterosis effect. Consequently, F_1 hybrid seeds have to be produced anew for each generation by the crossing of the parental lines, which is big business for seed companies. However, apomictic F_1 hybrids would be true-breeding for heterosis (Fig. 1); in general, any trait — no matter how complex its genetic control — could be fixed instantaneously through apomixis, starting from a single fortunate genotype. Apomixis therefore has the potential to revolutionize plant breeding and agriculture[2,3]. It is also the stuff of thrillers: a fictitious race for the first filing of a patent on an apomixis supergene, involving scientists, international corporations and intelligence services, was the central theme of a detective story published last year[4].

Apomixis involves the elimination of meiosis, such that a non-recombined, unreduced $2n$ egg cell is formed (apomeiosis), followed by its development into an embryo without fertilization (parthenogenesis). A further requirement for an apomictic seed is the development of the endosperm — a transient tissue that nourishes the developing embryo — either after fertilization or autonomously, as in some natural apomicts. Studies on the inheritance of apomixis in natural apomicts indicate that these elements of apomixis are genetically controlled[5]. So far, however, no genes controlling natural apomixis have been cloned.

Siddiqi and colleagues[1] looked for mutations in the sexually reproducing plant *Arabidopsis*. This is the main organism used for research in molecular plant biology, and in the mid-1990s three mutations, designated *fertilization-independent seed* mutations, were discovered that cause autonomous endosperm development[6]. Since then, a mutation that mimics the initial stages of parthenogenetic development has also been reported[7]. But fertile apomeiosis mutations were unknown.

Siddiqi and colleagues show that a recessive mutation called *dyad* results in functional apomeiotic egg cells. The *dyad* mutation is a variant copy of a gene involved in regulating chromosome organization during meiosis. In *dyad*/*dyad* plants, the two divisions of normal meiosis are replaced by a single one not involving meiotic recombination and reduction, the result is the formation of two unreduced ($2n$) spores instead of four reduced (n) spores. Developmental progression of *dyad* spores is usually blocked, leading to abortion of the cells. The authors show, however, that a few *dyad* spores escape this arrest and develop into fully functional, unreduced, diploid egg cells — which, after fertilization by haploid pollen grains, produce viable triploid ($3n$) offspring (viable parthenogenesis cannot yet be induced

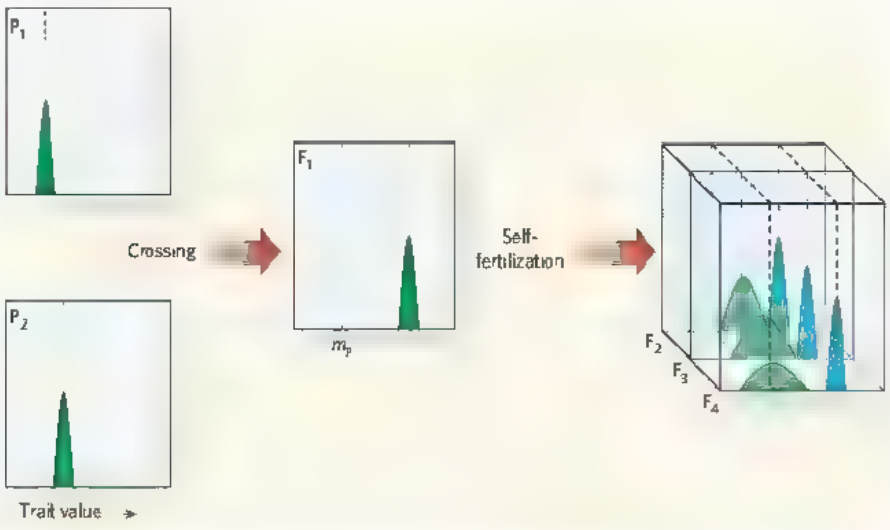

Figure 1 | The loss of heterosis (hybrid vigour) and its potential maintenance. The average trait value of the first generation (F_1) hybrids is higher than that of the mid-parent value (m_p) of the two parental inbred lines P_1 and P_2. Trait value is a measure of vigour, such as yield. Self-fertilization of the F_1, F_2 ... plants leads to a progressive reduction of heterosis in the following generations (green). With apomixis, such hybrids would be true-breeding for heterosis (blue).

BioMark
GENETIC ANALYSIS BY FLUIDIGM

THE NEW STANDARD IN HIGH THROUGHPUT REAL TIME PCR

You can learn from the past.

96-WELL MICROPLATES
- 24x more plates
- 48x more tips
- 125x more reagents
- 18x more time

You can improve on it.

384 WELL MICROPLATES
- 6x more plates
- 12x more tips
- 50x more reagents
- 5x more time

Or you can leave it behind.

The BioMark 48.48 Dynamic Array
- 1 simple, powerful, fast solution.

A single BioMark™ 48.48 Dynamic Array generates as much real-time PCR data as 24 96-well microplates. Surprisingly, this radically higher throughput requires 50-fold fewer pipetting steps and far less hands-on processing time. And you can switch to dynamic arrays and continue using the licensed PCR reagents already in your lab.

It's no wonder the BioMark system is emerging as the new standard for high-throughput gene expression profiling. Are you thinking about leaving the past behind? Contact Fluidigm to learn how the Biomark system can help your organization achieve a higher throughput future.

Heat Map View provides a macro-to-micro view of C_t values within the entire array.

Fluidigm

Toll-free: 1.866.FLUIDLINE (866.358.4354) | Fax: 650.871.7152 | www.fluidigm.com

Sales: North America: 1 650.266 6170 | biomark@fluidigm.com
Europe/EMEA: +31 20 578 8853 | biomarkeurope@fluidigm.com
Asia: +81 3 3555 2351 biomarkasia@fluidigm.com

in *Arabidopsis*). Using various tests, Siddiqi and colleagues exclude alternative origins of the triploid offspring, and convincingly show that the full maternal genome is transmitted by the unreduced egg cells.

The *dyad* mutation affects only female meiosis of a plant, not the male meiosis that produces pollen. This female specificity also applies to the genetic factors that control apomeiosis in natural populations. However, there are also notable differences between natural apomicts and plants carrying the *dyad* mutation. Apomeiosis in natural apomicts is always inherited dominantly, whereas *dyad* is recessive. Moreover, the expression of apomeiosis in natural settings is much higher than that of the *dyad* mutation in *Arabidopsis* — as witnessed by the fact that apomictic dandelions are highly prolific. The developmental block that usually prevents the development of *dyad* spores in *Arabidopsis* is perhaps modified in these dandelions.

The existence of *dyad* and other mutations shows that apomixis-like development is possible in *Arabidopsis*. In sexually reproducing crops, apomixis-like developmental errors, such as unreduced gametes and haploid offspring, occur at low frequencies. Thus, sexual plants have a latent capacity for apomictic seed development, and it should be possible to genetically engineer apomixis into sexual crops.

Plant breeding is confronted by towering challenges, among them the production of higher-yielding crops to feed the growing world population, the adaptation of crops to changing climates, and the development of crops for renewable industrial feedstock. Apomictic crops could be part of the answer. But the expression of *dyad* characteristics will have to be much improved; parthenogenesis will have to be introduced, and the problem of endosperm formation will have to be considered. Ideally, apomixis should be inducible in crops such that meiosis could be switched on when new variation is needed and switched off when the best results are to be maintained. To achieve this ultimate goal, vision and determination are needed, but the rewards could be tremendous. More than 9,000 years after the dawn of agriculture, it is high time to bring meiosis under control. ■

Peter J. van Dijk is at KeyGene NV, Agro Business Park 90, 6708 PW Wageningen, the Netherlands.
e-mail: peter.van-dijk@keygene.com

1. Ravi, M., Marimuthu, M. P. A. & Siddiqi, I. *Nature* **451,** 1121–1124 (2008).
2. Vielle-Calzada, J. P., Crane, C. F. & Stelly, D. M. *Science* **274,** 1322–1323 (1996).
3. Spillane, C., Curtis, M. D. & Grossniklaus, U. *Nature Biotechnol.* **22,** 687–691 (2004).
4. Pringle, P. *Day of the Dandelion* (Simon & Schuster, New York, 2007).
5. Ozias-Akins, P. & van Dijk, P. J. *Annu. Rev. Genet.* **41,** 465–507 (2007).
6. Chaudhury, A. M. *et al. Proc. Natl Acad. Sci. USA* **94,** 4223–4228 (1997).
7. Guitton, A. & Berger, F. *Curr. Biol.* **15,** 750–754 (2005).

HISTORY OF SCIENCE

Quinine steps back in time

Philip Ball

Chemists have long memories. The claim, dating back to 1918, that a crucial step in a synthesis of quinine had been carried out has been validated experimentally, closing a chapter in this fascinating story.

"One of the greatest scientific achievements in a century" was how *The New York Times* hailed the 'total synthesis' of quinine reported in 1944 by Robert Woodward and William Doering at Harvard University[1,2]. But had they really achieved it at all? The debate has continued, sometimes with considerable heat, into the twenty-first century.

In a paper[3] dedicated to Doering on his ninetieth birthday, Aaron Smith and Robert Williams now say that they have settled the matter. They show that the contentious 'missing step' in Woodward and Doering's synthesis, which the Harvard pair assumed to have been demonstrated previously by Paul Rabe and Karl Kindler in 1918, is indeed possible under the conditions sketchily described in that early work[4]. Figure 1 shows Woodward and Doering shortly after the announcement of their achievement.

There are several reasons why this apparent footnote in the history of natural-product synthesis takes on wider significance. Ever since the physician Juan del Vega allegedly administered *quina*, an extract of the bark of the New World 'fever tree' now known as cinchona, to the wife of the viceroy of Peru in the 1630s and cured her malaria, quinine was recognized as just about the only effective agent against this pervasive tropical disease. The gin and tonics of the British colonial Raj were considered a necessity rather than a luxury, providing a daily dose of quinine in the 'tonic' water. Identified as the active ingredient in 1820, quinine quickly became a desirable target for chemical synthesis; one failed attempt in 1856 by the young William Henry Perkin led serendipitously to the discovery of aniline dyes and the birth of the modern chemicals industry.

Woodward and Doering's synthesis was also the launching point of Woodward's stellar career, which saw him become an unrivalled master in the art of molecule-building and, in 1965, a Nobel laureate. In the 1940s, the synthesis of quinine looked urgent when the war in southeast Asia cut off supplies of the drug that were sorely needed by soldiers in the Pacific. But although Woodward had promoted the synthesis of quinine in this context since 1942, his immediate motivation was commercial rather than military: he was contracted by the Polaroid Corporation to look for synthetic alternatives to quinine as a precursor to light-polarizing molecules.

Quinine is a fearsome synthetic target: it is an alkaloid with a complicated, multi-ring framework that has four stereogenic centres (where the atoms can be arranged in mirror-image 'chiral' forms) and thus 16 stereoisomers. Delicate control of stereochemistry in organic synthesis was well beyond the capabilities of nineteenth-century chemists, who didn't even know of such things until the work of Jacobus Henricus van't Hoff and Joseph-Achille Le Bel in the 1870s. But by the time Woodward and Doering came to attack the problem, much of the pathway for quinine synthesis had already been solved.

Rabe and Kindler had claimed to have reconstituted quinine from a degradation product called *d*-quinotoxine, in which a carbon–

AP

Figure 1 | Gin and tonics all round. Robert Woodward (left) and William Doering were fêted for their 'formal' synthesis of quinine in 1944. This achievement has been questioned, but Smith and Williams[3] have now validated their work.

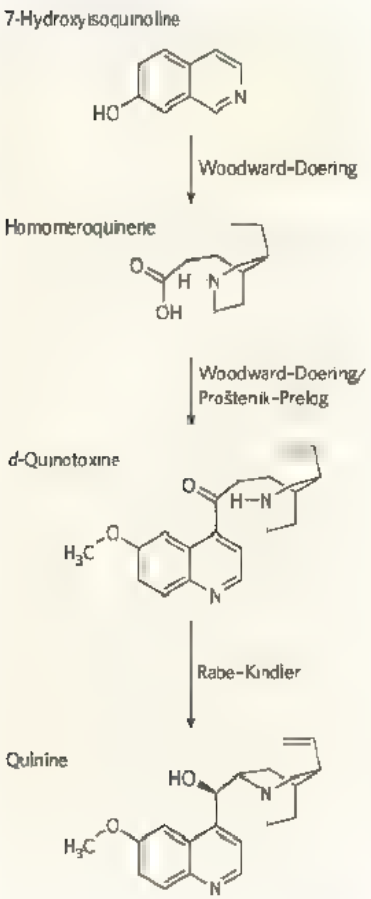

Figure 2 | The formal synthesis of quinine. This simplified scheme shows the steps achieved in the 1940s by Woodward and Doering (7-hydroxyisoquinoline to *d*-quinotoxine) and Prostenik and Prelog (homomeroquinene to *d*-quinotoxine). The claim to a full synthesis depended, however, on the final stage depicted here, which was published in 1918 by Rabe and Kindler and has only now been validated experimentally[3], in which quinine is a product.

nitrogen bond is cut (Fig. 2). And in the early 1940s, Vladimir Prelog and Mihovil Prostenik made *d*-quinotoxine from a still-simpler degradation product, homomeroquinene[5].

Woodward and Doering's contribution was to take the path right back to (relatively) simple starting materials, demonstrating the synthesis of homomeroquinene from 7-hydroxyisoquinoline and then on to *d*-quinotoxine[1,2] (Fig. 2). This then completed the 'formal' total synthesis, even though they had not seen the full pathway through themselves; this is standard practice for organic chemists. As well as giving organic chemistry a rare spate of media celebrity — the news reached *Time*, *Life* and *The New Yorker* — the paper is now widely viewed as heralding a new era in synthesis.

But had Rabe and Kindler really achieved stereochemical control of the final step? That wasn't apparent from their account[4], which was little more than a page long. Feeling that the case was unproven, Gilbert Stork, a graduate student who came to Harvard in 1944, began work on a new total synthesis in 1946 — a monumental effort that he completed, by a totally different route, only in 2001 (ref. 6).

Stork has asserted that the Woodward–Doering claim was a "widely believed myth ... in part based on wishful thinking", and that Rabe and Kindler's part of the synthesis would not have worked had they tried it[7]. This idea has found its way into both the technical and the popular literature, although it has been hotly contested. In an exhaustive analysis of published literature and private correspondence, Jeffrey Seeman[8] recently asserted that "Rabe and Kindler did convert *d*-quinotoxine into quinine" in 1918, and thus that "the Woodward–Doering/Rabe–Kindler total synthesis of quinine is a valid achievement".

Smith and Williams[3] have now validated Seeman's assertion experimentally: they have reproduced the Rabe–Kindler protocol (described in more detail for other *Cinchona* alkaloids in a later publication by Rabe[9]), and find that they can make quinine with about a 5% yield, along with comparable amounts of the diastereomer quinidine. Because diastereomers are stereoisomers (differing in the chirality of stereogenic centres) but not enantiomers (mirror images), they have different physical properties and can be separated from one another by straightforward crystallization as the salt of a chiral compound (in this case, tartrate).

But there's a twist. The key step is a reduction using aluminium powder, the purity and freshness of which seems to be crucial. Only when the powder was partly oxidized, did Smith and Williams[3] obtain an appreciable yield, suggesting that success of the method owes much to chance. Old, aerated aluminium powder generally works well, but Smith and Williams found that even the batch-to-batch variations in commercial-grade material significantly affect the outcome. It's not hard to imagine that Rabe and Kindler got lucky; pedants might even still argue that reporting "reduction with aluminium powder" doesn't quite convey what is really going on.

All the same, there's now no reason to doubt Rabe and Kindler's success. The new results, say Smith and Williams, "should serve to remove the blemish" not only on their reputations, but on those of Woodward and Doering. At the same time, it does nothing to diminish Stork's achievement, which has been labelled a classic of total synthesis in its own right. ■

Philip Ball is a consultant editor for *Nature*.
e-mail p.ball@nature.com

1. Woodward, R. B. & Doering, W. E. *J. Am. Chem. Soc.* **66**, 849 (1944)
2. Woodward, R. B. & Doering, W. E. *J. Am. Chem. Soc.* **67**, 860–874 (1945)
3. Smith, A. C. & Williams, R. M. *Angew. Chem. Int. Edn* **47**, 1736–1740 (2008)
4. Rabe, P. & Kindler, K. *Ber. Deutsch. Chem. Ges.* **51**, 466–467 (1918)
5. Prostenik, M. & Prelog, V. *Helv. Chim. Acta* **26**, 1965–1971 (1943)
6. Stork, G. *et al. J. Am. Chem. Soc.* **123**, 3239–3242 (2001)
7. Rouhi, A. M. *Chem. Eng. News* **79** (7 May), 54–56 (2001)
8. Seeman, J. I. *Angew. Chem. Int. Edn* **46**, 1378–1413 (2007)
9. Rabe, P. *Justus Liebigs Ann. Chem.* **492**, 242–266 (1932)

CANCER

Crossing over to drug resistance

David M. Livingston and Daniel P. Silver

Certain cancers stem from mutations that prevent a cell from repairing its damaged DNA efficiently. But antitumour chemotherapy that exploits that repair defect can in turn be nullified by counter-mutation.

Two papers[1,2] in this issue provide insight into a subset of breast and ovarian cancers, the action of drugs used to treat them, and a novel mechanism of chemotherapeutic drug resistance. The papers are by Edwards *et al.* (Ashworth and colleagues)[1] and Sakai *et al.* (Taniguchi and colleagues)[2], and appear on pages 1111 and 1116. These groups have analysed the molecular basis for resistance to specific anticancer drugs in tumours that have defects in a process known as homologous recombination (HR), a particular pathway for DNA-damage repair. The drugs in question — two platinum analogues, cisplatin and carboplatin, and PARP inhibitors — exploit defective HR in these tumours. Drug resistance develops when specific mutations restore HR and, thus, the cancer cells' ability to survive when exposed to these agents.

At the centre of events is *BRCA2*, a tumour-suppressor gene that encodes a protein with a key role in HR. Inactivation of *BRCA2* results in defective repair of DNA double-strand breaks. The most dramatic — and tragic — outcome is cancer, usually of the breast or ovary. The cancer cells cannot deal with DNA double-strand breaks using HR, and must rely on other DNA-repair processes for eliminating this otherwise lethal damage. *BRCA2*-deficient (*BRCA2*$^{-/-}$) cells also cannot remove abnormal DNA chemical crosslinks efficiently. This removal process requires a cell to deal with the crosslink itself, as well as with the double-strand break that results from crosslink removal. Thus, DNA crosslinking agents can be used to kill *BRCA2*-deficient tumour cells. Such agents include cisplatin and carboplatin (both referred to here as Pt), which are the current mainstay of ovarian cancer treatment.

Single-strand breaks in DNA must also be

repaired in *BRCA2*-deficient cells. Otherwise, during DNA replication, these breaks can evolve into deadly double-strand breaks. This requirement led to a proposal[3,4] of a new therapeutic strategy for HR-deficient tumour cells, including *BRCA2*$^{-/-}$ cells. Base-excision repair, another DNA-repair pathway, is involved in repairing single-strand DNA breaks. Among the proteins that are essential in base-excision repair is poly(ADP-ribose) polymerase (PARP). The idea was that an inhibitor of PARP would kill HR-deficient cells but not their normal counterparts. This is because HR-deficient cells, including those that are *BRCA2*$^{-/-}$, cannot rely on HR to repair the double-strand breaks that evolve from single-strand breaks when base-excision repair is inhibited. The results of tissue-culture experiments supported this hypothesis, and clinical trials of potent PARP inhibitors are afoot.

Ashworth's and Taniguchi's groups[1,2] now describe the results of analysing drug-resistant *BRCA2*-deficient tumour cells. The story is the same in clones derived from cultured *BRCA2*$^{-/-}$ tumour cells that are resistant to PARP inhibitors or Pt, and in Pt-resistant *BRCA2*$^{-/-}$ ovarian cancers from the clinic. Tumour cells carrying a known, disease-inducing mutation of the *BRCA2* gene that produces a shortened, defective protein incur a second mutation that results in the production of a functionally normal protein. More specifically, the consequences of the original ('frameshift') mutation are largely negated by a second mutation that re-establishes the normal *BRCA2* sequence. Consequently, unlike their predecessors, the revertant cells are HR 'competent' — that is, they can perform HR. As a result, they are resistant to the drug to which they were once sensitive. Transfer of the double-mutant, resistance-associated *BRCA2* gene variant to a *BRCA2*-deficient, HR defective cell line confers both HR competence and drug resistance. Thus, in patient tumour cells and cell lines alike, HR competence spells resistance to both PARP inhibitors and Pt. This result shows unequivocally that these drugs require faulty HR for antitumour activity in this setting.

The results have clinical implications for situations in which drug resistance has developed. Further treatment with chemotherapy that creates DNA crosslinks, or inhibits base-excision repair, is likely to be less effective in HR-competent cells than in HR-incompetent cells. Moreover, in HR-incompetent cells that have acquired drug resistance through other mechanisms (such as the action of cellular pumps that eject the drug), the use of treatments different from those to which resistance has arisen is an obvious course — a different form of DNA-crosslinking chemotherapy, for example, or a different class of agents that inhibit base-excision repair.

There is even a potential biomarker that could, in principle, be used to assess HR competence in tumour cells, and thus instruct therapeutic decisions. This biomarker is Rad51, a protein that catalyses a key step in HR. A sign of HR competence is the appearance of Rad51-containing foci in the nuclei of cells after double-strand breaks have occurred. Many HR-incompetent cells cannot produce these foci, whereas most HR-competent cells should contain them. When present, they can be readily visualized by immunofluorescence. Isolation of viable tumour cells by direct biopsy of a tumour mass, or even from the patient's bloodstream, as recently suggested[5], might make it possible to analyse post-damage Rad51 foci and help to clarify the nature of a patient's drug resistance.

The new findings[1,2] raise other considerations. Neither Pt nor PARP inhibitors interact directly with the mutant protein (BRCA2) whose functional reactivation leads to resistance. So, drug-design strategies that target anticipated resistance mutations, and that have been useful in other tumour-cell settings, will not apply in this one. Further, we may be seeing here the beginning of a new challenge in the growing discipline of pharmacogenomics, which deals with the influence of genetics on drug responsiveness. This is because different *BRCA2* mutations probably vary in their ability to undergo reversion by the kinds of mechanisms described by the authors[1,2]. One wonders, for example, whether patients with substantial *BRCA2* deletions have more durable clinical responses to Pt than patients with mutations that are more readily amenable to reversion, such as the ones studied in these reports.

Finally, there are broader implications. Many patients with ovarian cancer who have normal *BRCA2* genes respond to Pt. So it could be that their tumour cells are inherently less HR competent than the normal cells from which they are derived. Second, until now it has remained a possibility that continued BRCA2 deficiency is required for maintaining various features of cancer. This is especially so given recent evidence that the absence of BRCA1, a tumour-suppressor protein involved in many of the same processes as BRCA2, helps a tumour to recruit a blood-vessel supply, which is essential for tumour survival[6]. However, a tumour analysed by the Taniguchi group[2] contained a direct reversion of the HR-deficient *BRCA2* mutation after Pt therapy. This resulted in a completely normal *BRCA2* coding unit and therefore restoration of a normal BRCA2 protein, but no regression of the tumour. These findings imply that a temporary loss of BRCA2 function is enough to establish the cancer, which is consistent with the view that BRCA2 loss results in a substantially increased rate of DNA damage that, in turn, triggers cancer. In other words, the results reinforce the notion that *BRCA2* is a caretaker tumour-suppressor gene (inactivation of which allows mutation in other cancer-causing genes), and not a gatekeeper tumour-suppressor gene (which directly controls tumour growth)[7]. ■

David M. Livingston and Daniel P. Silver are at the Dana-Farber Cancer Institute, Harvard Medical School, 44 Binney Street, Boston, Massachusetts 02115, USA.
e-mails: david_livingston@dfci.harvard.edu; daniel_silver@dfci.harvard.edu

1 Edwards, S. L. *et al. Nature* **451**, 1111–1115 (2008)
2 Sakai, W. *et al. Nature* **451**, 1116–1120 (2008)
3 Bryant, H. E. *et al. Nature* **434**, 913–917 (2005)
4 Farmer, H. *et al. Nature* **434**, 917–921 (2005)
5 Nagrath, S. *et al. Nature* **450**, 1235–1239 (2007)
6 Furuta, S. *et al. Cancer Cell* **10**, 13–24 (2006)
7 Kinzler, K. W. & Vogelstein, B. *Nature* **386**, 761–763 (1997)

ENVIRONMENTAL ECONOMICS

To the rich man the spoils

R. Kerry Turner and Brendan Fisher

Global economic growth during the past century has lifted many into lives of unprecedented luxury. The cost has been the degradation of vital ecosystems — a cost borne disproportionately by the world's poor.

Through our rapacious exploitation, ecosystems and the benefits they bring to us are disappearing at an unprecedented and alarming rate. Qualitative evidence suggests that the rich world is profiting from this process, whereas poorer countries are bearing the brunt of the resulting environmental degradation. Srinivasan *et al.*[1], writing in *Proceedings of the National Academy of Sciences*, provide a quantitative basis for that claim, calculating the distribution of costs and benefits over a range of indicators of ecosystem change. The results might, in an ideal world, lead to a radical reassessment of who is in debt to whom.

Measured in terms of gross domestic product (GDP), the size of the world's economy has doubled almost three times since 1950. But the proposition that aggregate economic growth alone is the most important and powerful force for human progress and poverty reduction has increasingly been questioned[2,3]. Economic growth fuelled by international trade relies on the consumption of heavily advertised and marketed goods and services. Poorer people and the natural world, marginalized by the market economy, lose out.

Besides basic economic needs, a high quality of human life must include satisfactory human

relationships, communities, freedoms and opportunities[4,5]. Well-functioning ecosystems are even more fundamental. The buzz-word is 'ecosystem services': the favours such as food and fuel, protection from storms, disease and solar radiation; regulation of water and climate; creation of soils, and inspiration for art, literature, religion and culture that the natural world bestows on us. Current economic models undervalue this provision, because many ecosystem services are 'public goods', historically provided for free. This leaves them prone to overexploitation, a trend exacerbated by global population growth: 15 of the 24 ecosystem services identified in the seminal Millennium Ecosystem Assessment initiated by the United Nations in 2001 were found to be in decline at the global scale[6].

The current political focus on climate change has brought this pressure on our ecological support systems into sharper relief. Sustaining ecosystem processes is all the more difficult because many change abruptly and nonlinearly when pressed beyond a certain threshold. Qualitative or context- and case-specific evidence indicates that poorer countries bear most of this pressure[7]. An example is the widespread conversion of tropical mangrove forests to shrimp aquaculture. These farms supply Europe and North America with cheap shrimp, but nearby residents must pay the costs: the loss of the storm regulation, fish nurseries, and fuel and fibre sources that the mangrove forests provided[8].

This type of unequal exchange has been termed an 'ecological debt' owed by rich countries to the poor[7]. As raw materials — whether they be shrimp, palm oil, or crude oil and gas — become scarcer, and exploitation of them advances into new territories, this debt will probably increase. The prices at which exports are sold do not include compensation for the goods' local — or sometimes global — environmental costs. That problem is exacerbated by rich countries' disproportionate use of environmental sinks, such as the atmosphere, to take up their higher carbon emissions.

Srinivasan *et al.*[1] present for the first time a global-scale quantitative analysis of the distribution of major environmental costs across nations in three income groups: low (representing 32% of the world's population), middle (50%) and high (18%). The timescale of the study is 1961–2000, and it covers six categories of environmental change: climate change; stratospheric ozone depletion; agricultural intensification and expansion; deforestation, overfishing; and mangrove conversion. In the case of climate change, the authors calculate that nations in the low, middle and high income groups were responsible for 13%, 45% and 42% of greenhouse-gas emissions, respectively. The resulting climate damages were estimated to be distributed 29%, 45% and 25%. The same pattern of cost transfer to the poorest nations is observed for ozone depletion, overfishing and aquaculture. In the case of agricultural change and deforestation, the authors find that arguably the costs were largely generated and borne within nations.

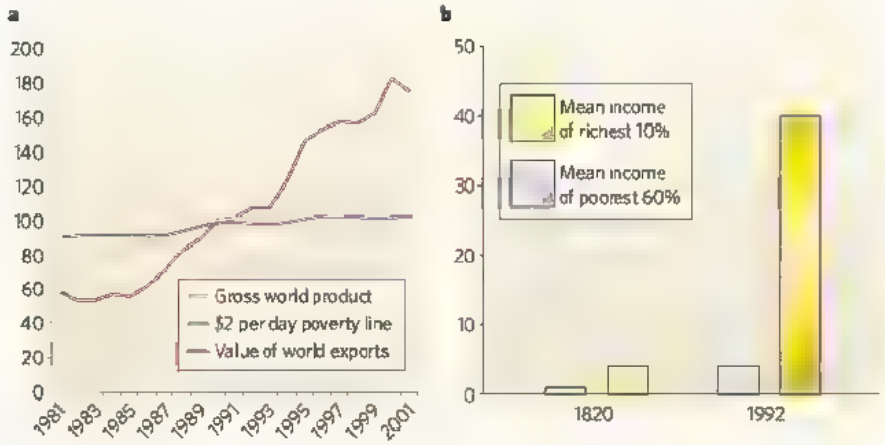

Figure 1 | Inequality in economic growth. **a**, Although gross world product and the value of exports throughout the world rose steadily during the period 1981–2001 (values relative to 1990 = 100), the number living below the US$2 per day poverty line has increased slightly[10]. **b**, Whereas in 1820 the difference between the mean incomes of the poorest 60% of countries and of the richest 10% was fourfold, by 1992 the disparity was tenfold (value of mean income of poorest countries in 1820 = 1)[9].

When the figures for the six categories are aggregated and adjusted for different currency purchasing power, the low-income group of nations bears 20% of the total costs, the middle-income group 60% and the high income group 20%. Taking into account equity weighting (the fact that a unit of income is not the same to a poor as to a rich person, making costs a heavier burden to shoulder) the percentages are 45%, 52% and 3%. A significant proportion of the cost burden of the low-income group is caused by the activities of the other groups looking at climate-change damage alone, rich countries might already have imposed costs on poor countries greater than the poor countries' existing foreign debt. The people bearing these costs include the one billion or so who already lack daily access to safe drinking water, electricity, secure food supplies and basic education.

Several caveats are needed to put these striking results into context. First, any study is only as good as the available data. Globally robust data sets on environmental externalities are incomplete, and therefore the results are indicative, not absolute. Some significant environmental changes have been omitted: the destruction of coral reefs, the dispersal of persistent pollutants and the costs of biodiversity loss. The authors are up-front about these limitations. But they justly suggest that the omissions indicate that their estimates of ecological debts are conservative.

Furthermore, the study does not look at the benefits of increased trade to material wealth and human health. But it is unlikely that this would change the balance of the results: the available, albeit partial, evidence indicates that, despite some gains by poorer countries through the liberalization of trade and finance, the number of people living in poverty has increased or stayed the same during the past 25 years, and the gains of economic globalization have been heavily skewed towards wealthy nations[2] (Fig. 1). One of the most detailed studies on global inequality concludes[9] that income divergence between rich and poor nations has "at best … decelerated after 1950, but [has] not reversed". Large areas of Central and South America, and almost all of sub-Saharan Africa, have been left behind.

Srinivasan and colleagues' work[1] should raise the scientific profile of issues vital to human well-being, including research into ecosystem services and the effects of large-scale ecosystem conversion, and how such changes both create and alleviate poverty. We must better understand the complex interactions between our economic, social and ecological systems, and the biological diversity that supports them. Scientists and society as a whole need to ask of our current economic paradigms in an era of globalization: why do they produce such inequities; who pays the costs; and are they ecologically and socially sustainable? ■

R. Kerry Turner and Brendan Fisher are at the Centre for Social and Economic Research on the Global Environment (CSERGE), School of Environmental Sciences, University of East Anglia, Norwich, Norfolk NR4 7TJ, UK.

1. Srinivasan, U. T. *et al. Proc. Natl Acad. Sci. USA* doi:10.1073/pnas.0709562104 (2008)
2. Stiglitz, J. E. *Globalization and its Discontents* (Norton, New York, 2003)
3. Wade, R. H. *World Dev.* **32**, 567–589 (2004)
4. Sen, A. *Development as Freedom* (Anchor, New York, 1999)
5. Layard, R. *Happiness: Lessons from a New Science* (Allen Lane, London, 2005)
6. *Millennium Ecosystem Assessment, Ecosystems and Human Well-Being: Synthesis* (Island, Washington DC, 2005)
7. Martinez-Alier, J. *The Environmentalism of the Poor* (Oxford Univ. Press, New Delhi, 2005)
8. Sathirathai, S. & Barbier, E. B. *Contemp. Econ. Pol.* **19**, 109–122 (2001)
9. Bourguignon, F. & Morrisson, C. *Am. Econ. Rev.* **92**, 727–744 (2002)
10. World Development Indicators 2007 www.worldbank.org/data (2007)

REVIEWS

Autophagy fights disease through cellular self-digestion

Noboru Mizushima[1], Beth Levine[2], Ana Maria Cuervo[3] & Daniel J. Klionsky[4]

Autophagy, or cellular self-digestion, is a cellular pathway involved in protein and organelle degradation, with an astonishing number of connections to human disease and physiology. For example, autophagic dysfunction is associated with cancer, neurodegeneration, microbial infection and ageing. Paradoxically, although autophagy is primarily a protective process for the cell, it can also play a role in cell death. Understanding autophagy may ultimately allow scientists and clinicians to harness this process for the purpose of improving human health.

At first glance, it may seem perplexing that a process of cellular self-eating could be beneficial. In its simplest form, however, autophagy probably represents a single cell's adaptation to starvation—if there is no food available in the surroundings, a cell is forced to break down part of its own reserves to stay alive until the situation improves. In single-cell organisms such as yeasts, this starvation response is one of the primary functions of autophagy, but in fact this role extends up through to humans. For example, even on a day-to-day basis, autophagy is activated between meals in organs such as the liver to maintain its metabolic functions, supplying amino acids and energy through catabolism[1,2].

There are various types of autophagy, including micro- and macroautophagy, as well as chaperone-mediated autophagy (CMA), and they differ in their mechanisms and functions (Fig. 1)[3,4]. Both micro- and macroautophagy have the capacity to engulf large structures through both selective and non-selective mechanisms, whereas CMA degrades only soluble proteins, albeit in a selective manner. The capacity for large-scale degradation is important in autophagic function, but it carries a certain risk, because unregulated degradation of the cytoplasm is likely to be lethal. On the other hand, basal levels of autophagy are important for maintaining normal cellular homeostasis. Thus, it is important that autophagy be tightly regulated (Fig. 2) so that it is induced when needed, but otherwise maintained at a basal level. Although a complete picture of autophagy regulation is not available, many aspects have been covered in recent reviews[5–8].

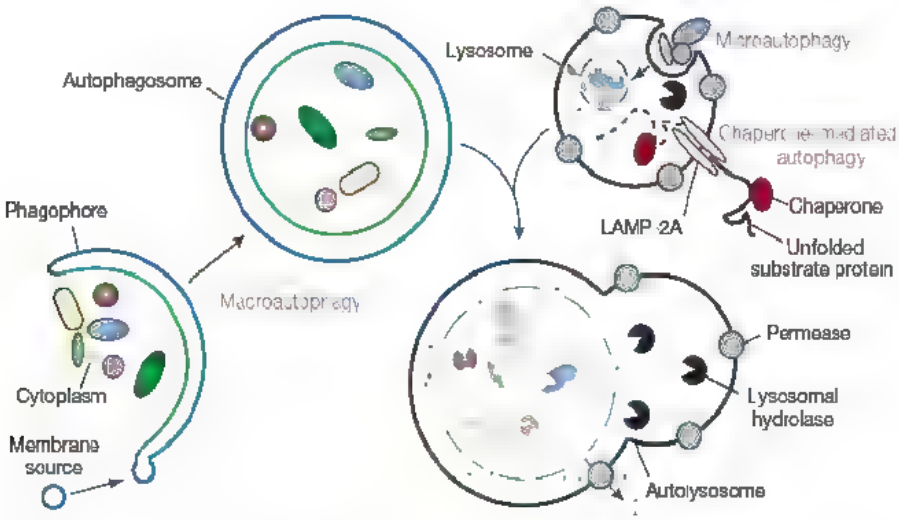

Figure 1 | Different types of autophagy. Microautophagy refers to the sequestration of cytosolic components directly by lysosomes through invaginations in their limiting membrane. The function of this process in higher eukaryotes is not known, whereas microautophagy-like processes in fungi are involved in selective organelle degradation. In the case of macroautophagy, the cargoes are sequestered within a unique double-membrane cytosolic vesicle, an autophagosome. Sequestration can be either nonspecific, involving the engulfment of bulk cytoplasm, or selective, targeting specific cargoes such as organelles or invasive microbes. The autophagosome is formed by expansion of the phagophore, but the origin of the membrane is unknown. Fusion of the autophagosome with an endosome (not shown) or a lysosome provides hydrolases. Lysis of the autophagosome inner membrane and breakdown of the contents occurs in the autolysosome, and the resulting macromolecules are released back into the cytosol through membrane permeases. CMA involves direct translocation of unfolded substrate proteins across the lysosome membrane through the action of a cytosolic and lysosomal chaperone hsc70, and the integral membrane receptor LAMP-2A (lysosome-associated membrane protein type 2A)

[1]Department of Physiology and Cell Biology, Tokyo Medical and Dental University, Tokyo 113-8519, Japan. [2]Departments of Internal Medicine and Microbiology, University of Texas Southwestern Medical Center, Dallas 75390, USA. [3]Departments of Anatomy and Structural Biology and of Developmental and Molecular Biology, Marion Bessin Liver Research Center, Albert Einstein College of Medicine, Bronx, New York 10461, USA. [4]Life Sciences Institute and Departments of Molecular, Cellular and Developmental Biology and Biological Chemistry, University of Michigan, Ann Arbor 48109, USA.

Both the non-selective and selective nature of autophagy, as well as basal and induced levels, are important in regard to the role of this process in human health and disease. Perhaps the most fundamental point is that either too little or too much autophagy can be deleterious, a complexity seen in its dual role in cytoprotection and cell death. With the identification of many *autophagy-related* (*ATG*) genes and improved methods for monitoring this process, future research on this topic should continue to progress.

Autophagy in cell survival and cell death

The pro-survival function of autophagy has been demonstrated at the cellular and organismal level in different contexts, including during nutrient and growth factor deprivation, endoplasmic reticulum stress, development, microbial infection, and diseases characterized by the accumulation of protein aggregates[8–11]. This pro-survival function is generally believed to be adaptive, but, in the context of cancer, is potentially maladaptive[12]. Metabolic stress is a common feature of the tumour microenvironment and most chemotherapeutic agents induce cellular stress. Thus, an area of intense investigation is whether autophagy-dependent survival should be blocked in these settings to promote tumour-cell death[13].

An apparent conundrum is that autophagy acts both in cytoprotection and in cell death. In response to most forms of cellular stress, autophagy plays a cytoprotective role, because *ATG* gene knockdown/knockout accelerates rather than delays cell death[9,11]. However, in certain settings where there is uncontrolled upregulation of autophagy (for example, overexpression of the autophagy protein Beclin 1 in mammalian cells[14], and Atg1 overexpression in *Drosophila*[15]), autophagy can lead to cell death, possibly through activating apoptosis[15] or possibly as a result of the inability of cells to survive the non-specific degradation of large amounts of cytoplasmic contents. Notably, many examples of *ATG*-gene-dependent cell death occur in cells deficient in apoptosis[9], suggesting that autophagy, as a route to cell death, may be a choice of last resort. One general caveat to these types of studies is that the overexpression or knockout of a single *ATG* gene could have unknown indirect effects beyond autophagy.

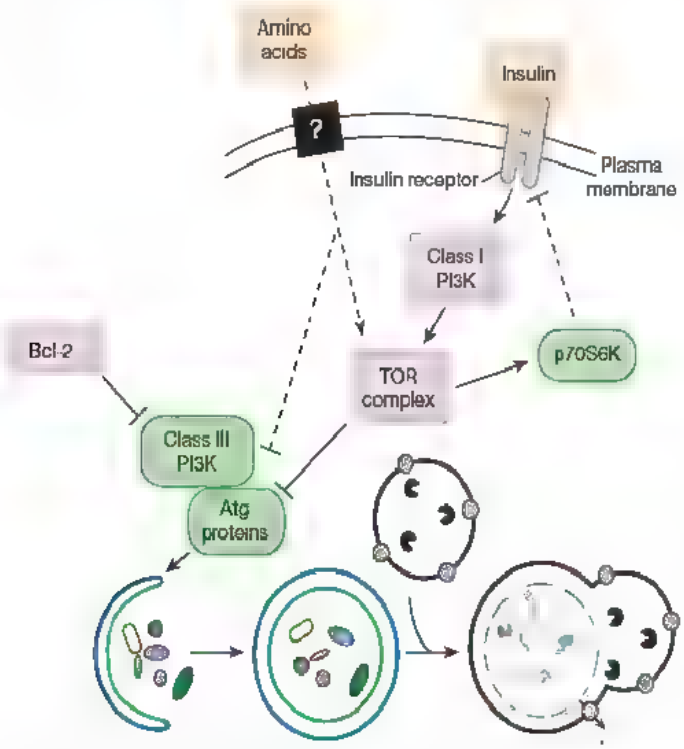

Figure 2 | A simplified model of autophagy regulation. Macroautophagy occurs at a basal level and can be induced in response to environmental signals including nutrients and hormones, and also microbial pathogens. The best-characterized regulatory pathway includes a class I PI3K and TOR, which act to inhibit autophagy, although the mechanism is not known. A class III PI3K is needed for activation of autophagy. TOR activity is probably regulated in part through feedback loops to prevent insufficient or excessive autophagy. For example, p70S6 kinase is a substrate of TOR that may act to limit TOR activity, ensuring basal levels of autophagy that are critical for homeostasis. Proteins in green and pink are stimulatory and inhibitory for autophagy, respectively. Dashed lines indicate possible regulatory effects.

Autophagic programmed cell death was originally described in tissues undergoing active development. Yet, not only is there no evidence that *ATG* gene inhibition prevents this death, but the opposite may be true. Nematodes lacking *bec-1*, the *Caenorhabditis elegans* orthologue of *ATG6/beclin 1*, and mice lacking *beclin 1* or *atg5* display increased numbers of apoptotic cells in embryonic tissues, arguing against a requirement for the autophagic machinery in developmental programmed cell death[16,17]. It may, however, be premature to conclude that autophagy deficiency results in the increased generation of apoptotic cells during development, because the *ATG* machinery also has a role in the heterophagic removal of apoptotic corpses[16]. In mature animals with tissue-specific *ATG* gene knockout, there is perhaps clearer evidence of an anti-apoptotic function of autophagy *in vivo*[18–20].

The cross-talk between autophagy, a pathway that functions primarily in cell survival, and apoptosis, a pathway that invariably leads to cell death, is complex. The two pathways are regulated by common factors, they share common components, and each can regulate and modify the activity of the other[9,11]. Many signals originally studied in the context of apoptosis activation induce autophagy, whereas signals that inhibit apoptosis also inhibit autophagy[5–7]. Anti-apoptotic proteins, such as Bcl-2 family members, inhibit Beclin 1[14], and pro-apoptotic factors, such as BH3-only proteins, disrupt this inhibitory interaction and thereby activate autophagy[21]. Another link between the autophagic machinery and apoptosis is the observation that Atg5 can undergo calpain-mediated cleavage to generate a pro-apoptotic fragment that functions in the intrinsic mitochondrial death pathway[22]. These examples may represent only the tip of the iceberg, as we clearly are just beginning to understand the intricate molecular interplay between autophagy and apoptosis. However, it does seem likely that the coordinated regulation of 'self-digestion' by autophagy and 'self-killing' by apoptosis may underlie diverse aspects of development, tissue homeostasis and disease pathogenesis.

Neurodegeneration

Growing evidence reveals that alterations in autophagy occur in many human diseases. Here we discuss only those disorders in which autophagy malfunction has been shown to contribute to their pathogenesis (Fig. 3). As mentioned above, autophagy occurs at basal, constitutive levels and recent studies have highlighted the importance of basal autophagy in intracellular quality control. The demand for basal autophagy differs among tissues; it is particularly important in the liver and in other tissues where the cells, such as neurons and myocytes, do not divide after differentiation[18,19,23–25]. In contrast to conventional *atg5*, *atg7* and *beclin 1* knockout mice, which die during embryogenesis or the neonatal period[1,23,26–29], those with neural-tissue-specific knockouts of these genes survive the postnatal starvation period. However, these mice develop progressive motor deficits and display abnormal reflexes, and ubiquitin-positive inclusion bodies accumulate in their neurons[18,19]. Although the levels of autophagosomes detected in neurons are very low under normal and even starvation conditions[30,31], these studies strikingly show that constitutive turnover of cytosolic contents by autophagy is indispensable, even in the absence of expression of any disease-associated mutant proteins.

Despite the important function of basal autophagy in healthy individuals, the requirement for autophagy is even more evident under disease conditions. Recent studies reveal that degradation of disease-related mutant proteins is highly dependent on autophagy, in addition to the ubiquitin–proteasome system. Examples include extended polyglutamine-containing proteins that cause various

neurodegenerative diseases such as Huntington's disease and spinocerebellar ataxia, and mutant forms of α-synuclein that cause familial Parkinson's disease[32–34]. CMA also participates in wild-type α-synuclein degradation, but mutant forms of α-synuclein block the lysosomal receptor, resulting in general CMA inhibition[35]. The affected cells attempt to compensate for the CMA blockage by upregulating macroautophagy, which guarantees cell survival but renders the cells more susceptible to stressors[4].

Considering all of the available data, there is no doubt that autophagy has a beneficial effect of protecting against neurodegeneration; however, how autophagy can prevent neurodegeneration is not completely understood. One hypothesis is that autophagy eliminates protein aggregates or inclusion bodies, possibly in a directed manner[36,37]. One possible adaptor is p62/sequestosome-1 (SQSTM1)[36]. Almost all protein aggregates are decorated with ubiquitin, and SQSTM1 has both LC3-binding (the mammalian homologue of the autophagy-related protein Atg8) and ubiquitin-binding domains, allowing it to mediate the recognition of protein aggregates by a protein (LC3) in the membrane of the forming autophagosome[36,38]. Furthermore, proper turnover of p62 by autophagy is critical to prevent spontaneous aggregate formation[39].

However, direct degradation of aggregates by autophagy is somehow contradictory to the recent hypothesis that the generation of protein aggregates is a protective mechanism[40,41]. Rather, the primary target of autophagy seems to be diffuse cytosolic proteins, not inclusion bodies themselves, suggesting that inclusion body formation in autophagy-deficient cells is an event secondary to impaired general protein turnover[18]. However, it is still possible that misfolded proteins in soluble or oligomeric states could be preferentially recognized by autophagosomal membranes, which might also be mediated by ubiquitin–p62–LC3 interactions.

Alterations of autophagy have also been observed in Alzheimer's disease, but in this case the contribution of autophagy may not be as simple as in other types of neurodegeneration. For example, autophagosome-like structures accumulate in dystrophic neurites of Alzheimer's disease patients and model mice, probably owing to impairment of autophagosome maturation into autolysosomes (Fig. 1)[42]. Surprisingly, the toxic proteolytic product Aβ can be produced within these partially degraded compartments because the Aβ precursor protein, APP, and the protease responsible for its cleavage, are both present in the endoplasmic reticulum sequestered in these structures[42]. Therefore, one hypothesis is that impaired autophagic flux provides a novel site for Aβ peptide production.

It is reasonable to assume that autophagy could be a therapeutic target for treatment of these neurodegenerative diseases because of its protective role[43]. For example, upregulation of autophagy by the regulatory protein kinase complex Target of Rapamycin (TOR) inhibitors such as rapamycin and its analogue CCI-779 protects against neurodegeneration seen in polyglutamine disease models in *Drosophila* and mice[44]. Recently, small-molecule enhancers of rapamycin were identified[45]. These improve the clearance of mutant huntingtin and α-synuclein, and protect against neurodegeneration in a fruit-fly Huntington's disease model. Importantly, the effects of small-molecule enhancers of rapamycin are independent of TOR, making

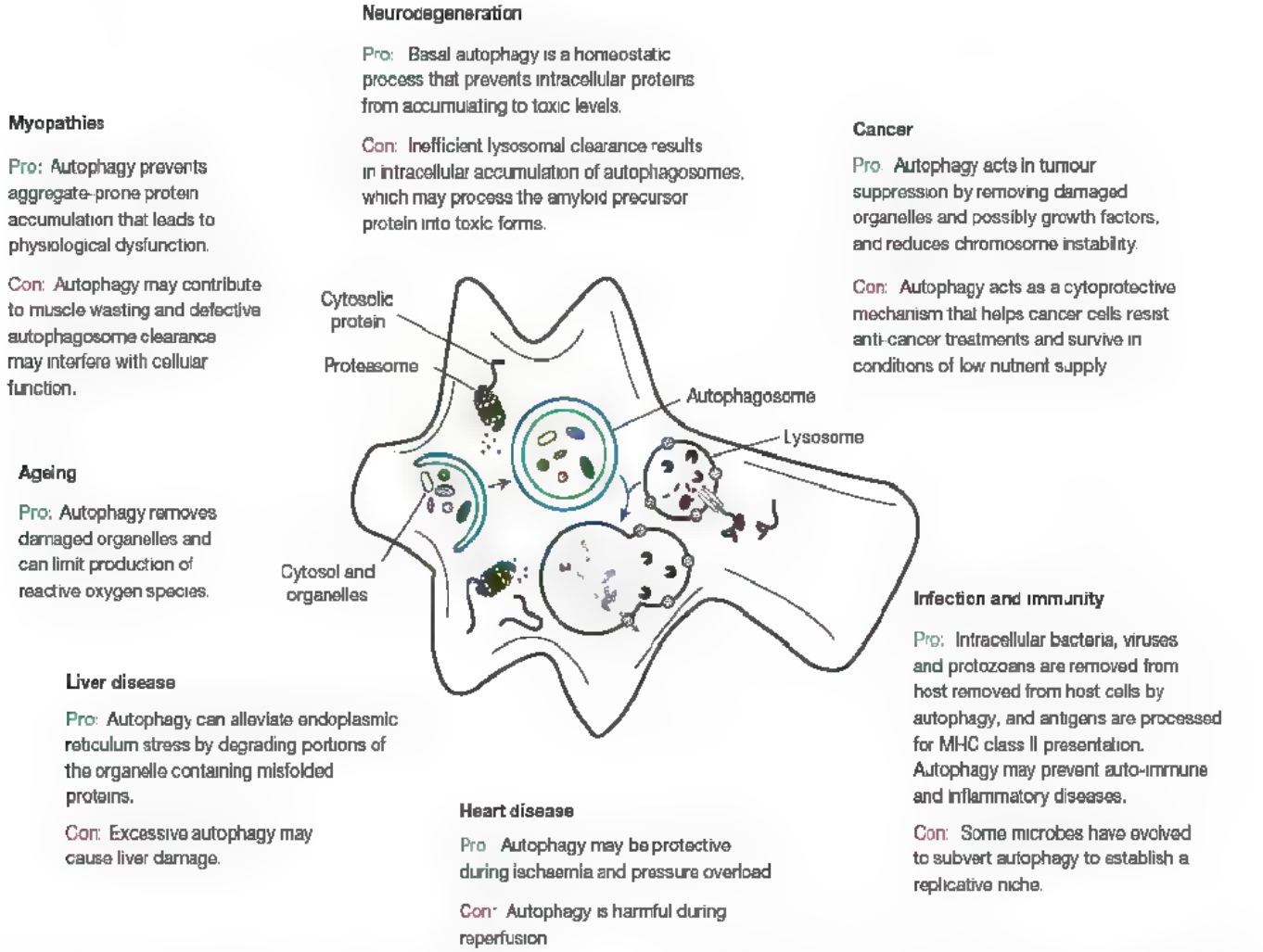

Figure 3 | The role of autophagy in human disease. Degradation, in particular through autophagy and the proteasome, is important in cellular physiology. Autophagy can act as a cytoprotective mechanism to prevent various diseases, and dysfunctional autophagy leads to pathology. In some cases, however, autophagy can be deleterious; for example, some microbes subvert autophagy for replication, and the cytoprotective action can allow cancer cells to resist anti-cancer treatments.

it possible to use them in combination with rapamycin for therapeutic purposes. In any attempt at manipulating autophagy therapeutically, however, it is important to take into account the dynamic nature of the changes that occur in the autophagic system during the pathogenic course of a disease (Fig. 3).

Innate and adaptive immunity

The disposal of intracellular organisms, similar to cellular organelles, represents a steric challenge for cellular degradative pathways that may be uniquely met by autophagy. The same autophagic machinery used to selectively capture cellular organelles is used for the selective delivery of microorganisms to lysosomes in a process termed xenophagy[46]. In mammals (and perhaps other metazoan organisms), the role of autophagy in antimicrobial defence probably extends beyond the direct elimination of pathogens. A growing number of studies indicate a role for autophagy in delivery of microbial antigenic material to the innate and adaptive immune system, as well as in maintaining lymphocyte homeostasis[47,48] (Fig. 3).

Xenophagy can target extracellular bacteria that invade intracellularly, bacteria and parasites that reside in the cytosol, phagosomes, or pathogen-containing vacuoles, as well as newly synthesized virions during their exit from the nucleus through the cytoplasm[47,49]. The cell biology of xenophagy is less well-studied than classical autophagy and despite the overlap in molecular components required for the two processes, it is not yet clear whether the membranes engulfing microorganisms have a biogenesis similar or different to that of classical autophagosomes. Pathogen-containing LC3-positive compartments can be considerably larger than classical autophagosomes consisting exclusively of cellular constituents[47], indicating a plasticity of the autophagic process that permits it to adapt to the need to engulf microbes that are larger than its own organelles, a capacity that reflects the unique mechanism of autophagosome formation (Fig. 1). Although xenophagy appears to be primarily a selective form of autophagy, almost nothing is known about how microbes (or membranous compartments containing microbes) are recognized by the autophagic machinery.

Beyond its direct role in pathogen elimination, autophagy may exert cytoprotective functions in infected cells and also mediate trafficking events required for innate and adaptive immunity. In the case of certain RNA viral infections, autophagy is required for the delivery of viral nucleic acids to the endosomal toll-like receptor TLR7, and subsequent activation of type I interferon signalling[47]. The autophagic machinery is also used for the major histocompatibility complex (MHC) class II presentation of certain endogenously synthesized viral antigens[47]. Not only does the autophagic machinery function in innate and adaptive immunity, but several innate and adaptive immune mediators involved in intracellular pathogen control stimulate autophagy[47].

Given the diverse roles of autophagy in innate and adaptive immunity, it is not surprising that many pathogens have devised strategies to outsmart autophagy. Some intracellular bacteria and viruses co-opt the autophagic machinery to use Atg protein-dependent dynamic membrane rearrangements to their own replicative advantage[49,50]. More commonly, successful intracellular pathogens modulate the signalling pathways that regulate autophagy or block the membrane trafficking events required for autophagy-mediated pathogen delivery to the lysosome[47]. Notably, in certain settings, microbial evasion of autophagy may be essential for microbial pathogenesis. For example, fatal herpes simplex virus encephalitis requires inhibition of the Beclin 1 autophagy protein by a virus neurovirulence protein[51]. Thus, the selective disruption of interactions between microbial virulence factors and their targeted host autophagy proteins may help reduce infection-induced pathology.

Other postulated roles of autophagy in immunity that warrant further scientific attention include T-cell homeostasis, central and peripheral tolerance induction, and the prevention of unwanted inflammation and autoimmunity[47]. We also note that several recent genome-wide scans have uncovered strong associations between a non-synonymous single nucleotide polymorphism in the autophagy gene *ATG16L1* as well as in the autophagy-stimulatory immunity-related GTPase IRGM, and susceptibility to Crohn's disease, an inflammatory disease of the intestine[13]. These associations suggest an intriguing potential role for autophagy deregulation in the pathogenesis of Crohn's disease. However, it is not known whether the ATG16L variant is defective in autophagy function and whether this genetic association is indicative of a mechanistic link between autophagy impairment and Crohn's disease pathogenesis. Studies in targeted mutant mice with a knock-in T300A mutation in *ATG16L1* should help clarify these important questions.

Cancer

Cancer is one of the first diseases genetically linked to autophagy malfunction[12,13]. The *ATG* gene *beclin 1* is monoallelically deleted in 40–75% of cases of human breast, ovarian, and prostate cancer. This is probably mechanistically important in tumorigenesis, because mice with heterozygous disruption of *beclin 1* have decreased autophagy and are more prone to the development of spontaneous tumours including lymphomas, lung carcinomas, hepatocellular carcinomas, and mammary precancerous lesions[27,29]. Further, immortalized kidney and mammary epithelial cells derived from *beclin 1* heterozygous-deficient mice are more tumorigenic when transplanted *in vivo*. Other components that enhance the autophagic activity of the Beclin 1/class III phosphatidylinositol 3-kinase (PI3K) complex, including ultraviolet irradiation resistance-associated gene (UVRAG), Ambra1 and Bif-1 may also play a role in cell growth control and/or tumour suppression[26,28]. In animal models, additional *ATG* genes including *atg4c* also exert tumour suppressor effects[52], suggesting that tumour suppression may be a shared property of autophagy proteins that act at different steps of the pathway (Fig. 3). Beyond a role for *ATG* genes in tumour suppression, there is accumulating evidence that autophagy signalling regulation is tightly linked to oncogenic signalling. Several commonly activated oncogenes (for example, those encoding class I PI3K, PKB, TOR, Bcl-2) inhibit autophagy, whereas commonly mutated or epigenetically silenced tumour suppressor genes (such as those encoding p53, PTEN, DAPk, TSC1/TSC2) stimulate autophagy[1].

These genetic links between defects in autophagy regulation or execution and cancer suggest that autophagy is a true tumour suppressor pathway. However, the mechanisms by which it functions in tumour suppression remain largely undetermined. Autophagy may directly regulate cell growth, functioning as a brake to prevent cells from inappropriately dividing in the absence of appropriate trophic support (even though it may promote cell survival in this setting)[13]. The increased frequency of mitochondrial DNA mutations in autophagy-deficient yeast suggests that mitochondrial turnover mediated by basal autophagy may prevent genotoxic stress and DNA damage[12,13]. Indeed, recent studies strikingly reveal that both *beclin 1* and *atg5* function as 'guardians' of the cellular genome. Immortalized epithelial cells with mono-allelic or bi-allelic loss of *beclin 1* or *atg5*, respectively, display increased DNA damage, gene amplification, and aneuploidy, especially during ischaemic stress, in parallel with increased tumorigenicity[12]. It is not yet known how autophagy deficiency compromises genomic stability.

A seeming paradox is that autophagy, a pathway that functions primarily in cell survival, also functions in tumour suppression (Fig. 3), but two hypotheses have recently been proposed to explain this paradox[12]. First, when tumour cells cannot die by apoptosis upon exposure to metabolic stress, autophagy may prevent death by necrosis, a process that might exacerbate local inflammation and thereby increase tumour growth rate. Second, as noted above, even though autophagy promotes cell survival in the setting of metabolic stress in the tumour microenvironment, it acts concurrently to prevent genomic instability. An additional possibility is that despite its pro-survival effects, autophagy activation during metabolic stress

(and high density conditions) prevents cell growth[13]. Although the pro-survival effects of autophagy may often be counterbalanced by its tumour suppressor effects, an area of growing interest is the potential contribution of these pro-survival effects to tumour cell resistance to chemotherapy; recent studies have shown that genetic or pharmacological inhibition of autophagy enhances cytoxicity of cancer chemotherapeutic agents[53,54]. Consequently, clinical trials are in progress (based on studies in mouse models[55]) to disrupt autophagic degradation to maximize the effects of cancer cytotoxic agents. Thus, much as in neurodegenerative and cardiac diseases, it may be necessary to differentially target autophagy in a context-specific and disease-stage-specific manner; autophagy augmentation may be effective in preventing tumour formation and progression, whereas autophagy inhibition may be helpful in promoting tumour regression.

Ageing and longevity

A common characteristic of all ageing cells is the accumulation of damaged proteins and organelles, even in the absence of any mutations that predispose the cells to a pathogenic phenotype such as aggregate-prone mutant proteins (Fig. 4). As discussed above, these deposits of altered components are particularly detrimental in non-dividing differentiated cells, such as neurons and cardiomyocytes, where the characteristic functional decline with age usually manifests itself sooner than in other cell types. Both macroautophagy and CMA activity decrease with age[56,57]. In light of the dramatic phenotypes observed in the recently generated genetic mouse models with impaired autophagy[18,19,23,24], it is easy to infer that a gradual decrease in autophagic activity with age could play a major role in the functional deterioration of ageing organisms. Conversely, caloric restriction, the only intervention known to slow down ageing, seems to improve autophagy induction, possibly owing to lower levels of insulin, an autophagy inhibitor (Fig. 2). Current efforts to prevent or restore the decline in macroautophagy with age are aimed at reproducing the observed beneficial effect of caloric restriction on this pathway through the use of anti-lipolytic drugs (that mimic the starvation state induced by caloric restriction)[58].

Outlook

In the past decade there has been a tremendous advance in our knowledge about the molecular mechanism of macroautophagy, including the identification of many of the components of the protein machinery. By comparison, our understanding of regulation, particularly the complex interplay of multiple stimulatory and inhibitory inputs, is relatively limited. To manipulate autophagy for therapeutic purposes, especially considering its dual capacity in cytoprotection and cell death, we need to improve our understanding of the various regulatory pathways.

In contrast to the rapid advance in the molecular dissection of macroautophagy and growing information about its regulation and its pathophysiological relevance, our understanding of other forms of autophagy is still limited. Critical molecular players have been identified for CMA, but it is clear, by comparison with other membrane

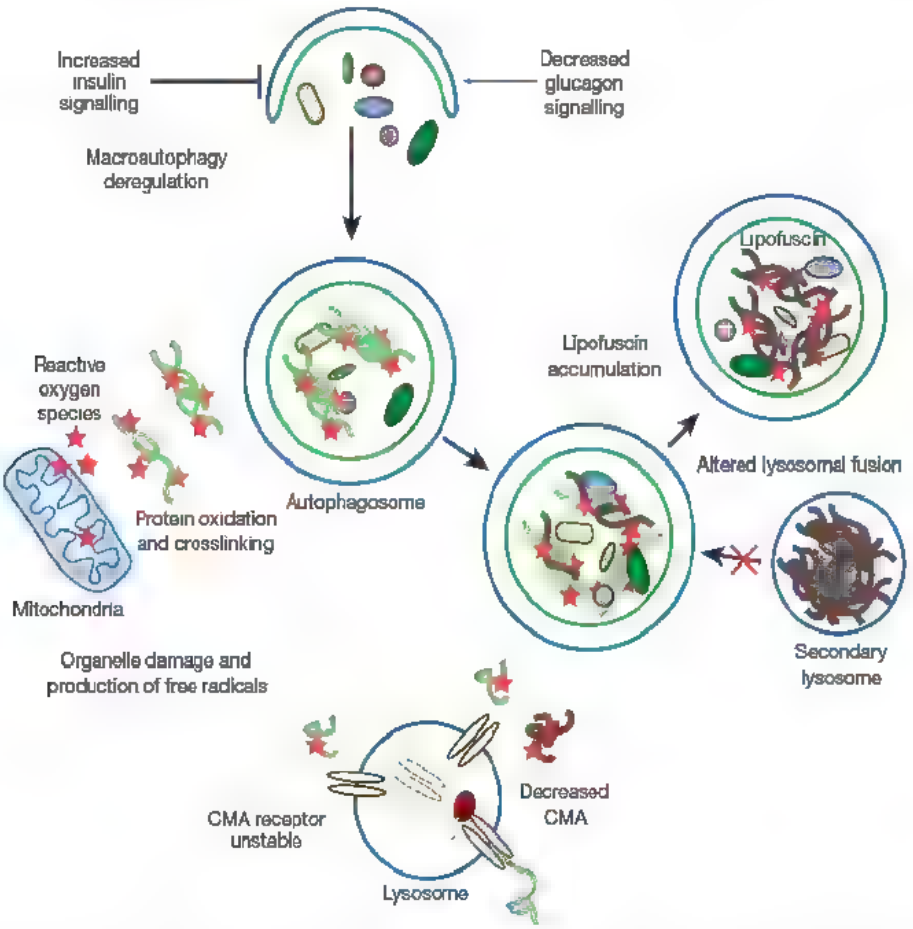

Figure 4 | Autophagy and ageing. Defective lysosomal function has been reported in almost all tissues of ageing organisms, from nematode worms to mammals, and both macroautophagy and CMA activity decrease with age[56]. Problems in the regulation and execution of macroautophagy contribute to its functional decline during ageing[57]. Upregulation of macroautophagy by increased levels of glucagon in serum (that is, between meals) is lost in older organisms, possibly owing to persistently enhanced basal activity of the insulin receptor in response to the higher content of reactive oxygen species in ageing cells[59]. Also, accumulation of undigested material (lipofuscin) inside secondary lysosomes (for example, autolysosomes) interferes with their ability to fuse with autophagosomes and to degrade their cargo. Changes with age in the lysosomal membrane make the CMA receptor unstable. The age-dependent decrease in the levels of this receptor is responsible for low CMA activity in older organisms[60]. Some predicted consequences of the decline in autophagy with age are the inefficient clearance of damaged components, a poor response to stress, and a possible precipitating effect on disease.

translocation systems, that other regulatory components are yet to be discovered. The current available information about microautophagy is even more limited and the absence of reliable markers or assays to track this process has prevented any connection of microautophagic changes with physiological or pathological conditions.

Although starvation or stress adaptation is an evolutionarily conserved function of autophagy under physiological conditions, the degradation of intracellular components may be a more important function when considering the role of autophagy in disease. One area of future interest is to study how autophagy functions in preventing neurodegeneration, although at present we do not know the direct cause of the toxicity of neuropeptides such as Aβ and α-synuclein. In addition, we need to understand the issue of functional autophagy serving a protective role, as opposed to compromised autophagy and the accompanying accumulation of cytosolic autophagosomes, which contributes to pathogenesis in neurodegeneration, liver disease and myopathies, because induction of autophagy in these latter situations can exacerbate the disease pathology. Similarly, we should carefully consider the type and progression of diseases such as cancer when attempting to determine whether autophagy inhibition or stimulation is likely to be beneficial. To understand immunity better, it will be important to identify the mechanisms by which autophagy is activated in response to microbial invasion, the targets that allow specific recognition of intracellular pathogens, and the roles of autophagy in immune cell function.

One of the current challenges in the study of autophagy in ageing is that most of the genetic mouse models with impaired autophagy do not reproduce the main characteristics of the ageing-dependent changes. In these models there is complete blockage of autophagy and this blockage is present from birth. The recent introduction of conditional knockout mice should help in part to overcome this problem, because these make it possible to compare the consequences of impaired autophagy from birth, when compensatory mechanisms are likely to be activated, with that occurring in the adult organism.

Thus, although tremendous advances have been made in our understanding of autophagy, many unanswered questions remain. A fuller understanding of all types of autophagy is necessary before we can hope to manipulate these pathways to treat human disease.

1 Kuma, A. *et al.* The role of autophagy during the early neonatal starvation period *Nature* 432, 1032–1036 (2004)
2. Mizushima, N & Klionsky, D. J. Protein turnover via autophagy: implications for metabolism *Annu. Rev. Nutr.* 27, 19–40 (2007)
3. Klionsky D. J. The molecular machinery of autophagy: unanswered questions. *J. Cell Sci.* 118, 7–18 (2005).
4. Massey, A. C., Zhang, C. & Cuervo, A. M. Chaperone-mediated autophagy in aging and disease. *Curr. Top. Dev. Biol.* 73, 205–235 (2006)
5. Botti, J., Djavaheri-Mergny, M., Pilatte, Y. & Codogno, P. Autophagy signaling and the cogwheels of cancer *Autophagy* 2, 67–73 (2006)
6. Gozuacik, D. & Kimchi, A. Autophagy and cell death. *Curr. Top. Dev. Biol.* 78, 217–245 (2007)
7. Meijer, A. J. & Codogno, P. Signalling and autophagy regulation in health, aging and disease. *Mol. Aspects Med.* 27, 411–425 (2006)
8. Yorimitsu, T. & Klionsky, D. J. Eating the endoplasmic reticulum: quality control by autophagy. *Trends Cell Biol.* 17, 279–285 (2007).
9. Levine, B. & Yuan, J. Autophagy in cell death: an innocent convict? *J. Clin. Invest.* 115, 2679–2688 (2005)
10. Lum, J. J., DeBerardinis, R. J. & Thompson, C. B. Autophagy in metazoans: cell survival in the land of plenty. *Nature Rev. Mol. Cell Biol.* 6, 439–448 (2005)
11. Maiuri, C., Zakkvar, E., Kimchi, A. & Kroemer G. Self-eating and self-killing: crosstalk between autophagy and apoptosis. *Nature Rev. Mol. Cell Biol.* 8, 741–752 (2007)
12. Mathew R., Karantza-Wadsworth, V. & White, E. Role of autophagy in cancer *Nature Rev. Cancer* 7, 961–967 (2007).
13. Levine, B. & Kroemer G. Autophagy in the pathogenesis of disease. *Cell* 132, 27–42 (2008).
14. Pattingre, S. *et al.* Bcl-2 antiapoptotic proteins inhibit Beclin 1-dependent autophagy *Cell* 122, 927–939 (2005)
15. Scott, R. C., Juhasz, G. & Neufeld, T. P. Direct induction of autophagy by Atg1 inhibits cell growth and induces apoptotic cell death. *Curr. Biol.* 17, 1–11 (2007)
16. Qu, X. *et al.* Autophagy gene-dependent clearance of apoptotic cells during embryonic development. *Cell* 128, 931–946 (2007).
17 Takacs-Vellai, K. *et al.* Inactivation of the autophagy gene *bec-1* triggers apoptotic cell death in *C. elegans*. *Curr. Biol.* 15, 1513–1517 (2005).
18 Hara, T. *et al.* Suppression of basal autophagy in neural cells causes neurodegenerative disease in mice. *Nature* 441, 885–889 (2006)
19 Komatsu, M. *et al.* Loss of autophagy in the central nervous system causes neurodegeneration in mice. *Nature* 441, 880–884 (2006)
20 Pua, H. H., Dzhagalov, I., Chuck, M., Mizushima, N. & He, Y. W. A critical role for the autophagy gene Atg5 in T cell survival and proliferation. *J. Exp. Med.* 204, 25–31 (2007).
21 Maiuri, M. C. *et al.* Functional and physical interaction between Bcl-X_L and a BH3-like domain in Beclin-1 *EMBO J.* 26, 2527–2539 (2007).
22 Yousefi, S. *et al.* Calpain-mediated cleavage of Atg5 switches autophagy to apoptosis. *Nature Cell Biol.* 8, 1124–1132 (2006).
23 Komatsu, M. *et al.* Impairment of starvation-induced and constitutive autophagy in *Atg7*-deficient mice. *J. Cell Biol.* 169, 425–434 (2005).
24 Nakai, A. *et al.* The role of autophagy in cardiomyocytes in the basal state and in response to hemodynamic stress. *Nature Med.* 13, 619–624 (2007)
25 Komatsu, M. *et al.* Essential role for autophagy protein Atg7 in the maintenance of axonal homeostasis and the prevention of axonal degeneration. *Proc. Natl Acad. Sci. USA* 104, 14489–14494 (2007)
26. Fimia, G. M. *et al.* Ambral regulates autophagy and development of the nervous system *Nature* 447, 1121–1125 (2007)
27 Qu, X. *et al.* Promotion of tumorigenesis by heterozygous disruption of the *beclin 1* autophagy gene. *J. Clin. Invest.* 112, 1809–1820 (2003)
28. Takahashi, Y. *et al.* Bif-1 interacts with Beclin 1 through UVRAG and regulates autophagy and tumorigenesis. *Nature Cell Biol.* 9, 1142–1151 (2007)
29 Yue, Z., Jin, S., Yang, C., Levine, A. J. & Heintz, N. Beclin 1, an autophagy gene essential for early embryonic development, is a haploinsufficient tumor suppressor *Proc. Natl Acad. Sci. USA* 100, 15077–15082 (2003)
30. Mizushima, N., Yamamoto, A., Matsui, M., Yoshimori, T. & Ohsumi, Y. *In vivo* analysis of autophagy in response to nutrient starvation using transgenic mice expressing a fluorescent autophagosome marker *Mol. Biol. Cell* 15, 1101–1111 (2004)
31 Nixon. R. A. *et al.* Extensive involvement of autophagy in Alzheimer disease: an immuno-electron microscopy study. *J. Neuropathol. Exp. Neurol.* 64, 113–122 (2005)
32 Martinez-Vicente, M. & Cuervo, A. M. Autophagy and neurodegeneration: when the cleaning crew goes on strike. *Lancet Neurol.* 6, 352–361 (2007)
33. Rubinsztein, D. C. The roles of intracellular protein-degradation pathways in neurodegeneration. *Nature* 443, 780–786 (2006
34. Rubinsztein, D. C. *et al.* Autophagy and its possible roles in nervous system diseases, damage and repair *Autophagy* 1, 11–22 (2005)
35 Cuervo, A. M., Stefanis, L., Fredenburg, R., Lansbury, P. T. & Sulzer, D. Impaired degradation of mutant α-synuclein by chaperone-mediated autophagy *Science* 305, 1292–1295 (2004)
36. Bjørkøy, G *et al.* p62/SQSTM1 forms protein aggregates degraded by autophagy and has a protective effect on huntingtin-induced cell death. *J. Cell Biol.* 171, 603–614 (2005)
37 Iwata, A., Riley, B. E., Johnston, J. A. & Kopito, R. R. HDAC6 and microtubules are required for autophagic degradation of aggregated huntingtin. *J. Biol. Chem.* 280, 40282–40292 (2005)
38. Pankiv, S. *et al.* p62/SQSTM1 binds directly to Atg8/LC3 to facilitate degradation of ubiquitinated protein aggregates by autophagy *J. Biol. Chem.* 282, 24131–24145 (2007).
39. Komatsu, M. *et al.* Homeostatic levels of p62 control cytoplasmic inclusion body formation in autophagy-deficient mice. *Cell* 131, 1149–1163 (2007)
40 Arrasate, M., Mitra, S., Schweitzer, E. S., Segal, M. R. & Finkbeiner, S. Inclusion body formation reduces levels of mutant huntingtin and the risk of neuronal death *Nature* 431, 805–810 (2004).
41. Tanaka, M. *et al.* Aggresomes formed by α-synuclein and synphilin-1 are cytoprotective. *J. Biol. Chem.* 279, 4625–4631 (2004)
42 Yu, W. H. *et al.* Macroautophagy—a novel β-amyloid peptide-generating pathway activated in Alzheimer's disease. *J. Cell Biol.* 171, 87–98 (2005).
43. Rubinsztein, D. C., Gestwicki, J. E., Murphy, L. O. & Klionsky, D. J. Potential therapeutic applications of autophagy *Nature Rev. Drug Discov.* 6, 304–312 (2007)
44. Ravikumar, B. *et al.* Inhibition of mTOR induces autophagy and reduces toxicity of polyglutamine expansions in fly and mouse models of Huntington disease. *Nature Genet.* 36, 585–595 (2004).
45. Sarkar, S. *et al.* Small molecules enhance autophagy and reduce toxicity in Huntington's disease models *Nature Chem. Biol.* 3, 331–338 (2007)
46. Levine, B. Eating oneself and uninvited guests: autophagy-related pathways in cellular defense. *Cell* 120, 159–162 (2005)
47 Levine, B. & Deretic, V. Unveiling the roles of autophagy in innate and adaptive immunity *Nature Rev. Immunol.* 7, 767–777 (2007)
48. Schmid, D. & Münz, C. Innate and adaptive immunity through autophagy *Immunity* 27, 11–21 (2007)
49 Huang, J. & Klionsky, D. J. Autophagy and human disease. *Cell Cycle* 6, 1837–1849 (2007).
50. Kirkegaard, K., Taylor, M. P. & Jackson, W. T. Cellular autophagy: surrender, avoidance and subversion by microorganisms. *Nat. Rev. Microbiol.* 2, 301–314 (2004)

51. Orvedahl, A. *et al.* HSV-1 ICP34.5 confers neurovirulence by targeting the Beclin 1 autophagy protein. *Cell Host Microbe* 1, 23–35 (2007)
52. Mariño, G. *et al.* Tissue-specific autophagy alterations and increased tumorigenesis in mice deficient in Atg4C/autophagin-3. *J. Biol. Chem.* 282, 18573–18583 (2007)
53. Abedin, M. J., Wang, D., McDonnell, M. A., Lehmann, U. & Kelekar, A. Autophagy delays apoptotic death in breast cancer cells following DNA damage. *Cell Death Differ.* 14, 500–510 (2007)
54. Carew, J. S. *et al.* Targeting autophagy augments the anticancer activity of the histone deacetylase inhibitor SAHA to overcome Bcr-Abl-mediated drug resistance. *Blood* 110, 313–322 (2007).
55. Amaravadi, R. K. *et al.* Autophagy inhibition enhances therapy-induced apoptosis in a Myc-induced model of lymphoma. *J. Clin. Invest.* 117, 326–336 (2007)
56. Cuervo, A. M. *et al.* Autophagy and aging: the importance of maintaining "clean" cells. *Autophagy* 1, 131–140 (2005)
57. Del Roso, A. *et al.* Ageing-related changes in the *in vivo* function of rat liver macroautophagy and proteolysis. *Exp. Gerontol.* 38, 519–527 (2003).
58. Bergamini, E. Targets for anti-ageing drugs. *Expert Opin. Ther. Targets* 9, 77–82 (2005)
59. Hildebrandt, W. *et al.* Effect of thiol antioxidant on body fat and insulin reactivity. *J. Mol. Med.* 82, 336–344 (2004)
60. Kiffin, R. *et al.* Altered dynamics of the lysosomal receptor for chaperone-mediated autophagy with age. *J. Cell Sci.* 120, 782–791 (2007)

Supplementary Information is linked to the online version of the paper at www.nature.com/nature.

Acknowledgements This work was funded in part by grants from the National Institutes of Health (NCI, NIA, NIAID, NIGMS) the American Cancer Society, the Ellison Medical Foundation, Grants-in-Aid Scientific Research from the Ministry of Education, Culture, Sports, Science and Technology of Japan, and the Toray Science Foundation.

Author Information Reprints and permissions information is available at www.nature.com/reprints. Correspondence should be addressed to D.J.K. (klionsky@umich.edu)

ARTICLES

Proteomic analysis of active multiple sclerosis lesions reveals therapeutic targets

May H. Han[1]*, Sun-Il Hwang[3]*, Dolly B. Roy[4]*, Deborah H. Lundgren[3], Jordan V. Price[1], Shalina S. Ousman[1], Guy Haskin Fernald[5], Bruce Gerlitz[6], William H. Robinson[2], Sergio E. Baranzini[5], Brian W. Grinnell[6], Cedric S. Raine[7], Raymond A. Sobel[8], David K. Han[3] & Lawrence Steinman[1]

Understanding the neuropathology of multiple sclerosis (MS) is essential for improved therapies. Therefore, identification of targets specific to pathological types of MS may have therapeutic benefits. Here we identify, by laser-capture microdissection and proteomics, proteins unique to three major types of MS lesions: acute plaque, chronic active plaque and chronic plaque. Comparative proteomic profiles identified tissue factor and protein C inhibitor within chronic active plaque samples, suggesting dysregulation of molecules associated with coagulation. *In vivo* administration of hirudin or recombinant activated protein C reduced disease severity in experimental autoimmune encephalomyelitis and suppressed Th1 and Th17 cytokines in astrocytes and immune cells. Administration of mutant forms of recombinant activated protein C showed that both its anticoagulant and its signalling functions were essential for optimal amelioration of experimental autoimmune encephalomyelitis. A proteomic approach illuminated potential therapeutic targets selective for specific pathological stages of MS and implicated participation of the coagulation cascade.

Multiple sclerosis (MS) is an inflammatory and degenerative disease of the central nervous system (CNS) with diverse clinical presentations and heterogeneous histopathological features. Understanding the neuropathology of MS is essential to develop improved therapies. MS lesions or 'plaques' in the CNS white matter have distinct histological and immunocytological characteristics depending on disease activity[1–3]. This heterogeneity implies that there are discrete molecular events at different pathogenic stages of MS[1,4,5]. Therefore, identification of targets specific to pathological types of MS lesions may have therapeutic benefits during different stages of disease.

In recent years, a 'systems biology' approach using large-scale analysis of proteins and gene transcripts has illuminated new aspects of pathogenesis for complex disease networks including malignancies, neurodegenerative disorders and infections[6–8]. Similarly, large-scale transcriptional profiling of MS lesions has identified involvement of novel molecules and pathways such as osteopontin and Notch/Jagged signalling, respectively[9,10]. However, transcriptomic analysis fails to provide a comprehensive understanding of effector molecules involved in MS pathogenesis because of the susceptibility of messenger RNA to degradation and the discrepancy between mRNA and protein expression levels. Transcriptomic analysis also overlooks signalling molecules from serum, hormones and neurotransmitters. Therefore, a focused proteomic analysis of well-characterized human MS brain lesions, enriched by laser-capture microdissection (LCM) and analysed by sensitive tools such as mass spectrometry, will provide functional insights into the pathogenesis of MS.

Here we classified MS brain lesions into distinct histological types: acute plaque, chronic active plaque (CAP) and chronic plaque. We then isolated the lesions by LCM and performed saturated sequencing by mass spectrometry. We selected two candidate proteins, tissue factor and protein C inhibitor (PCI), by an analysis using a computer-guided system. We then validated their potential therapeutic roles in experimental autoimmune encephalomyelitis (EAE). We also studied the cellular and molecular mechanism of how activated protein C (aPC), an intrinsic inhibitor of PCI, ameliorates EAE. These findings emphasize how lesion-specific proteomic profiling of diseased tissue from patients with MS can identify potential therapeutic targets. In addition, we reveal the extensive interface between the coagulation system and brain inflammation.

Results

Histological characterization of MS lesions. Brain autopsy samples from patients with different clinical subtypes of MS (Table 1) were evaluated by staining with haematoxylin and eosin (H&E), Luxol fast blue (LFB) and immunohistochemistry. Lesions with florid parenchymal and perivascular inflammatory cell infiltration, abundant astroglial hypertrophy, myelin fragmentation, oedema and ongoing demyelination with indistinct margins were classified as acute plaque (Fig. 1a–c and Supplementary Fig. 1a–c)[11]. CAP lesions had chronic demyelination, sharply defined margins and recent areas of inflammatory demyelination at the edges (Fig. 1d–f and Supplementary Fig. 1d–h). Chronic plaque lesions had areas of demyelination with well-demarcated borders and abundant astrogliosis, but few or no inflammatory cells (Fig. 1g–i and Supplementary Fig. 1i). Age-matched control brain samples were analysed similarly and were devoid of CNS abnormalities.

Proteomic profiling of MS lesions. We compared the different histological stages of MS lesions by proteomics analysis to determine their global protein expression profiles. LCM enabled selective isolation of MS lesions from the adjacent white matter from the same tissue blocks evaluated for histological characterization. Samples

[1]Department of Neurology and Neurological Sciences, [2]Division of Immunology and Rheumatology, Stanford University School of Medicine, Stanford, California 94305, USA [3]Department of Cell Biology, Center for Vascular Biology, University of Connecticut Health Center, Farmington, Connecticut 06030, USA [4]Northridge Neurological Center, Northridge, California 91325, USA [5]Department of Neurology, University of California at San Francisco School of Medicine, California 94143, USA [6]Biotechnology Discovery Research, Lilly Research Laboratories, Lilly Corporate Center, Indianapolis, Indiana 46285, USA [7]Department of Pathology, Albert Einstein College of Medicine, Bronx, New York 10461, USA [8]Department of Pathology (Neuropathology), Stanford, California 94305, USA.
*These authors contributed equally to this work.

Table 1 | Characteristics of the MS patients and controls in the study

	Age/gender	Type of MS	Disease duration	Prior treatment	Lesion type	Cause of death	Autopsy interva
MS1	42/F	Acute	2 weeks	None	AP	Respiratory failure	12 h
MS2	54/F	Acute	2½ months	Corticosteroids	AP	Respiratory failure	12 h
MS3	31/F	Chronic	11 years	Corticosteroids	CAP	Respiratory failure	1.5h
MS4	27/F	Progressive	10 years	Corticosteroids	CAP	Broncho-pneumonia	4 h
MS5	47/M	Secondary progressive	20 years	Corticosteroids	CP	Respiratory failure	24 h
MS6	46/M	Chronic progressive	15 years	Lioresal; compazine	CP	Cardiac arrest	4 h
Control 1	23/F	Fallopian tube cancer	N/A	N/A		Respiratory failure	12 h
Control 2	52/F	Ovarian cancer	N/A	N/A		Respiratory failure	15.5 h

Two separate samples of brain lesions were obtained from MS1 and MS2, and three separate samples were obtained from MS3 to MS6 and normal controls. None of the patients with MS were treated with disease-modifying agents. Full CNS autopsies were performed on all cases. AP, acute plaque; CP, chronic plaque.

isolated by LCM were separately analysed by nanoliquid chromatography and tandem mass spectrometry (Fig. 2a). To ascertain reliable protein identification, we used the criteria of stringent mass tolerance and eliminated false-positive proteins by searching against a forward and reverse human protein database[12]. Furthermore, to enhance maximal protein detection coverage, MS samples were analysed repeatedly by mass spectrometric analysis (four to seven times) until a saturation point was reached (Supplementary Fig. 2). Analysis of control, acute plaque, CAP and chronic plaque samples yielded 2,574 proteins with high confidence. Among these, 2,302 proteins were related to MS samples (three types of lesion combined), and 1,492 proteins belonged to control samples (see Supplementary Table 1 for a complete listing). For individual MS lesion types we identified 1,082, 1,728 and 1,514 proteins for acute plaque, CAP and chronic plaque samples, respectively (Table 2). To our knowledge, this is the largest and the most comprehensive proteome of MS brain lesions characterized so far (Supplementary Tables 1 and 3).

CAP expresses coagulation proteins. After mass spectrometric protein identification, we used INTERSECT software to determine proteins specific to each MS lesion type. There were 158, 416 and 236 proteins unique to acute plaque, CAP and chronic plaque[13] (Supplementary Fig. 3 and Supplementary Table 2). We then applied PROTEOME-3D software to assign biological functions and subcellular localization to these proteins[14]. The analysis revealed that proteins of unknown function made up more than half of the unique proteins identified in all three MS lesion types (Supplementary Fig. 4). Of the proteins with known function, structural proteins, adhesion molecules, cell surface receptors and components of channels were among the most numerous (6% or greater). They were followed by proteins involved in the cell cycle, in synaptic transmission, in cellular signalling and in the components of the machinery for transcription and translation (2–6%). Least numerous were proteins with functions associated with molecular chaperones and cellular metabolism (less than 2%). Interestingly, the analysis revealed five proteins involved in coagulation: tissue factor, PCI, thrombospondin, fibronectin and vitronectin (Fig. 2b, c). These coagulation proteins were unique to CAP samples.

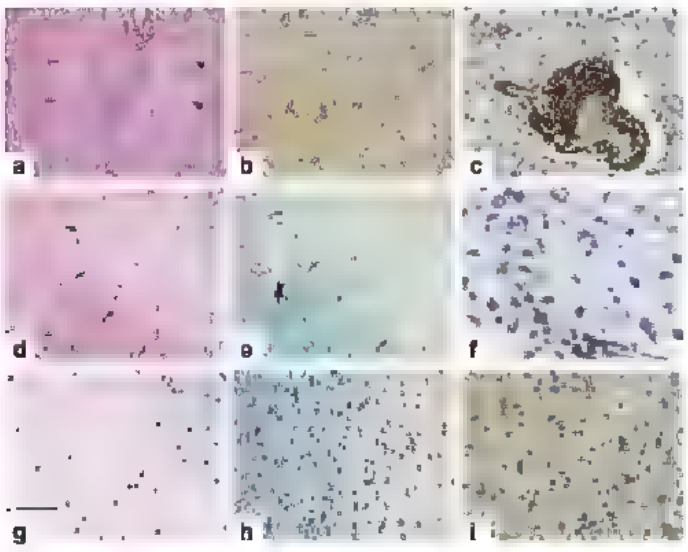

Figure 1 | Histopathology of MS brain lesions. Staining: **a**, **d**, **g**, H&E; **e**, **h**, LFB; **b**, **c**, **f**, **i**, immunohistochemistry. **a–c**, Acute plaque. **a**, Marked inflammation, vacuolation (arrowheads) and oedema. **b**, Patchy demyelination (normal myelin, brown), anti-$PLP_{200–219}$. **c**, Perivenous and parenchymal (arrows) inflammatory cells; anti-CD45. **d–f**, CAP. **d**, **e**, Well-demarcated edge (arrows); recent inflammation (**e**) (large arrow). **f**, Macrophages within CAP; anti-CD68. **g–i**, Chronic plaque. **g**, Hypocellular fibrotic lesion. **h**, Well-demarcated edge. **i**, Astrogliosis; anti-GFAP. Scale bars: **d**, 50 μm (also applies to **a**, **b**, **e**); **g**, 50 μm (also applies to **c**, **h**) and 25 μm **f**, **i**.

Thrombin inhibition attenuates EAE. Tissue factor, a coagulation factor, is expressed in monocytes and astrocytes during inflammation[15,16]. It promotes pro-inflammatory thrombin signalling through the protease activated receptor (PAR) family of proteins[17]. PCI is a serum protein that accumulates in the CAP lesions probably secondary to the disruption of the blood–brain barrier during neuroinflammation. PCI inhibits aPC. aPC also signals through PAR-1 and endothelial protein C receptor (EPCR)[18]. Despite sharing a common signalling pathway with procoagulant tissue factor, aPC is an anticoagulant with cytoprotective properties. The combined presence of tissue factor and PCI suggests pro-inflammatory thrombin formation and suppression of protein C pathway in CAP lesions.

To test the role of thrombin signalling during neuroinflammation, SJL/J mice that had been immunized with myelin proteolipid protein ($PLP_{139–151}$) peptide were treated daily with either intravenous injection of the thrombin inhibitor hirudin (see Methods Summary), or with PBS, at the peak of clinical disease. Mice treated with hirudin showed dramatic improvement in disease severity (Fig. 3a). This was accompanied by decreased immune cell proliferation (Fig. 3b) and suppression of cytokines interleukin (IL)-6, tumour-necrosis factor (TNF) and IL-17 (Fig. 3d, e). There were no differences in the production of IL-4, IL-10, IL-12 and interferon-γ (IFN-γ) cytokines between the vehicle-treated and the hirudin-treated groups (not shown). Hirudin had no effect on relapse rates or disease course (not shown). The brains and spinal cords of mice treated with hirudin showed fewer inflammatory foci (Fig. 3c and Supplementary Fig. 5a, b). Amelioration of EAE by hirudin treatment was observed only up to day 35, probably secondary to development of auto-antibodies against hirudin (see Discussion)[19].

aPC administration ameliorates EAE. aPC has anti-inflammatory and anti-apoptotic functions, and its therapeutic benefits have previously been observed in meningococcemia and in systemic inflammatory response syndrome[15,20–22]. The presence of PCI in CAP samples and evidence of low serum levels of protein C in patients with MS suggest suppression of the protein C pathway during MS[23]. To determine the effects of aPC during neuroinflammation, we induced EAE in 7- to 8-week-old SJL/J mice and treated them with either recombinant murine aPC ($0.2\ mg\ kg^{-1}$) or vehicle (PBS) beginning at the peak of disease. During the course of EAE, mice treated with aPC showed significant amelioration of disease severity (Fig. 4a). Treatment had no effect on relapse rates, nor did it alter the disease course (not shown). This effect was accompanied by decreased immune cell proliferation in splenocytes and lymph-node cells (Fig. 4b) and inhibition of Th1 and Th17 cytokines in

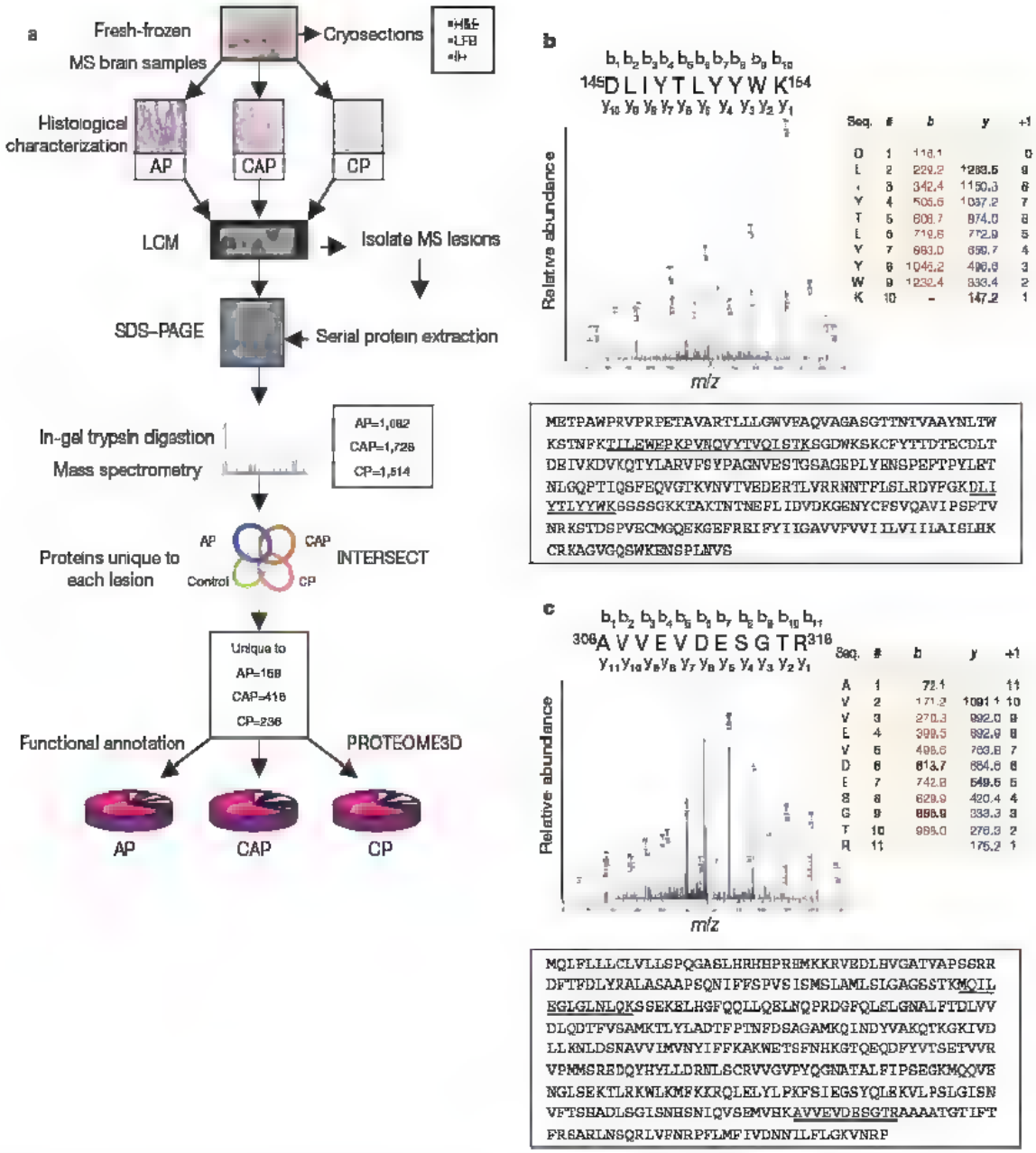

METPAWPRVPRPETAVARTLLLGWVFAQVAGASGTTNTVAAYNLTW
KSTNFKTILEWEPKPVNQVYTVQISTKSGDWKSKCFYTTDTECDLT
DEIVKDVKQTYLARVFSYPAGNVESTGSAGEPLYENSPEFTPYLET
NLGQPTIQSFEQVGTKVNVTVEDERTLVRRNNTFLSLRDVFGKDLI
YTLYYWKSSSSGKKTAKTNTNEFLIDVDKGENYCFSVQAVIPSRTV
NRKSTDSPVECMGQEKGEFREIFYIIGAVVFVVIILVIILAISLHK
CRKAGVGQSWKENSPLNVS

MQLPLLLCLVLLSPQGASLHRHEPREMKKRVEDLHVGATVAPSSRR
DFTFDLYRALASAAPSQNIFFSPVSISMSLAMLSLGAQESTKMQIL
EGLGLNLQKSSEKELHGFQQLLQELNQPRDGFQLSLGNALFTDLVV
DLQDTFVSAMKTLYLADTFPTNFDSAGAMKQINDYVAKQTKGKIVD
LLKNLDSNAVVIMVNYIFFKAKWETSFNHKGTQEQDFYVTSETVVR
VPMMSREDQYHYLLDRNLSCRVVGVPYQGNATALFIPSEGKMQQVE
NGLSEKTLRKWLKMFKKRQLELYLPKFSIEGSYQLEKVLPSLGISN
VFTSHADLSGISNHSNIQVSEMVHKAVVEVDESGTRAAAATGTIFT
FRSARLNSQRLVFNRPFLMFIVDNNILFLGKVNRP

Figure 2 | Proteomic analysis of MS lesions. **a**, Schematic procedure of the proteomic analysis of MS lesions. **b**, Representative tandem mass spectra of peptide(s) identified from (**b**) tissue factor or (**c**) PCI from CAP samples. Sequences of identified peptides are shown above the mass spectra and underlined in the protein sequence; b_n or y_n denote the ion generated by cleavage of the peptide bond after the *n*th amino acid from the amino terminus or the carboxy terminus; identified b and y ions and values of *m/z* (mass/charge) for ions are indicated in the table.

aPC-treated mice (Fig. 4c, d). Additionally, fewer inflammatory foci were observed in the CNS tissue of EAE mice treated with aPC (Fig. 4e and Supplementary Fig. 5c, d)

Molecular mechanism of aPC during EAE. aPC functions both as an anticoagulant and a signalling molecule[18]. Structure–function studies have identified the domain of aPC required for its anticoagulant function as distinct from its signalling function[24]. To determine whether the amelioration of EAE by aPC treatment is mediated through anti-coagulant or signalling functions, we induced EAE in SJL/J mice and treated them with two recombinant aPC mutants, aPC-L8W and aPC-K193E[25]. One mutant, aPC-L8W, retains anti-coagulant properties but lacks PAR-1 signalling because of the defective interaction with its receptor EPCR at L8[26]. The other mutant, aPC-K193E, mainly participates in PAR-1 signalling and lacks anti-coagulant activities[18]. The clinical status of the mice treated with aPC mutants was compared with those treated with either vehicle (PBS) or aPC wild type (WT) Mice treated with aPC-L8W and aPC-K193 showed significant amelioration early in the disease course (days 20–25), whereas mice treated with aPC-WT showed improvement in the latter part of disease course (days 25–30) (Fig. 5a–c). These data suggest that both activities of aPC may be required for maintaining an extended effect in this model.

To understand the effects of aPC on CNS and immune cells, we separately isolated peritoneal macrophages, astrocytes and T cells and activated them *in vitro* with either lipopolysaccharide (LPS) or

Table 2 | Summary of the proteomic data

	AP	CAP	CP	CTL
Peptide	40,819	64,678	54,339	68,478
Unique peptide	6,321	10,143	8,967	8,991
Protein*	1,082	1,728	1,514	1,492
Reverse peptide identifications	39	34	10	12
Forward peptide identifications	3,612	4,937	3,687	4,020
False positive (%)†	1.08	0.69	0.27	0.3

*Identification filtering criteria: X_{corr} 1.9 (1+), 2.2 (2+), 3.7 (3+), delta correlation > 0.1, excluding trypsin, including keratin, excluding single peptide identification. The files used to compute false-positive rate were searched against concatenated forward and reverse human databases.
†Formula for the false positive (%): number of reverse identifications × 100/number of forward identifications, based on a representative subset of each category

CD3/CD28 after pre-treatment with recombinant murine aPC. Activated macrophages and astrocytes treated with aPC produced less IL-6 and IL-17 (Fig. 5 d–g). Similarly, low levels of IL-17 were detected in T cells exposed to aPC (Fig. 5h). These data suggest that aPC suppresses inflammation in both the CNS and the periphery.

Because aPC suppressed NF-κB signalling during neuronal injury[27], we analysed protein extracts from cultured T cells treated with murine aPC in cell activation assays by western blot analysis. The results demonstrate less IκB breakdown in cells treated with aPC. This implies inhibition of NF-κB signalling by aPC (Fig. 5i).

Discussion

This study provides the first information on large-scale protein identification from highly characterized MS brain lesions. Proteomic expression profiling of MS brain lesions has identified several candidate therapeutic targets. Reversing the physiological effects of two of these newly implicated proteins (tissue factor and PCI) ameliorates disease in EAE. A parallel approach in identification of targets in EAE had previously led to development of new therapies in MS, as in the case of natalizumab, which targets a critical integrin involved in homing of monocytes to the inflamed brain[28]. Thus, this exercise has precedents in leading ultimately to new and effective therapies in MS.

Brück and Lucchinetti have classified active MS lesions according to their distinct histological and immunocytological characteristics[1]. The proteomic analysis of MS lesions illuminates the dynamic biological events that influence lesion development and pathogenesis. It will be possible to refine these proteomics techniques to analyse specific areas in MS tissues (for example, normal-appearing white matter, areas of oligodendrocyte destruction) in order to identify proteins unique to these particular regions of interest.

The reversal of neurological deficits in EAE by administration of thrombin inhibitor and aPC suggests several new options for MS therapy. Heparin therapy was shown to improve symptoms during MS relapses and active EAE[29,30], but treating patients with MS with an anticoagulant such as hirudin would not be optimal because of the increased risk of bleeding. Serum of EAE mice treated with hirudin also showed the presence of anti-hirudin antibodies (not shown), which may have interfered with the protective effects of hirudin during EAE. On the other hand, aPC may be a drug for future therapy in MS, especially if an aPC variant with reduced bleeding potential could be engineered by genetic modification[18,22].

Experiments using function-specific aPC mutants raise several intriguing questions about the pharmacological properties of aPC. Our results suggest that both the anticoagulant and signalling properties of aPC ameliorate EAE, perhaps through different mechanisms. One possible explanation consistent with our findings centres on PAR-1 activation such that either sending a cytoprotective signal

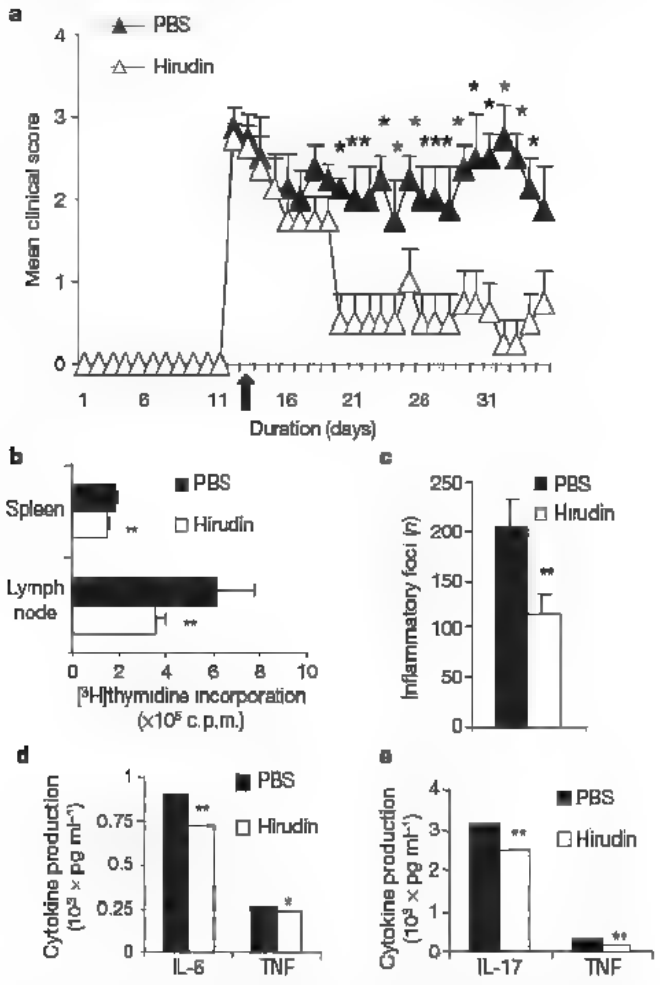

Figure 3 | Thrombin inhibition suppresses inflammation in EAE. **a**, Mean clinical scores ± s.e.m. of EAE mice treated with PBS (black) or recombinant hirudin (white) (10 mg kg^{-1}) ($n = 10$ per group) at the peak of disease (arrow) ($P < 0.05$, Mann–Whitney analysis). **b**, *In vitro* proliferation rates of splenocytes and lymph-node cells activated with PLP (20 μg ml^{-1}) and cytokine production from (**d**) splenocytes and (**e**) lymph-node cells of mice treated with PBS or hirudin. Mean ± s.e.m. *$P < 0.05$, **$P < 0.02$ (*t*-test) (from triplicate culture wells). **c**, Quantitation of inflammatory lesions from brain and spinal cord of EAE mice treated with PBS or hirudin ($n = 5$ per group). Data represent means ± s.e.m. (**$P < 0.01$).

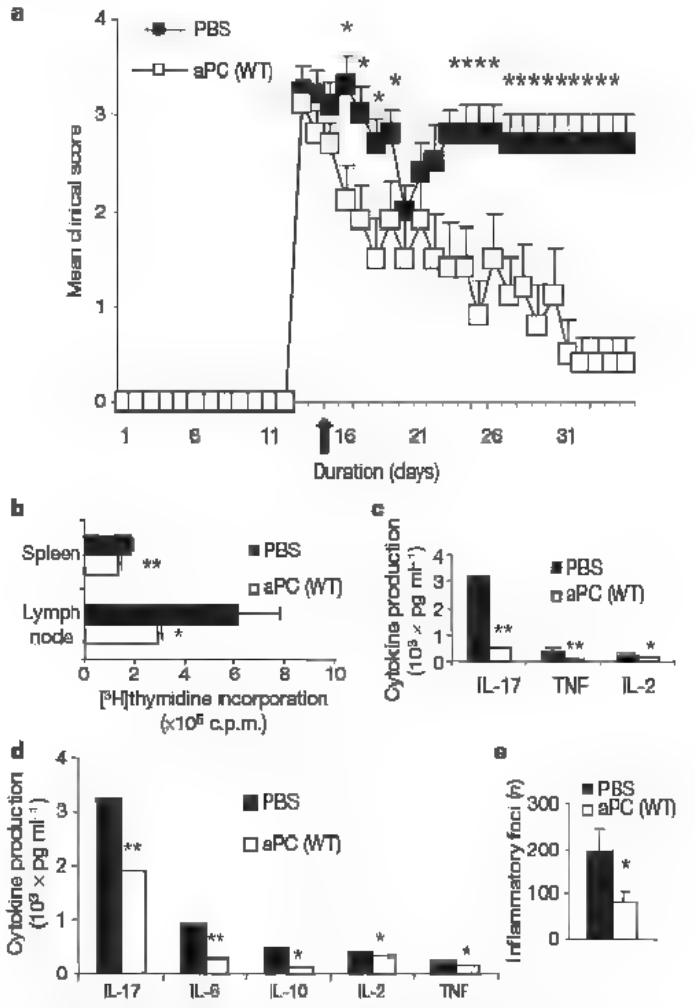

Figure 4 | aPC modulates Th1 and Th17 responses in EAE. **a**, Mean clinical scores ± s.e.m. of EAE mice treated with PBS (black) and aPC (white) at maximal paralysis (arrow) ($P < 0.05$, Mann–Whitney analysis); **b**, proliferation rates of splenocytes and lymph-node cells after activation with PLP peptide in culture and cytokine levels of c) lymph nodes and d) splenocytes from PBS and aPC-treated EAE mice. Means ± s.e.m. (picograms per millilitre) (*$P < 0.05$, **$P < 0.02$, *t*-test) **e**, Quantitation of inflammatory foci from paraffin-embedded sections from brain and spinal cord of EAE mice treated with PBS or aPC. Data represent mean ± s.e.m., ($P < 0.05$, *t*-test)

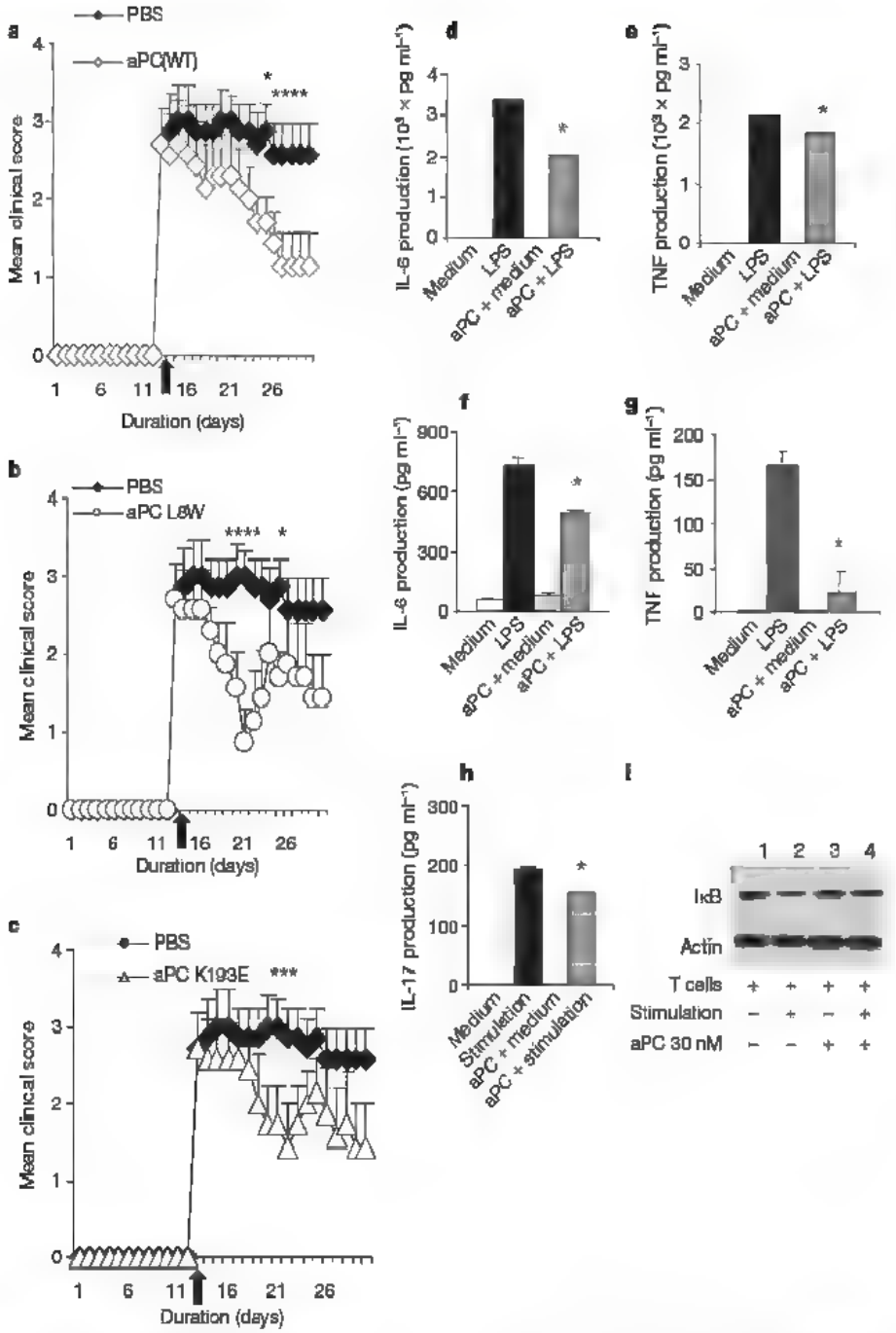

Figure 5 | Molecular mechanism of aPC during EAE. SJL/J mice with established EAE ($n = 7$ per group) were treated with (arrow) PBS or aPC-WT (**a**), aPC-L8W (**b**) or aPC-K193E (**c**) (0.46 mg kg^{-1}). Mean clinical scores ± s.e.m. (*$P < 0.05$, Mann–Whitney analysis). **d–h**, Macrophages (**d**, **e**), primary astrocytes (**f**, **g**) or purified T cells (**h**) were pre-treated with recombinant murine aPC-WT (30 nM) and activated with LPS (100 ng ml^{-1}) (**d–g**) or CD3/CD28 (5 μg ml^{-1}) (**h**), and cytokine levels were measured from culture supernatant. Means ± s.e.m. (pictograms per millilitre) ($P < 0.05$, *t*-test). **i**, Immunoblot of total cell lysate (50 μg) from purified T cells treated with aPC (30 min time point) probed with anti-IκB-α.

(through EPCR and PAR-1 by aPC-K193E) or inhibiting the generation of thrombin (by aPC-L8W, and thus suppressing its pro-inflammatory signals through PAR-1) is independently sufficient to improve function in EAE. Experiments to understand the molecular interplay of EPCR, PAR-1 and aPC signalling in the CNS and immune cells are underway. This may provide a direct application for MS therapy because PAR-1 signalling alone by aPC was sufficient to suppress EAE.

We used the approach of systems biology to identify the molecular composition of the proteins in defined MS lesions. The lesion-specific proteome reveals a 'new world', with most of the unique proteins identified in all three MS lesions possessing functions currently unknown within today's knowledge of physiology. Other proteins whose functions are known, like those of the coagulation cascade, are clearly playing new and perhaps unexpected pathobiological roles beyond our current understanding. The intersection of the coagulation cascade and inflammation in MS is the first of many new discoveries that will emerge from such a catalogue of proteins. These proteomes constitute a mere vocabulary for the biological language whose rules and structures must be deciphered to understand a disease like MS.

METHODS SUMMARY

Histopathological characterization of MS lesions. Cryosections from MS and control samples were analysed by H&E, LFB and immunohistochemistry as previously described[9]. MS lesions were classified according to the criteria used by Lock *et al.*[11]. Normal control brain samples were ruled out for obvious CNS pathology.

LCM, in-gel trypsin digestion, mass spectrometry, database searching. Cryosections (15 μM) from brain samples were cut on Molecular Machines and Industries (MMI) membranes and MS lesions were isolated by LCM as previously described[31]. Protein samples were extracted and resolved by

one-dimensional SDS–polyacrylamide gel electrophoresis (SDS–PAGE). Then, protein bands were digested with trypsin, and tryptic peptides were analysed repeatedly (four to seven times) with a linear trap quadrupole (LTQ) ion-trap mass spectrometer[33]. Data obtained from each gel band were searched independently against a non-redundant human protein database using the SEQUEST algorithm[32]. Files from acute plaque, CAP and chronic plaque were then combined using the INTERACT program[33] and filtered as previously described[32,34]. False-positive rates were estimated by searching against a concatenated forward and reverse human protein database[35].

EAE. EAE was induced in 7- to 8-week-old SJL/J female mice by subcutaneous immunization with 100 μg $PLP_{139-151}$ in emulsion[36]. For hirudin (Refludan, recombinant lepirudin, Berlex) or aPC treatment, EAE mice ($n = 10$ per group) were treated with daily intravenous injection of hirudin (10 mg kg^{-1}) or mouse recombinant aPC-WT (0.2 mg kg^{-1}) beginning at the peak of disease. Mice were assessed daily and scored according to: 0, no clinical disease; 1, tail weakness; 2, hindlimb weakness; 3, complete hindlimb paralysis; 4, hindlimb paralysis and some forelimb weakness; 5, moribund or dead.

Statistical analysis. Data are presented as means ± s.e.m. A *t*-test ($n = 2$ groups) was used for parametric data, and a Mann–Whitney *U*-test for non-parametric data ($n = 2$ groups) to detect between-group differences. A *P* value of 0.05 or lower was considered significant.

Full Methods and any associated references are available in the online version of the paper at www.nature.com/nature.

Received 25 October; accepted 20 December 2007.
Published online 17 February 2008.

1. Lassmann, H., Bruck, W. & Lucchinetti, C. Heterogeneity of multiple sclerosis pathogenesis: implications for diagnosis and therapy. *Trends Mol. Med.* 7, 115–121 (2001).
2. Frohman, E. M., Racke, M. K. & Raine, C. S. Multiple sclerosis – the plaque and its pathogenesis. *N. Engl. J. Med.* 354, 942–955 (2006).
3. Wekerle, H. Immune pathogenesis of multiple sclerosis. *Neurol. Sci.* 26 (suppl. 1), S1–S2 (2005).
4. Benito, C. *et al.* Cannabinoid CB1 and CB2 receptors and fatty acid amide hydrolase are specific markers of plaque cell subtypes in human multiple sclerosis. *J. Neurosci.* 27, 2396–2402 (2007).
5. Kagitani-Shimono, K. *et al.* Lipocalin-type prostaglandin D synthase (beta-trace) is upregulated in the αB-crystallin-positive oligodendrocytes and astrocytes in the chronic multiple sclerosis. *Neuropathol. Appl. Neurobiol.* 32, 64–73 (2006).
6. Minn, A. J. *et al.* Genes that mediate breast cancer metastasis to lung. *Nature* 436, 518–524 (2005).
7. Rubinsztein, D. C. & Serra, H. G. Protein–protein interaction networks in the spinocerebellar ataxias. *Genome Biol.* 7, 229.1–229.3 (2006).
8. Sam-Yellowe, T. Y. *et al.* A *Plasmodium* gene family encoding Maurer's cleft membrane proteins: structural properties and expression profiling. *Genome Research* 14, 1052–1059 (2004).
9. Chabas, D. *et al.* The influence of the proinflammatory cytokine, osteopontin, on autoimmune demyelinating disease. *Science* 294, 1731–1735 (2001).
10. John, G. R. *et al.* Multiple sclerosis: re-expression of a developmental pathway that restricts oligodendrocyte maturation. *Nature Med.* 8, 1115–1121 (2002).
11. Lock, C. *et al.* Gene-microarray analysis of multiple sclerosis lesions yields new targets validated in autoimmune encephalomyelitis. *Nature Med.* 8, 500–508 (2002).
12. Peng, J., Elias, J. E., Thoreen, C. C., Licklider, L. J. & Gygi, S. P. Evaluation of multidimensional chromatography coupled with tandem mass spectrometry (LC/LC-MS/MS) for large-scale protein analysis: the yeast proteome. *J. Proteome Res.* 2, 43–50 (2003).
13. Hwang, S. I. *et al.* Systematic characterization of nuclear proteome during apoptosis: a quantitative proteomic study by differential extraction and stable isotope labeling. *Mol. Cell. Proteomics* 5, 1131–1145 (2006).
14. Lundgren, D. H., Eng, J., Wright, M. E. & Han, D. K. PROTEOME-3D: an interactive bioinformatics tool for large-scale data exploration and knowledge discovery. *Mol. Cell. Proteomics* 2, 1164–1176 (2003).
15. Esmon, C. T. Crosstalk between inflammation and thrombosis. *Maturitas* 47, 305–314 (2004).
16. Eddleston, M. *et al.* Astrocytes are the primary source of tissue factor in the murine central nervous system. A role for astrocytes in cerebral hemostasis. *J. Clin. Invest.* 92, 349–358 (1993).
17. Riewald, M. & Ruf, W. Orchestration of coagulation protease signaling by tissue factor. *Trends Cardiovasc. Med.* 12, 149–154 (2002).
18. Mosnier, L. O., Zlokovic, B. V. & Griffin, J. H. The cytoprotective protein C pathway. *Blood* 109, 3161–3172 (2007).
19. Song, X., Huhle, G., Wang, L., Hoffmann, U. & Harenberg, J. Generation of anti-hirudin antibodies in heparin-induced thrombocytopenic patients treated with r-hirudin. *Circulation* 100, 1528–1532 (1999).
20. de Kleijn, E. D. *et al.* Activation of protein C following infusion of protein C concentrate in children with severe meningococcal sepsis and purpura fulminans: a randomized, double-blinded, placebo-controlled, dose-finding study. *Crit. Care Med.* 31, 1839–1847 (2003).
21. Laterre, P. F. *et al.* Severe community-acquired pneumonia as a cause of severe sepsis: data from the PROWESS study. *Crit. Care Med.* 33, 952–961 (2005).
22. Bernard, G. R. *et al.* Efficacy and safety of recombinant human activated protein C for severe sepsis. *N. Engl. J. Med.* 344, 699–709 (2001).
23. Kinchuk, V. F. & Streknev, A. G. Rol' sistemy gemostaza v patogeneze i lechenii rasseiannogo skleroza. *Zh. Nevrol. Psikhiatr. Im. S. S. Korsakova* (special issue 2), 103, 34–38 (2003).
24. Gerlitz, B. G. Mutation of protease domain residues Lys37–39 in human protein C inhibits activation by the thrombomodulin-thrombin complex without affecting activation by free thrombin. *J. Biol. Chem.* 271, 22285–22288 (1996).
25. Grinnell, B. W. *et al.* Differentiation of cytoprotective vs. anticoagulant function with variants of activated protein C in LPS-induced renal microvascular dysfunction. *Crit. Care Med.* 35, (suppl.) abstr. 42 (2007).
26. Preston, R. J. *et al.* Multifunctional specificity of the protein C/activated protein C Gla domain. *J. Biol. Chem.* 281, 28850–28857 (2006).
27. Cheng, T. *et al.* Activated protein C inhibits tissue plasminogen activator-induced brain haemorrhage. *Nature Med.* 12, 1278–1285 (2006).
28. Steinman, L. Blocking adhesion molecules as therapy for multiple sclerosis: natalizumab. *Nature Rev. Drug Discov.* 4, 510–518 (2005).
29. Maschmeyer, J., Shearer, R., Lonser, E. & Spindle, D. Heparin potassium in the treatment of chronic multiple sclerosis. *Bull. Los Angel. Neuro. Soc.* 26, 165–171 (1961).
30. Lider, O. *et al.* Suppression of experimental autoimmune diseases and prolongation of allograft survival by treatment of animals with low doses of heparins. *J. Clin. Invest.* 83, 752–756 (1989).
31. Bagnato, C. *et al.* Proteomics analysis of human coronary atherosclerosis plaques: a feasibility study of direct tissue proteomics by liquid chromatography and tandem mass spectrometry. *Mol. Cell. Proteomics* 6, 1088–1102 (2007).
32. Yates, J. R. III, Eng, J. K., McCormack, A. L. & Schieltz, D. Method to correlate tandem mass spectra of modified peptides to amino acid sequences in the protein database. *Anal. Chem.* 67, 1426–1436 (1995).
33. Han, D. K., Eng, J., Zhou, H. & Aebersold, R. Quantitative profiling of differentiation-induced microsomal proteins using isotope-coded affinity tags and mass spectrometry. *Nature Biotechnol.* 19, 946–951 (2001).
34. Liu, H., Sadygov, R. G. & Yates, J. R. III. A model for random sampling and estimation of relative protein abundance in shotgun proteomics. *Anal. Chem.* 76, 4193–4201 (2004).
35. Peng, J. *et al.* A proteomics approach to understanding protein ubiquitination. *Nature Biotechnol.* 21, 921–926 (2003).
36. Platten, M. *et al.* Treatment of autoimmune neuroinflammation with a synthetic tryptophan metabolite. *Science* 310, 850–855 (2005); erratum 311, 954 (2006).

Supplementary Information is linked to the online version of the paper at www.nature.com/nature.

Acknowledgements We thank Mary Jane Eaton for help with histopathology and Jian Luo for help with imaging microscopy. This work was funded by the National Institutes of Health and the National Multiple Sclerosis Society to L.S., the National Institutes of Health to D.H., and Ruth L. Kirschstein National Research Service Award and T32 Adult and Pediatric Rheumatology and Immunology Fellowship awards to M.H.H. B.W.G. and B.G. are employed by Lilly Research Laboratories, a division of Eli Lilly & Co.

Author Contributions M.H.H. and L.S. formulated the hypothesis and designed all the experiments. D.K.H., S.-I.H. and D.H.L. contributed the proteomic studies. D.B.R. performed the EAE experiment with hirudin treatment. R.A.S. and C.S.R. contributed to the histopathological analysis. B.G. and B.W.G. provided the recombinant aPC proteins. J.V.P. performed studies on NF-κB signalling. S.S.O. performed the *in vitro* assays with astrocytes. D.K.H. and L.S., the senior authors, contributed equally to this work.

Author Information Reprints and permissions information is available at www.nature.com/reprints. The authors declare competing financial interests: details accompany the full-text HTML version of the paper at www.nature.com/nature. Correspondence and requests for materials should be addressed to L.S. (steinman@stanford.edu).

LETTERS

A minimum column density of 1 g cm^{-2} for massive star formation

Mark R. Krumholz[1,2] & Christopher F. McKee[3]

Massive stars are very rare, but their extreme luminosities make them both the only type of young star we can observe in distant galaxies and the dominant energy sources in the Universe today. They form rarely because efficient radiative cooling keeps most star-forming gas clouds close to isothermal as they collapse, and this favours fragmentation into stars of one solar mass or lower[1–3]. Heating of a cloud by accreting low-mass stars within it can prevent fragmentation and allow formation of massive stars[4,5], but the necessary properties for a cloud to form massive stars—and therefore where massive stars form in a galaxy—have not yet been determined. Here we show that only clouds with column densities of at least 1 g cm^{-2} can avoid fragmentation and form massive stars. This threshold, and the environmental variation of the stellar initial mass function that it implies, naturally explain the characteristic column densities associated with massive star clusters[6–9] and the difference between the radial profiles of Hα and ultraviolet emission in galactic disks[10,11]. The existence of a threshold also implies that the initial mass function should show detectable variation with environment within the Galaxy, that the characteristic column densities of clusters containing massive stars should vary between galaxies, and that star formation rates in some galactic environments may have been systematically underestimated.

Consider a simple model system: a spherical gas cloud of mass M, column density Σ, radius $R=\sqrt{[M/(\pi\Sigma)]}$, and density profile $\rho \propto r^{-k_\rho}$, with a point source of luminosity L at its centre, representing the radiation output by stars beginning to form within it. In the limit $L \to 0$, the cloud falls to a background temperature T_b set by the balance between cosmic-ray heating and molecular and dust cooling. We are interested in the earliest stages of cloud collapse, so we adopt $k_\rho = 1$. This puts most of the mass at low density, and is expected if clouds are in rough hydrostatic balance and obey the observed linewidth–size relation[12] $\sigma \propto r^q$ for molecular clouds, where σ is the velocity dispersion, r is the size scale and $q \approx 0.5$. However, any choice in the range $1 \leq k_\rho \leq 2$ yields the same qualitative conclusions.

The dust in a spherical cloud with a central source of illumination has a power-law temperature structure $T = T_{ch}(r/R_{ch})^{-k_T}$, where T_{ch}, R_{ch} and k_T are functions of the cloud column density Σ, the light to mass ratio $\eta = L/M$, and the dust opacity, which we characterize through a parameter δ that we define below[13]. As we show in the Supplementary Information using a grain–gas energy exchange code[14–16], at the high densities with which we are concerned, the gas temperature will be nearly identical to the dust temperature. The temperature will be everywhere greater than T_b if

$$T_{ch}(\eta,\Sigma,\delta)\left[\frac{R}{R_{ch}(\eta,\Sigma,\delta)}\right]^{-k_T(\eta,\Sigma,\delta)} = T_b \qquad (1)$$

Because k_T is generally close to 0.4 for strong sources of internal illumination and large R/R_{ch}, a cloud satisfying this condition has an effective adiabatic index $\gamma \approx 1.4$ throughout its volume. As even $\gamma \approx 1.1$–1.2 is sufficient to suppress fragmentation[5], equation (1) implicitly defines a critical light-to-mass ratio η_{halt} above which fragmentation will halt in a cloud with a given Σ, δ and T_b. We describe our procedure for solving this equation in the Supplementary Information.

We approximate the infrared dust opacity as $\kappa = \delta\kappa_0(\lambda_0/\lambda)^2$, where δ is a dimensionless number that we define to be unity at solar metallicity, λ is the radiation wavelength, and $\lambda_0 = 100\,\mu$m. Observations in the Milky Way indicate[13,17] that, in cold regions where dust grains are coated with ice mantles, $\kappa_0 \approx 0.54$ cm^2 g^{-1}. Under Milky Way conditions the minimum temperature for interstellar gas is $T_b \approx 10$ K, with a weak density dependence that we ignore for simplicity. In addition to the Milky Way case, we also consider $\delta = 0.25$, $T_b = 10$ K, appropriate for a low-metallicity galaxy today, and $\delta = 0.25$, $T_b = 15$ K, typical of a galaxy at $z \approx 6$ that has low metallicity but a temperature floor of 15 K imposed by the cosmic microwave background. Figure 1 shows the value of η_{halt} calculated for the three cases. We find that η_{halt} declines with Σ because at higher Σ a cloud of fixed mass has a smaller radiating area and remains warmer at fixed luminosity.

Clouds containing massive stars can have light-to-mass ratios of $100L_\odot/M_\odot$ (ref. 18), more than sufficient to stop fragmentation, but we are interested in clouds where no massive stars have yet formed because fragmentation breaks all collapsing objects down to small masses. For a low-mass protostar the dominant energy source is gravitational potential energy radiated away by accreting gas. We plot the energy released per unit mass accreted, ψ, in Fig. 2. Consider a cloud converting its mass into stars at a rate $\dot{M}_*$ with a mass distribution $dn/d\ln m_*$ and a mean mass $m_* = \int m_*(dn/d\ln m_*)d\ln m_*$. Once the rate at which new stars in a cloud begin accreting balances the rate at which other stars reach their final mass and stop accreting, the light-to-mass ratio is

$$\eta_{grav} = \frac{1}{M}\left(\frac{\dot{M}_*}{\dot{m}_*}\right)\int \frac{dn}{d\ln m_*}\psi m_* d\ln m_* \qquad (2)$$

$$= \frac{SFR_{ff}}{t_{ff}}\langle\psi\rangle_{IMF} \qquad (3)$$

where $SFR_{ff} = (\dot{M}_* t_{ff})/M$ is the fraction of a cloud's mass that it turns into stars per mean density free-fall time t_{ff}, and $\langle\psi\rangle_{IMF} = \bar{m}_*^{-1}\int(dn/d\ln m_*)\psi m_* d\ln m_*$ is the value of ψ averaged over the initial mass function (IMF). For a Chabrier IMF[19] truncated at a maximum mass of $1M_\odot$, $\langle\psi\rangle_{IMF} = 2.1\times10^{14}$ erg g^{-1} $= 0.11(GM_\odot/R_\odot)$. Observations constrain SFR_{ff} to be a few per cent[20,21], and in the Supplementary Information we use an analytic fitting formula[22] to estimate $SFR_{ff} \approx 0.041\left(M_2\Sigma_0/T_{b,1}^2\right)^{-0.08}$, where $M_2 = M/(100M_\odot)$, $\Sigma_0 =$

[1]Astrophysics Department, Princeton University, Princeton, New Jersey 08544, USA. [2]Astrophysics Department, University of California Santa Cruz, Santa Cruz, California 95064, USA. [3]Physics and Astronomy Departments, University of California Berkeley, Berkeley, California 94720, USA

$\Sigma/(1\,\mathrm{g\,cm^{-2}})$, and $T_{b,1} = T_b/(10\,\mathrm{K})$. Combining our estimates for $\langle\psi\rangle_{IMF}$ and SFR_{ff} with the definition of the mean density free-fall time ($t_{ff} = \sqrt{3\pi/(32G\bar{\rho})} = 38.6 M_2^{1/4}\Sigma_0^{-3/4}\,\mathrm{kyr}$), we find that the light-to-mass ratio of a cloud powered by accretion onto low-mass stars is

$$\eta_{grav} \approx 3.6 M_2^{\ 0.33}\Sigma_0^{0.67}T_{b,1}^{0.16}\left(\frac{L_\odot}{M_\odot}\right) \quad (4)$$

For the models shown in Fig. 2 a cloud reaches its equilibrium light-to-mass ratio within about $3t_{ff}$ after star formation begins, and because SFR_{ff} is less than about 0.05, at most ~15% of the mass will have gone into low-mass stars at this point. If star formation accelerates in time, as predicted by some models[23], then η_{grav} will reach the value given by equation (4) even earlier.

In Fig. 1, we show η_{grav} computed for some typical parameters overplotted with η_{halt}. For each cloud mass M, we solve equations (1) and (4) to find the column density Σ_{th} such that $\eta_{halt} \geq \eta_{grav}$, and plot the result in Fig. 3. This is the threshold required for fragmentation to halt. We find that thresholds of 0.7–1.5 $\mathrm{g\,cm^{-2}}$ are required to form stars of 10–200$M_\odot$ under Milky Way conditions. Lower-metallicity galaxies (0.25 solar metallicity) with comparable background temperatures require column densities that are about a factor of 3 smaller, whereas galaxies at $z \approx 6$ with 0.25 solar metallicity but high cosmic microwave background temperatures require higher column densities by a similar factor.

The existence of a threshold for massive star formation both explains current observations and predicts future ones. Regions with column densities above about 1 $\mathrm{g\,cm^{-2}}$ are rare even among star-forming clouds, and contain only a small fraction of the molecular mass in the Galaxy, but our threshold explains why all nearby regions of massive star formation have Σ at or above this value[6–9]. We further predict that clusters formed with $\Sigma \ll 1\,\mathrm{g\,cm^{-2}}$ should be deficient in massive stars. This is probably unobservable in individual low-Σ clusters because they contain too few stars, but a statistical analysis of many clusters might reveal the effect.

Conversely, suppression of fragmentation should produce top-heavy IMFs at high gas column densities. This prediction can be tested by X-ray searches for low-mass protostars in high-Σ clouds that are not detected by Spitzer at 24 μm and therefore contain no massive protostars[24]. We predict that any low-mass protostellar populations detected will constitute at most 15% of the total mass. This prediction provides a sharp test for distinguishing our model from competitive accretion models, which predict that the mass of the most massive star forming in a cloud is related to the mass of low-mass stars around it by $(M_{max}/M_\odot) \approx (M_{low\text{-}mass}/M_\odot)^{2/3}$ (ref. 23). Thus we would predict that a cloud of mass $100M_\odot$ and $\Sigma > 1\,\mathrm{g\,cm^{-2}}$ with no stars larger than $10M_\odot$ should have a total stellar content below $15M_\odot$, whereas competitive accretion would allow up to $42M_\odot$ of low-mass stars. However, because radiation does not halt fragmentation until some low-mass stars have formed, we do expect most massive stars to form surrounded by a cluster.

Environmental variation at the top end of the IMF has even more profound consequences for extragalactic astronomy, as observations of distant galaxies are generally sensitive only to massive stars. The threshold explains why Hα emission in galactic disks ends at sharp edges where the disks transition from gravitationally unstable to gravitational stable[10], but ultraviolet emission declines smoothly with radius and does not show a feature at the Hα edge[11]. Ultraviolet and

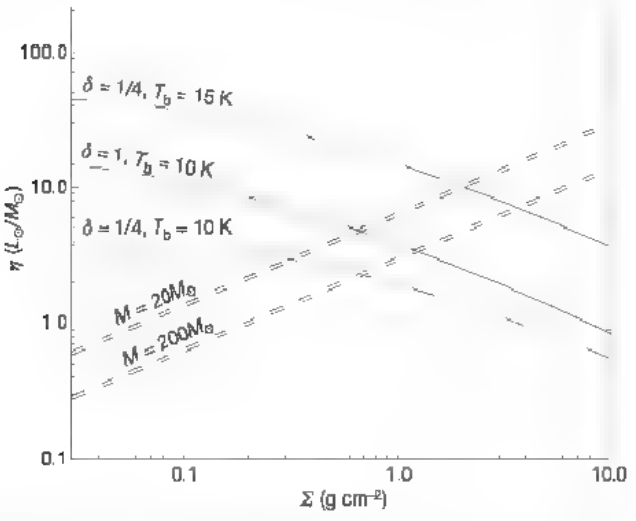

Figure 1 | Critical and equilibrium light-to-mass ratios versus cloud column density. The plot shows the critical light-to-mass ratio η_{halt} (solid lines) and the equilibrium light-to-mass ratio η_{grav} due to low-mass star formation (dashed lines) as a function of the cloud column density Σ. The three curves for η_{halt} are computed for $\delta = 1$, $T_b = 10$ K, for $\delta = 1/4$, $T_b = 10$ K, and for $\delta = 1/4$, $T_b = 15$ K, as indicated. The two sets of curves for η_{grav} are computed for $M = 20M_\odot$ and $M = 200M_\odot$, as indicated, corresponding to the clouds that would be required to form $10M_\odot$ and $100M_\odot$ stars for a typical star-formation efficiency[27] of 50%. In each pair the lower curve corresponds to $T_b = 10$ K and the upper to $T_b = 15$ K. Note that the background temperature can be higher than our assumed T_b in regions near massive stars, but it is unclear whether massive stars in a cluster ever form close enough in time that the first to form can affect the formation of subsequent ones. In the Orion Nebula[28] and W3 Main[29] clusters, all the stars larger than $10M_\odot$ that remain today formed over a time spread of less than about 10^5 yr. This is comparable to the formation time of a single massive star[30], so that the last massive star to form must have been well in progress by the time the first began to heat its envelope. Even in non-coeval clusters, our approach applies to the first massive stars.

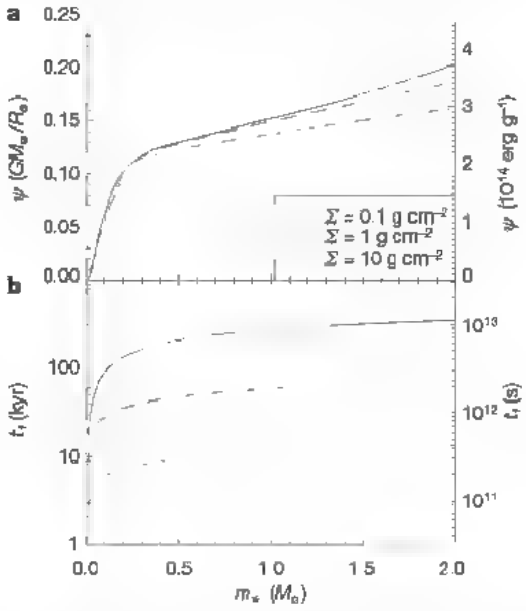

Figure 2 | Energy per unit mass radiated and formation time versus protostellar mass. a, The energy per unit mass, ψ, radiated away in the process of forming a star of mass m_*; **b**, the time required to form the star, t_f. The tracks shown are computed using a one-zone protostellar evolution code[9] applied to the accretion histories predicted previously[9,30] using their fiducial parameters, for protostellar cores born in environments where the column density is $\Sigma = 0.1$, 1.0 or 10.0 $\mathrm{g\,cm^{-2}}$ as indicated. However, alternative accretion histories give qualitatively identical results. Note that ψ is nearly independent of both accretion history and final stellar mass because the entropy distribution within a protostar and the protostellar mass–radius relation are nearly constant on timescales that are short compared with the Kelvin–Helmholtz time t_{KH}, and for low-mass stars $t_f \ll t_{KH} \approx 10$ Myr. This means that ψ, which is a measure of the gravitational energy released, is nearly independent of accretion history. Moreover, because low-mass stars have nearly linear mass–radius relations, ψ is also nearly independent of the final stellar mass. Although our calculation of ψ uses a code calibrated to solar metallicity, our results should also apply over a very wide range of metallicities because even for low-metallicity stars $t_f \ll t_{KH}$.

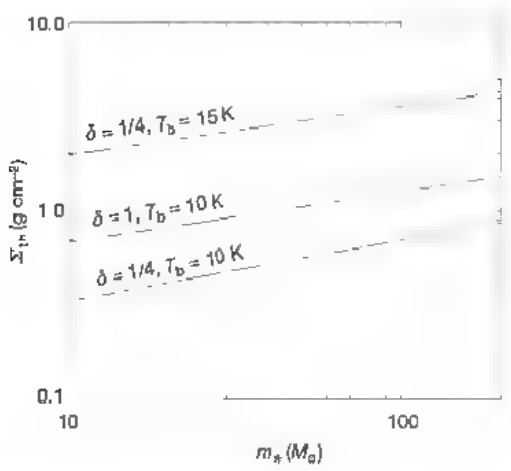

Figure 3 | Threshold column density versus stellar mass. The plot shows the threshold column density Σ_{th} required to form a star of mass m_* for $\delta = 1$, $T_b = 10$ K, for $\delta = 1/4$, $T_b = 10$ K, and for $\delta = 1/4$, $T_b = 15$ K, as indicated. In making the plot we assumed an efficiency of 50% (ref. 27), so that the cloud mass required to make a star of mass m_* is $M = 2m_*$.

Hα emission are both tracers of recent star formation but are sensitive to different parts of the IMF. Outside the gravitational stability radius, the molecular-to-atomic surface density ratio drops sharply[25], probably because purely local instabilities create small molecular clouds but not giant complexes like those in the inner parts of disks. Because compressing gas to column densities of Σ_{th} requires a huge amount of weight that can only be provided by such giant complexes, their absence will selectively suppress the formation of the most massive stars, leading to a truncated IMF. If in such a region no stars larger than, for example, $15M_\odot$ were to form, this would reduce ultraviolet emission by ~50% but would eliminate more than 99% of the Hα light[26], explaining the sharp drop in Hα but not in the ultraviolet.

An important corollary is that estimates of the star formation rate assuming a standard IMF in regions that do not contain giant clouds (such as much of the volume of dwarf galaxies and the outer parts of disk galaxies) may be systematically too low. At this point our theory is too approximate to allow a precise calculation of the underestimate.

Our calculation of Σ_{th} also enables us to predict how the characteristic column densities of young clusters containing massive stars will vary between galaxies. We predict that clusters that have cleared their gas but not yet dynamically expanded should show a minimum column density near Σ_{th} (probably slightly below Σ_{th}, owing to gas removal), and this should be lower at low metallicity and higher at high redshift, as indicated in Fig. 3.

Received 17 October; accepted 20 December 2007.

1. Larson, R. B. Thermal physics, cloud geometry and the stellar initial mass function. *Mon. Not. R. Astron. Soc.* 359, 211–222 (2005).
2. Jappsen, A.-K., Klessen, R. S., Larson, R. B., Li, Y. & Mac Low, M.-M. The stellar mass spectrum from non-isothermal gravoturbulent fragmentation. *Astron. Astrophys.* 435, 611–623 (2005).
3. Bonnell, I. A., Clarke, C. J. & Bate, M. R. The Jeans mass and the origin of the knee in the IMF. *Mon. Not. R. Astron. Soc.* 368, 1296–1300 (2006).
4. Krumholz, M. R. Radiation feedback and fragmentation in massive protostellar cores. *Astrophys. J.* 641, L45–L48 (2006).
5. Krumholz, M. R., Klein, R. I. & McKee, C. F. Radiation-hydrodynamic simulations of collapse and fragmentation in massive protostellar cores. *Astrophys. J.* 656, 959–979 (2007).
6. Plume, R., Jaffe, D. T., Evans, N. J., Martin-Pintado, J. & Gomez-Gonzalez, J. Dense gas and star formation: Characteristics of cloud cores associated with water masers. *Astrophys. J.* 476, 730–749 (1997).
7. Mueller, K. E., Shirley, Y. L., Evans, N. J. & Jacobson, H. R. The physical conditions for massive star formation: Dust continuum maps and modeling. *Astrophys. J. Suppl. Ser.* 143, 469–497 (2002).
8. Shirley, Y. L., Evans, N. J., Young, K. E., Knez, C. & Jaffe, D. T. A CS $J = 5 \rightarrow 4$ mapping survey toward high-mass star-forming cores associated with water masers. *Astrophys. J. Suppl. Ser.* 149, 375–403 (2003).
9. McKee, C. F. & Tan, J. C. The formation of massive stars from turbulent cores. *Astrophys. J.* 585, 850–871 (2003).
10. Martin, C. L. & Kennicutt, R. C. Star formation thresholds in galactic disks. *Astrophys. J.* 555, 301–321 (2001).
11. Boissier, S. *et al.* Radial variation of attenuation and star formation in the largest late-type disks observed with GALEX. *Astrophys. J. Suppl. Ser.* 173, 524–537 (2007).
12. Heyer, M. H. & Brunt, C. M. The universality of turbulence in galactic molecular clouds. *Astrophys. J.* 615, L45–L48 (2004).
13. Chakrabarti, S. & McKee, C. F. Far-infrared SEDs of embedded protostars and dusty galaxies. I. Theory for spherical sources. *Astrophys. J.* 631, 792–808 (2005).
14. Neufeld, D. A., Lepp, S. & Melnick, G. J. Thermal balance in dense molecular clouds: Radiative cooling rates and emission-line luminosities. *Astrophys. J. Suppl. Ser.* 100, 132–147 (1995).
15. Young, K. E., Lee, J.-E., Evans, N. J. II, Goldsmith, P. F. & Doty, S. D. Probing pre-protostellar cores with formaldehyde. *Astrophys. J.* 614, 252–266 (2004).
16. Urban, A., Evans, N. J. II & Doty, S. D. A parameter study of the dust and gas temperature in a field of young stars. *Astrophys. J.* (submitted), preprint at (http://arXiv.org/abs/0710.3906) (2007).
17. Weingartner, J. C. & Draine, B. T. Dust grain-size distributions and extinction in the Milky Way, Large Magellanic Cloud, and Small Magellanic Cloud. *Astrophys. J.* 548, 296–309 (2001).
18. Wu, J. *et al.* Connecting dense gas tracers of star formation in our galaxy to high-*z* star formation. *Astrophys. J.* 635, L173–L176 (2005).
19. Chabrier, G. in *The Initial Mass Function 50 Years Later* (ed. Corbelli, E., Palla, F. & Zinnecker, H.) 41–50 (Springer, Dordrecht, 2005).
20. Tan, J. C., Krumholz, M. R. & McKee, C. F. Equilibrium star cluster formation. *Astrophys. J.* 641, L121–L124 (2006).
21. Krumholz, M. R. & Tan, J. C. Slow star formation in dense gas: Evidence and implications. *Astrophys. J.* 654, 304–315 (2007).
22. Krumholz, M. R. & McKee, C. F. A general theory of turbulence-regulated star formation, from spirals to ultraluminous infrared galaxies. *Astrophys. J.* 630, 250–268 (2005).
23. Bonnell, I. A., Vine, S. G. & Bate, M. R. Massive star formation: nurture, not nature. *Mon. Not. R. Astron. Soc.* 349, 735–741 (2004).
24. Motte, F. *et al.* The earliest phases of high-mass star formation: a 3 square degree millimeter continuum mapping of Cygnus X. *Astron. Astrophys.* 476, 1243–1260 (2007).
25. Braine, J., Ferguson, A. M. N., Bertoldi, F. & Wilson, C. D. The detection of molecular gas in the outskirts of NGC 6946. *Astrophys. J.* 669, L73–L76 (2007).
26. Parravano, A., Hollenbach, D. J. & McKee, C. F. Time dependence of the ultraviolet radiation field in the local interstellar medium. *Astrophys. J.* 584, 797–817 (2003).
27. Matzner, C. D. & McKee, C. F. Efficiencies of low-mass star and star cluster formation. *Astrophys. J.* 545, 364–378 (2000).
28. Huff, E. M. & Stahler, S. W. Star formation in space and time: The Orion Nebula Cluster. *Astrophys. J.* 644, 355–363 (2006).
29. Feigelson, E. D. & Townsley, L. K. The diverse stellar populations of the W3 star forming complex. *Astrophys. J.* 673, 354–362 (2008), preprint at (http://arXiv.org/abs/0710.0090) (2007).
30. McKee, C. F. & Tan, J. C. Massive star formation in 100 000 years from turbulent and pressurized molecular clouds. *Nature* 416, 59–61 (2002).

Supplementary Information is linked to the online version of the paper at www.nature.com/nature.

Acknowledgements We acknowledge S. Boissier, I. Bonnell, B. Elmegreen, E. Feigelson and C. Martin for discussions. We thank A. Urban, N. Evans and S. Doty for providing a copy of their grain–gas coupling code. This work was supported by NASA through the Hubble Fellowship program and by the NSF. Parts of this work were performed while the authors were in residence at the Kavli Institute for Theoretical Physics at UCSB.

Author Information Reprints and permissions information is available at www.nature.com/reprints. Correspondence and requests for materials should be addressed to M.R.K. (krumholz@astro.princeton.edu).

LETTERS

Designing metallic glass matrix composites with high toughness and tensile ductility

Douglas C. Hofmann[1], Jin-Yoo Suh[1], Aaron Wiest[1], Gang Duan[1], Mary-Laura Lind[1], Marios D. Demetriou[1] & William L. Johnson[1]

The selection and design of modern high-performance structural engineering materials is driven by optimizing combinations of mechanical properties such as strength, ductility, toughness, elasticity and requirements for predictable and graceful (non-catastrophic) failure in service[1]. Highly processable bulk metallic glasses (BMGs) are a new class of engineering materials and have attracted significant technological interest[2–6]. Although many BMGs exhibit high strength and show substantial fracture toughness, they lack ductility and fail in an apparently brittle manner in unconstrained loading geometries[7]. For instance, some BMGs exhibit significant plastic deformation in compression or bending tests, but all exhibit negligible plasticity (<0.5% strain) in uniaxial tension. To overcome brittle failure in tension, BMG–matrix composites have been introduced[8,9]. The inhomogeneous microstructure with isolated dendrites in a BMG matrix stabilizes the glass against the catastrophic failure associated with unlimited extension of a shear band and results in enhanced global plasticity and more graceful failure. Tensile strengths of ~1 GPa, tensile ductility of ~2–3 per cent[9], and an enhanced mode I fracture toughness of $K_{1C} \approx 40\ \mathrm{MPa\,m^{1/2}}$ were reported[8,9]. Building on this approach, we have developed 'designed composites' by matching fundamental mechanical and microstructural length scales. Here, we report titanium–zirconium-based BMG composites with room-temperature tensile ductility exceeding 10 per cent, yield strengths of 1.2–1.5 GPa, K_{1C} up to ~170 $\mathrm{MPa\,m^{1/2}}$, and fracture energies for crack propagation as high as $G_{1C} \approx 340\ \mathrm{kJ\,m^{-2}}$. The K_{1C} and G_{1C} values equal or surpass those achievable in the toughest titanium or steel alloys, placing BMG composites among the toughest known materials.

Uniaxial compression tests are often used to assess the ductility of BMG materials to distinguish them from glassy alloys, which all lack tensile ductility[10–21]. Under compression, an operating shear band is subject to a normal stress that closes the band. Variations in local material properties caused, for example, by nanoscale inhomogeneities[20] and frictional forces (due to closing stresses) combine to arrest persistent slip on individual shear bands. Multiple shear bands are sequentially activated, giving rise to global plasticity (~1–10% strain). A geometry that better differentiates the ductility is bending. Here, the sample is subject to both compressive and tensile stresses. Shear bands initiate on the tensile surface but are arrested as they propagate towards the neutral stress axis[22,23]. Deformation is stable unless the shear band at the tensile surface evolves to an opening crack[23,24]. In bending, plasticity is greatly enhanced when the characteristic dimension R_p of a crack tip's 'plastic zone' exceeds ~$D/2$, where D is sample thickness[22,24] and R_p is a material length scale related to fracture toughness. For a mode I opening crack, it can be expressed as[25]:

$$R_p \approx (1/2\pi)(K_{1C}/\sigma_Y)^2$$

R_p varies from ~1 μm up to ~1 mm on going from relatively brittle to tough BMGs[26]. R_p is associated with the maximum spatial extension (band length) of shear bands originating at an opening crack tip. For a specific geometry (for example, a mode I opening crack in tension tests), R_p is related to a maximum allowable shear offset along the band[23,24]. In bending, the most ductile BMG reported is $Pt_{57.5}Cu_{14.7}Ni_{5.3}P_{22.5}$, with $R_p \approx 0.5$ mm ($K_{1C} = 83\ \mathrm{MPa\,m^{1/2}}$). A 4-mm-thick square beam showed 3% plastic bending strain without cracking[27]. Despite large bending and compressive ductility, the $Pt_{57.5}Cu_{14.7}Ni_{5.3}P_{22.5}$ glass has negligible (<0.5%) ductility in uniaxial tensile tests. In tension, the opening stress on the shear bands enhances strain softening and instability, frictional forces are absent,

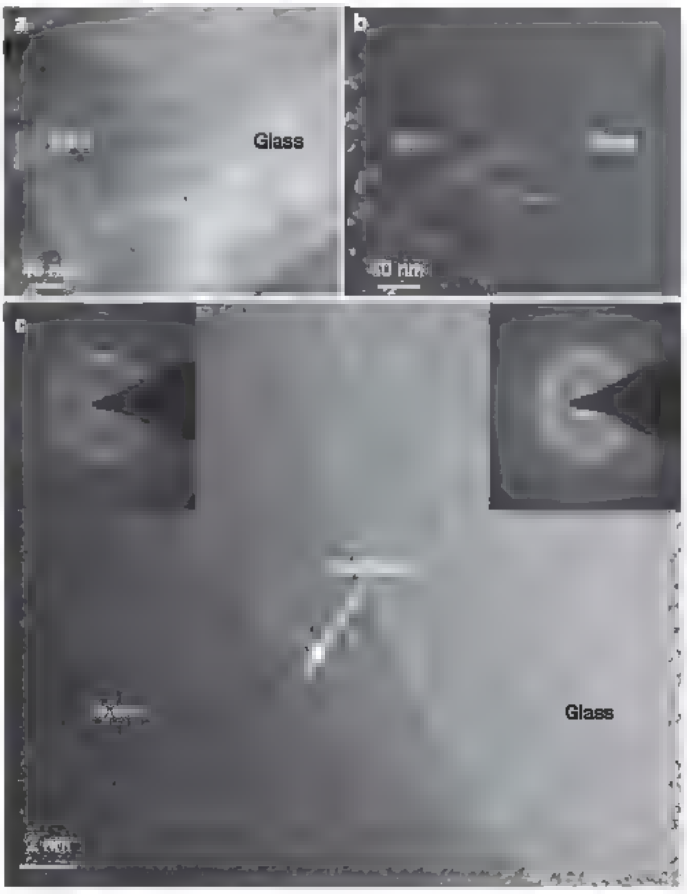

Figure 1 | High-resolution TEM images from the alloy DH1. a, Bright-field TEM micrograph showing a b.c.c. dendrite in the glass matrix. **b**, The corresponding dark-field micrograph of the same region. **c**, A high-resolution micrograph showing the interface between the two phases, with corresponding diffraction patterns shown in the inset.

[1]Keck Laboratory of Engineering Materials, California Institute of Technology Pasadena, California 91125, USA

and a propagating shear band lengthens and slips without limit. Cavitation ultimately ensues within the slipping band and an opening failure follows.

Suppression of tensile instability requires a mechanism to limit shear band extension. Bending produces an inherently inhomogeous stress state where a shear band is arrested by the gradient in applied stress, $\nabla\sigma = 2\sigma_Y/D$. Stability against crack opening is geometrically ensured when $D/2 < R_p$ (refs 23 and 24). Under uniaxial tension, applied stress is uniform. By introducing inhomogeneity in elastic or plastic material properties at a microstructural length scale L, 'microstructural' stabilization mechanisms become possible. Shear bands initiated in plastically soft regions (with lower σ_Y or lower shear modulus G) can be arrested in surrounding regions of higher yield stress or stiffness. Stabilization requires that $L \approx R_p$. This fundamental concept underlies enhancement of ductility and toughening and is similar to that used in the toughening of plastic by inclusion of rubber particles (see, for example, ref. 28).

Compared to previous *in situ* composites, the new BMG composites have increased Ti content to reduce density and contain no Ni. Removal of Ni enhances fracture toughness of the glass and suppresses nucleation of brittle intermetallics during processing. Three alloys—$Zr_{36.6}Ti_{31.4}Nb_7Cu_{5.9}Be_{19.1}$, $Zr_{38.3}Ti_{32.9}Nb_{7.3}Cu_{6.2}Be_{15.3}$ and $Zr_{39.6}Ti_{33.9}Nb_{7.6}Cu_{6.4}Be_{12.5}$ (DH1, DH2 and DH3)—are discussed. We varied the Be content, $x = 12.5$–19.1 (in atom %), while fixing the mutual ratios of Zr, Ti, Nb and Cu. As x decreases, we obtained an increasing volume (or molar) fraction of dendritic phase in a glass matrix. Scanning electron microscopy (SEM), energy dispersive X-ray spectrometry (EDS) and X-ray diffraction (XRD) analysis show that the composition of the dendrites and glass matrix remain approximately constant with varying x. The dendritic phase is a body-centred cubic (b.c.c.) solid solution containing primarily Zr, Ti and Nb, as verified by X-ray and EDS analysis.

Partition of DH1, DH2 and DH3 by volume fraction yielded 42%, 51% and 67% dendritic phase in a glass matrix, respectively. These percentages were obtained by analysing the contrast from SEM images using computer software. They were independently verified by analysing the heat of crystallization from DH1, DH2 and DH3 in differential scanning calorimetry (DSC) scans relative to the heat of crystallization from a fully glassy matrix alloy (see Supplementary Information). Dendrite compositions measured using EDS ranged over $Zr_{40-44}Ti_{42-45}Nb_{11-14}Cu_{1-3}$, while glass matrix compositions ranged over $Zr_{31-34}Ti_{17-22}Nb_{1-2}Cu_{9-13}Be_{31-38}$. These are reported with an estimated error of 1 atom %. The volume fraction of the dendritic phase can be controlled by varying x (data not presented here) from 0 to 100%. Ultrasonic measurements for the composites give average elastic constants following a 'volume rule of mixtures' with varying x. In DH1, for example, we obtained a shear modulus $G = 33.2$ GPa and Young's modulus $E = 89.7$ GPa for the glass matrix phase and $G = 28.7$ GPa and $E = 78.3$ GPa for the dendritic phase. The two-phase composite has a volume-weighted average value of the two, $G = 30.7$ GPa and $E = 84.3$ GPa. The dendrites are elastically soft inclusions relative to the matrix (see Supplementary

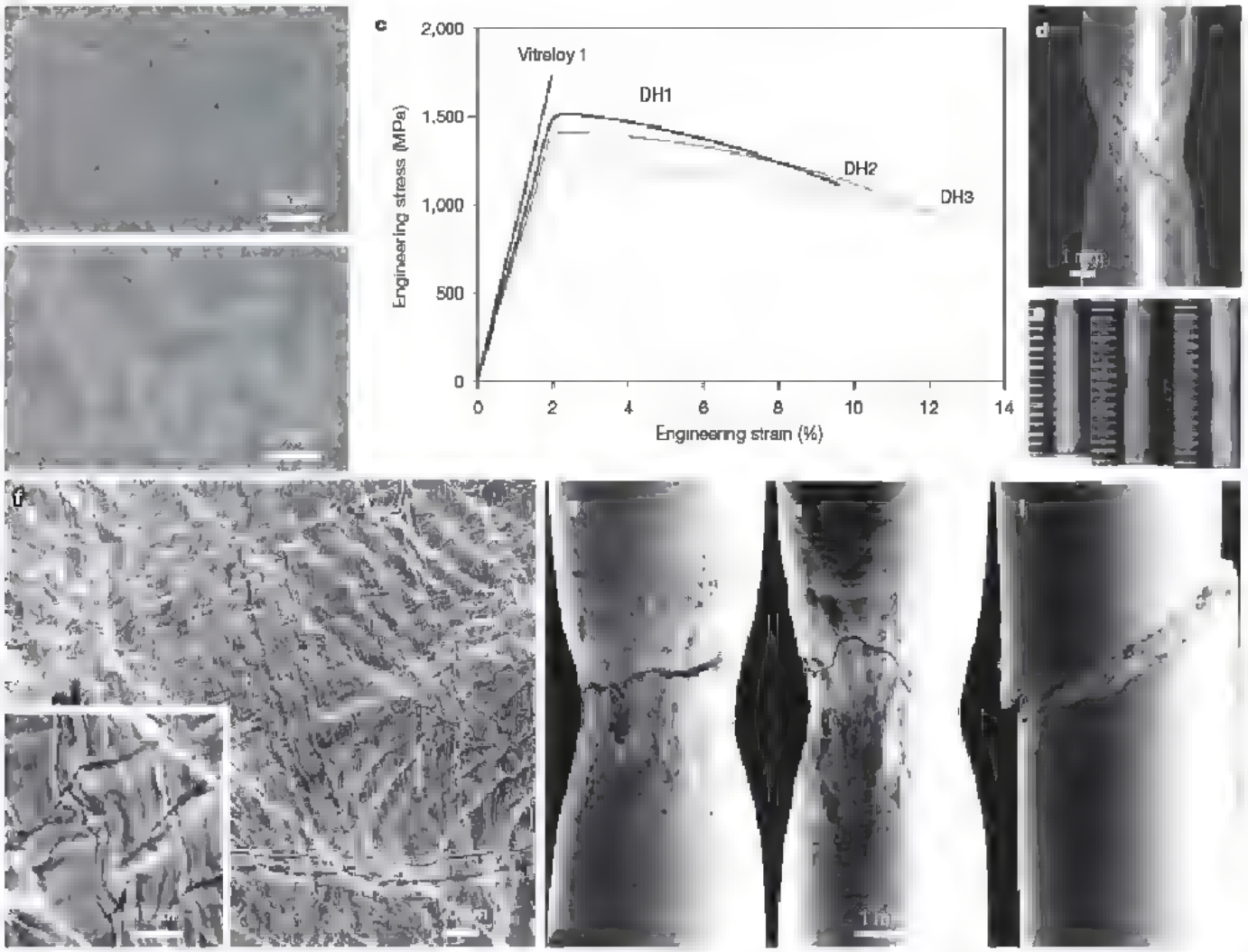

Figure 2 | Enhanced room-temperature tensile ductility of DH1, DH2 and DH3. Backscattered SEM micrographs showing the microstructure of DH1 (**a**) and DH3 (**b**) where the dark contrast is from the glass matrix and the light contrast is from the dendrites. **c**, Engineering stress–strain curves for Vitreloy 1 and DH1, DH2 and DH3 in room-temperature tension tests. **d**, Optical micrograph of necking in DH3. **e**, Optical micrographs showing an initially undeformed tensile specimen contrasted with DH2 and DH3 specimens after tension testing. **f**, SEM micrograph of the tensile surface in DH3 with higher magnification shown in the inset. SEM micrographs of necking in DH2 (**g**) and DH3 (**h**). **i**, Brittle fracture representative of all monolithic BMGs.

Information). Under loading, yielding and deformation are promoted in the dendrite vicinity and limited by the surrounding matrix.

Earlier reported *in situ* composites[8,9] were solidified from the melt in an arc melter. Owing to cooling rate variations within the ingots, the overall dendrite length scale and interdendrite spacings showed large variation from ~1 to 100 μm (refs 8 and 21). To produce a more uniform microstructure, we heated the present alloys into the semi-solid two-phase region (T = ~800–900 °C) between the alloy liquidus and solidus temperature[21] and held them there isothermally for several minutes, remaining entirely below the molten state (T > 1,100 °C). The semi-solid mixture was then quenched sufficiently rapidly to vitrify the remaining liquid phase. This process yields a more uniform 'near-equilibrium' two-phase microstructure throughout the ingot, which was characterized using TEM, as shown in Fig. 1. A bright-field/dark-field pair showing the b.c.c. dendrite in the glass matrix is shown in Fig. 1a and b for the alloy DH1. The interface between a dendrite and the glass matrix is shown in high resolution in Fig. 1b. The micrograph confirms that the interface between the two phases is atomically sharp. Diffraction patterns are shown in the insets of Fig. 1c for both the dendrite and the matrix glass. The dendrite exhibits a b.c.c. diffraction pattern whereas the glass matrix exhibits two broad, diffuse halos typical of an amorphous material. The dendrite–glass interfaces in DH2 and DH3 are similar to those seen in Fig. 1.

SEM analysis was used to characterize the bulk microstructure of the composites. Two selected areas are shown in Fig. 2a and b for the alloys DH1 and DH3. After analysing an array of micrographs, we found dendrite size varied over L ≈ 60–120 μm while inter-dendrite spacings varied over S ≈ 80–140 μm. (S is the distance from the centre of a single dendrite tree to the centre of an adjacent one, and L is the total spanning length of a single dendrite tree.) Primary or secondary 'trunk' diameters noticeably increased from DH1 to DH3 with DH1 (or DH3) exhibiting a more (or less) developed tree structure. The rationale for selecting these microstructures lies in uniformly matching the length scales L and S to be less than, but of the order of, R_p. The R_p for the glass matrix can be estimated from its K_{1C} ≈ 70 MPa $m^{1/2}$ to be R_p ≈ 200 μm.

The ambient-temperature (23 °C) engineering stress–strain tensile curves for DH1, DH2 and DH3 (Fig. 2c) show total strain to failure in the range 9.6–13.1% at ultimate tensile strengths of 1.2–1.5 GPa. Sample-to-sample variation in total strain was typically ±1% and variation in strength was typically ±0.1 GPa. The stress decreases at large strains owing to necking in the gauge section. The alloy DH2 demonstrates the most necking (50% reduction in area), and fails at a true stress of 2.15 GPa in the necked region. Optical images of tensile gauge sections in DH2 and DH3 are shown in Figs 2d and e. The *in situ* composites exhibit plastic elongation of approximately 1.3 mm (8.6%) and 1.7 mm (11.3%) from their undeformed gauge lengths of ~15 mm. Figure 2g and h shows the necked regions from DH2 and DH3 at higher magnification. In contrast, monolithic BMGs fail on a single shear band oriented at roughly 45° (Fig. 2i).

The observed tensile ductility of DH1, DH2 and DH3 is associated with patterns of locally parallel primary shear bands that form in domains defined by individual dendrites (Fig. 2f, taken near the necked region). The primary shear bands have a dominant spacing of d_p ≈ 15 μm, or roughly $S/10 \approx L/10$. The plane of shear slip of the primary bands changes orientation (often by a 90° rotation) on moving from one dendrite domain to a neighbouring dendrite domain. The length of individual primary shear bands (~60–100 μm) is of the order of L (and S), and somewhat less than, but of the order of, R_p. The inset of Fig. 2f shows a magnified image of secondary shear band patterns between two primary shear bands. Dense secondary shear bands with spacing d_s ≈ 1–2 μm are uniformly distributed within primary bands. We note that $d_p \approx L/10$ and $d_s \approx d_p/10$. Similar

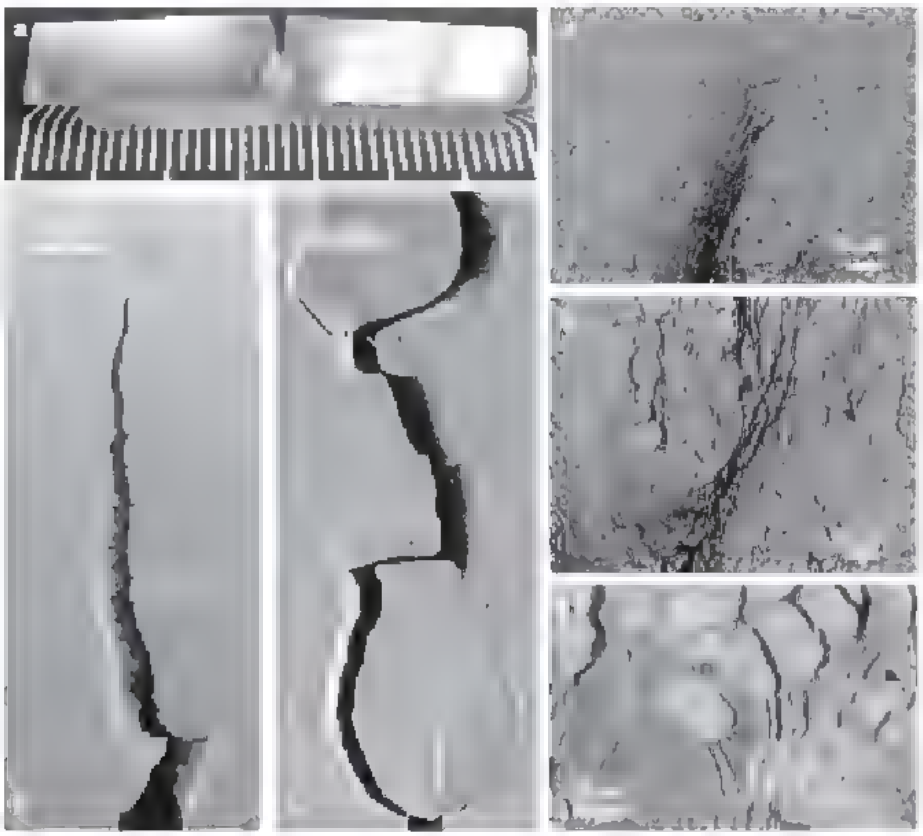

Figure 3 | High fracture toughness obtained by matching of key fundamental mechanical and microstructural length scales. **a**, Optical image of an unbroken fracture toughness (K_{1C}) specimen in DH1, showing plasticity around the crack tip of the order of several millimetres. **b**, SEM micrograph of an arrested crack in DH1 during a K_{1C} test. **c**, SEM micrograph of K_{1C} test in Vitreloy 1. **d**, **e** Backscattered SEM micrographs showing the plastic zone in front of the crack in DH1 (**d**) and DH3 (**e**). **f**, Higher-magnification SEM micrograph of DH3, showing shear bands of the order of 0.3–0.9 μm.

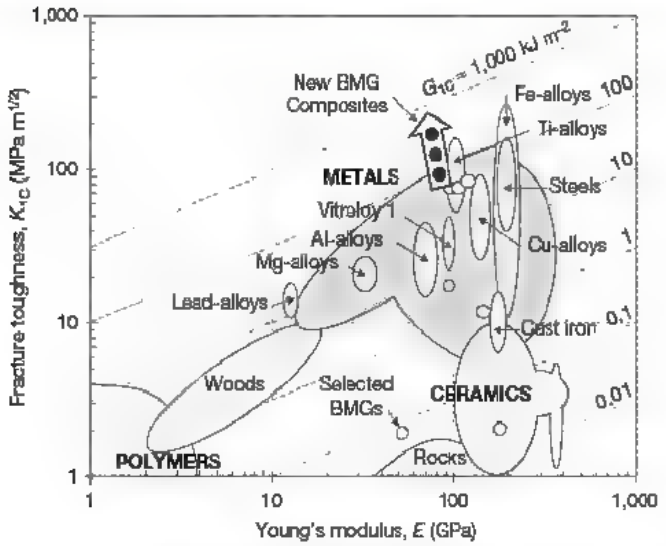

Figure 4 | Piercing the envelope of toughness for common engineering materials. An Ashby plot for materials selection. The dashed contour lines separated by an order of magnitude of G_{1C}. The plot shows a large range of common engineering materials along with selected metallic glass ribbons and BMGs. Owing to their high K_{1C} and low stiffness, the semi-solidly processed composites DH1, DH2 and DH3 (Zr-Ti-Nb-Cu-Be) have among the highest G_{1C} values of all known engineering materials.

geometric 'scaling' of shear band spacings is also observed for primary/secondary patterns in bending experiments[23,24].

Mode I fracture toughness tests in the three-point bend geometry (K_{1C}) were used to assess the resistance to crack propagation of DH1, DH2 and DH3 (Fig. 3a). From an initial cut notch, a precrack was generated by fatigue cracking. On subsequent loading, we observed extensive plasticity before crack growth. The load displacement curves start to turn over at a stress intensity of $K = 55$–75 MPa m$^{1/2}$, but unloading compliance shows that failure at the blunted precrack front initiates much later. Thus, the J-integral and J–R curves were used to assess K_{1C} according to method ASTM E399.A3 and formula ASTM E1820. In fact, the final propagating crack was arrested before sample failure occurred (Fig. 3b). This contrasts sharply with the behaviour of monolithic BMGs (Fig. 3c) in which crack arrest is never observed. Although an array of shear bands form at the precrack tip, the monolithic glass fails catastrophically along a single shear band when overloaded. Figure 3d and e shows backscattered SEM micrographs of the arrested crack tip in DH1 and DH3, showing a complex plastic zone with primary and secondary shear band patterns. DH3, which has the highest fracture toughness, exhibits more extensive deformation at the crack tip than DH1 (Fig. 3d, e).

High-resolution SEM was used to image the shear band formation in the interdendrite regions, shown in Fig. 3f. Primary and secondary shear band patterns are visible with spacing 5–10 μm and 0.3–0.9 μm, respectively. This matches closely with the secondary to primary shear band relation $d_s \approx d_p/10$. The fracture toughnesses of DH1, DH2 and DH3 were estimated to be $K_{1C} \approx 87$ MPa m$^{1/2}$, 128 MPa m$^{1/2}$ and 173 MPa m$^{1/2}$. DH1, DH2 and DH3 have high K_{1C} in load-limited failure, but have extremely high values of G_{1C} ($\sim K_{1C}^2/E$) in energy-limited failure (due in part to their relatively low Young's modulus). For example, the fracture toughness of DH3 is $K_{1C} \approx 173$ MPa m$^{1/2}$, while the fracture energy is $G_{1C} \approx 341$ kJ m^{-2}. This is comparable to G_{1C} in highly toughened steels, which have stiffness nearly three times higher than DH3 ($E \approx 200$ GPa versus $E = 75$ GPa). We note that the apparent plastic zone radius R_p of the composite is of the order of several millimetres (Fig. 3a), comparable to many structural crystalline metals.

To illustrate the unusual properties of the new composites, an 'Ashby Map', used for selection of materials in load, deflection and energy-limited structural applications, is shown in Fig. 4. The parallel dashed lines correspond to constant G_{1C} contours. Whereas the K_{1C} values of DH1, DH2 and DH3 are comparable to those of the toughest steels and crystalline Ti alloys, the G_{1C} values appear to pierce the limiting envelope defined by all alloys. The new BMG composites have benchmark G_{1C} values.

Table 1 summarizes some of the properties observed for DH1, DH2 and DH3. The properties are compared with those of monolithic BMGs and with earlier reported composites (other data obtained not shown). For example, Charpy impact energies were measured and found to be of the order of 40–50 J cm^{-2}, much higher than values for either monolithic glass or previous composites (Table 1). These results will be discussed elsewhere. Further details (backscattered SEM, XRD, DSC curves and optical images) of the current alloys are shown in the Supplementary Information.

To conclude, the present materials were created using the strategy of microstructural toughening and ductility enhancement in metallic glasses. The two basic principles are: (1) introduction of 'soft' elastic/plastic inhomogeneities in a metallic glass matrix to initiate local shear banding around the inhomogeneity; and (2) matching of microstructural length scales (for example, L and S) to the characteristic length scale R_p (for plastic shielding of an opening crack tip) to limit shear band extension, suppress shear band opening, and avoid crack development. These principles are applicable to other ductile-phase reinforced metallic glass systems provided several criteria are met: the new alloy system must be a highly processable metallic glass in which a shear-soft dendritic phase nucleates and grows while the remaining liquid is vitrified on subsequent cooling. At least one other alloy system has been reported that successfully uses this strategy[29]. A BMG matrix composite was discovered in $La_{74}Al_{14}(Cu,Ni)_{12}$ whereby 5% tensile ductility was achieved with 50% volume fraction of soft second phases. Although the La-based composite exhibited an ultimate tensile strength of only 435 MPa, the alloy demonstrated that the properties of the monolithic metallic glass ($La_{62}Al_{14}(Cu,Ni)_{24}$) could be greatly improved through the introduction of a soft second phase. Other desirable composite systems are those with lower density (as with Al-containing alloys) or with higher strength (as with Fe-based alloys).

METHODS SUMMARY

The alloys used in this research were prepared in a two-step process. First, ultrasonically cleansed pure elements were arc-melted under a Ti-gettered argon atmosphere. Second, the ingots were placed on a water-cooled Cu boat and heated via induction, with temperature monitored by pyrometer. The second step is used as a way of semi-solidly processing the alloys between their solidus and the liquidus temperatures. This procedure coarsens the dendrites, produces radio-frequency stirring, and homogenizes the mixture. Samples were produced with masses up to 35 g and with thicknesses ~1 cm, based on the geometry of the Cu boat. Samples for mechanical testing were machined directly from these

Table 1 | Mechanical and material properties of the new composites

Alloy	σ_{max} (MPa)	ε_{tot} (%)	σ_y (MPa)	ε_y (%)	E (GPa)	ρ (g cm^{-3})	G (GPa)	CIT (J)	RoA (%)	ν
$Zr_{36.6}Ti_{31.4}Nb_7Cu_{5.9}Be_{19.1}$ (DH1)	1,512	9.58	1,474	1.98	84.3	5.6	30.7	26	44	0.371
$Zr_{38.3}Ti_{32.9}Nb_{7.3}Cu_{6.2}Be_{15.3}$ (DH2)	1,411	10.80	1,367	1.92	79.2	5.7	28.8	40	50	0.373
$Zr_{39.6}Ti_{33.9}Nb_{7.6}Cu_{6.4}Be_{12.5}$ (DH3)	1,210	13.10	1,096	1.62	75.3	5.8	27.3	45	46	0.376
$Zr_{41.2}Ti_{13.8}Cu_{12.5}Ni_{10}Be_{22.5}$ (Vitreloy 1)	1,737	1.98	–	–	97.2	6.1	35.9	8	0	0.355
$Zr_{56.2}Ti_{13.8}Nb_{5.0}Cu_{6.9}Ni_{5.6}Be_{12.5}$ (LM2)	1,302	5.49	1,046	1.48	78.8	6.2	28.6	24	22	0.375

A comparison of the alloys DH1, DH2 and DH3, Vitreloy 1, and the *in situ* composite of refs 8 and 9 (LM2). The properties listed are yield strength (σ_y), ultimate tensile strength (σ_{max}), yield strain (ε_y), total strain to failure (ε_{tot}), reduction in area (RoA), density (ρ), modulus of elasticity (E), shear modulus (G), Charpy impact toughness (CIT) and Poisson's ratio (ν).

ingots and tests were performed in accordance with ASTM standards, where applicable. Elastic properties were measured ultrasonically

Full Methods and any associated references are available in the online version of the paper at www.nature.com/nature.

Received 18 October; accepted 11 December 2007.

1. Ashby M. F., *Materials Selection in Mechanical Design* Ch. 6 (Pergamon, Oxford, 1992).
2. Peker, A. & Johnson, W. L. A highly processable metallic glass: $Zr_{41.2}Ti_{13.8}Cu_{12.5}Ni_{10.0}Be_{22.5}$. *Appl. Phys. Lett.* **63**, 2342–2344 (1993)
3. Johnson, W. L. Bulk glass-forming metallic alloys: science and technology. *MRS Bull.* **24**, 42–56 (1999)
4. Ashby, M. F. & Greer, A. L. Metallic glasses as structural materials. *Scr. Mater.* **54**, 321–326 (2006)
5. Salimon, A. I. *et al.* Bulk metallic glasses: what are they good for? *Mater. Sci. Eng. A* **375**, 385–388 (2004).
6. Greer, A. L. Metallic glasses. *Science* **267**, 1947–1953 (1995)
7. Rao, X. *et al.* Preparation and mechanical properties of a new Zr-Al-Ti-Cu-Ni-Be bulk metallic glass. *Mater. Lett.* **50**, 279–283 (2001)
8. Hays, C. C., Kim, C. P. & Johnson, W. L. Microstructure controlled shear band pattern formation and enhanced plasticity of bulk metallic glasses containing in situ formed ductile phase dendrite dispersions. *Phys. Rev. Lett.* **84**, 2901–2904 (2000).
9. Szuecs, F., Kim, C. P. & Johnson, W. L. Mechanical properties of $Zr_{56.2}Ti_{13.8}Nb_{5.0}Cu_{6.9}Ni_{5.6}Be_{12.5}$ ductile phase reinforced bulk metallic glass composite. *Acta Mater.* **49**, 1507–1513 (2001)
10. Liu, Y. H. *et al.* Super plastic bulk metallic glasses at room temperature. *Science* **315**, 1385–1388 (2007)
11. Hofmann, D. C., Duan, G. & Johnson, W. L. TEM study of structural evolution in a copper mold cast $Cu_{46}Zr_{54}$ bulk metallic glass. *Scr. Mater.* **54**, 1117–1122 (2006)
12. Fan, C. & Inoue, A. Ductility of bulk nanocrystalline composites and metallic glasses at room temperature. *Appl. Phys. Lett.* **77**, 46–48 (2000)
13. Eckert, J. *et al.* Structural bulk metallic glasses with different length-scale of constituent phases. *Intermetallics* **10**, 1183–1190 (2002)
14. He, G., Löser, W. & Eckert, J. Microstructure and mechanical properties of the $Zr_{66.4}Cu_{10.5}Ni_{8.7}Al_8Ta_{6.4}$ metallic glass-forming alloy. *Scr. Mater.* **48**, 1531–1536 (2003)
15. Lee, M. H. *et al.* Mechanical behavior of Ni-based metallic glass matrix composites deformed by cold rolling. *Mater. Lett.* **58**, 3312–3315 (2004)
16. Lee, M. H. *et al.* A development of Ni-based alloys with enhanced plasticity. *Intermetallics* **12**, 1133–1137 (2004)
17. Das, J. *et al.* "Work-hardenable" ductile bulk metallic glass. *Phys. Rev. Lett.* **94**, 205501 (2005).
18. Yao, K. F. *et al.* Superductile bulk metallic glass. *Appl. Phys. Lett.* **88**, 122106 (2006).
19. Eckert, J. *et al.* High strength ductile Cu-base metallic glass. *Intermetallics* **14**, 876–881 (2006)
20. Chen, M. *et al.* Extraordinary plasticity of ductile bulk metallic glasses. *Phys. Rev. Lett.* **96**, 245502 (2006).
21. Lee, S. Y. *et al.* Pseudo-binary phase diagram for Zr-based in-situ beta phase composites. *J. Mater. Res.* **22**, 538–543 (2007).
22. Conner, R. D. *et al.* Shear bands and cracking of metallic glass plates in bending. *J. Appl. Phys.* **94**, 904–911 (2003).
23. Ravichandran, G. & Molinari, A. Analysis of shear banding in metallic glasses under bending. *Acta Mater.* **53**, 4087–4095 (2005)
24. Conner, R. D. *et al.* Shear band spacing under bending of Zr-based metallic glass plates. *Acta Mater.* **52**, 2429–2434 (2004)
25. Myers, M. A. *Mechanical Metallurgy: Principles and Applications* (Prentice Hall, Englewood Cliffs, New Jersey, 1984).
26. Lewandowski, J. J., Wang, W. H. & Greer, A. L. Intrinsic plasticity or brittleness of metallic glasses. *Phil. Mag. Lett.* **85**, 77–87 (2005).
27. Schroers, J. & Johnson, W. L. Ductile bulk metallic glasses. *Phys. Rev. Lett.* **93**, 255506 (2004)
28. Liang, J. Z. & Li, R. K. Y. Rubber toughening in polypropylene: a review. *J. Appl. Polym. Sci.* **77**, 409–417 (2000).
29. Lee, M. L. *et al.* Effect of a controlled volume fraction of dendritic phases on the tensile and compressive ductility in La-based metallic glass matrix composites. *Acta Mater.* **52**, 4121–4131 (2004)

Supplementary Information is linked to the online version of the paper at www.nature.com/nature.

Acknowledgements We acknowledge the Office of Naval Research for partial support of this work. D.C.H. acknowledges financial support from the Department of Defense through the NDSEG fellowship programme. This work benefited from the use of the Caltech Kavli Nanoscience Institute and the Mat. Sci. TEM facilities supported by the MRSEC Program of the National Science Foundation. We thank C. Garland for assistance with the TEM work. We also thank S. Y. Lee, K. S. Vecchio, C. P. Kim and C. E. Hofmann for their comments and advice.

Author Information Reprints and permissions information is available at www.nature.com/reprints. Correspondence and requests for materials should be addressed to D.C.H. (dch@caltech.edu)

LETTERS

Millennial- and orbital-scale changes in the East Asian monsoon over the past 224,000 years

Yongjin Wang[1], Hai Cheng[1,2], R. Lawrence Edwards[2], Xinggong Kong[1], Xiaohua Shao[1], Shitao Chen[1], Jiangyin Wu[1], Xiouyang Jiang[1], Xianfeng Wang[2] & Zhisheng An[3]

High-resolution speleothem records from China have provided insights into the factors that control the strength of the East Asian monsoon[1–4]. Our understanding of these factors remains incomplete, however, owing to gaps in the record of monsoon history over the past two interglacial–glacial cycles. In particular, missing sections have hampered our ability to test ideas about orbital-scale controls on the monsoon[5–7], the causes of millennial-scale events[8,9] and relationships between changes in the monsoon and climate in other regions. Here we present an absolute-dated oxygen isotope record from Sanbao cave, central China, that completes a Chinese-cave-based record of the strength of the East Asian monsoon that covers the past 224,000 years. The record is dominated by 23,000-year-long cycles that are synchronous within dating errors with summer insolation at 65° N (ref. 10), supporting the idea that tropical/subtropical monsoons respond dominantly and directly to changes in Northern Hemisphere summer insolation on orbital timescales[5]. The cycles are punctuated by millennial-scale strong-summer-monsoon events (Chinese interstadials[1]), and the new record allows us to identify the complete series of these events over the past two interglacial–glacial cycles. Their duration decreases and their frequency increases during glacial build-up in both the last and penultimate glacial periods, indicating that ice sheet size affects their character and pacing. The ages of the events are exceptionally well constrained and may thus serve as benchmarks for correlating and calibrating climate records.

The last glacial period is characterized by millennial-scale events, first identified in Greenland, including 25 Greenland interstadials (GIS) during the last interglacial–glacial period[11–13]. We previously identified a number of Chinese interstadial (CIS) events[2,4] (relatively strong summer millennial-scale East Asian monsoon, EAM, events) and correlated them with analogous GIS events. We also identified CIS events from portions of the penultimate glacial period, and established a nomenclature with last glacial period CIS denoted CIS A1, A2, and so on, from youngest to oldest, and those of the penultimate glacial period denoted CIS B1, B2, and so on[1]. Here we present an EAM record from Sanbao cave, together with our previous Hulu records[1,2], and characterize the complete CIS series for the last and penultimate interglacial–glacial cycles, including events not previously identified.

Sanbao cave is in Hubei province, central China, on the northern slope of Mt Shennongjia, near the southern edge of the Chinese loess plateau (110° 26′ E, 31° 40′ N, 1,900 m above sea level). Regional climate is dominated by the EAM, a sub-system of the Asian monsoon (AM) (Supplementary Fig. 1), with a mean annual rainfall of 1,900–2,000 mm and a mean temperature of 8–9 °C. During boreal summer (June to September), warm/humid air from the equatorial Pacific penetrates to the northern slope of Mt Shennongjia, delivering more than 80% of annual precipitation. Twelve stalagmites, collected ~1,500 m from the cave entrance, were dated, with 127 ^{230}Th dates with typical errors in age (2σ) of less than 1% (see Methods, Supplementary Table 1 and Supplementary Fig. 2). The record was established with 3,779 δ^{18}O data (see Methods and Supplementary Table 2) with an average resolution of ~70 yr between 224 and 55 kyr before present (BP) and ~40 yr or better between 19 and 0.5 kyr BP.

Virtually identical fluctuations of δ^{18}O from different stalagmites over contemporaneous growth periods (Fig. 1) provide a robust replication test for equilibrium calcite deposition[14] (Supplementary Fig. 3). Furthermore, the Sanbao δ^{18}O record is broadly similar to Hulu and Dongge records[1–4] for all overlapping time intervals (Supplementary Fig. 4), providing another replication test, and indicating that changes in climate have been similar over broad regions of China. Previous studies showed that shifts in stalagmite δ^{18}O largely reflect changes in δ^{18}O values of meteoric precipitation at Hulu and Dongge caves. These shifts, in turn, relate to changes in summer EAM intensity[1–3]. The similarities among the Sanbao, Hulu and Dongge records indicate that the Sanbao record is also a summer EAM proxy.

The EAM fluctuations recorded at Sanbao and Hulu broadly follow orbitally induced Northern Hemisphere summer insolation[10] (NHSI; Fig. 1) and are punctuated by many millennial-scale strong monsoon events (25 in the last glacial cycle, CIS A1–A25, and 24 in the penultimate glacial cycle, CIS B1–B24, Fig. 2 and Supplementary Fig. 5). We previously correlated most of the CIS A events with GIS events[2,4]. The Sanbao data complete this set of correlations through the full set of 25 GIS[13] and CIS A events, including identification of CIS A21, A22 and A25, and their correlation with analogous GIS events. For the penultimate glacial period, we have identified an additional 9 CIS B events so that the full CIS B sequence includes 24 events (Fig. 2 and Supplementary Fig. 5).

When directly compared to each other, there are some striking similarities in the character of analogous CIS A and CIS B events, particularly the older events, CIS A17–A24 and CIS B17–B24 (Fig. 2). In the penultimate interglacial–glacial cycle, the CIS events between 224 and 160 kyr BP (CIS B24–B12) are, in general, longer in duration (average ~3 kyr) and less frequent (~1 event in 5 kyr on average) in comparison with those between 160 and 130 kyr BP (CIS B15–B1, average duration of ~1.5 kyr and frequency of ~1 event in 2.5 kyr) (Fig. 2 and Supplementary Fig. 5). These relationships are similar to the variations of the CIS in the last interglacial–glacial cycle, with an average duration of ~3 kyr and frequency of ~1 event in 4.5 kyr between 110 and 50 kyr BP, and an average duration of ~2 kyr and frequency of ~1 event in 2.5 kyr between 50 and 10 kyr BP. Time–frequency analysis supports this generalization (Supplementary Fig. 6).

Furthermore, cross-spectral analysis between δ^{18}O records of Sanbao/Hulu and Greenland ice[14] over the past 120 kyr also reveals

[1]College of Geography Science, Nanjing Normal University, Nanjing, Jiangsu 210097, China. [2]Department of Geology and Geophysics, University of Minnesota, Minneapolis, Minnesota 55455, USA. [3]State Key Laboratory of Loess and Quaternary Geology, Institute of Earth Environment, Chinese Academy of Sciences, Xi'an, Shanxi 710054, China.

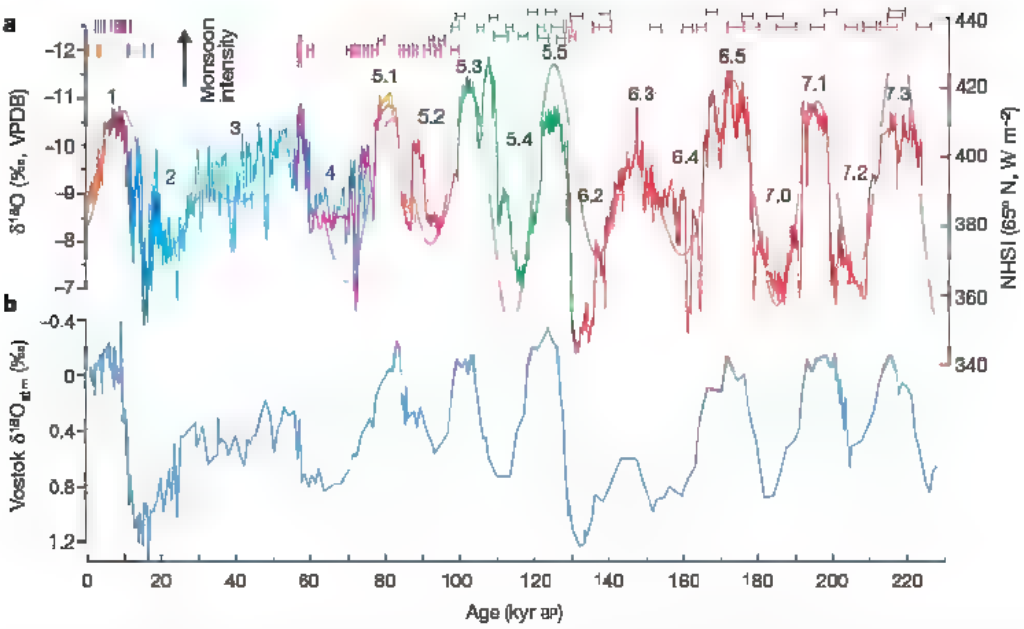

Figure 1 | Comparison of Sanbao/Hulu $\delta^{18}O$ records with NHSI and atmospheric $\delta^{18}O$ record over the past 224 kyr BP. **a**, Time versus Sanbao $\delta^{18}O$ records (red, stalagmite SB11, green, SB23, yellow, SB25-1, pink, SB22, dark blue, SB3, purple, SB10 and orange, SB26) and Hulu cave (blue)[3], and NHSI (Northern Hemisphere summer insolation, 21 July) at 65° N[10] (grey). For comparison, the Hulu $\delta^{18}O$ record is plotted 1.6‰ more negative to account for the higher Hulu values than Sanbao cave (see Supplementary Fig. 4). The ^{230}Th ages and errors (2σ error bars at top) are colour-coded by stalagmites. Numbers indicate the marine isotope stages and substages. **b**, The atmospheric $\delta^{18}O$ record from Vostok ice core, Antarctica[28].

significant common cycles centred at 6.1, 4.7, 4.2, 3.0, 1.6 and 1.2 kyr, similar to North Atlantic ice-rafted debris[15] and/or interstadial cycles[16](Supplementary Fig. 7), supporting the close link between the CIS and GIS. Forcing mechanisms for millennial-scale events have been explained by changing rates of North Atlantic Deep Water formation, resulting in changing heat transport to the North Atlantic[17]. Our data further indicate that (1) the duration and frequency of the millennial-scale events change systematically throughout the course of a glacial period, and (2) that the general nature of these changes is reproducible for the last two glacial periods. These observations suggest a link between ice volume, which could have changed in broadly the same fashion during the last two glacial periods, and the character, duration and pacing of millennial-scale events, consistent with recent simulation results that the mean climate state represented by global ice-volume can pace climatic events[8,9]. Therefore, ice volume, affecting ice dynamics, probably with feedbacks affecting atmospheric and oceanic circulation, may have a significant influence on GIS and CIS events.

The Sanbao/Hulu $\delta^{18}O$ records are characterized by a broadly sinusoidal pattern with a ~23 kyr cycle throughout (Supplementary

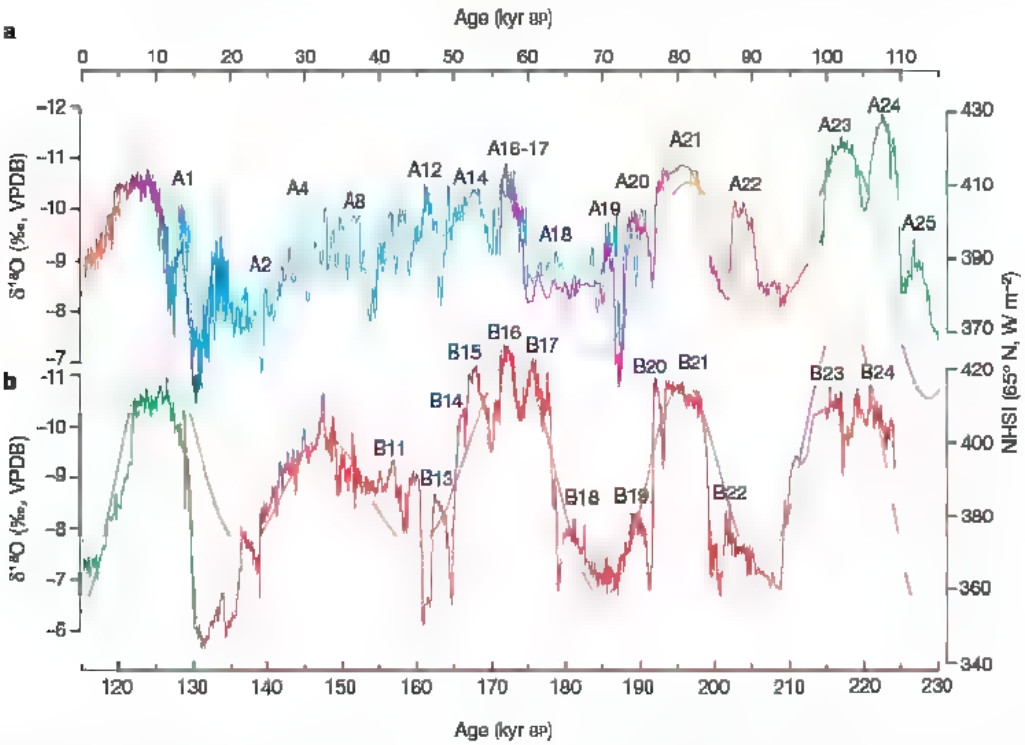

Figure 2 | Comparison of millennial-scale oscillations of the AM between the last and penultimate interglacial-glacial cycles. **a**, Last cycle; **b**, penultimate cycle. The same colours as in Fig. 1 are used to denote samples. Numbers indicate Chinese interstadials[1] (A25 to A1 in the last interglacial–glacial cycle and B24 to B1 in the penultimate interglacial–glacial cycle). See detailed plots of Hulu CIS A1–A13 and B1–B10 in refs 1 and 2. The summer (21 July) insolation at 65° N[10] (grey curves) is also plotted for comparison.

Figs 8 and 9), closely following precession-dominated NHSI (for example, 21 July) changes at 65° N[30] (Fig. 1). This strongly suggests that EAM orbital changes respond approximately linearly to orbital forcing. Spectral analysis ($r = 0.70$, $n = 3,206$) further shows no significant phase difference between 21 July insolation and the average EAM signal (lags of the EAM by 0.77 ± 0.45 kyr coherently at 23 kyr cyclicity or $12° \pm 7°$, with 30° equivalent to one month phase shift) (Supplementary Fig. 9).

At higher frequency, millennial-scale events (including CIS events and 'Mystery Intervals' before EAM Terminations I and II[1]) are superimposed on orbital-scale EAM variations. Depending on the relative timing of the millennial-scale and orbital-scale variations, the superposition may result in the appearance of a monsoon lead or lag relative to insolation. The EAM Termination II, dated at 129 ± 1 kyr BP here and in the Hulu and Dongge records[1,3], occurs after the initial rise in insolation by 4–6 kyr. This lag probably results from the occurrence of Heinrich event H11 (correlated to the Weak Monsoon Interval[1]) and its effect on the monsoon during the initial portion of the insolation rise. Similarly, the EAM lead relative to insolation at around 110 to 115 kyr BP might be explained by CIS A24 and A25 (Fig. 1). In addition, the monsoon shift associated with the last deglaciation begins at about 21 kyr BP, synchronous with the insolation minimum. The shift to interglacial values was punctuated by monsoon shifts that correlate with the Oldest Dryas (Heinrich event 1) and the Younger Dryas, explaining apparent EAM lags[7] of ~2 kyr relative to insolation during the last deglaciation (Fig. 2).

Given the observations above, our EAM records confirm an earlier hypothesis[5] that tropical monsoons vary dominantly and directly in response to the changes in Northern Hemisphere summer solar radiation on orbital scales. Onset of the modern Asian summer monsoon occurs in late May–early June as seasonal insolation change results in the reversal of the temperature gradient between land and ocean. Overall EAM rainfall reaches its peak in July in China. Analogous to the seasonal change of the modern EAM, our data show that NHSI change also drives the EAM on orbital scales through similar changes in the temperature gradient between land and ocean[1]. This contrasts with an idea that ties the AM precession cycle to latent heat transfer from the Southern Hemisphere, on the basis of a lag of the AM (as inferred from sediment cores from the Indian[18] and Pacific Oceans[19]) of $\sim 6 \pm 1$ kyr relative to 21 July insolation. Our data do not support this interpretation, nor do they support the idea of a monsoon lag relative to insolation.

One could plausibly reconcile the data sets if the western part of the AM (recorded in the ocean cores) behaved differently from the eastern portion (recorded in our Chinese cave work). However, this does not seem viable either, as cave studies show synchronous shifts for both regions on millennial[20,21] and orbital scales[3,22]. A second possible explanation[6] suggests that the oceanic monsoon proxies represent a more complicated signal that is not solely representative of the Indian summer monsoon. Here we raise a third possibility. From our correlations[1] between cave-based monsoon records and North Atlantic marine records[23], we know that during Termination II, the marine termination (benthic $\delta^{18}O$) led the abrupt transition into the last interglacial monsoon by several kyr. On the basis of this correlation, the SPECMAP timescale[24] is young by several kyr at Termination II. The idea is also supported by a number of earlier studies[25–27]. As the oceanic monsoon records are tied to the SPECMAP timescale[18], SPECMAP offsets might explain the difference in monsoon-insolation phasing inferred for the ocean and cave records.

The amplitudes of EAM variations follow NHSI in general. However, there are differences in $\delta^{18}O$ amplitudes. The monsoon peaks corresponding to marine isotope stage (MIS) 5.5 and 7.3 are relatively low, and the peak at MIS 6.5 is relatively high (Fig. 1). These differences are similar to precessional features in $\delta^{18}O$ variations of atmospheric O_2 ($\delta^{18}O_{atm}$) recorded in the Vostok ice core[28] (Fig. 1). Using the original timescale for $\delta^{18}O_{atm}$, we calculate a correlation coefficient of $r = 0.58$ ($n = 225$, between the $\delta^{18}O_{atm}$ and our records), a likely minimum value as differential errors in age may well lower the calculated coefficient substantially. This minimum, as well as the visual relationship in Fig. 1, indicate a clear relationship between the EAM and $\delta^{18}O_{atm}$, confirming earlier work linking low-latitude climate and $\delta^{18}O_{atm}$ (refs 26, 29). Today, $\delta^{18}O_{atm}$ differs from that of the ocean, the ultimate source of atmospheric O_2, by ~23.5‰ as a consequence of global photosynthesis (known as the Dole effect[29]). Sea water is the ultimate source of oxygen to the atmosphere, with terrestrial photosynthesis contributing to the isotopic difference through a combination of fractionations associated with evaporation from the ocean, Rayleigh processes in the atmosphere, meteoric precipitation, transpiration and photosynthesis[29]. The ultimate source of oxygen for EAM precipitation is also sea water, with isotopic compositions largely governed by the first three of the above processes.

The likely mechanistic link between changes in the Dole effect and changes in the EAM is changes in the average isotopic composition of terrestrial leaf water, through changes in the isotopic composition of meteoric precipitation and relative humidity, both of which might reasonably correlate with changes in the monsoon. As land photosynthesis contributes on the order of 63% of the oxygen to the atmosphere[29], a shift of only 1.6‰ in leafwater $\delta^{18}O$ would generate a 1‰ shift in $\delta^{18}O_{atm}$ (out of a full amplitude of about 1.6‰ for the whole record). As our monsoon record has an amplitude of about 6‰, changes in the isotopic composition of terrestrial meteoric precipitation (that include and correlate with our observed changes monsoon isotopic composition) could easily account for most of the $\delta^{18}O_{atm}$ shift. Furthermore, as leafwater $\delta^{18}O$ is very sensitive to relative humidity[29], changes in terrestrial relative humidity that correlate with (and include) our observed changes in the monsoon probably contribute to the observed changes in the Dole effect as well. Thus, our data support the idea[26,29] that varying AM intensity plays a key part in changing the Dole effect. This relationship will prove critical in correlating ice-core and monsoon records.

METHODS SUMMARY

All of the stalagmites were cut into halves along the growth axis and the surface polished. Subsamples were drilled along growth axes for ^{230}Th dating at the Minnesota Isotope Laboratory on an inductively coupled plasma mass spectrometer (Thermo-Finnigan ELEMENT) using procedures described in refs 3 and 4. A total of 127 ^{230}Th dates were obtained with typical errors in age (2σ) of less than 1%. Typical uncertainties in age (2σ) are less than 0.5 kyr between 10 and 60 kyr BP, 0.7 kyr between 60 and 130 kyr BP, 1.5 kyr between 130 and 180 kyr BP, and 2.0 kyr between 180 and 224 kyr BP. Linear interpolations between ^{230}Th dates were used to establish chronologies. Among these stalagmites, sample SB1. grew for the longest period of time, from 224 ± 2 to 129.3 ± 0.7 kyr BP. Sample SB11, together with four other stalagmites (see Supplementary Fig. 2 for lithologic profiles and dating positions), were used to reconstruct a monsoon history covering time ranges between 224 and 55 kyr BP and between 19.2 and 0.5 kyr BP, as shown in Fig. 1. Analytical procedures for oxygen isotope ratios ($\delta^{18}O$) are similar to those described in ref. 3 and are further described in Supplementary Table 2. Approximately 100 μg of powder samples were drilled along growth axes of stalagmites and analysed with an on-line, automated carbonate preparation system (Kiel III), linked to a Finnigan MAT-253 gas-source mass spectrometer at the Isotope Laboratory at Nanjing Normal University, China. Standards (NBS19) were run every nine samples to check reproducibility. The standard deviation calculated from the NBS19 measurements is ~0.06‰ for $\delta^{18}O$ values. The subsampling interval is ~1 mm or ~0.5 mm along stalagmite axes, depending on sample growth rates.

Received 6 July 2007; accepted 16 January 2008.

1. Cheng, H. *et al.* A penultimate glacial monsoon record from Hulu Cave and two-phase glacial terminations. *Geology* 34, 217–220 (2006)
2. Wang, Y. J. *et al.* A high-resolution absolute-dated late Pleistocene monsoon record from Hulu Cave, China. *Science* 294, 2345–2348 (2001)
3. Yuan, D. X. *et al.* Timing, duration and transition of the last interglacial Asian Monsoon. *Science* 304, 575–578 (2004)
4. Kelly, M. J. *et al.* High resolution characterization of the Asian Monsoon between 146,000 and 99,000 years B.P. from Dongge Cave and global correlation of events surrounding Termination II. *Palaeogeogr. Palaeoclimatol. Palaeoecol.* 236, 20–38 (2006)

5 Kutzbach, J E Monsoon climate of the Early Holocene: Climate experiment with the Earth's orbital parameters for 9000 years ago *Science* 214, 59–61 (1981)
6. Ruddiman, W F What is the timing of orbital-scale monsoon changes? *Quat. Sci. Rev.* 25, 657–658 (2006)
7 Clemens, S, C. & Prell, W L. The timing of orbital-scale Indian monsoon changes. *Quat. Sci. Rev* 26, 275–278 (2007)
8 Sima, A., Paul, A. & Schulz, M. The Younger Dryas — an intrinsic feature of late Pleistocene climate change at millennial timescales. *Earth Planet. Sci. Lett.* 222, 741–750 (2004)
9 Wang, Z. & Mysak, L. A. Glacial abrupt climate changes and Dansgaard-Oeschger oscillations in a coupled climate model. *Paleoceanography* 21, PA2001, doi:10.1029/2005PA001238 (2006)
10. Berger, A. L. Long-term variations of caloric insolation resulting from the Earth s orbita elements. *Quat. Res.* 9, 139–167 (1978).
11. Dansgaard, W *et al.* Evidence for general instability of past climate from a 250-kyr ice-core record. *Nature* 364, 218–220 (1993).
12 Meese, D. A. *et al.* The Greenland Ice Sheet Project 2 depth-age scale: Methods and results. *J. Geophys. Res.* 102, 26411–26423 (1997)
13. North Greenland Ice Core Project members. High-resolution record of Northern Hemisphere climate extending into the last interglacial period *Nature* 431, 147–151 (2004)
14. Hendy, C. H The isotope geochemistry of speleothems - I. The calculation of the effects of different modes of formation on the isotopic composition of speleothems and their applicability as paleoclimatic indicators. *Geochim. Cosmochim. Acta* 35, 801–824 (1971)
15. Bond, G *et al.* A pervasive millennial-scale cycle in North Atlantic Holocene and Glacial climates *Science* 278, 1257–1266 (1997)
16. Clemens, S. C. Millennial-band climate spectrum resolved and linked to centennial-scale solar cycles. *Quat. Sci. Rev.* 24, 521–531 (2005).
17 Broecker, W S. Massive iceberg discharges as triggers for global climate change. *Nature* 372, 421–424 (1994).
18. Clemens, S. C. & Prell. W. L. A 350,000 year summer-monsoon multi-proxy stack from the Owen ridge, Northern Arabian Sea *Mar. Geol.* 201, 35–51 (2003).
19. Morley, J., & Heusser, L. E. Role of orbital forcing in East Asian monsoon climates during the last 350 kyr: Evidence from terrestrial and marine climate proxies from core RC14–99 *Paleoceanography* 12, 483–494 (1997)
20 Sinha, A. *et al.* Variability of Southwest Indian summer monsoon precipitation during the Bølling-Allerød. *Geology* 33, 813–816 (2005)
21. Cai, Y., *et al.* High-resolution absolute-dated Indian Monsoon record between 53 and 36 ka from Xiaobailong Cave, southwestern China *Geology* 34, 621–624 (2006).
22. Fleitmann, D. *et al.* Holocene forcing of the Indian Monsoon recorded in a stalagmite from southern Oman. *Science* 300, 1737–1739 (2003).
23. McManus, J F., Oppo, D. W & Cullen, J. L. A 0.5-million-year record of millennial-scale climate variability in the North Atlantic. *Science* 283, 971–975 (1999)
24. Imbrie, J. *et al.* in *Milankovitch and Climate* Part 1 (eds Berger, A. L., Imbrie, J., Hays, J., Kukla, G. & Saltzman, B.) 269–305 (Riedel, Hingham, 1984).
25. Pisias, N. G., Mix A. C. & Zahn, R. Nonlinear response in the global climate system: Evidence from benthic oxygen isotopic record in core RC13–110 *Paleoceanography* 5, 147–160 (1990).
26. Shackleton, N. J. The 100,000 year Ice-Age cycle identified and found to lag temperature, carbon dioxides and orbital eccentricity *Science* 289. 1897–1902 (2000)
27 Ruddiman, W F. Orbital insolation, ice volume, and greenhouse gases. *Quat. Sci. Rev.* 22, 1597–1629 (2003).
28. Petit, J R. *et al.* Climate and Atmospheric history of the past 420,000 years from the Vostok ice core, Antarctic *Nature* 399, 429–436 (1999).
29. Bender, M., Sowers, T & Labeyrie, L. The Dole effect and its variations during the last 130,000 years as measured in the Vostok ice core. *Glob. Biogeochem. Cycles* 8, 363–376 (1994).

Supplementary Information is linked to the online version of the paper at www.nature.com/nature.

Acknowledgements We thank W. S. Broecker and the late G. Comer for their support of our work, and J. E. Kutzbach, W.F. Ruddiman and Y. Wang for their comments on an early version of the manuscript. This work was supported by National Basic Research Program of China, a Gary Comer Science and Education Foundation Grant, and NSF and NSFC grants

Author Information Reprints and permissions information is available at www.nature.com/reprints. Correspondence and requests for materials should be addressed to Y.W. (yjwang@njnu.edu.cn), or H.C. (cheng021@umn.edu), or R.L.E. (edwar001@umn.edu)

LETTERS

Arc-parallel flow in the mantle wedge beneath Costa Rica and Nicaragua

Kaj Hoernle[1,2], David L. Abt[3], Karen M. Fischer[3], Holly Nichols[1], Folkmar Hauff[2], Geoffrey A. Abers[4]†, Paul van den Bogaard[1,2], Ken Heydolph[1], Guillermo Alvarado[5], Marino Protti[6] & Wilfried Strauch[7]

Resolving flow geometry in the mantle wedge is central to understanding the thermal and chemical structure of subduction zones, subducting plate dehydration, and melting that leads to arc volcanism, which can threaten large populations and alter climate through gas and particle emission. Here we show that isotope geochemistry and seismic velocity anisotropy provide strong evidence for trench-parallel flow in the mantle wedge beneath Costa Rica and Nicaragua. This finding contradicts classical models, which predict trench-normal flow owing to the overlying wedge mantle being dragged downwards by the subducting plate. The isotopic signature of central Costa Rican volcanic rocks is not consistent with its derivation from the mantle wedge[1–3] or eroded fore-arc complexes[4] but instead from seamounts of the Galapagos hotspot track on the subducting Cocos plate. This isotopic signature decreases continuously from central Costa Rica to northwestern Nicaragua. As the age of the isotopic signature beneath Costa Rica can be constrained and its transport distance is known, minimum northwestward flow rates can be estimated (63–190 mm yr^{-1}) and are comparable to the magnitude of subducting Cocos plate motion (~85 mm yr^{-1}). Trench-parallel flow needs to be taken into account in models evaluating thermal and chemical structure and melt generation in subduction zones.

Preferential alignment of the minerals olivine and orthopyroxene occurs as a result of deformation, and produces anisotropy in seismic-wave velocities within the upper mantle. Assuming classical trench-normal 'corner flow' and standard models of crystallographic fabric development, the direction of fast shear-wave polarization will be normal to the arc in the warmer wedge beneath the arc and back-arc, although the fast shear-wave polarization may be parallel to the arc in the cold corner of the wedge beneath the fore-arc[5,6]. Whereas this pattern of seismic anisotropy is observed in some subduction zones[7,8], many display more variable fast directions further from the trench beneath the arc and back-arc, often with a roughly arc-parallel trend[9–12]. The origin of this arc-parallel fast anisotropy, in particular whether it is related to along-arc flow within the mantle wedge or some other process, is vigorously debated[5,6,13–16].

Although arc volcanic rocks from Costa Rica have ocean-island-basalt (OIB)-type compositions similar to those found in Galapagos hotspot rocks[17], the origin of this geochemical signature is controversial. In some models, OIB signatures are contained in the mantle wedge beneath central Costa Rica, reflecting (1) residual Galapagos-type mantle remaining after the formation of the Caribbean large igneous province (CLIP) in the Cretaceous period[1], or flow of OIB-type asthenospheric mantle either (2) from beneath the northwest margin of South America[2] or (3) through a slab window[3] into the mantle wedge beneath central Costa Rica. Alternatively, subduction erosion of older Galapagos and CLIP terranes in the Costa Rican fore-arc may have introduced this signature beneath Costa Rica[4]. The geochemical evidence presented here, however, suggests that the OIB signature is primarily derived from the subducting Galapagos hotspot track.

Central American volcanism results from subduction of the Cocos plate beneath the Caribbean plate (Fig. 1). Normal oceanic crust formed at the East Pacific Rise (EPR) subducts beneath Guatemala

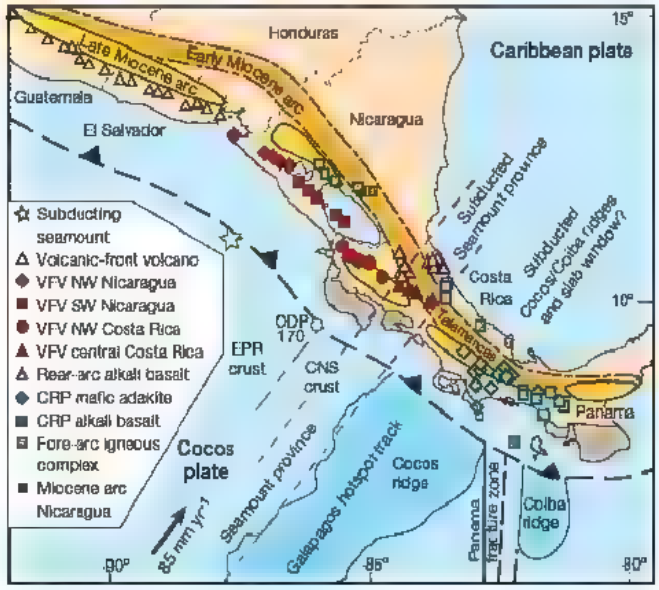

Figure 1 | Reference map of Central America illustrating the subduction of the Galapagos hotspot Seamount province beneath central Costa Rica and the westward migration of the volcanic arc that extends from Costa Rica to southwestern Guatemala. Positions of the arc are shown from the Early Miocene (11–24 Myr ago) to the Late Miocene (6–12 Myr ago) to the Quaternary[30]. The Seamount province of the Galapagos hotspot track is subducting beneath the central Costa Rican volcanic front and Late Pliocene-Holocene (0–2 Myr ago) rear- and back-arc alkali basalts (northeastern occurrences dated at 2 Myr ago). The Cocos and Coiba ridges of the Galapagos hotspot tracks are subducting beneath Pliocene-Holocene mafic adakites and alkali basalts from southeastern Costa Rica and western Panama (CRP), where there has been no volcanic-front volcanism since the Late Miocene. The heavy dashed purple lines project the Seamount province beneath Costa Rica. The boundary between crust formed at the East Pacific Rise (EPR) and the Cocos Nazca (Galapagos) spreading centre (CNS) and the Panama fracture zone are also shown. Volcanic-front volcanoes (VFV) are indicated. A window in the subducting Cocos and Nazca plates may be located beneath southern Costa Rica and western Panama[3].

[1]SFB 574, [2]Leibniz Institute of Marine Sciences (IFM-GEOMAR), University of Kiel, Wischhofstrasse 1-3, Kiel 24148, Germany. [3]Department of Geological Sciences, Brown University, Box 1846, Providence, Rhode Island 02912, USA. [4]Boston University, Department of Earth Sciences, 675 Commonwealth Avenue, Boston, Massachusetts 02215, USA. [5]Observatorio Sismológico y Vulcanológico de Arenal y Miravalles (OSIVAM), Instituto Costarricense de Electricidad (ICE), Apdo. 10032-1000, Costa Rica. [6]Observatorio Vulcanológico y Sismológico de Costa Rica, Universidad Nacional, Apdo. 86-3000, Heredia, Costa Rica. [7]Instituto Nicaragüense de Estudios Territoriales, Apdo. 2110, Managua, Nicaragua. †Present address: Lamont-Doherty Earth Observatory, Columbia University, Palisades, New York 10964, USA.

to northwestern Costa Rica, whereas crust formed at the Cocos-Nazca spreading centre (CNS) with the Galapagos hotspot track on it subducts beneath central Costa Rica to Panama. The Galapagos hotspot tracks (and islands) are chemically zoned[18,19], with the Seamount province having distinctly higher $^{208}Pb/^{204}Pb$ (Figs 1, 2) and lower $^{143}Nd/^{144}Nd$ (Supplementary Fig. 1.1) for a given $^{206}Pb/^{204}Pb$ isotope ratio compared with the Cocos and Coiba ridges.

Radiogenic isotope ratios, which are not fractionated by physical processes such as partial melting and magma differentiation, can be used as tracers to determine the sources contributing to arc magmatism. Along the volcanic front from central Costa Rica to northwestern Nicaragua, Nd isotope ratios increase and Pb isotope ratios decrease continuously (Fig. 2a, b). $^{206}Pb/^{204}Pb$ and $^{208}Pb/^{204}Pb$ isotope data from the volcanic-front rocks also form an excellent linear correlation ($R^2 = 0.997$; Fig. 2c). Although normal arc magmatism ceased in the Late Miocene-Pliocene in southern Costa Rica and western Panama, Pliocene-Quaternary adakitic/alkalic volcanic rocks are widely distributed but volumetrically insignificant[3,20,21]. Lead isotope data from these rocks also form an excellent linear correlation ($R^2 = 0.976$) below, but sub-parallel to, the trend formed by volcanic-front rocks. The highest Pb isotope ratios in the arc rocks occur in the areas situated above the subducting hotspot track, also characterized by radiogenic Pb.

At least three endmembers are required to explain the Pb and Nd isotope data of the Nicaraguan to Panamanian volcanic rocks (see also Supplementary Fig. 1.1). The northwestern Nicaraguan endmember with unradiogenic Pb and radiogenic Nd reflects addition to the depleted mantle wedge of a slab fluid that contains Pb primarily from the subducting crust (as represented by samples from a subducting seamount) (Figs 1, 2). The southern Costa Rica/Panama endmember with radiogenic Pb but intermediate $^{208}Pb/^{204}Pb$ and $^{143}Nd/^{144}Nd$ could be derived from the subducting Cocos/Coiba ridges[3] and/or eroded fore-arc igneous complexes[4], consisting of CLIP basement and accreted early Cenozoic Galapagos seamounts[22–24]. The only source with the appropriate Pb (radiogenic Pb and high $^{208}Pb/^{204}Pb$) and Nd isotopic composition to derive the central Costa Rica endmember is the Seamount province subducting beneath central Costa Rica. Other potential sources for Pb and Nd, such as tectonically eroded Costa Rica fore-arc[4] and input of Galapagos hotspot mantle through a slab window[3] (which would be expected to have a composition similar to the voluminous Cocos/Coiba ridges—representing the primary composition of the Galapagos plume), have isotopic compositions distinct from the Seamount province and thus cannot explain the observed mixing trends.

If the Galapagos seamount slab component has melt-like properties (is a supercritical fluid/hydrous melt), it could readily transport rare-earth elements (for example, La, Nd) and high-field-strength elements (for example, Nb), consistent with the decrease in La/Yb and increase in Ba/La, U/Th and Ba/Th observed in the volcanic-front lavas from central Costa Rica to northwestern Nicaragua[2,25,26] (see Supplementary Information Section 1 for the role of subducted sediments). The transition from a dominantly fluid-like slab component beneath Nicaragua to melt-like slab components in Costa Rica and Panama may be related to the influx of hot mantle through a slab window in the south[3].

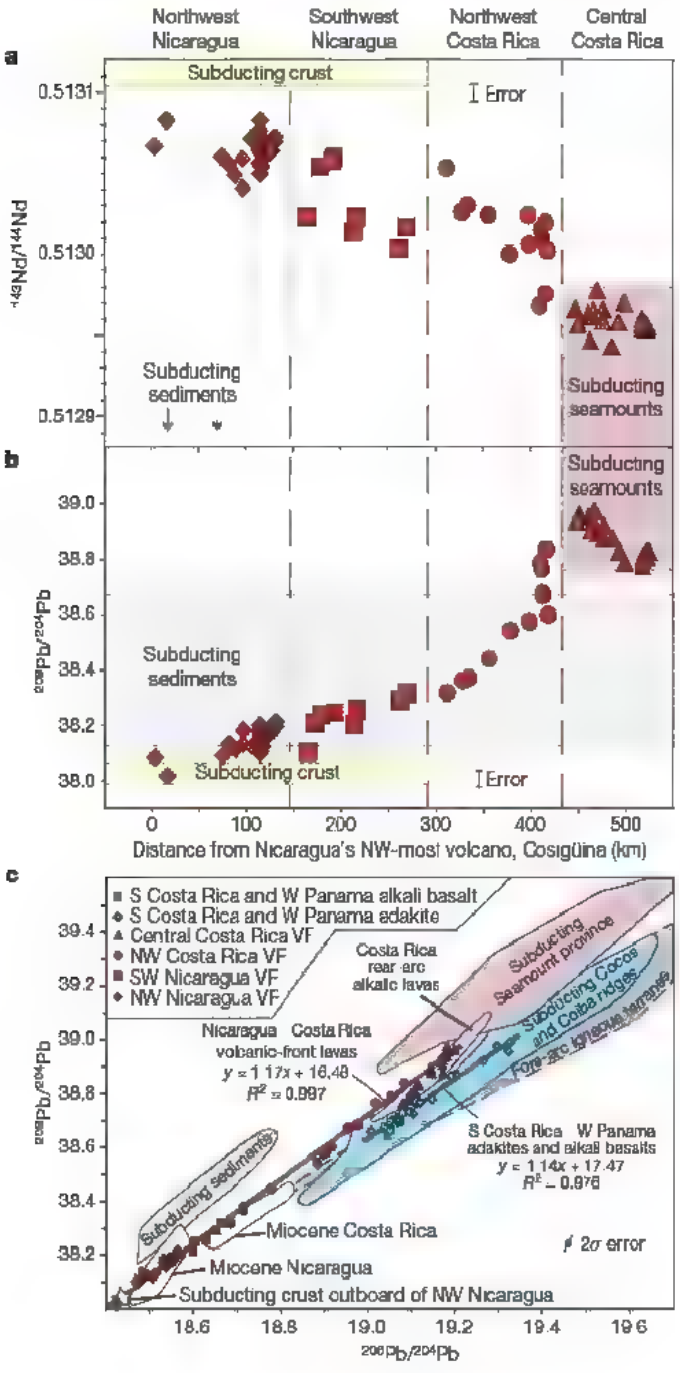

Figure 2 | Systematic variation in lead and neodymium isotopic composition along the volcanic front from Costa Rica to northwest Nicaragua indicates northwestward flow of mantle wedge material. **a**, **b**, Isotope ratios, $^{143}Nd/^{144}Nd$ (**a**) and $^{208}Pb/^{204}Pb$ (**b**), show systematic trends along the arc that indicate mixing of mantle wedge enriched with melts from the subducting Galapagos hotspot Seamount province with mantle wedge enriched with hydrous fluids from the ocean crust subducting beneath Nicaragua. In **c**, Quaternary volcanic front (VF) lavas from Nicaragua and Costa Rica form an excellent linear correlation (longer solid grey line, $R^2 = 0.997$) on the thorogenic Pb isotope diagram. Late Pliocene-Quaternary rear- and back-arc alkalic lavas in northeastern Costa Rica overlap in composition with Costa Rica volcanic-front lavas but extend to more radiogenic compositions, consistent with a greater contribution from a melt-like slab component. Low volume, scattered Pliocene-Quaternary mafic adakites and alkali basalts from southern Costa Rica and western Panama, where there has been no volcanic-front volcanism since the Late Miocene, form a distinct linear array (shorter solid grey line, $R^2 = 0.976$) below but subparallel to the volcanic-front lavas, having lower $^{208}Pb/^{204}Pb$ for a given $^{206}Pb/^{204}Pb$ isotope ratio. Whereas the adakites may represent direct melts of subducted Galapagos rocks, the alkali basalts most probably reflect interaction between carbon-rich fluids/melts from Galapagos material and the overlying mantle wedge. The difference in Pb isotopic composition between the Pliocene-Quaternary central Costa Rica and the southern Costa Rica/western Panama lavas correlates closely with the boundary between the subducting Seamount province and Cocos/Coiba ridges of the chemically zoned Galapagos hotspot track. The subducting Seamount province and the Cocos/Coiba ridges, which have distinct Pb and Nd (Supplementary Fig. 1.1) isotopic compositions[18,19], could serve as the endmembers necessary for generating the distinct isotopic compositions of the central Costa Rica and southern Costa Rica/western Panama lavas, respectively. Fields for (1) fore-arc igneous terranes, which includes CLIP basement from Costa Rica and Panama[22,23,25] and (2) sediments and ocean crust subducting beneath Nicaragua[1,19] are also shown. All errors are reported as 2σ of the mean.

The along-arc variations in volcanic-front isotopic composition indicate that the Galapagos seamount component diminishes in quantity towards northwestern Nicaragua. These trends cannot be produced by upper plate variation. Although CLIP lithosphere underlies Costa Rica, its composition (included in the fore-arc igneous terranes field in Fig. 2c) is distinct from that of the Seamount province[22,23]. The volcanic-front isotopic trends also cannot be explained by systematic changes in the composition of the subducting plate. During ODP Leg 170, gabbro sills with OIB-type geochemical characteristics were drilled about 80 km north of the Seamount province[27], suggesting that the Galapagos hotspot may have affected a larger area than represented by the morphological expression of the hotspot track. However, it is unlikely that the plume spread out 500 km north of the Cocos ridge. When the hotspot track off Costa Rica formed, the CNS was located to the south of the hotspot[19], and plume material would have flowed south towards the ridge (not north). In addition, the gabbro sills from Leg 170 do not have Pb isotopic compositions that plot within the Seamount province, but rather compositions that plot within the Cocos/Coiba ridge field (Supplementary Information Section 1). Finally, a seamount on the Cocos plate subducting beneath central Nicaragua shows no evidence for the presence of Galapagos-type material in this area[19] but rather has the appropriate composition to serve as the depleted Nicaraguan endmember.

As the seamount component only appears to be present on the incoming plate off the Pacific coast of central Costa Rica, this signature must have been introduced into the wedge by a melt-like slab component from the subducting Seamount province and then transported northwest in the mantle wedge in melt pockets (possibly crystallized to form pyroxenite after leaving the slab and reacting with the overlying mantle wedge peridotite). Fluids from the subducting plate beneath Nicaragua flux the wedge, causing melting and mixing with the Galapagos seamount component. As the mantle is transported northwestwards, the seamount component will be progressively flushed out of the wedge, causing a decrease in Pb and increase in Nd isotopic composition.

Seismic anisotropy in the mantle wedge beneath Nicaragua and Costa Rica provides corroborating evidence for arc-parallel flow. Shear-wave splitting was measured in local S phases recorded by a dense temporary deployment of broadband seismometers (Supplementary Fig. 2.1), and a three-dimensional model of anisotropy was obtained (Fig. 3) by tomographically inverting the splitting measurements[28]. Beneath the arc where the Galapagos geochemical signature is observed and further into the back-arc, anisotropy is dominated by roughly arc-parallel alignment of the olivine fast symmetry axis (*a* axis). These *a* axes extend well into the warmer wedge where they should align roughly parallel to flow[6]. A zone of arc-normal *a* axes appears beneath the northwestern end of the Nicaraguan arc where geochemical evidence for the Galapagos seamount component is nearly absent, perhaps suggesting a reduction in arc-parallel flow.

The isotope data allow an along-arc flow rate for the mantle in the wedge to be directly estimated. Given that samples from the Miocene Nicaraguan arc (7–24 Myr old) adjacent to Quaternary southwest Nicaraguan rocks (Fig. 1) have Pb isotope ratios that overlap the range in the Quaternary northwest Nicaraguan volcanic front (Fig. 2), the component with elevated Pb isotope ratios was presumably introduced into the mantle beneath Nicaragua after the Miocene. Igneous rocks from the Miocene arc (6–26 Myr old) in Costa Rica have slightly more radiogenic isotopic compositions than those from Nicaragua, which could reflect interaction with CLIP lithosphere or derivation from subduction of older Galapagos hotspot tracks[24]. The Seamount province composition is not however observed in the Miocene volcanic rocks, providing a maximum age for the appearance of this component of ~6 Myr. Assuming that the oldest part of the subducted Seamount province lies along its boundary with the Panama fracture zone (Fig. 1), it would have passed beneath the central Costa Rican volcanic front 2–3 Myr ago[21] (reversing subduction at a rate of 85 mm yr^{-1}), providing a minimum age of 2 Myr for the appearance of the seamount component beneath the arc.

These dates (2–6 Myr ago) imply that the minimum arc-parallel wedge flow ranges from 63 to 190 mm yr^{-1}, assuming the Galapagos seamount component is transported a distance of 380 km. This distance is measured from the northwesternmost Nicaraguan volcano (Casitas) that shows a clear geochemical influence of the subducting

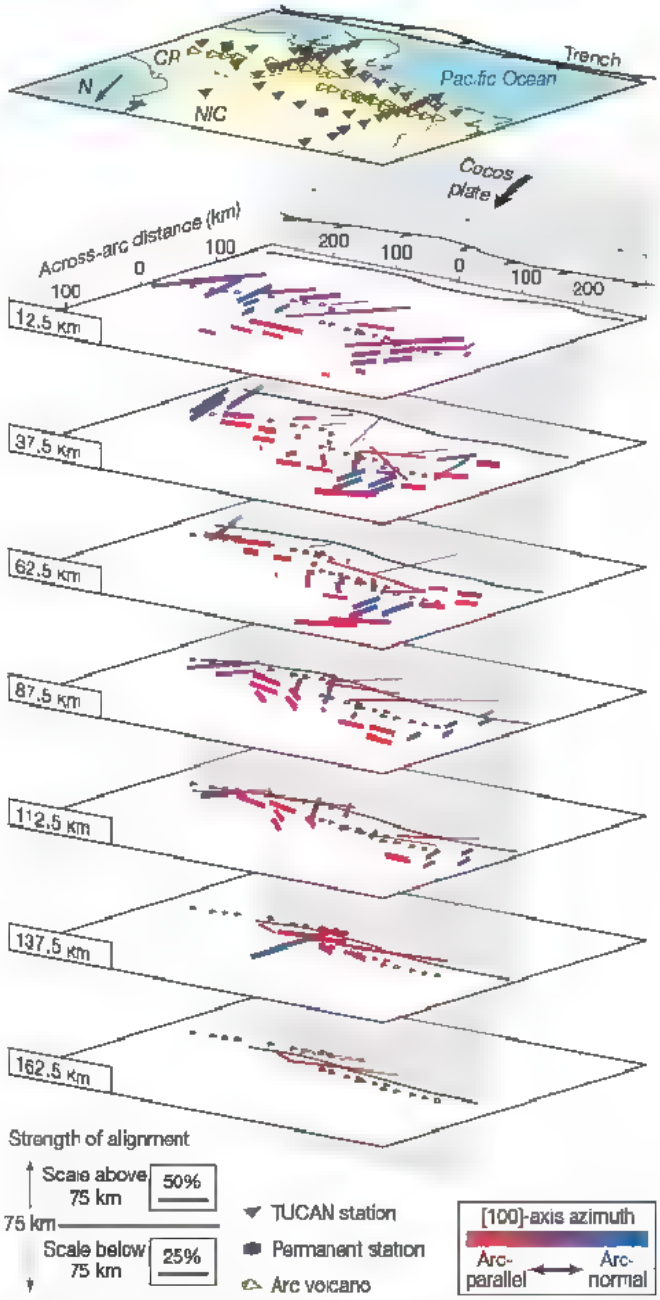

Figure 3 | Model of anisotropy obtained by inverting shear-wave splitting measurements from events in the Nicaragua (NIC)-Costa Rica (CR) subduction zone. The inversion used a tomographic approach[28] (see Methods and Supplementary Information Section 2). The vectors represent well-resolved olivine *a* axes in an olivine-orthopyroxene model, with orientation and colour indicating horizontal azimuth. Vector length corresponds to the strength of anisotropy relative to single-crystal values, note the change in strength scale at 75 km depth. We also invert for *a*-axis dip, but for clarity here we project *a* axes onto map-view planes. Effective block size in the rear- and back-arc is larger. Only well-resolved regions of the model are shown, and vector thickness corresponds to model parameter resolution. The TUCAN seismic array and volcanic arc are shown at the surface, and for reference, the volcanic arc is plotted on each slice through the model. The slab–wedge interface, based on earthquake locations, is shown by grey shading. The top two layers primarily lie within the upper plate; the mantle wedge is located in front of the slab in the layers spanning 50–175 km. Roughly arc-parallel *a* axes dominate well-resolved wedge regions beneath the arc and the rear- and back-arc at depths of 50–150 km, with the exception of a zone of arc-normal *a* axes at the northwestern end of the arc in Nicaragua and one isolated model block deep beneath the back-arc.

Seamount province (more radiogenic Pb and less radiogenic Nd than Cosigüina volcano and the crust subducting beneath Nicaragua) to the location of maximum Pb isotopic composition (greatest amount of Galapagos seamount component) in central Costa Rica. These transport rates are of the order of the Cocos plate subduction rate (~85 mm yr^{-1} off Costa Rica), suggesting that lateral (arc/trench-parallel) flow in the mantle wedge can compete with flow entrained by subduction.

Lead isotope data demonstrate that rapid arc-parallel flow occurs in the mantle wedge beneath Costa Rica and Nicaragua, allowing arc-parallel fast anisotropy to be explained without atypical mechanisms of generating anisotropic fabrics[5,14]. Trench rollback, variations in slab dip, and arc-parallel shearing within the upper plate may all contribute to along-arc wedge flow[9,13,15]. In Costa Rica and Nicaragua, the fore-arc is translating to the northwest, although at less than 15 mm yr^{-1} (ref. 29). Westward migration of the volcanic front since the early Miocene was greatest in Nicaragua and Honduras/El Salvador[30] (Fig. 1) where slab dips are steepest, suggesting differential slab roll-back that could draw wedge material towards northwestern Nicaragua, possibly from a slab window to the south. Collision (indenture) of the thickened Cocos ridge crust with the margin could also have helped drive arc material northwards. Regardless of the mechanism for generating flow, this study demonstrates a rate of arc-parallel flow beneath Costa Rica and Nicaragua that rivals downgoing Cocos plate motion.

METHODS SUMMARY

Nd and Pb isotope analyses were carried out at IFM-GEOMAR by thermal ionization mass spectrometry (TIMS), using a Triton and a MAT262 RPQ^{2+} TIMS, respectively. Over the course of the study, La Jolla produced $^{143}Nd/^{144}Nd = 0.511846 \pm 0.000005$ ($N = 49$) and the long-term reproducibility of NBS 981 ($n = 184$) is $^{206}Pb/^{204}Pb = 16.899 \pm 0.007$, $^{207}Pb/^{204}Pb = 15.437 \pm 0.009$, $^{208}Pb/^{204}Pb = 36.525 \pm 0.028$. Total chemistry blanks were <100 pg for Nd and Pb, and thus are considered negligible.

We solve for a best-fitting model of anisotropy through an iterative, damped, least-squares inversion[28] of 791 local-S splitting measurements from the TUCAN broadband seismic experiment. Anisotropy is described by a hexagonal average of olivine and orthopyroxene elastic coefficients, and parameters in each model block are the azimuth and plunge of the olivine *a* axis and a scalar that controls the strength of anisotropy. A total of 100 iterations were realized, with a moderate relaxation of damping after iteration 40. Model blocks are 25 km on each side, although in back-arc regions constraints were applied after iteration 70 that forced model parameters to be uniform across groups of blocks. Predicted splitting measurements and partial derivatives were calculated at every iteration for each hypocentre–station pair by progressively splitting an initially linearly polarized wavelet to account for the anisotropy encountered in each model block along the phase path.

Full Methods and any associated references are available in the online version of the paper at www.nature.com/nature.

Received 23 July; accepted 5 December 2007.
Published online 21 January 2008.

1. Feigenson, M. D., Carr, M. J., Maharaj, S. V., Juliano, S. & Bolge, L. L. Lead isotope composition of Central American volcanoes: Influence of the Galapagos plume. *Geochem. Geophys. Geosyst.* 5, Q06001, doi:10.1029/2003GC000621 (2004).
2. Herrstrom, E. A., Reagan, M. K. & Morris, J. D. Variations in lava composition associated with flow of asthenosphere beneath southern Central America. *Geology* 23, 617–620 (1995).
3. Abratis, M. & Wörner, G. Ridge collision, slab window formation, and the flux of Pacific asthenosphere into the Caribbean realm. *Geol. Soc. Am.* 29, 127–130 (2001).
4. Goss, A. R. & Kay, S. M. Steep REE patterns and enriched Pb isotopes in southern Central American arc magmas: Evidence for forearc subduction erosion? *Geochem. Geophys. Geosyst.* 7, Q05016, doi:10.1029/2005GC001163 (2006).
5. Jung, H. & Karato, S.-i. Water-induced fabric transition in olivine. *Science* 293, 1460–1463 (2001).
6. Kneller, E. A., van Keken, P. E., Karato, S.-i. & Park, J. B-type olivine fabric in the mantle wedge: Insights from high-resolution non-Newtonian subduction zone models. *Earth Planet. Sci. Lett.* 237, 781–797 (2005).
7. Nakajima, J., Shimizu, J., Hori, S. & Hasegawa, A. Shear-wave splitting beneath the southwestern Kurile arc and northeastern Japan arc: A new insight into mantle return flow. *Geophys. Res. Lett.* 33, L05305, doi:10.1029/2005GL025053 (2006).
8. Long, M. D. & van der Hilst, R. D. Upper mantle anisotropy beneath Japan from shear wave splitting. *Phys. Earth Planet. Inter.* 151, 206–222 (2006).
9. Smith, G. P. *et al.* A complex pattern of mantle flow in the Lau backarc. *Science* 292, 713–716 (2001).
10. Levin, V., Droznin, D., Park, J. & Gordeev, E. Detailed mapping of seismic anisotropy with local shear waves in southeastern Kamchatka. *Geophys. J. Int.* 158, 1009–1023 (2004).
11. Anderson, M. L., Zandt, G. & Wagner, L. Along-strike mantle flow variations in a segment of the South American subduction zone, Chile and Argentina. *Earth Planet. Sci. Lett.* (submitted).
12. Pozgay, S. H., Wiens, D. A., Conder, J. A., Shiobara, H. & Sugioka, H. Complex mantle flow in the Mariana subduction system: Evidence from shear wave splitting. *Geophys. J. Int.* 107, 371–386 (2007).
13. Hall, C. E., Fischer, K. M. & Parmentier, E. M. The influence of plate motions on three dimensional back-arc mantle flow and shear wave splitting. *J. Geophys. Res.* 105, 28009–28033 (2000).
14. Holtzman, B. K. *et al.* Melt segregation and strain partitioning: Implications for seismic anisotropy and mantle flow. *Science* 301, 1227–1230 (2003).
15. Behn, M. D., Hirth, G. & Kelemen, P. B. Trench-parallel anisotropy produced by foundering of arc lower crust. *Science* 317, 108–111 (2007).
16. Kneller, E. A. & van Keken, P. E. Trench-parallel flow and seismic anisotropy in the Mariana and Andean subduction systems. *Nature* 450, 1222–1225 (2007).
17. Reagan, M. K. & Gill, J. B. Coexisting calcalkaline and high-niobium basalts from Turrialba volcano, Costa Rica: Implications for residual titanates in arc magma sources. *J. Geophys. Res.* 94, 4619–4633 (1989).
18. Hoernle, K. A., Werner, R., Phipps Morgan, J., Bryce, J. & Mrazek, J. Existence of a complex spatial zonation in the Galapagos plume for at least 14.5 Ma. *Geology* 28, 435–438 (2000).
19. Werner, R., Hoernle, K., Barckhausen, U. & Hauff, F. Geodynamic evolution of the Galapagos hot spot system (Central East Pacific) over the past 20 m.y.: Constraints from morphology, geochemistry, and magnetic anomalies. *Geochem. Geophys. Geosyst.* 4, doi:10.1029/2003GC000576 (2003).
20. Defant, M. J. *et al.* The geology and geochemistry of El Valle volcano, Panama: Andesite and dacite genesis via contrasting processes. *Contrib. Mineral. Petrol.* 106, 309–324 (1991).
21. MacMillan, I., Gans, P. B. & Alvarado, G. Middle Miocene to present plate tectonic history of southern Central American volcanic arc. *Tectonophysics* 392, 325–348 (2004).
22. Hoernle, K., Hauff, F. & van den Bogaard, P. 70 m.y. history (139–69 Ma) for the Caribbean large igneous province. *Geology* 32, 697–700 (2004).
23. Hauff, F., Hoernle, K. A., van den Bogaard, P., Alvarado, G. E. & Garbe-Schönberg, D. Age and geochemistry of basaltic complexes in Western Costa Rica: Contributions to the geotectonic evolution of Central America. *Geochem. Geophys. Geosyst.* 1, doi:10.1029/1999GC000020 (2000).
24. Hoernle, K. A. *et al.* The missing history (16–71 Ma) of the Galápagos hotspot: Implications for the tectonic and biological evolution of the Americas. *Geology* 30, 795–798 (2002).
25. Patino, L. C., Carr, M. J. & Feigenson, M. D. Local and regional variations in Central American arc lavas controlled by variations in subducted sediment input. *Contrib. Mineral. Petrol.* 138, 265–283 (2000).
26. Carr, M. J., Feigenson, M. D. & Bennett, E. A. Incompatible element and isotopic evidence for tectonic control of source mixing and melt extraction along the Central American arc. *Contrib. Mineral. Petrol.* 105, 369–380 (1990).
27. Kimura, G. *et al.* SITE 1039 (Ch. 3), SITE 1040 (Ch. 4). *Proc. ODP Init. Rep.* 170, 45–152 (1997).
28. Abt, D. L. & Fischer, K. M. Resolving three-dimensional anisotropic structure with shear-wave splitting tomography. *Geophys. J. Int.* (submitted).
29. Turner, H. L. *et al.* Kinematics of the Nicaraguan forearc from GPS geodesy. *Geophys. Res. Lett.* 34, L02302, doi:10.1029/2006GL027586 (2007).
30. Alvarado, G. E. *et al.* in *Central America: Geology, Resources and Hazards* (eds Bundschuh, J. & Avarado, G.) 345–394 (Taylor and Francis, Leiden, 2007).

Supplementary Information is linked to the online version of the paper at www.nature.com/nature.

Acknowledgements Reviewers (J. Walker and S. Schwartz), J. Phipps-Morgan, T. Plank, R. Werner, M. Portnyagin and members of SFB574 and MARGINS are thanked for comments/discussions that helped significantly improve the manuscript. The IRIS PASSCAL programme provided seismometers and technical assistance to the TUCAN experiment. This research was supported by the German Science Foundation Collaborative Research Centre (SFB574) and the National Science Foundation MARGINS programme.

Author Contributions K.H., D.L.A. and K.M.F. collected samples/data, processed and interpreted the data, developed the ideas and wrote the paper, with significant input from G.A.A. and discussions with other co-authors. H.N., F.H. and K.H. generated the geochemical data and P.v.d.B. age data. G.A.A., M.P. and W.S. were key in collecting the seismic data; P.v.d.B., G.A. and H.N. assisted in the collection of the volcanic samples. Central American partners provided geological overviews and logistical support.

Author Information Reprints and permissions information is available at www.nature.com/reprints. Correspondence and requests for materials should be addressed to K.H. (thoernle@ifm-geomar.de)

LETTERS

Scaling laws of marine predator search behaviour

David W. Sims[1,2], Emily J. Southall[1], Nicolas E. Humphries[1], Graeme C. Hays[4], Corey J. A. Bradshaw[5]†, Jonathan W. Pitchford[6], Alex James[6,7], Mohammed Z. Ahmed[3], Andrew S. Brierley[8], Mark A. Hindell[9], David Morritt[10], Michael K. Musyl[11], David Righton[12], Emily L. C. Shepard[4], Victoria J. Wearmouth[1], Rory P. Wilson[4], Matthew J. Witt[+3] & Julian D. Metcalfe[12]

Many free-ranging predators have to make foraging decisions with little, if any, knowledge of present resource distribution and availability[1]. The optimal search strategy they should use to maximize encounter rates with prey in heterogeneous natural environments remains a largely unresolved issue in ecology[1–3]. Lévy walks[4] are specialized random walks giving rise to fractal movement trajectories that may represent an optimal solution for searching complex landscapes[3]. However, the adaptive significance of this putative strategy in response to natural prey distributions remains untested[6,7]. Here we analyse over a million movement displacements recorded from animal-attached electronic tags to show that diverse marine predators—sharks, bony fishes, sea turtles and penguins—exhibit Lévy-walk-like behaviour close to a theoretical optimum[2]. Prey density distributions also display Lévy-like fractal patterns, suggesting response movements by predators to prey distributions. Simulations show that predators have higher encounter rates when adopting Lévy-type foraging in natural-like prey fields compared with purely random landscapes. This is consistent with the hypothesis that observed search patterns are adapted to observed statistical patterns of the landscape. This may explain why Lévy-like behaviour seems to be widespread among diverse organisms[3], from microbes[8] to humans[9], as a 'rule' that evolved in response to patchy resource distributions.

Predators can sometimes fine-tune their foraging by using sensory information of resource abundance and distribution at near-distance scales dominated by proximal clues[10], and at very broad scales some may have awareness of seasonal and geographical prey distributions[11]. However, across the broad range of mesoscale boundaries (a few to hundreds of kilometres), the necessary spatial knowledge required for successful foraging will depend largely on the search strategy used. Over these scales some predators are more like probabilistic or 'blind' hunters than deterministic foragers. Fully aquatic marine vertebrates that feed on ephemeral resources like zooplankton and small pelagic fish typify this type of predator because they have sensory detection ranges limited by the seawater medium and experience extreme variability in food supply[7,10–12] over a broad range of spatio-temporal scales[13–15].

Probabilistic search patterns described by a category of random-walk models known as Lévy walks[4] appear to describe foraging movements of some species[3]. These specialized random walks have super-diffusive properties comprising 'walk clusters' of short move step lengths (distance moved per unit time) with longer re-orientation jumps between them. This pattern is repeated across all scales, with the resultant scale-invariant clusters creating trajectories with fractal patterns[3]. Lévy-walk move steps are drawn from a probability distribution with a power-law tail: $P(l_i) \sim l_i^{-\mu}$, with $1 < \mu \leq 3$, where l_i is the move-step length and μ is the power-law (Lévy) exponent (here '$\sim$' means 'distributed as'). Theoretical studies[2,3,16] show that Lévy walks and Lévy flights (the turning points in a Lévy walk[4]) across random prey distributions increase new-patch encounter probability compared with simple brownian motion, with an optimal search having an exponent $\mu \cong 2$. Recent studies[17–19] contend that Lévy walks or flights have been wrongly ascribed to some species through use of incorrect methods, while others indicate Lévy-like behaviour with optimal power-law exponents[3,20,21] for highest-efficiency searches, supporting the hypothesis that Lévy behaviour may represent an evolutionary optimal value of the Lévy exponent[3,5,22].

We hypothesized that fully aquatic (non-aerial) marine predators should adopt a movement (search) strategy that optimises prey-patch encounter rates, thus conferring an advantage when foraging within naturally non-random prey distributions[13–15]. Long-term movements of large marine predators can be recorded accurately at fine temporal resolution (seconds) for long periods (months) using electronic data-logging tags[23]. In the largest such analysis yet attempted, we collated the vertical movements resulting from recorded diving activity within the foraging range of seven large vertebrate species that feed on patchily distributed prey (for example, zooplankton, small fish) (see Methods). Numerous investigations have tracked a predator's horizontal movements but none have studied vertical movements for which the same considerations of 'blind' hunting probably hold over much shorter vertical spatial scales (tens of metres), particularly outside the well-lit near-surface zones[24]. We analysed a total of 1,209,088 vertical move steps for 31 individual predators from seven species and found that the large-scale structure of vertical movement was similar for the majority of species (Fig. 1). Model fits to move-step-length frequency distributions for five species across diverse taxa (shark, teleosts, sea turtle, penguin) closely resembled an inverse-square power law[25] with a heavy tail of increasingly longer steps intermittently distributed within the time series that is typical of ideal Lévy walks[3,4] (Fig. 1; Supplementary Information). Lévy exponents derived from

[1]Marine Biological Association of the United Kingdom, The Laboratory, Citadel Hill, Plymouth PL1 2PB, UK. [2]Marine Biology and Ecology Research Centre, School of Biological Sciences, [3]School of Computing, Communications and Electronics, University of Plymouth, Drake Circus, Plymouth PL4 8AA, UK. [4]Department of Biological Sciences, Institute of Environmental Sustainability, Swansea University, Singleton Park, Swansea SA2 8PP, UK. [5]School for Environmental Research, Charles Darwin University, Darwin, Northern Territory 0909, Australia. [6]Department of Biology and York Centre for Complex Systems Analysis, University of York, York YO10 5YW, UK. [7]Department of Mathematics and Statistics, University of Canterbury, Christchurch, New Zealand. [8]Gatty Marine Laboratory, School of Biology, University of St Andrews, Fife KY16 8LB, UK. [9]School of Zoology, University of Tasmania, Private Bag 05, Hobart, Tasmania 7001, Australia. [10]School of Biological Sciences, Royal Holloway, University of London, Egham TW20 0EX, UK. [11]Joint Institute for Marine and Atmospheric Research, Pelagic Fisheries Research Programme, University of Hawaii at Manoa, Kewalo Research Facility/NOAA Fisheries, 1125-B Ala Moana Boulevard, Honolulu, Hawaii 96814, USA. [12]Centre for Environment, Fisheries and Aquaculture Science, Lowestoft Laboratory, Pakefield Road, Lowestoft NR33 0HT, UK. [13]Centre for Ecology and Conservation, University of Exeter in Cornwall, Tremough TR10 9EZ, UK. †Present address: Research Institute for Climate Change and Sustainability, School of Earth and Environmental Sciences, University of Adelaide, Adelaide, South Australia 5005, Australia.

Lévy-like move-step-length frequency distributions for the five species were maintained for individuals, and it is striking that they were close to a theoretically optimal $\mu \approx 2$ exponent ($\bar{\mu} \pm$ s.d. = 2.12 ± 0.31, $n = 24$; species range: $1.34 \leq \mu \leq 2.91$) (Fig. 1; Supplementary Information). Relative likelihood estimates of model fits to the move-step-length frequency distributions for all species supported only an exponential function typifying random motion for two species (catshark, elephant seal), confirming that Lévy-like processes may not predominate within vertical search strategies in all species (see Supplementary Information).

To test for the presence of long-term correlations that also characterize scale-invariant Lévy walks[3], we used the root-mean-square fluctuation of the displacement, $F(t)$, in each time series. Uncorrelated time series arise from uncorrelated random walks for which $\alpha = 0.5$ for the relationship $F(t) \sim t^{\alpha}$ (ref. 26); in contrast, weighted means of α for each species tested here were between 0.80 and 1.24 ($\alpha \pm$ s.d. = 1.08 ± 0.17, $n = 5$), confirming the presence of long-range correlations in diving time series across the five species (Supplementary Information). The scaling exponent β of the sum of the spectra against frequency in the dive time series was 0.8 in the low-frequency regime, also consistent with long-range correlations in scale-invariant systems[26] because $\beta \cong 0$ when behaviour is temporally uncorrelated (Supplementary Information). We considered vertical foraging movements only in one dimension (depth) through time (that is, the total dimensionality is two dimensional, 2D), so we were unable to determine randomness in turning angles which would further confirm the existence of Lévy-like motion[21] over the full range of underwater movements; however, considering the data as 2D projections of three-dimensional (3D) movements presents no obstacle to their statistical treatment. The projection of spatially homogeneous 3D Lévy movements into 2D preserves the power-law relationship with an unchanged exponent at all length scales greater than the minimum move step of the original 3D trajectory. This invariance under projection does not hold for other move-step distributions (Supplementary Information). The Lévy-like vertical movements described here, therefore, reflect the more complex 3D movements made by a range of phylogenetically distinct marine vertebrate species, implying that Lévy-like walks may be a common strategy employed by open-ocean foragers.

Lévy-walk-like behaviour of foragers may show mechanistic links with natural prey fields if the search pattern emerges from the underlying pattern of food distribution[20], or if the strategy evolved to

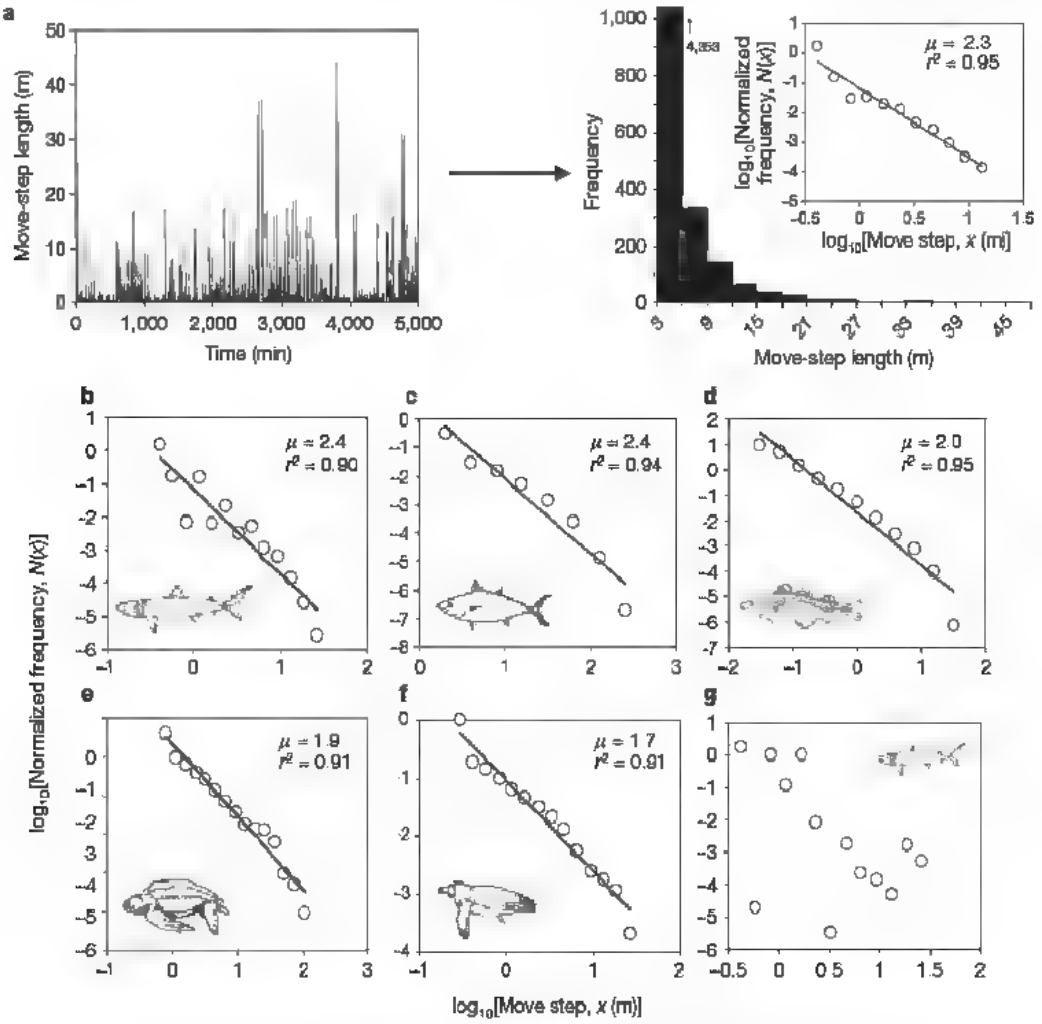

Figure 1 | Lévy-like scaling law among diverse marine vertebrates. **a**, Movement time series recorded by electronic tags were analysed to determine the Lévy exponent to the heavy-tailed power-law distribution. Left, time series of vertical move (dive) steps ($n = 5{,}000$) of an individual basking shark (*Cetorhinus maximus*) over 3.5 days, showing an intermittent structure of longer steps. Right, the move-step-length frequency distribution for the same data. Inset, the normalized log–log plot of move-step frequency versus move-step length, giving an exponent μ within ideal Lévy limits ($\mu = 2.3$). The Lévy exponent is conserved across longer temporal scales, for example, expanding the time series for this individual to 30 days ($n = 43{,}200$ steps) maintains $\mu = 2.3$ (data not shown), indicating scale-invariance in move-step distribution. **b–g**, Normalized log–log plots of the move-step frequency distributions for: **b**, sub-adult and adult basking shark ($n = 503{,}447$ move steps); **c**, bigeye tuna (*Thunnus obesus*) ($n = 222{,}282$ steps), **d**, Atlantic cod (*Gadus morhua*) ($n = 94{,}314$ steps); **e**, leatherback turtle (*Dermochelys coriacea*) ($n = 4{,}393$ steps); and **f**, Magellanic penguin (*Spheniscus magellanicus*) ($n = 9{,}727$ steps). Lévy exponents were maintained at the individual level for 24 sub-adult and adult animals (see Supplementary Information). **g**, Normalized log–log plot of move-step-length frequency distribution for a 2.5-m-long, <1-year-old basking shark showing nonlinear form. Relative likelihood model fits to rank-frequency plots for the five species also indicated that move-step distributions were Lévy-like and not purely random (Supplementary Information).

enhance foraging success in particular prey distributions. To examine these contrasting hypotheses we analysed the structure of two different prey fields (krill, total zooplankton) consumed by some predators considered here (planktivorous shark, penguin). Krill (*Euphausia superba*) densities occurring horizontally in a current passing a moored echosounder[27] were measured throughout the 200m water column at consecutive, equally spaced time intervals. Krill densities showed extreme variance in amplitude through time, with an intermittent structure of large 'jumps' (Fig. 2a). The frequency distribution of krill density changes also closely resembled a power law

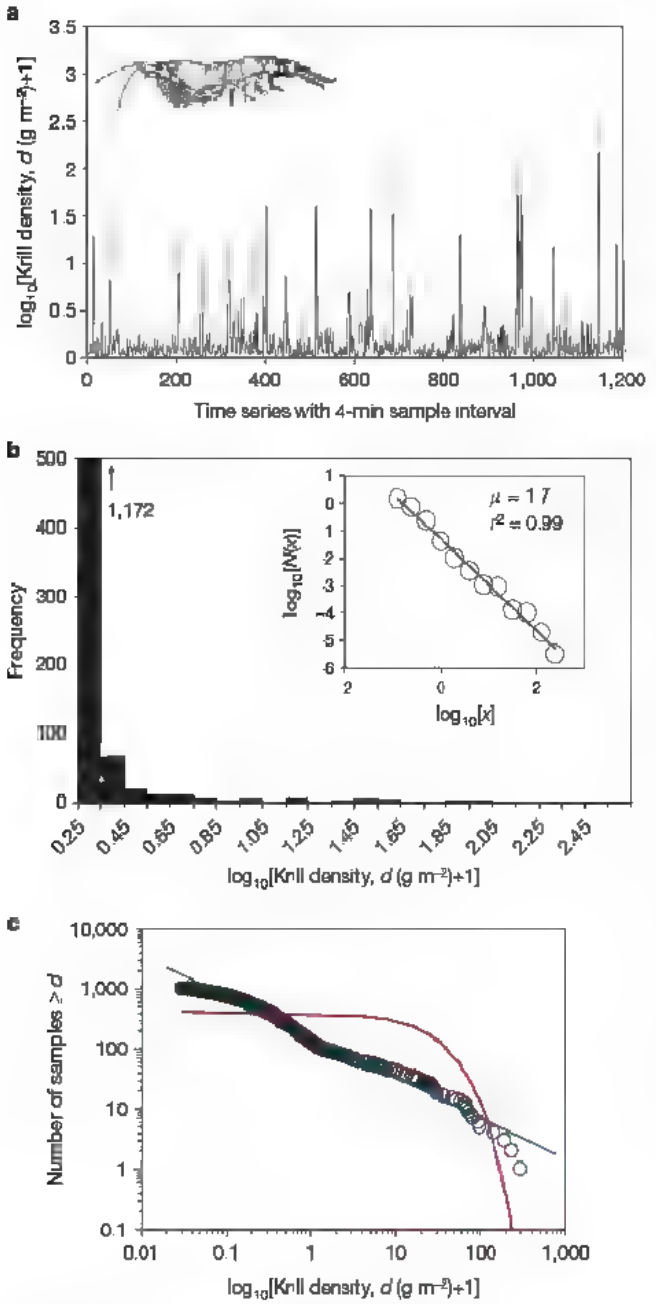

Figure 2 | Macroscopic properties of a prey field. a, Krill (*Euphausia superba*) density d (in g m^{-2}) ($n = 1{,}215$ samples) occurring horizontally and integrated vertically within the current flowing past a moored, upward-looking echosounder off South Georgia. **b**, The move-step frequency distribution of krill density follows a heavy-tailed power law reminiscent of those obtained for Lévy-walk-like predators, and as for the predators, it shows an exponent within Lévy limits and close to the optimum $\mu \approx 2$. **c**, Cumulative distribution or rank-frequency plot[17] of krill density change showing a straight-line form consistent with power-law-like and Lévy-like processes. This plot gives a Lévy exponent of 1.64. The relative likelihood model fit to the rank-frequency plot also indicated that the density-change distribution was Lévy-like and not purely random (see Supplementary Information).

with a heavy tail, giving a Lévy exponent of 1.7 (Fig. 2b, c). Root-mean-square fluctuations gave $\alpha = 0.9$ for krill and spectral analysis revealed low-frequency changes at $\beta = 0.3$ (Supplementary Information). Similar results were found for the zooplankton time series ($\mu = 1.8$ and 2.0, $\alpha = 0.9$; Supplementary Information). Therefore, the presence of long-range correlations and scale invariance in the spatial changes in prey density are properties in common with marine predator movements. The Lévy exponents describing the slopes of the power-law-like distributions were also similar, as were frequency spectra of predator movements and prey distribution. The similarity of Lévy exponents and frequency spectra between predator movements and prey distributions does not necessarily prove the existence of a mechanistic link between a predator's foraging movement response and natural prey assemblages, but the close resemblance does indicate that Lévy properties (describing fractal processes) underlie both predator movements and prey distribution. Thus, for these specific ecological cases, the exponent of the searcher may represent an optimization to the heterogeneous prey fields demonstrating fractal properties.

There are, however, two competing hypotheses to explain the predator–prey interactions we propose: (1) animal search patterns are adapted stochastically to their prey field structures because their environment is so heterogeneous (predators actively search following rules of optimality), or (2) apparently 'optimal' search patterns may arise simply as a function of the underlying distribution of the prey field (a predator's patterns are a by-product of the prey distribution it encounters). The results of a recent modelling study[20] support the latter explanation by showing that scale-free foraging patterns (Lévy walks) emerge from the interaction of animals with a particular resource distribution. Likewise, field observations of primates moving between fruiting trees fit the expected pattern probably because primates possess complex mental maps of resource location; hence, the underlying resource landscape determines the distribution of move steps[20]. However, this process is unlikely to account for the move-step distributions of marine species we measured because they have an incomplete knowledge of resource location. First, behavioural kineses to prey are limited to relatively small vertical distances in the ocean[24], so when threshold prey densities are reached, a predator should initiate searches aimed at traversing distances exceeding the sensory detection range[2,7,10]. Second, strict fidelity of a marine predator to small target locations (analogous to the trees visited by primates) will be ineffective because locations of prey such as zooplankton, squid and shoaling fish often change rapidly and dynamically across a range of spatio-temporal scales[7,10,14]. So our empirical results favour the first explanation—predators feeding on patchy, heterogeneous prey should adapt the best probabilistic search strategy given that they are essentially 'blind' hunters at the spatial and temporal scales over which they typically forage. This conclusion regarding adaptation is strengthened by the vertical move-step-length frequency distribution of a 2.5-m-long, <1-year-old basking shark that we tracked for 7 months that did not conform to Lévy-like behaviour (Fig. 1g). We suggest that this striking difference in search pattern from those of mature individuals reflects ontogenetic behavioural development[28], that is, juveniles learn about the underlying structure of prey distributions as they gain foraging experience.

Further support for the hypothesis that movement processes are linked to prey distributions could be inferred if there were an advantage to predators adopting Lévy walks in fractal landscapes compared to other distribution types. For a particular search strategy to evolve, it must confer an advantage in terms of higher fitness resulting from greater efficiency in energy acquisition[29]. To test this, we investigated the foraging success (total energy acquisition) of a Lévy searcher adapted to a natural-like, fractal prey field by simulating a Lévy-walk predator's vertical diving movements within a virtual prey field defined by either a Lévy or random distribution. Lévy searches ($\mu = 2.0$) reflecting marine predator

Table 1 | Comparison of foraging success for simulated searchers

Ratio	Mean foraging success (% difference)	Standard error of the mean
LL:LR	14.47	2.49
RL:RR	−0.52	0.73
RL:LL	−10.89	1.32

See text for explanation of the ratio and Supplementary Information for further details of simulation results. The mean foraging success ratio was calculated from ten replicate simulation sets, with each replicate comprising three runs of each forager type per prey field type, with each run estimating foraging success (prey encountered per distance moved) for each of 100,000 foragers. Hence, each pair of sets making up a replicate summarized searching by 600,000 foragers.

movements within Lévy (fractal)-distributed prey fields (LL, denoting a Lévy searcher in a Lévy prey field) were compared with encounter rates in ordinary, random prey fields (LR) (defined as a prey distribution resulting from a homogeneous spatial Poisson point process) (see Methods). Our expectation was that the foraging success ratio LL:LR should not deviate substantially from 1.0 (zero difference) if adapting to a fractal prey field presents no particular foraging advantage to a Lévy searcher. However, the LL:LR ratio always exceeded 1.0, and LL was 14% higher on average than LR (Table 1), which thus supports the optimality hypothesis. We next compared random with Lévy searchers in fractal fields (RL, denoting a random searcher in a Lévy prey field) and found that the RL:LL ratio, by contrast, showed a negative foraging gain (−10%), whereas comparing RL with a random forager in a random field (RR) indicated similar levels of search performance (RL:RR ≅ 1.0; Table 1 and Supplementary Information). These results are consistent with the hypothesis that Lévy-like searches may represent an adaptation to complex prey distributions by evolving optimal search strategies.

Our findings indicate that animals in stochastic environments necessitating probabilistic foraging may derive benefits from adapting movements described by Lévy processes. Lévy models express behavioural minimalism[3], so not all movements made by marine vertebrates and other animals will be associated with optimal foraging (for example, resting, breeding and migration) and, in addition, it is unlikely that animals search with Lévy-like motion at all times, especially if, for some species, foraging decisions are predominantly deterministic within stable environments. However, evidence that Lévy-walk search patterns apply to a diverse range of taxa[3,8,9,21], together with our results, suggest that foragers are adapted to optimal behaviour in complex landscapes. Hence, Lévy-like walks may be useful for developing more realistic models of how animals redistribute themselves in response to shifting resources as a consequence of climate change, fisheries extractions and other habitat modifications[30]. Such general and simple laws of movement as optimal Lévy walks could prove useful in robotics—for example, in an algorithm controlling the movements of autonomous robots designed to sample optimally in hostile and heterogeneous environments such as the deep sea, active volcanoes or on other planets.

METHODS SUMMARY

Electronic tagging. Pressure (depth)-sensitive data-logging tags were attached to basking sharks *Cetorhinus maximus* ($n = 6$ individuals) and small spotted catshark *Scyliorhinus canicula* ($n = 3$) in the northeast Atlantic Ocean, bigeye tuna *Thunnus obesus* ($n = 3$) in the North Pacific near Hawaii, Atlantic cod *Gadus morhua* ($n = 5$) in the North Sea, leatherback turtles *Dermochelys coriacea* ($n = 4$) in the Atlantic Ocean, Magellanic penguins *Spheniscus magellanicus* ($n = 7$) off Patagonia, Argentina, and southern elephant seals *Mirounga leonina* ($n = 3$) in the Pacific sector of the Southern Ocean. Full details of deployments, animal body sizes, tag types and data sources are given in Supplementary Table 1.

Prey sampling. Antarctic krill (*Euphausia superba*) in the top 200 m were detected at 4-min intervals within the current flowing past a moored, upward-looking data-logging echosounder at South Georgia, South Atlantic Ocean[27]. Logged data were processed to provide a prey-field time series of horizontal changes in krill density at a point location integrated vertically in the water column, and scaled to account for variable current flow over time. Two zooplankton time series were also analysed (see Supplementary Information).

Simulation program. The purpose of simulating searches was to test the hypothesis that foraging success (biomass consumed per distance moved) by optimal Lévy walkers ($\mu_{opt} = 2.0$) in fractal (natural) prey distributions exceeded prey acquisition rates within random prey fields. We developed a simulation where vertical trajectories (y, time) of Lévy foragers were routed through seascapes with heterogeneous prey patches distributed according to Lévy (describing fractal processes) or random distributions. This simulated a predator searching vertically for patchy resources.

Full Methods and any associated references are available in the online version of the paper at www.nature.com/nature.

Received 17 October; accepted 29 November 2007.

1. Stephens, D. W. & Krebs, J. R. *Foraging Theory* (Princeton Univ. Press, Princeton, 1986)
2. Viswanathan, G. M. *et al.* Optimizing the success of random searches. *Nature* 401, 911–914 (1999).
3. Bartumeus, F., da Luz, M. G. E., Viswanathan, G. M. & Catalan, J. Animal search strategies: a quantitative random-walk analysis. *Ecology* 86, 3078–3087 (2005)
4. Shlesinger, M. F., Zaslavsky, G. M. & Klafter, J. Strange kinetics. *Nature* 363, 31–37 (1993)
5. Viswanathan, G. M. *et al.* Lévy flights in random searches. *Physica A* 282, 1–12 (2000)
6. Russell, R. W., Hunt, G. L., Coyle, K. O. & Cooney, R. T. Foraging in a fractal environment: spatial patterns in a marine predator-prey system. *Landscape Ecol.* 7, 195–209 (1992).
7. Sims, D. W., Witt, M. J., Richardson, A. J., Southall, E. J. & Metcalfe, J. D. Encounter success of free-ranging marine predator movements across a dynamic prey landscape. *Proc. R. Soc. Lond. B* 273, 1195–1201 (2006)
8. Schuster, F. L. & Levandowsky, M. Chemosensory responses of *Acanthamoeba castellanii*: Visual analysis of random movement and responses to chemical signals. *J. Eukaryot. Microbiol.* 43, 150–158 (1996)
9. Brockmann, D., Hufnagel, L. & Geisel, T. The scaling laws of human travel. *Nature* 439, 462–465 (2006).
10. Sims, D. W. & Quayle, V. A. Selective foraging behaviour of basking sharks on zooplankton in a small-scale front. *Nature* 393, 460–464 (1998).
11. Bradshaw, C. J. A., Hindell, M. A., Sumner, M. D. & Michael, K. J. Loyalty pays: potential life history consequences of fidelity to marine foraging regions by southern elephant seals. *Anim. Behav.* 68, 1349–1360 (2004)
12. Houghton, J. D. R., Doyle, T. K., Wilson, M. W., Davenport, J. & Hays, G. C. Jellyfish aggregations and leatherback turtle foraging patterns in a temperate coastal environment. *Ecology* 87, 1967–1972 (2006)
13. Mackas, D. L. & Boyd, C. M. Spectral analysis of zooplankton spatial heterogeneity. *Science* 204, 62–64 (1979)
14. Makris, N. C. *et al.* Fish population and behaviour revealed by instantaneous continental shelf-scale imaging. *Science* 311, 660–663 (2006)
15. Steele, J. H. The ocean 'landscape'. *Landscape Ecol.* 3, 185–192 (1989)
16. Bartumeus, F., Catalan, J., Fulco, U. L., Lyra, M. L. & Viswanathan, G. M. Optimizing the encounter rate in biological interactions: Lévy versus Brownian strategies. *Phys. Rev. Lett.* 88, 097901 (2002)
17. Sims, D. W., Righton, D. & Pitchford, J. W. Minimizing errors in identifying Lévy flight behaviour of organisms. *J. Anim. Ecol.* 76, 222–229 (2007)
18. Benhamou, S. How many animals really do the Lévy walk? *Ecology* 88, 1962–1969 (2007)
19. Edwards, A. M. *et al.* Revisiting Lévy flight search patterns of wandering albatrosses, bumblebees or deer. *Nature* 449, 1044–1048 (2007).
20. Boyer, D. *et al.* Scale-free foraging by primates emerges from their interaction with a complex environment. *Proc. R. Soc. Lond. B* 273, 1743–1750 (2006)
21. Bartumeus, F., Peters, F., Pueyo, S., Marrase, C. & Catalan, J. Helical Levy walks: adjusting search statistics to resource availability in microzooplankton. *Proc. Natl Acad. Sci. USA* 100, 12771–12775 (2003)
22. Bartumeus, F. Lévy processes in animal movement: an evolutionary hypothesis. *Fractals* 15, 151–162 (2007).
23. Ropert-Coudert, Y. & Wilson, R. P. Trends and perspectives in animal-attached remote sensing. *Front. Ecol. Environ.* 3, 437–444 (2005)
24. Myers, A. E. & Hays, G. C. Do leatherback turtles *Dermochelys coriacea* forage during the breeding season? A combination of data-logging devices provide new insights. *Mar. Ecol. Prog. Ser.* 322, 259–267 (2006)
25. Bradshaw, C. J. A. & Sims, D. W. Solutions to problems associated with identifying Lévy walk patterns in animal movement data. *J. Anim. Ecol.* (submitted)
26. Viswanathan, G. M. *et al.* Lévy flight search patterns of wandering albatrosses. *Nature* 381, 413–415 (1996).
27. Brierley, A. S. *et al.* Use of moored acoustic instruments to measure short-term variability in abundance of Antarctic krill. *Limnol. Oceanogr. Methods* 4, 18–29 (2006).

28. Field, I. C., Bradshaw, C. J. A., Burton, H. R., Sumner, M. D. & Hindell, M. A. Resource partitioning through oceanic segregation of foraging juvenile southern elephant seals (*Mirounga leonina*). *Oecologia* 142, 127–135 (2005).
29. Perry, G. & Pianka, E. R. Animal foraging past, present and future. *Trends Ecol. Evol.* 12, 360–364 (1997).
30. McMahon, C. R. & Hays, G. C. Thermal niche, large-scale movements and implications of climate change for a critically endangered marine vertebrate. *Glob. Change Biol.* 12, 1330–1338 (2006).

Supplementary Information is linked to the online version of the paper at www.nature.com/nature.

Acknowledgements This research was facilitated through the European Tracking of Predators in the Atlantic (EUTOPIA) programme in the European Census of Marine Life (EuroCoML). Funding was provided by the UK Natural Environment Research Council (NERC) grant-in-aid to the Marine Biological Association of the UK (MBA), the NERC 'Oceans 2025' Strategic Research Programme (Theme 6 Science for Sustainable Marine Resources), UK Defra, The Royal Society and the Fisheries Society of the British Isles. D.W.S. thanks G. Budd, P. Harris, N. Hutchinson and D. Uren for field assistance. G.C.H. thanks Ocean Spirits Incorporated, J. Houghton and A. Myers for logistical help in the field. A.S.B. thanks E. Murphy, M. Brandon, R. Saunders, D. Bone and P. Enderlein for their contributions to mooring sampling at South Georgia. NERC Plymouth Marine Laboratory provided L4 zooplankton data. This research complied with all animal welfare laws of the countries or sovereign territories in which it was conducted. D.W.S. was supported by a NERC-funded MBA Research Fellowship.

Author Contributions D.W.S. conceived and planned the study, led the data analysis and wrote the manuscript. All co-authors contributed to subsequent drafts. Field data of animal movements and/or prey distributions were collected by D.W.S., E.J.S., J.D.M., G.C.H., C.J.A.B., A.S.B., M.A.H., D.M., M.K.M., D.R., V.J.W. and R.P.W. The simulation model was conceived by N.E.H. and D.W.S. with N.E.H. writing the programming code, J.W.P. and A.J. were responsible for analysis of projections of 3D Lévy movements, M.Z.A. and E.L.C.S. coded the power spectrum analysis, C.J.A.B. completed the relative likelihood modelling, and G.C.H. and M.J.W. provided additional data analysis.

Author Information Reprints and permissions information is available at www.nature.com/reprints. Correspondence and requests for materials should be addressed to D.W.S. (dws@mba.ac.uk)

LETTERS

Selection overrides gene flow to break down maladaptive mimicry

George R. Harper Jr[1]† & David W. Pfennig[1]

Predators typically avoid dangerous species, and batesian mimicry evolves when a palatable species (the 'mimic') co-opts a warning signal from a dangerous species (the 'model') and thereby deceives its potential predators[1,2]. Because predators would not be under selection to avoid the model and any of its look-alikes in areas where the model is absent (that is, allopatry)[2–5], batesian mimics should occur only in sympatry with their model. However, contrary to this expectation, batesian mimics often occur in allopatry[6–8]. Here we focus on one such example—a coral snake mimic[3,8]. Using indirect DNA-based methods, we provide evidence suggesting that mimics migrate from sympatry, where mimicry is favoured[3,9], to allopatry, where it is disfavoured[10]. Such gene flow is much stronger in nuclear genes than in maternally inherited mitochondrial genes, indicating that dispersal by males may explain the presence of mimetic phenotypes in allopatry. Despite this gene flow, however, individuals from allopatry resemble the model less than do individuals from sympatry. We show that this breakdown of mimicry probably reflects predator-mediated selection acting against individuals expressing the more conspicuous mimetic phenotype in allopatry. Thus, although gene flow may explain why batesian mimics occur in allopatry, natural selection may often override such gene flow and promote the evolution of non-mimetic phenotypes in such areas.

We examined whether mimics occur in allopatry because of gene flow[11,12] from regions where the model is present (and where mimics are selectively favoured) to regions where the model is absent. We also asked whether gene flow maintains mimetic phenotypes in allopatry or whether such phenotypes ultimately break down in these areas.

We focused on a well-known snake mimicry complex[8,13]. In the eastern United States, non-venomous scarlet kingsnakes, *Lampropeltis triangulum elapsoides*, closely resemble highly venomous eastern coral snakes, *Micrurus fulvius*[8,13] (Fig. 1a, b). Both species are brightly coloured, with conspicuous rings of red, yellow (or white), and black encircling the body. Predators avoid such tricolour ringed patterns[3,14], possibly without previous experience[15], but only in areas where *M. fulvius* actually occurs[3]. However, *L. t. elapsoides* occurs hundreds of kilometres outside the range of *M. fulvius* (Fig. 1c).

To determine whether mimics occur in allopatry because of gene flow, we used indirect DNA-based methods[12]. In particular, we used neutral DNA markers and the computer program MIGRATE-n[16] to estimate the number of migrants per generation (*Nm*) from sympatry into allopatry. We focused on two recipient *L. t. elapsoides* populations: one in eastern allopatry, and one in western allopatry (Fig. 1c). We began by sequencing three mitochondrial (mtDNA) loci (*ND4*, *CytB* and *16S*). Because mitochondria are haploid and are passed only from mother to offspring, such markers measure female dispersal[17]. Estimates of *Nm* based on these markers were extremely low (Fig. 1d, e). Indeed, none of these estimates was significantly greater than zero (Fig. 1d, e), indicating little or no gene flow in the mitochondrial genome.

Because males are more likely than females to disperse in species such as snakes[18,19] that have polygynous mating systems[17,20], we also estimated gene flow based on five nuclear (microsatellite) loci, which measure gene flow caused by both sexes. These estimates of *Nm* were significantly greater than zero in both populations (Fig. 1d, e). Moreover, in both populations, estimates of *Nm* were significantly higher in the nuclear genome than in the mitochondrial genome (Fig. 1d, e), indicating that dispersal by males may explain the presence of mimetic phenotypes in allopatry (however, gene flow was not directional: northward gene flow into allopatry was no stronger than southward gene flow into sympatry; Supplementary Table 1)

However, according to batesian mimicry theory, mimics should fail to receive protection from predation in allopatry[2–5]. Because mimics (like their models) are often conspicuous[7], allopatric mimics should generally experience increased predation pressure relative to less noticeable types[10] If such selection is strong compared with gene flow, then allopatric mimics should either go extinct or evolve less conspicuous (non-mimetic) phenotypes. Clearly, *L. t. elapsoides* has not gone extinct in allopatry (Fig. 1c). We therefore used morphometric analyses to determine whether *L. t. elapsoides* has evolved to become less phenotypically similar to *M. fulvius* in allopatry than in sympatry.

As predicted, allopatric *L. t. elapsoides* individuals are less similar to *M. fulvius* than are sympatric *L. t. elapsoides* individuals in terms of two morphological characters that predators use to discriminate between good and poor mimics[9]: the proportion of a snake's dorsum that is black, and the proportion that is red (Tukey–Kramer Honestly Significant Difference, $P < 0.05$ for both traits; overall analysis of variance (ANOVA) for black: $F_{2,110} = 6.941$, $P = 0.002$ (Fig. 2a, b); overall ANOVA for red: $F_{2,110} = 4.608$, $P = 0.012$ (Fig. 2a, c)). Indeed, a discriminant analysis that compared allopatric and sympatric *L. t. elapsoides* with *M. fulvius* mistakenly classified sympatric *L. t. elapsoides* as *M. fulvius* significantly more often than allopatric *L. t. elapsoides* (36 of 78 sympatric *L. t. elapsoides* versus 24 of 85 allopatric *L. t. elapsoides* individuals were mistakenly classified as *M. fulvius*; Fisher's exact test, $P = 0.023$, two-tailed test). Furthermore, allopatric *L. t. elapsoides* individuals became increasingly dissimilar to *M. fulvius* as the distance from the sympatry/allopatry boundary increased (Spearman correlation between distance from sympatry/allopatry boundary and proportion of dorsum black $= -0.40$, $N = 89$, $P = 0.0001$ (Fig. 2d); Spearman correlation between distance from sympatry/allopatry boundary and proportion of dorsum red $= 0.27$, $N = 89$, $P = 0.0115$ (Fig. 2e)). This gradual decrease in morphological similarity to the model correlates significantly with

[1]Department of Biology, University of North Carolina, Chapel Hill, North Carolina 27599, USA. †Present address: Department of Biology, Hendrix College, Conway, Arkansas 72032, USA

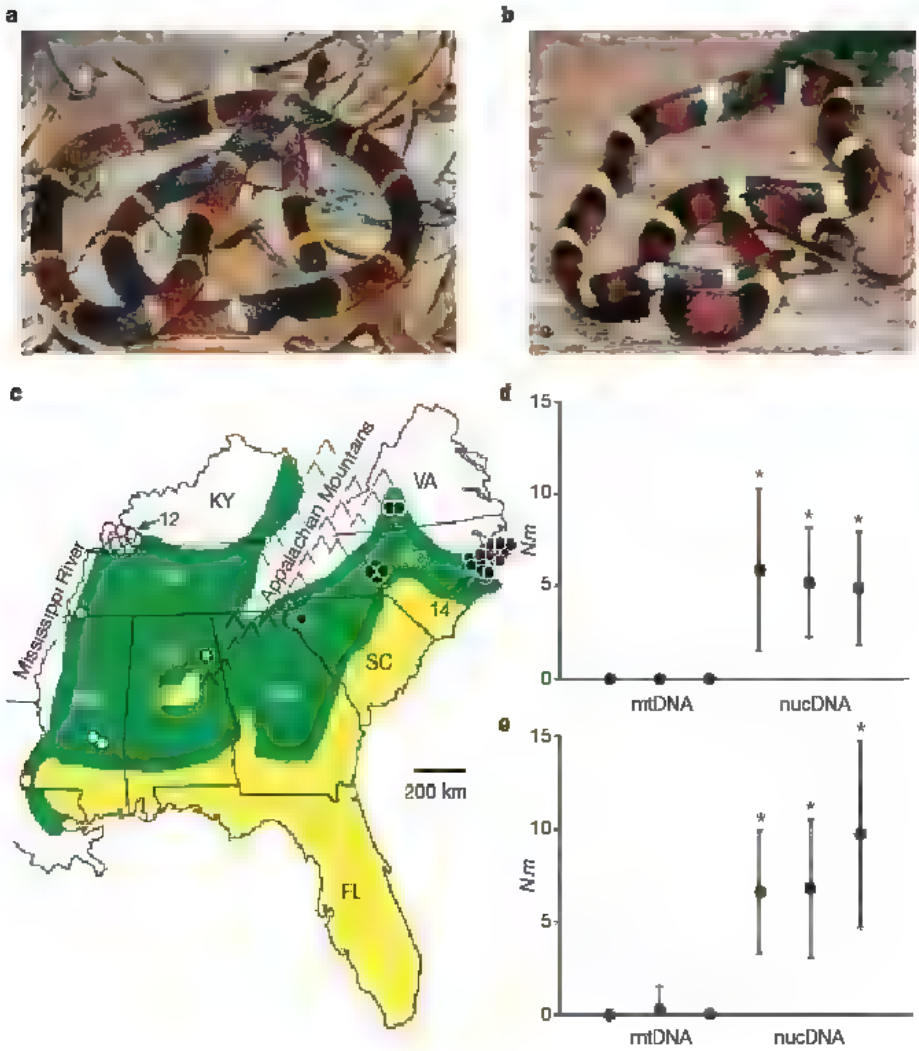

Figure 1 | Gene flow among coral snake mimics. **a**, **b**, The venomous eastern coral snake (*Micrurus fulvius*; **a**) and its non-venomous mimic, the scarlet kingsnake (*Lampropeltis triangulum elapsoides*; **b**) **c**, Geographical distributions of model (yellow) and mimic (yellow, green). For simplicity, sampling locations for genetic analyses are shown for allopatry only (open circles, western allopatry; filled circles, eastern allopatry) **d**, **e**, Gene flow among *L. t. elapsoides* (number of migrants per generation, *Nm*, shown as means ± 95% confidence interval) from sympatry into each of two allopatric recipient populations (eastern (**d**) and western allopatry (**e**)), as measured in mitochondrial (mtDNA) and nuclear (nucDNA) genomes (the three estimates in each population and genome reflect three runs of MIGRATE-n). Asterisks indicate estimates significantly greater than 0.

distance from the sympatry/allopatry boundary and not with latitude (partial correlation for distance from sympatry/allopatry boundary and proportion of dorsum black controlling for latitude = −0.27, d.f. = 86, $P < 0.01$; partial correlation for distance from sympatry/allopatry boundary and proportion of dorsum red controlling for latitude = 0.29, d.f. = 86, $P < 0.01$). Thus, mimicry seems to be breaking down in allopatry, and this erosion of the mimetic pattern does not reflect latitudinal variation in phenotype.

Three hypotheses can explain the evolution of a less mimetic form in allopatry. First, erosion of the mimetic phenotype may reflect genetic mixing of *L. t. elapsoides* with other, less mimetic *L. triangulum* subspecies in allopatry. Yet population genetic surveys of all *L.*

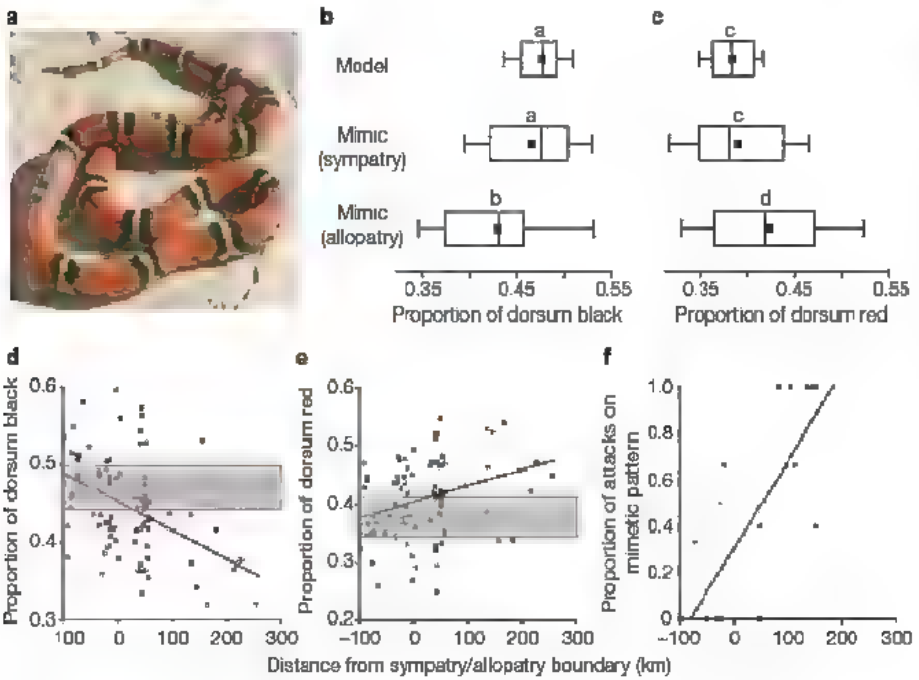

Figure 2 | Breakdown of mimicry. **a**, An *L. t. elapsoides* individual from allopatry. **b**, **c**, Colour patterns of model and mimic in sympatry and in allopatry. Box plots show 10th, 25th, 50th (median), 75th and 90th centiles; black squares show means. Different superscripts denote means that are significantly different. **d**, **e**, Geographical variation in colour pattern of *L. t. elapsoides* as a function of the distance from the sympatry/allopatry boundary (0) (more negative values are deeper into sympatry, and more positive values are deeper into allopatry). The grey area represents the 95% confidence interval for the model. **f**, Geographical variation in selection on the mimetic phenotype, as measured by proportion of attacks on the mimetic phenotype by natural predators (where the proportion is less than 0.5, predators avoided the mimetic phenotype; where it is more than 0.5, predators preferentially attacked the mimetic phenotype).

triangulum subspecies in the United States, with the use of both mitochondrial and nuclear genomes, revealed no evidence of recent hybridization between *L. t. elapsoides* and any other subspecies of *L. triangulum*[21,22]. For example, none of the allopatric *L. t. elapsoides* individuals contained a mtDNA sequence (at the *ND4*, *CytB* or *16S* locus) characteristic of, or closely related to, any other currently recognized subspecies of *L. triangulum* in the United States. Indeed, given that the subspecies *L. t. elapsoides* seems to be only distantly related to other subspecies of *L. triangulum* in the eastern United States (Fig. 3), recent hybridization between the two groups seems unlikely.

Second, erosion of the mimetic phenotype may reflect the action of random genetic drift. Many characters degrade through random genetic drift when selection is relaxed (as might occur when selection no longer favours mimicry). Yet drift is unlikely to explain the breakdown of the mimetic pattern. Coloration of allopatric *L. t. elapsoides* predictably degrades with distance from the sympatry/allopatry boundary (Fig. 2d, e). Under random genetic drift we would expect no such relationship.

Third, erosion of the mimetic phenotype may reflect the action of predator-mediated natural selection. As noted above, previous field experiments[3,9,10] revealed that predators preferentially attack mimetic phenotypes in allopatry. When we pooled estimates of selection against the mimetic phenotype obtained from these experiments, we found that the intensity of selection against the mimetic phenotype increases in allopatry with increasing distance from the sympatry/allopatry boundary (Spearman correlation between distance from sympatry/allopatry boundary and proportion of attacks on the mimetic pattern = 0.78, $N = 20$ sites, $P < 0.0001$; Fig. 2f). Indeed, the gradual increase in attacks on mimetic phenotypes mirrors the gradual breakdown of the mimetic phenotype (Fig. 2d, e), indicating that predator-mediated natural selection was probably predominant in eroding the mimetic pattern.

The above analysis assumes that *L. t. elapsoides* evolved in sympatry and migrated into allopatry secondarily, and that poor mimics in allopatry evolved from good ones in sympatry. However, it might be contended that *L. t. elapsoides* evolved in allopatry before moving into sympatry, and that good mimics in sympatry evolved from poor ones in allopatry. Three lines of evidence argue against this hypothesis, however. First, phylogenetic analysis[21] of the genus *Lampropeltis* indicates that the mimetic phenotype evolved in an ancestor of *L. t. elapsoides* and that the ancestral clade within *L. t. elapsoides* occurs in Florida (that is, deep sympatry); all allopatric individuals belong to one of the most recently derived clades (Fig. 3). Second, within the clade that contains both sympatric and allopatric individuals, the mitochondrial haplotypes found in allopatry seem to be recently descended from the sympatric haplotypes possessed by good mimics (Fig. 4). Third, given the close association of *L. t. elapsoides* with longleaf pine forests[23], it seems unlikely that the species would have existed in modern allopatry until about 10,000 years ago, when longleaf pine from refugia in the south began to move north into present-day allopatry[24]. Thus, *L. t. elapsoides*

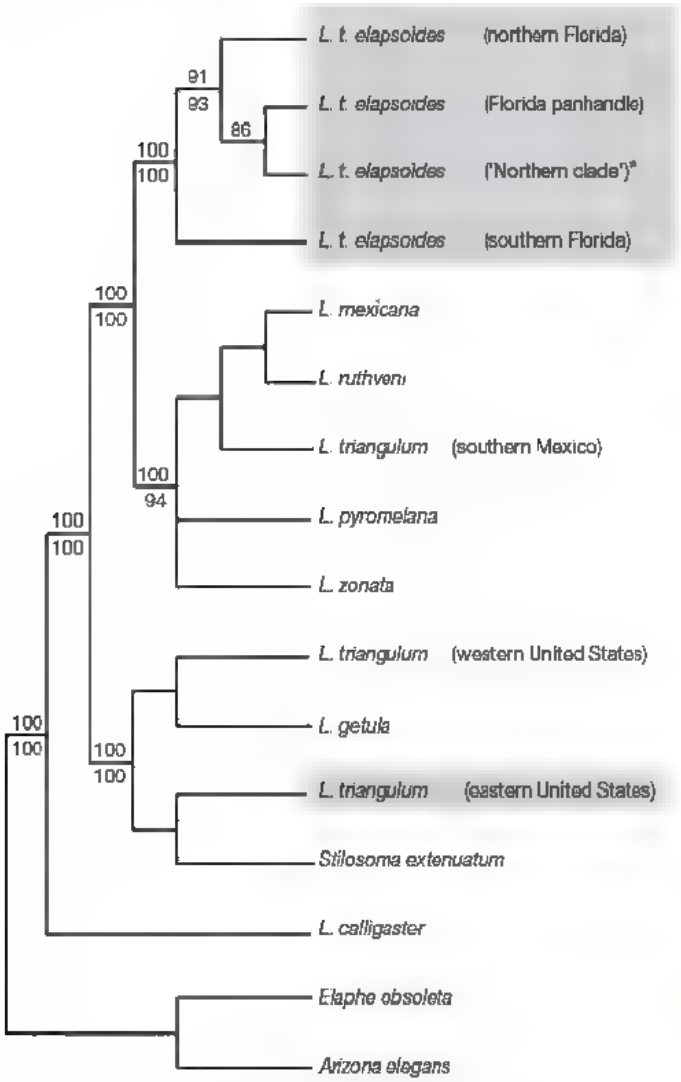

Figure 3 | Summary cladogram of North American *Lampropeltis*. Cladogram based on sequences from three mitochondrial genes and determined by maximum likelihood and Bayesian inference (upper numbers are parsimony-based bootstrap values over 80%; lower numbers are Bayesian posterior probability values over 90%). *L. t. elapsoides* (the mimic, in the upper grey rectangle) contains four clades, only one of which (the 'Northern clade') occurs in both sympatry and allopatry (indicated by the asterisk). In addition, *L. t. elapsoides* seems to be only distantly related to other *L. triangulum* subspecies, namely *L. t. triangulum* and *L. t. syspila*, from the eastern United States (in lower grey rectangle).

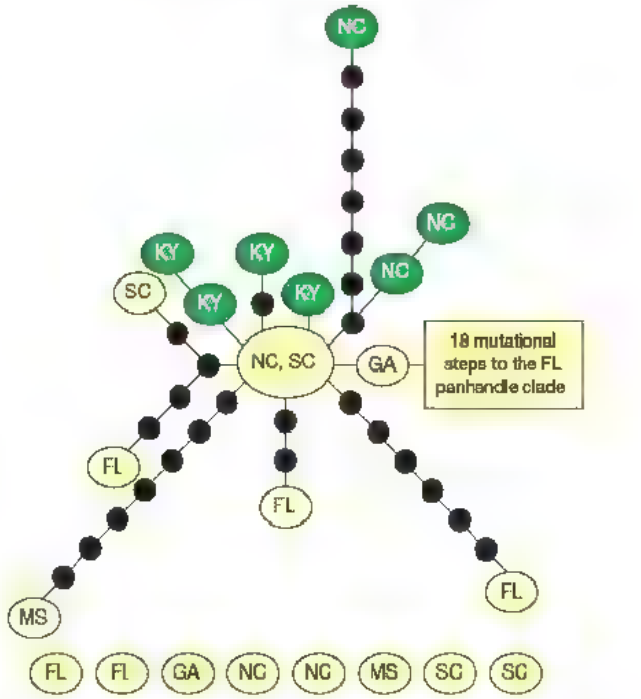

Figure 4 | Haplotype network for the 'Northern clade' of *L. t. elapsoides*. The network was based on three mitochondrial genes and determined by statistical parsimony. Shaded ovals containing two-letter US state abbreviations represent haplotypes and locations where they were found, green indicates that haplotypes were found in allopatry, and yellow that they were found in sympatry. Black circles represent an inferred missing haplotype (not found in individuals sampled), and each gap between circles or ovals represents one mutational step. The central oval represents the most common haplotype (found in six individuals, all other haplotypes were found in one or two individuals). The eight unconnected haplotypes at the bottom are each one mutational step away from the most common haplotype.

probably evolved in sympatry and subsequently migrated into allopatry, where erosion of the mimetic pattern occurred.

Our results provide an evolutionary explanation for why batesian mimics often occur in allopatry[6–8]. Generally, gene flow may carry alleles for mimetic phenotypes from sympatry, where mimics are favoured[3,9], to allopatry, where they are disfavoured[10]. However, in accord with batesian mimicry theory[2–5], selection, and possibly random genetic drift, may override such gene flow and break down maladaptive mimicry in regions where the model is absent, leading to the evolution of a less mimetic phenotype in allopatry.

METHODS SUMMARY

Gene flow estimation. We sequenced three mitochondrial genes (*ND4*, *CytB* and *16S*) and amplified five microsatellite (nuclear) loci from *L. t. elapsoides* collected in sympatry and in allopatry (Supplementary Tables 2, 3). We then used MIGRATE-n 2.1.3 (ref. 16) to calculate the number of migrants per generation (*Nm*) from sympatry into each of two recipient, allopatric populations (Fig. 1c). For each genome and recipient population we performed three runs of MIGRATE-n. For each estimate of *Nm* we generated 95% confidence intervals, which allowed us to assess whether the estimate was significantly greater than zero or different from values calculated for the other genome.

Colour pattern analysis. We evaluated the similarity of sympatric and allopatric mimics to the model by conducting morphometric analyses on snakes collected from North Carolina (Supplementary Table 4), where previous field experiments of mimicry had been conducted[3,9,10]. We focused on two colour characteristics—the proportion of a snake's dorsum that was black and the proportion that was red—that predation trials had shown to distinguish 'good' from 'poor' mimics[9]. We measured these characters from digital images of preserved specimens and used an ANOVA to compare the three groups of snakes. To determine whether mimicry degrades with increasing distance into allopatry, we estimated the sympatry/allopatry boundary from published accounts[21] and used a non-parametric Spearman correlation to assess the relationship between each snake's colour pattern and distance from this boundary.

Selection on mimics. To estimate selection against allopatric mimics, we re-analysed data from previously published field experiments[3,9,10]. Replicas of snakes with a mimetic or a non-mimetic pattern were exposed to free-ranging predators and the proportion of total attacks on mimetic replicas at each site was calculated. We used a non-parametric Spearman correlation to determine whether this proportion increased with distance from the sympatry/allopatry boundary.

Full Methods and any associated references are available in the online version of the paper at www.nature.com/nature.

Received 6 October; accepted 3 December 2007.

1. Bates, H. W. Contributions to an insect fauna of the Amazon valley. Lepidoptera Heliconidae. *Trans. Linn. Soc.* 23, 495–566 (1862).
2. Ruxton, G. D., Sherratt, T. N. & Speed, M. P. *Avoiding Attack: The Evolutionary Ecology of Crypsis, Warning Signals and Mimicry* (Oxford Univ. Press, Oxford, 2004).
3. Pfennig, D. W., Harcombe, W. R. & Pfennig, K. S. Frequency-dependent Batesian mimicry. *Nature* 410, 323 (2001).
4. Waldbauer, G. P. & Sternburg, J. G. Experimental field demonstration that two aposematic butterfly color patterns do not confer protection against birds in Northern Michigan. *Am. Midl. Nat.* 118, 145–152 (1987).
5. Wallace, A. R. *Contributions to the Theory of Natural Selection* (Macmillan, London, 1870).
6. Brower, L. P. & Brower, J. V. Z. The relative abundance of model and mimic butterflies in natural populations of the *Battus philenor* mimicry complex. *Ecology* 43, 154–158 (1962).
7. Clarke, C. & Sheppard, P. M. The genetics of the mimetic butterfly *Hypolimnas bolina* (L.). *Phil. Trans. R. Soc. B* 272, 229–265 (1975).
8. Greene, H. W. & McDiarmid, R. W. Coral snake mimicry: does it occur? *Science* 213, 1207–1212 (1981).
9. Harper, G. R. Jr & Pfennig, D. W. Mimicry on the edge: why do mimics vary in resemblance to their model in different parts of their geographical range? *Proc. R. Soc. Lond. B* 274, 1955–1961 (2007).
10. Pfennig, D. W., Harper, G. R. Jr, Brumo, A. F., Harcombe, W. R. & Pfennig, K. S. Population differences in predation on Batesian mimics in allopatry with their model: selection against mimics is strongest when they are common. *Behav. Ecol. Sociobiol.* 61, 505–511 (2007).
11. King, R. B. & Lawson, R. Color-pattern variation in Lake Erie water snakes: the role of gene flow. *Evolution Int. J. Org. Evolution* 49, 885–896 (1995).
12. Bohonak, A. J. Dispersal, gene flow, and population structure. *Q. Rev. Biol.* 74, 21–45 (1999).
13. Brodie, E. D. III & Brodie, E. D. Jr. in *The Venomous Reptiles of the Western Hemisphere* (eds Campbell, J. A. & Lamar, W. W.) Vol. II 617–633 (Comstock Publishing Associates, Ithaca, NY, 2004).
14. Brodie, E. D. III. Differential avoidance of coral snake banded patterns by free-ranging avian predators in Costa Rica. *Evolution Int. J. Org. Evolution* 47, 227–235 (1993).
15. Smith, S. M. Innate recognition of coral snake pattern by a possible avian predator. *Science* 187, 759–760 (1975).
16. Beerli, P. & Felsenstein, J. Maximum likelihood estimation of migration rates and population numbers of two populations using a coalescent approach. *Genetics* 152, 763–773 (1999).
17. Prugnolle, F. & de Meeus, T. Inferring sex-biased dispersal from population genetic tools: a review. *Heredity* 88, 161–165 (2002).
18. Blouin-Demers, G. & Weatherhead, P. J. Implications of movement patterns for gene flow in black rat snakes (*Elaphe obsoleta*). *Can. J. Zool.* 80, 1162–1172 (2002).
19. Keogh, J. S., Webb, J. K. & Shine, R. Spatial genetic analysis and long-term mark–recapture data demonstrate male-biased dispersal in a snake. *Biol. Lett.* 3, 33–35 (2007).
20. Clobert, J., Danchin, E. & Dhondt, A. A. (eds) *Dispersal* (Oxford Univ. Press, Oxford, 2001).
21. Harper, G. R. Jr. *Evolution of a Snake Mimicry Complex*. PhD thesis, Univ. North Carolina (2006).
22. Armstrong, M. P., Frymire, D. & Zimmerer, E. J. Analysis of sympatric populations of *Lampropeltis triangulum syspila* and *Lampropeltis triangulum elapsoides*, in western Kentucky and adjacent Tennessee with relation to the taxonomic status of the scarlet kingsnake. *J. Herpetol.* 35, 688–693 (2001).
23. Palmer, W. M. & Braswell, A. L. *Reptiles of North Carolina* (Univ. North Carolina Press, Chapel Hill, NC, 1995).
24. Soltis, D. E., Morris, A. B., McLachlan, J. S., Manos, P. S. & Soltis, P. S. Comparative phylogeography of unglaciated eastern North America. *Mol. Ecol.* 15, 4261–4293 (2006).

Supplementary Information is linked to the online version of the paper at www.nature.com/nature.

Acknowledgements We thank the museums and individuals listed in Supplementary Tables 2 and 4 for donating samples for the genetic and colour pattern analyses; M. Landstrom for measuring colour patterns; W. Van Devender for providing photographs in Figs 1a, b and 2a; and K. Pfennig, P. Marko, J. Wiens, A. Rice, R. Martin, C. Ledon-Rettig, J. Kingsolver, M. Servedio and D. Swofford for comments. Funding was provided by the National Science Foundation.

Author Contributions G.R.H. performed the genetic and morphological analyses and helped write the manuscript. D.W.P. designed the study, contributed to the interpretation of the data, and wrote the manuscript.

Author Information Reprints and permissions information is available at www.nature.com/reprints. Correspondence and requests for materials should be addressed to D.P. (dpfennig@unc.edu).

LETTERS

Facultative cheater mutants reveal the genetic complexity of cooperation in social amoebae

Lorenzo A. Santorelli[1], Christopher R. L. Thompson[2]†, Elizabeth Villegas[2], Jessica Svetz[2], Christopher Dinh[3], Anup Parikh[2,4], Richard Sucgang[3], Adam Kuspa[1,2,3], Joan E. Strassmann[1], David C. Queller[1] & Gad Shaulsky[1,2,4]

Cooperation is central to many major transitions in evolution, including the emergence of eukaryotic cells, multicellularity and eusociality[1]. Cooperation can be destroyed by the spread of cheater mutants that do not cooperate but gain the benefits of cooperation from others[1,2]. However, cooperation can be preserved if cheaters are facultative, cheating others but cooperating among themselves[2]. Several cheater mutants have been studied before, but no study has attempted a genome-scale investigation of the genetic opportunities for cheating. Here we describe such a screen in a social amoeba and show that cheating is multifaceted by revealing cheater mutations in well over 100 genes of diverse types. Many of these mutants cheat facultatively, producing more than their fair share of spores in chimaeras, but cooperating normally when clonal. These findings indicate that phenotypically stable cooperative systems may nevertheless harbour genetic conflicts. The opportunities for evolutionary moves and countermoves in such conflicts may select for the involvement of multiple pathways and numerous genes.

Only a few cheater mutants have been identified[3,4], but this situation is improving as model systems for the study of cheating have emerged, including the eukaryotic amoeba *Dictyostelium discoideum*[5–9] and the bacterium *Myxococcus xanthus*[10–12]. Solitary *D. discoideum* cells grow while feeding on bacteria but develop cooperatively into multicellular organisms on starvation[13]. At the end, 80% of the amoebae differentiate into viable spores and 20% differentiate into dead stalk cells, which facilitate spore dispersal[13]. The multicellular organism is formed by aggregation rather than by clonal cell division as in metazoa, so it is vulnerable to cheating by variant genotypes. *D. discoideum* cheaters are defined as strains that produce more than their fair share of spores in chimaeras, and losers as strains that produce less than their fair share of spores. Cheating occurs in chimaeras between wild isolates[9], and chimaeras are found in the wild[7], suggesting that cheating occurs in nature.

Clones with mutations in cooperation genes would cheat on the wild type during the social stage. To identify cooperation genes we selected cheaters by mutating *D. discoideum* cells and subjecting mixed mutant populations to successive rounds of growth, development, spore selection and germination. A previous screen that was limited to cheater mutants with obvious developmental defects produced one cheater, *fbxA*$^-$ (ref. 5), and cheaters from wild populations of *D. mucoroides* also displayed overt morphological defects[14,15]. In the wild, *D. discoideum* cells often develop clonally, preventing the spread of obligate cheaters that cooperate poorly when clonal[7]. Successful cheaters are therefore likely to be facultative, and indeed some wild strains of both *D. discoideum* and *M. xanthus* cheat facultatively[9,16]. Accordingly, we focused on facultative cheaters and selected against obligate cheaters by including one round of development and spore selection under clonal conditions, forcing the mutants to sporulate on their own.

We selected cheaters from a population of 10,000 mutant strains through ten rounds of germination, growth and development. At the tenth round we germinated spores and developed the strains clonally. After that round, we screened 2,448 clones and found 27 (1.1%) that exhibited aberrant morphology. Most strains (six out of seven tested) contained mutations in the *fbxA* gene[5] (Supplementary Table 1 and data not shown), suggesting that obligatory cheaters were rare in the population.

To determine whether cheater frequency increased during the selection, we mixed the populations with equal numbers of wild-type cells labelled with green fluorescent protein (GFP), induced development and counted the resulting spores. The controls behaved as expected (Fig. 1): the neutral control (unlabelled wild type) produced 50% of the spores, the loser control (*dimA*$^-$) contributed fewer than 50% and the cheater control (*fbxA*$^-$) produced more than 50%. The population from the first round did not cheat, but the populations

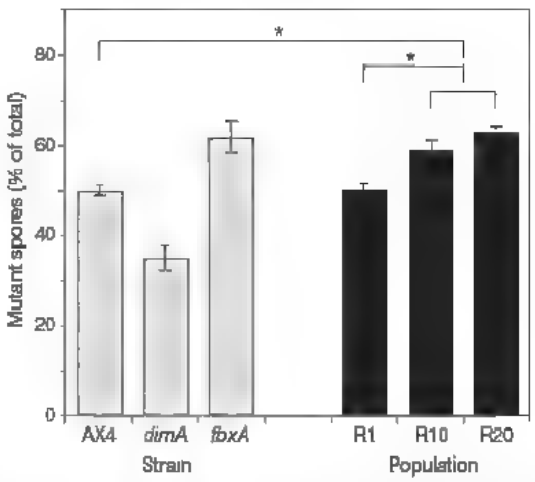

Figure 1 | Cheater selection. We mutated cells by using REMI and selected cheaters by development, followed by spore collection, germination and growth, all in mixed populations. We tested the population for cheating against GFP-labelled wild-type cells after the 1st, 10th and 20th rounds (R1, R10 and R20, respectively). Cheating is indicated as the proportion (percentage) of mutant spores recovered. The R10 and R20 populations were significantly different from the wild type and from the R1 population, but not from each other, as indicated by asterisks above the brackets (*t*-tests, $P < 0.001$, $n = 3$). Controls (left) were unlabelled wild type (AX4) as a neutral strain, *dimA*$^-$ cells as losers and *fbxA*$^-$ cells as cheaters. Results are shown as means and s.d. for at least three independent measurements.

[1]Department of Ecology and Evolutionary Biology, Rice University, Houston, Texas 77005, USA. [2]Department of Molecular and Human Genetics, [3]Department of Biochemistry and Molecular Biology. [4]Graduate Program in Structural Computational Biology and Molecular Biophysics, Baylor College of Medicine, Houston, Texas 77030, USA. †Present address: Faculty of Life Sciences, Michael Smith Building, University of Manchester, Manchester M13 9PT, UK.

from the 10th and 20th rounds did, indicating that the populations became enriched in cheaters (Fig. 1). To prevent interactions between cheaters, we also performed cheater selections on populations of 250 mutants each, which simplified into a few mutants over ten rounds (Supplementary Table 2, and data not shown).

We cloned and sequenced the insertion sites from 167 of the strains that we selected (Supplementary Table 2). To confirm the phenotypes, we tested a subset of the strains for cheating by growing them clonally, starving them, and mixing each with starved wild-type cells (the cells do not replicate genomic DNA during development[17,18], so cheating in this test cannot be attributed to differential growth rates). From the population of 10,000 mutants, we tested 11 random clones. Of these, ten were cheaters and one was a loser (Fig. 2 and Supplementary Table 1). From the populations of 250 mutants, we tested 29 clones and found 21 cheaters, 3 neutral (indistinguishable from the wild type) and 5 losers (Supplementary Table 1). Because 31 of the 40 tested strains were cheaters (77.5%), we estimate that 129 of the 167 strains would be cheaters.

We found that three loci were independently mutated at the same site in both screens; six others were mutated in two independent pools of mutants, and three cases revealed two different insertion sites of each gene (Supplementary Table 2). These results are consistent with near-saturation mutagenesis (at least 73% coverage), suggesting that the *D. discoideum* genome contains roughly 180 cooperation genes that could produce cheaters if mutated. That number would probably be higher if we tested other forms of mutation such as point mutations.

Finding independent alleles of several genes also indicated that the mutations caused the cheating phenotypes. To test causality further, we recapitulated 11 mutations in wild-type cells. The phenotypes were identical with those of the original strains in all cases (nine cheaters, one loser, one neutral; Supplementary Table 1, and data not shown), confirming that the insertional mutations were the cause of the phenotypes.

Previous studies suggested that cheating is limited by a mutant's inability to sporulate cooperatively in a pure population[5,7,11,14–16]. We found that all except one of the cheaters (LAS32) were morphologically indistinguishable from the wild type under clonal conditions (data not shown), suggesting that most are facultative cheaters whose fixation would leave cooperation intact. To test that idea further, we measured the sporulation efficiency of the 40 mutants shown in Fig. 2b. Of the 31 cheaters, 14 (45%) were indistinguishable from the wild type and 4 (13%) produced more spores than the wild type, suggesting that they are facultative cheaters, which are socially competent on their own. The latter might not be viewed as cheaters because they produce more spores clonally, but that would also be expected for cheaters that reduce allocation to stalk cells both clonally and in chimaeras.

Thirteen cheaters produced fewer spores than the wild type in pure populations (Fig. 2b and Supplementary Table 1). These mutants are not facultative because they have a clonal cost that might limit their spread, but they are also not obligatory because that cost does not eliminate cooperation completely. It is possible that the cost of the other mutations could be revealed under different conditions.

To test whether the cooperation genes have common characteristics, we examined nucleotide content, codon usage, expression, chromosomal location, recent duplications, Gene Ontology terms, and predicted protein domains. We considered all the genes together and the 31 cooperation genes separately, and in both cases we found only a few common features (Supplementary Figs 1–5 and Supplementary Table 3). However, the Gene Ontology annotations revealed several common functions, including protein and amino-acid metabolism, protein modification and signal transduction (Supplementary Fig. 5). Five genes are implicated in ubiquitin-mediated protein

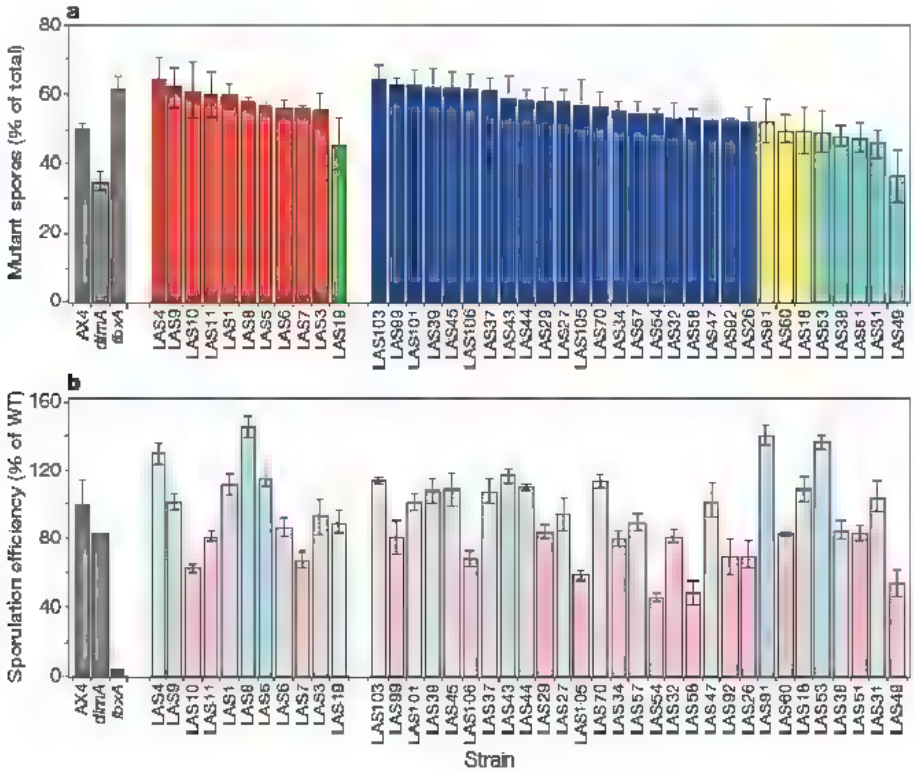

Figure 2 | Cheating ability and sporulation of isolated mutant strains. We grew the strains indicated clonally. **a**, Testing for cheating against GFP-labelled wild-type cells. Results (percentage mutant spores recovered) are shown as means ± s.d. for at least three independent measurements. Grey bars represent controls (as in Fig. 1); red (cheaters) and green (loser) bars represent strains from the population of 10,000 mutants; blue (cheaters), yellow (neutrals) and pale blue (losers) bars represent strains from the pools of 250 mutants. All the strains were statistically significantly different from the wild type (*t*-tests, $P < 0.05$, $n \geq 3$) except for the neutrals (complete data are given in Supplementary Table 1). **b**, Testing the sporulation efficiency of each strain after clonal development. Results (percentage sporulation efficiency relative to the wild type) are shown as means ± s.d. for four replications. Dark grey bars, controls; light grey bars, indistinguishable from the wild type (WT) (*t*-tests, $P > 0.05$, $n = 4$); light blue bars, sporulation was higher than in the wild type; rose bars, sporulation was lower than in the wild type (*t*-tests, $P > 0.05$, $n = 4$).

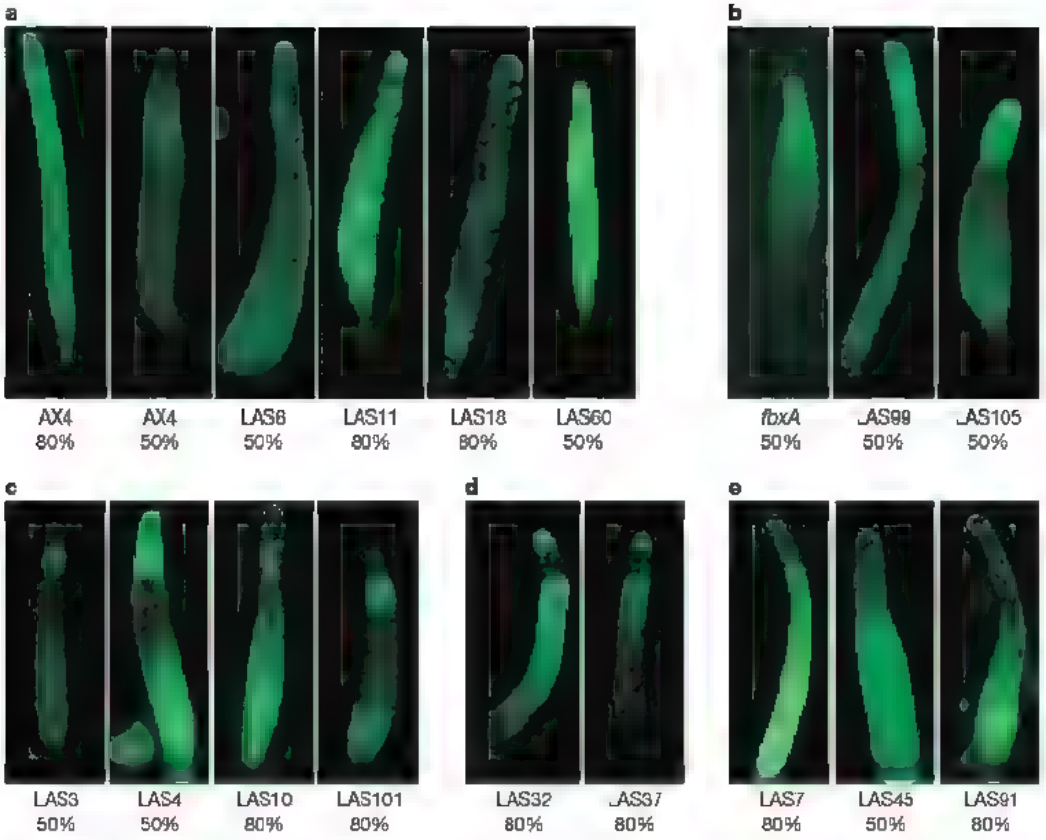

Figure 3 | Spatial distribution of cheater and wild-type cells in developing chimaeras. We grew strains clonally and mixed them with GFP-labelled wild-type cells in the indicated percentages. We photographed multicellular structures by using fluorescent microscopy after 16 h of development (anterior end up) **a**, The wild-type cells are evenly distributed in the structure (AX4 is the parental control) **b**, The wild-type cells are enriched in the prestalk (anterior) region. **c**, The wild-type cells are enriched in the PST-O (the posterior compartment of the prestalk region) and posterior prespore regions. **d**, The wild-type cells are almost excluded from the PST-O region. **e**, The wild-type cells are enriched in the prespore (posterior) region. All photographs were taken at the same magnification, the length of the top panels represents 1 mm. Cheating ability (sporulation) was confirmed in every case (data not shown).

degradation (*fbxA* and LAS3, LAS57, LAS81 and LAS103) and 12 are implicated in guanine nucleotide-mediated signalling (LAS13, LAS18, LAS32, LAS39/40, LAS45/46, LAS77, LAS86, LAS90, LAS104, LAS105, LAS110 and LAS143) (Supplementary Tables 1 and 2). These findings indicate that some of the cooperation genes have common functions, but in general they encode proteins with different structures and functions.

Despite the lack of common protein structure or function, the mutations could have conferred cheating by common mechanisms. We tested that possibility on 35 strains in chimaeras with GFP-labelled wild-type cells. We examined the distribution of GFP-labelled cells in slugs, in which the anterior consists of prestalk cells and the posterior contains mainly prespore cells[19]. In 23 cases the cheater and the wild-type cells were evenly distributed in the slugs (see, for example, Fig. 3a). In three cases the wild-type cells were enriched in the prestalk region, which is consistent with a cheating mechanism that diverts cell-type proportioning and forces the wild type to become prestalk (Fig. 3b). In four cases the wild-type cells were enriched in the posterior part of the prestalk region (PST-O[20]) and in the posterior part of the prespore region (Fig. 3c). In two cases the wild-type cells were almost excluded from the PST-O region (Fig. 3d) and in three cases they were enriched in the prespore region (Fig. 3e). There was no obvious correlation between the gene annotations and the spatial patterns, suggesting that many different pathways underlie cheating.

The mutant cheater strains that we found should pave the way to understanding the mechanisms that regulate cooperation in this system. The large number of genes and pathways involved suggest that it may be easy to evolve cheating and difficult to control it fully. However, our findings also show that complete control of cheating may not be required for maintaining cooperation and that the apparently serene surface of stable phenotypes may conceal underlying currents of molecular conflict with complex effects. Conflict is known to generate evolutionary churning, for example through rapid sequence evolution[21] or through copy-number changes[3]. Our results suggest that conflict-generated churning may also involve the recruitment of new genes and pathways, resulting in baroque networks.

METHODS SUMMARY

Strains, cell growth and maintenance. We used the laboratory wild-type strain AX4 (ref. 22) for mutagenesis, and GFP-labelled AX4 (ref. 6) to monitor cheating. *dimA*$^-$ was the loser control[23]; *fbxA*$^-$ was the cheater control[5]. We grew strains as described[24].

Mutagenesis and cheater selection. We mutated AX4 cells by insertional mutagenesis (REMI[25]). We allowed a mutant population of 10,000 clones to grow and develop in mixed populations, selected spores[26], and grew them again 20 times. At the tenth round, we grew and developed the cells clonally. We also generated 27 pools of 250 mutants each, selected them clonally for sporulation and then subjected them to ten rounds of selection as above.

Strain isolation, gene cloning and recapitulation of insertion events. We cloned individual strains, tested them for cheating, and cloned and sequenced the mutated genes[25]. In selected cases we regenerated the insertion by homologous recombination in AX4 cells[25].

Chimaeric testing for cheating and spatial distribution. We mixed cells from two strains, developed them and selected spores[24]. We counted all the spores as well as the GFP-positive spores in at least three independent replicates with neutral, loser and cheater controls. To examine the spatial distribution of strains in chimaeras, we mixed and developed strains as above and examined slugs after 16 h.

Sporulation efficiency. We grew and developed the cells in four replicates, counted the spores, and calculated the sporulation efficiency as the ratio between the number of cells plated and the number of spores recovered divided by the sporulation efficiency of AX4.

Full Methods and any associated references are available in the online version of the paper at www.nature.com/nature.

Received 26 October; accepted 20 December 2007.
Published online 13 February 2008.

1. Maynard Smith, J. & Szathmary, E. *The Major Transition in Evolution* (Freeman, Oxford, 1995).
2. Travisano, M. & Velicer, G. J. Strategies of microbial cheater control. *Trends Microbiol.* 12, 72–78 (2004).
3. Greig, D. & Travisano, M. The Prisoner's Dilemma and polymorphism in yeast SUC genes. *Proc. R. Soc. B* 271 (Suppl. 3), S25–S26 (2004).
4. Griffin, A. S., West, S. A. & Buckling, A. Cooperation and competition in pathogenic bacteria. *Nature* 430, 1024–1027 (2004).
5. Ennis, H. L., Dao, D. N., Pukatzki, S. U. & Kessin, R. H. *Dictyostelium* amoebae lacking an F-box protein form spores rather than stalk in chimeras with wild type. *Proc. Natl Acad. Sci. USA* 97, 3292–3297 (2000).
6. Foster, K. R., Shaulsky, G., Strassmann, J. E., Queller, D. C. & Thompson, C. R. L. Pleiotropy as a mechanism to stabilize cooperation. *Nature* 431, 693–696 (2004).
7. Gilbert, O. M., Foster, K. R., Mehdiabadi, N. J., Strassmann, J. E. & Queller, D. C. High relatedness maintains multicellular cooperation in a social amoeba by controlling cheater mutants. *Proc. Natl Acad. Sci. USA* 104, 8913–8917 (2007).
8. Queller, D. C., Ponte, E., Bozzaro, S. & Strassmann, J. E. Single-gene Greenbeard effects in the social amoeba *Dictyostelium discoideum*. *Science* 299, 105–106 (2003).
9. Strassmann, J. E., Zhu, Y. & Queller, D. C. Altruism and social cheating in the social amoeba *Dictyostelium discoideum*. *Nature* 408, 965–967 (2000).
10. Velicer, G. J., Kroos, L. & Lenski, R. E. Loss of social behaviors by *Myxococcus xanthus* during evolution in an unstructured habitat. *Proc. Natl Acad. Sci. USA* 95, 12376–12380 (1998).
11. Velicer, G. J., Kroos, L. & Lenski, R. E. Developmental cheating in the social bacterium *Myxococcus xanthus*. *Nature* 404, 598–601 (2000).
12. Velicer, G. J. *et al.* Comprehensive mutation identification in an evolved bacterial cooperator and its cheating ancestor. *Proc. Natl Acad. Sci. USA* 103, 8107–8112 (2006).
13. Kessin, R. H. *Dictyostelium—Evolution, Cell Biology, and the Development of Multicellularity* (Cambridge Univ. Press, Cambridge, 2001).
14. Buss, L. W. Somatic cell parasitism and the evolution of somatic tissue compatibility. *Proc. Natl Acad. Sci. USA* 79, 5337–5341 (1982).
15. Filosa, M. F. Heterocytosis in cellular slime molds. *Am. Nat.* 96, 79–91 (1962).
16. Fiegna, F. & Velicer, G. J. Exploitative and hierarchical antagonism in a cooperative bacterium. *PLoS Biol.* 3, e370 (2005).
17. Chen, G., Shaulsky, G. & Kuspa, A. Tissue-specific G1-phase cell-cycle arrest prior to terminal differentiation in *Dictyostelium*. *Development* 131, 2619–2630 (2004).
18. Shaulsky, G. & Loomis, W. F. Mitochondrial DNA replication but no nuclear DNA replication during development of *Dictyostelium*. *Proc. Natl Acad. Sci. USA* 92, 5660–5663 (1995).
19. Sternfeld, J. & David, C. N. Fate and regulation of anterior-like cells in *Dictyostelium* slugs. *Dev. Biol.* 93, 111–118 (1982).
20. Jermyn, K. A., Duffy, K. T. & Williams, J. G. A new anatomy of the prestalk zone in *Dictyostelium*. *Nature* 340, 144–146 (1989).
21. Nielsen, R. Molecular signatures of natural selection. *Annu. Rev. Genet.* 39, 197–218 (2005).
22. Knecht, D. A., Cohen, S. M., Loomis, W. F. & Lodish, H. F. Developmental regulation of *Dictyostelium discoideum* actin gene fusions carried on low-copy and high-copy transformation vectors. *Mol. Cell. Biol.* 6, 3973–3983 (1986).
23. Thompson, C. R., Fu, Q., Buhay, C., Kay, R. R. & Shaulsky, G. A bZIP/bRLZ transcription factor required for DIF signaling in *Dictyostelium*. *Development* 131, 513–523 (2004).
24. Sussman, M. Cultivation and synchronous morphogenesis of *Dictyostelium* under controlled experimental conditions. *Methods Cell Biol.* 28, 9–29 (1987).
25. Kuspa, A. & Loomis, W. F. Tagging developmental genes in *Dictyostelium* by restriction enzyme-mediated integration of plasmid DNA. *Proc. Natl Acad. Sci. USA* 89, 8803–8807 (1992).
26. Shaulsky, G., Escalante, R. & Loomis, W. F. Developmental signal transduction pathways uncovered by genetic suppressors. *Proc. Natl Acad. Sci. USA* 93, 15260–15265 (1996).

Supplementary Information is linked to the online version of the paper at www.nature.com/nature.

Acknowledgements We thank past and present members of our groups, especially A. Khare, E. Roberge, K. Foster and N. Mehdiabadi, for discussions and for technical assistance; R. H. Kessin for the *fbxA*⁻ strain and for discussions; and W. F. Loomis for encouragement and advice. This work was supported by a grant from the National Science Foundation; L.A.S. was supported by a Wray–Todd Fellowship. C.R.L.T. was supported by the Wellcome Trust International Prize Traveling Research Fellowship.

Author Contributions L.A.S., C.R.L.T., E.V., J.S. and C.D. conducted the experimental work. A.P. and R.S. performed computational analyses. A.K., C.R.L.T., D.C.Q., G.S. and J.E.S. conceived of the study and wrote the paper. All authors discussed the results and commented on the manuscript.

Author Information Reprints and permissions information is available at www.nature.com/reprints. Correspondence and requests for materials should be addressed to G.S. (gadi@bcm.tmc.edu).

LETTERS

Resistance to therapy caused by intragenic deletion in *BRCA2*

Stacey L. Edwards[1], Rachel Brough[1], Christopher J. Lord[1], Rachael Natrajan[1], Radost Vatcheva[1], Douglas A. Levine[2], Jeff Boyd[3], Jorge S. Reis-Filho[1] & Alan Ashworth[1]

Cells with loss of BRCA2 function are defective in homologous recombination (HR) and are highly sensitive to inhibitors of poly(ADP-ribose) polymerase (PARP)[1,2], which provides the basis for a new therapeutic approach. Here we show that resistance to PARP inhibition can be acquired by deletion of a mutation in *BRCA2*. We derived PARP-inhibitor-resistant (PIR) clones from the human CAPAN1 pancreatic cancer cell line, which carries the protein-truncating c.6174delT frameshift mutation. PIR clones could form DNA-damage-induced RAD51 nuclear foci and were able to limit genotoxin-induced genomic instability, both hallmarks of a competent HR pathway. New BRCA2 isoforms were expressed in the resistant lines as a result of intragenic deletion of the c.6174delT mutation and restoration of the open reading frame (ORF). Reconstitution of BRCA2-deficient cells with these revertant *BRCA2* alleles rescued PARP inhibitor sensitivity and HR deficiency. Most of the deletions in *BRCA2* were associated with small tracts of homology, and possibly arose from error-prone repair caused by BRCA2 deficiency[3,4]. Similar ORF-restoring mutations were present in carboplatin-resistant ovarian tumours from c.6174delT mutation carriers. These observations have implications for understanding drug resistance in *BRCA* mutation carriers as well as in defining functionally important domains within BRCA2.

Heterozygous germline mutations in *BRCA2* strongly predispose to cancer[5]. BRCA2 is critically important for the repair of double-strand breaks (DSBs) by HR, and loss of BRCA2 function probably fosters tumorigenesis by causing genome instability[6]. BRCA2 facilitates DSB repair by interacting with the recombinase RAD51 through eight well-conserved BRC-repeat motifs and a distinct RAD51-binding domain close to the carboxy terminus[7,8]. In response to DNA damage, BRCA2 localizes RAD51 to the site of DSBs and mediates repair[6]. Potent PARP inhibitors are synthetically lethal with BRCA2 deficiency as inhibition of PARP probably leads to the persistence of DNA lesions that would normally be repaired by BRCA2-mediated HR[1,2]. These observations have led to the assessment of these agents as monotherapy for cancer in *BRCA* mutation carriers[9]. However, it seems likely that some tumours may have *de novo* resistance or acquire resistance. To model this, we derived PIR clones from the BRCA2-deficient cell line CAPAN1 (ref. 10).

CAPAN1 cells originate from a pancreatic epithelial tumour and lack a wild-type *BRCA2* gene but carry an allele with a c.6174delT frameshift mutation that encodes a truncated protein of 2,002 amino-acid residues (about 224 kDa), in contrast with the wild-type 3,418-residue protein (about 390 kDa)[10]. The mutant protein lacks two whole BRC repeats, the DNA-binding/DSS1 interaction domain (DBD)[11] and the C terminus, which contains a second RAD51-binding domain (TR2)[7,8] and nuclear localization sequences[12]. CAPAN1 cells are defective in the ability to form damage-induced RAD51 foci and HR[13] and are extremely sensitive to treatment with potent inhibitors of PARP[14].

PIR clones were developed either by a continuous stepwise exposure to increasing concentrations of the PARP inhibitor KU0058948 (ref. 1) (from 1 nM to 50 μM; clones PIR1–6) or by continuous treatment with 100 nM KU0058948 (clones PIR7–12). PIR clones were highly resistant (1,370-fold) to KU0058948 (Fig. 1a). For CAPAN1, the SF_{50} (the dose at which 50% of cells survive) was 5.75 nM, in contrast with 7.35 μM for PIR1–12. PIR clones were also resistant to the DNA crosslinking agent cisplatin but not to the microtubule-stabilizing taxane docetaxel (Fig. 1a). Both KU0058948 and cisplatin are thought to exert their BRCA-selective effects by increasing the frequency of stalled and collapsed replication forks, leading to mis-repaired DSBs in the absence of effective HR[4,15], indicating that the resistance of PIR clones to KU0058948 might involve the restoration of functional HR.

The extent of stalled and collapsed replication forks and DSBs can be assessed by quantifying nuclear γ-H2AX foci[16]. KU0058948 induced the formation of γ-H2AX foci to the same extent in both CAPAN1 and PIR clones (Fig. 1b), indicating that resistance was unlikely to be explained by enhanced drug metabolism or efflux. CAPAN1 cells are deficient in the ability to form RAD51 foci after DNA damage, a hallmark of competence for HR. However, clones PIR1–11 had acquired the ability to form RAD51 foci after treatment with KU0058948 or exposure to X-rays (Fig. 1c). The ability of MMC to cause genomic instability is indicative of a defect in HR[3]. MMC-induced chromosomal aberrations were frequent in CAPAN1 cells but were significantly decreased in PIR cells (Fig. 1d and Table 1).

Given the possibility that KU0058948 resistance in PIR clones was a consequence of restored HR, and the critical role of BRCA2 in this pathway[3,4], we investigated whether PIR clones expressed wild-type BRCA2. PIR clones continued to express RNA from the c.6174delT allele (data not shown). We used western blot/immunoprecipitation analysis with antibodies recognizing the N-terminal region of BRCA2, present in the c.6174delT product, or the C-terminal region, which is absent from the c.6174delT protein, to investigate BRCA2 protein expression. Clones PIR1–11 expressed a BRCA2 species that was of similar size to the c.6174delT protein but included both N- and C-terminal epitopes, indicative of new BRCA2 proteins lacking amino-acid residues between these two regions (Fig. 2a) In addition to the c.6174delT product, PIR12 also expressed a BRCA2 species that was of similar size to wild-type BRCA2 and contained both N- and C-terminal epitopes. Newly identified BRCA2 proteins were also capable of nuclear translocation and RAD51 interaction (Fig. 2b).

[1]The Breakthrough Breast Cancer Research Centre, The Institute of Cancer Research, Fulham Road, London SW3 6JB, UK. [2]Department of Surgery, Memorial Sloan-Kettering Cancer Center, 1275 York Avenue, New York, NY 10021, USA. [3]Anderson Cancer Institute, Memorial Health University Medical Center, 4700 Waters Avenue, Savannah, GA 31404, USA

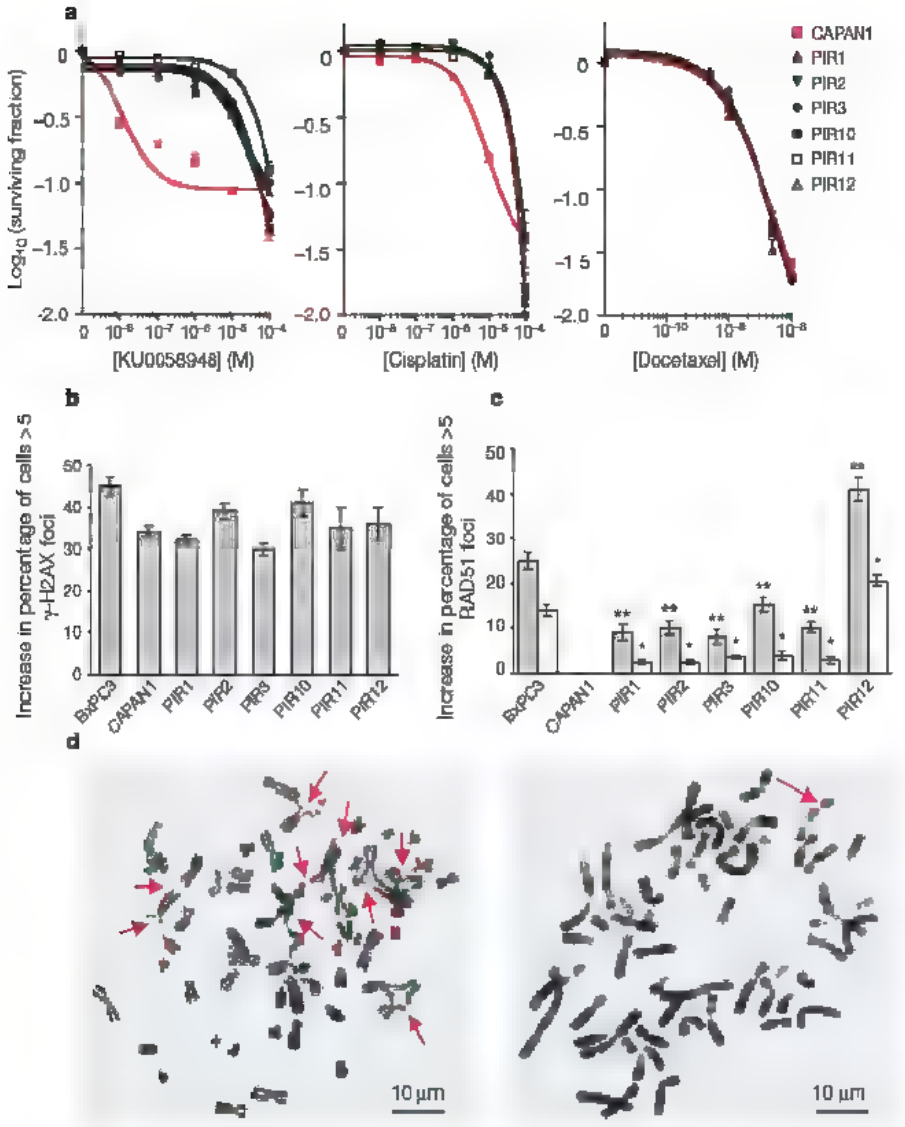

Figure 1 | PIR CAPAN1clones. a, Survival curves of cell lmes after 15 days of exposure to KU0058948, cisplatin or docetaxel. Means and s.d. for three experiments with internal duplication are shown. **b**, γ-H2AX focus formation after exposure to 10 μM KU0058948 for 24 h. Cells containing more than five γ-H2AX foci per nucleus were counted as positive[1]. More than 100 cells were assessed for each cell line and treatment. The means and s.d. for three independent experiments are shown. BxPC3 cells are shown as a positive control. **c**, RAD51 focus formation after exposure to 10-Gy X-rays (grey bars) followed by recovery for 6 h, or to 10 μM KU0058948 (white bars) for 24 h. Cells containing more than five RAD51 foci per cell were counted as positive[1]. More than 100 cells were assessed for each cell line and treatment. Means and s.d. for three independent experiments are shown. BxPC3 cells are shown as a control. *P* values were determined with a two-tailed *t*-test. Asterisk, $P \leq 0.005$ compared with CAPAN1 treated with KU0058948, two asterisks, $P \leq 0.0004$ compared with CAPAN1 exposed to X-rays. **d**, Chromosome analysis of CAPAN1 cells (left) and PIR1 cells (right) exposed to MMC for 24 h. Arrows indicate chromatid breaks, triradials and other chromosome aberrations.

Comparative genomic hybridization (CGH) in combination with fluorescence *in situ* hybridization (FISH) indicated that CAPAN1 and PIR12 cells possessed three copies of the *BRCA2* gene (Supplementary Fig. 1). This contrasted with five *BRCA2* copies in PIR1–6. Sequencing of complementary DNA and genomic DNA from PIR1–12 showed that all PIR clones carried the c.6174delT *BRCA2* allele (data not shown). PIR1–11 also expressed *BRCA2* alleles carrying deletions of up to 58 kb, all of which resulted in the elimination of the c.6174delT mutation and restoration of an ORF including five BRC repeats, the C-terminal nuclear localization sequence and the TR2 RAD51 interaction domain[7,8] (Fig. 2c and Table 2). These new BRCA2 species lacked three BRC repeats (BRC 6, 7 and 8) and all or most of the proposed DBD (Fig. 2d). Sequencing of *BRCA2* in PIR12 indicated the presence of a 458-base-pair (bp) deletion surrounding the original c.6174delT mutation, restoring the ORF and producing an almost full-length BRCA2 protein lacking 153 amino-acid residues and two BRC repeats (BRC 7 and 8).

Table 1 | MMC-induced chromosomal aberrations per cell

Cell line	Gaps/breaks*	*P*	Total aberrations†	*P*
CAPAN1	1.52 ± 1.31	–	2.44 ± 1.88	–
PIR1	0.98 ± 1.20	0.03	1.08 ± 1.25	<0.0001

Average aberrations per cell (50 metaphases scored per cell line) are shown. *P* values were determined with a two-tailed *t*-test.
*Chromatid and chromosome gaps and breaks, means ± s.d.
†Includes breaks, ring chromosomes, triradials, quadriradials, dicentrics, tricentrics and other aberrations, means ± s.d.

In the absence of functional BRCA2, single-strand annealing and non-homologous end joining compensate and repair DSBs by aligning short regions of homology flanking the DSB, deleting the intervening sequence[3,17]. Examination of the nucleotide sequences surrounding the *BRCA2* deletions in PIR1–12 revealed, in almost all cases, short regions of sequence identity associated with the ends of the deleted region (Table 2). It therefore seems possible that these deletions arose as a consequence of the DNA repair defect in CAPAN1 cells.

To validate our observations, we inhibited BRCA2 expression by using short interfering RNA (siRNA). Sensitivity to KU0058948 was partly restored in representative PIR clones after transfection with

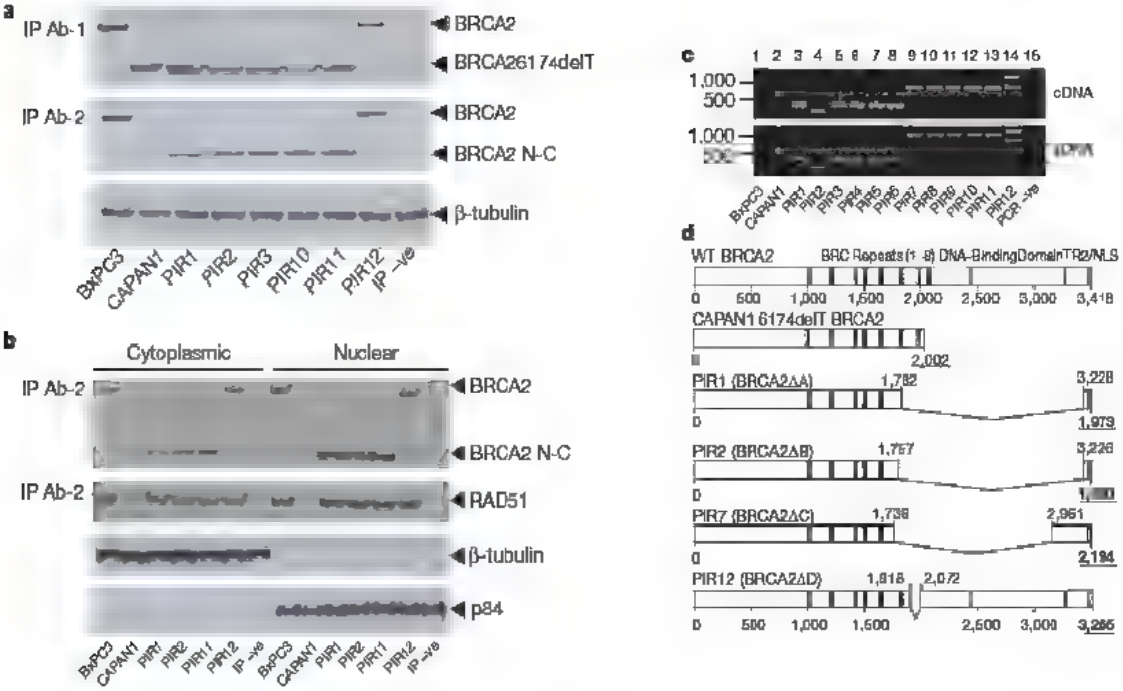

Figure 2 | BRCA2 expression in PIR clones. **a**, Immunoprecipitation (IP) and western blotting of lysates with anti-BRCA2 antibodies recognizing N-terminal (residues 1651–182. (Ab-1) or residues 188–563 (3E6)) or C-terminal (residues 3245–3418 (Ab-2)) epitopes. BRCA2 was immunoprecipitated with antibodies Ab-1 or Ab-2 and detected on immunoblots with 3E6. New BRCA2 species containing N-terminal and C-terminal epitopes (BRCA2 N-C) are indicated. **b**, Subcellular fractionation and immunoprecipitation of lysates with anti-BRCA2 (Ab-2) followed by probing with anti-BRCA2 (3E6) or anti-RAD51 (H-92) antibodies. The fractionation procedure was validated on separate blots with antibodies against cytoplasmic β-tubulin or nuclear p84. **c**, *BRCA2* PCR on cDNA and genomic DNA (gDNA). Lanes 3–8, B2Ex11F1/B2Ex27R1 (first round) and B2Ex11F2/B2Ex27R2 (second round) primers were used to amplify transcripts and alleles from PIR1–6. Lanes 9–13, B2Ex11F1/B2Ex24R1 (first round) and B2Ex11F3/B2Ex24R2 (second round) primers were used for PIR7–11. Lane 14, B2Ex11F4/B2Ex11R1 primers amplified both the c.6174delT transcript (larger band) and the new transcripts and alleles (smaller band) from PIR12. **d**, Diagram of new BRCA2 proteins in PIR1, PIR2, PIR7 and PIR12, as predicted from cDNA and genomic sequencing of *BRCA2*. The predicted number of amino acids for each new isoform is shown in bold and underlined. WT, wild type.

BRCA2 siRNA (Fig. 3a and Supplementary Fig. 2), and the acquired ability to form DNA damage-induced RAD51 foci was abrogated (Fig. 3b). Furthermore, we reconstituted BRCA2-deficient cell lines with BRCA2 expression constructs and assessed their ability to rescue KU0058948 sensitivity and perform efficient HR. Constructs that expressed either wild-type BRCA2, BRCA2 with the c.6174delT mutation (p6174delT) or two representative PIR mutant BRCA2 proteins, PIR1 and PIR12, were transfected into CAPAN1 cells. Wild-type BRCA2, PIR1 and PIR12 proteins partly rescued sensitivity to KU0058948, whereas expression of the 6174delT protein had no significant effect (Fig. 3c and Supplementary Fig. 3). To assess HR we used an I*Sce*I-dependent DR-green fluorescent protein (GFP) reporter assay integrated into BRCA2-deficient VC8 cells[18]. BRCA2 constructs were stably transfected into the VC8-DR-GFP cell line and HR was assayed (Fig. 3d and Supplementary Fig. 3). Expression of either the full-length or the PIR mutant BRCA2 proteins significantly increased HR (about fourfold), compared with the vector control, in contrast with expression of the c.6174delT-encoded protein, which had no effect (Fig. 3d).

Trials of potent PARP inhibitors for the treatment of BRCA-associated cancer are still in the early stages of assessment[9] and it is not yet possible to assess mechanisms of resistance in material from patients. However, patients with ovarian carcinoma, some of whom harbour *BRCA1* or *BRCA2* mutations, have long been treated with agents such as cisplatin and carboplatin, which probably exert their BRCA-selective effects by a similar mechanism to PARP inhibitors[1]. *BRCA1* or *BRCA2* mutation carriers with ovarian cancer tend to respond better to carboplatin than patients with no family history of the disease[19,20]; however, resistance does eventually occur[21]. To examine the mechanism of resistance, we sequenced *BRCA2* in tumours from two patients with the *BRCA2* c.6174delT mutation, whose ovarian cancers were resistant to carboplatin treatment. In

Table 2 | *BRCA2* genomic deletions observed in CAPAN1 and PIR clones

Clone name	Name of allele	Sequence of genomic deletion (5′→3′)*	No. of bases deleted	No. of clones
CAPAN1	c.6174delT†	(Exon 11) 26050 26052 (Exon 11) TTGTGGGATTTTTAGCACAGCAAG(T)GGAAAATCTGTCCAGGTATCAGAT	1	–
PIR1, 3–6	BRCA2ΔA‡	(Exon 11) 25451 83997 (Exon 27) AATGTTGAAG**ATCAAA**(AAAACACT...TT**ATCAAA**)GTCCTTTATCACT	58,545	5
PIR2	BRCA2ΔB‡	(Exon 11) 25375 83990 (Exon 27) TTCTGATGAGG**TATAT**(AATGATTC...AGA**TATAT**)TATCAAAGTCCTTT	58,614	1
PIR7–11	BRCA2ΔC‡	(Exon 11) 25312 65211 (Exon 22) TCTCTCCGAAA**AACAA**(GATACTTA...GG**AACAA**)GGTTTATCAAGGGA	39,898	5
PIR12	BRCA2ΔD‡	(Exon 11) 25857 26316 (Exon 11) TAGCACGCATTCACA**T**(AAGGTTTT...TAGAAAG**T**)TCCTTACACAAAG	458	1

Nucleotide sequences at the *BRCA2* deletion sites in the clones are shown.
* Sequence numbers flanking the deletions are shown and are based on GenBank accession no. AY436640.
† Reference 10
‡ New deletions. Microhomologies are indicated with overlapping sequences in bold and underlined with deleted sequences shown in parentheses.

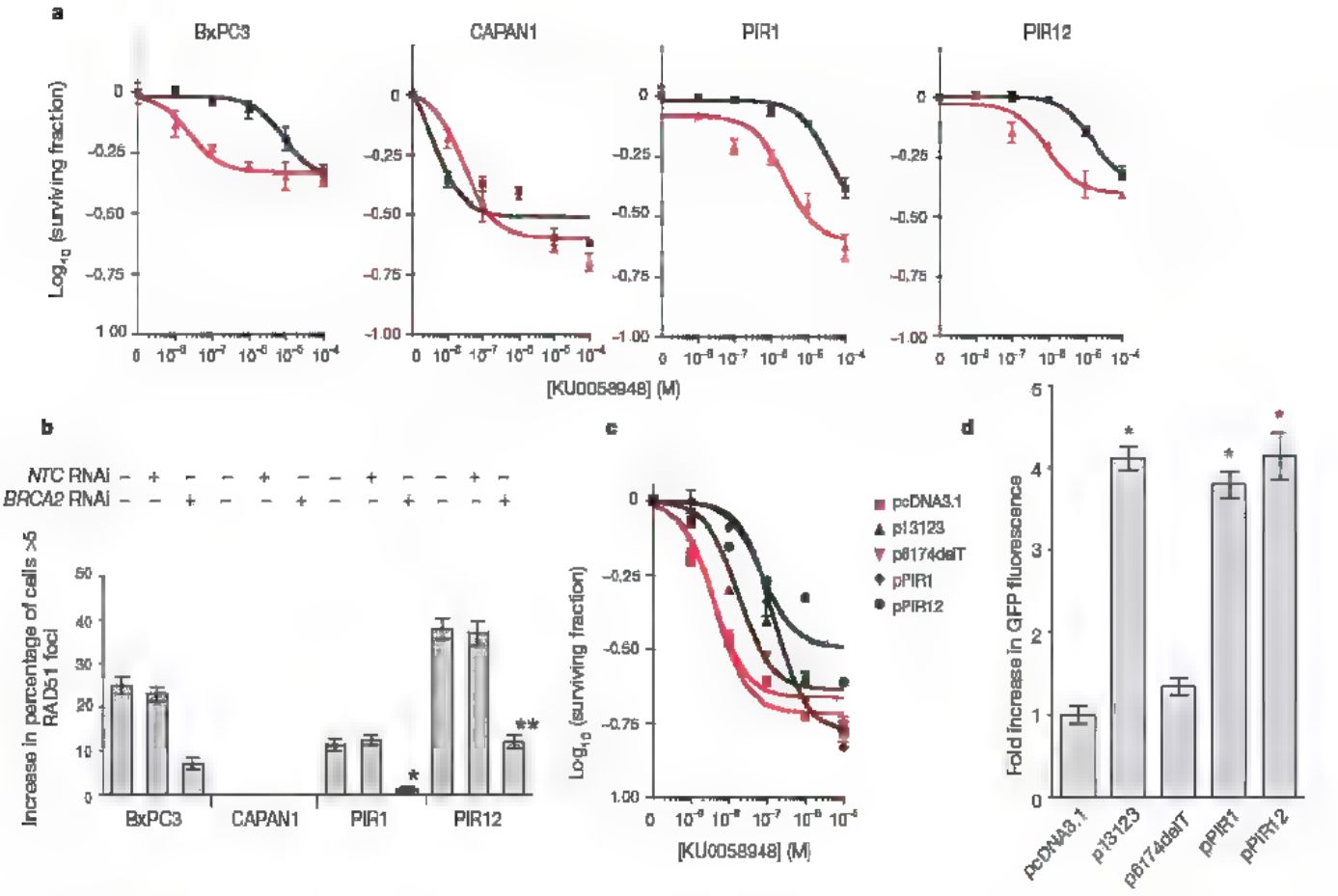

Figure 3 | Expression of new mutant BRCA2 isoforms restores KU0058948 resistance and increases HR in BRCA2 deficient cells. **a**, Survival curves after transfection with a non-targeting control siRNA (black) or *BRCA2* siRNA (red) and exposure to KU0058948 for 15 days. Means and s.d. for three independent experiments with internal duplication are shown. **b**, RAD51 focus formation in cells after transfection with siRNA and exposure to 10-Gy X-rays. Cells containing more than five RAD51 foci per nucleus were counted as positive[3]. More than 100 cells were assessed for each cell line and treatment. The means and s.d. for three independent experiments are shown. *P* values were determined with a two-tailed *t*-test. Asterisk, $P = 0.007$ compared with PIR1 NTC; two asterisks, $P = 0.0003$ compared with PIR12 NTC. **c**, Survival curves of G418-selected CAPAN1 cells expressing either wild-type or mutant forms of BRCA2, after 15 days of exposure to KU0058948. The means and s.d. for two independent experiments with internal duplication are shown. **d**, Quantification of ISceI-induced HR in VC8-DR-GFP cells stably expressing either wild-type or mutant forms of BRCA2. The fold increase in GFP-expressing cells compared to pcDNA3.1 is shown. The means and s.d. for three independent experiments with internal duplication are shown. *P* values were determined with a two-tailed *t*-test. Asterisk, $P < 0.0001$ compared with pcDNA3.1.

patient UK1999 we identified a 137-bp deletion within exon 11 of the gene, 7 bp 3′ to the c.6174delT mutation (Fig. 4). This resulted in the restoration of the BRCA2 ORF, with the deletion of 46 residues. Sequencing of *BRCA2* from patient UK2223 identified an 8-bp deletion in exon 11, 5 bp 3′ to the c.6174delT mutation (Fig. 4), which resulted in the restoration of the BRCA2 ORF, with the loss of three amino acids. A 6-bp direct repeat was associated with the deletion in one of the tumours (UK1999; Fig. 4).

Here we suggest that mutation in *BRCA2* and sensitivity to therapeutics in *BRCA2* mutation carriers can be suppressed by intragenic deletion. Multiple mechanisms have been described for the reversion of mutations in humans, but the size and nature of the deletions we have observed are uncommon[22]. However, a similar phenomenon has been noted in a *PALB2*/*FANCN* mutant cell line[23]. Our observation that variants of BRCA2 lacking a significant fraction of the protein—including putative functionally important domains such as BRC repeats 6–8 and the DBD—are competent in mediating PARP resistance and HR is perhaps surprising. Although these domains are clearly not absolutely required for these functions, their strong evolutionary conservation[11] suggests that they are important and may be involved in processes such as the fine-tuning of DSB repair or in meiosis[24]. The profound sensitivity of BRCA2-deficient cells to PARP inhibitors and platinum salts is probably determined by their defect in error-free repair[15]. It is therefore perhaps ironic that the deletions we observe leading to resistance may also arise because of this same HR deficiency. It remains to be seen whether resistance will arise in patients treated with PARP inhibitors, but these observations suggest a possible route to treatment failure for carriers of the common c.6174delT *BRCA2* mutation.

METHODS SUMMARY

CAPAN1 and BxPC3 cells were obtained from the ATCC. DNA sequencing confirmed the presence of a *BRCA2* c.6174delT mutation in the CAPAN1 cells. Twelve KU0058948-resistant subclones were developed as described in the text and derivation of clones from the parental CAPAN1 cell line was confirmed by DNA profiling (data not shown). The PARP inhibitor KU0058948 (IC_{50} 3.4 nM) was used as described previously[3]. Survival assays were performed over 15 days, and cell viability was assessed either by cell counting or by the use of a Sulforhodamine B colorimetric assay[25]. Chromosomal breakage analysis was performed by arresting cells in metaphase by using colcemid and staining chromosomes with 4,6-diamidino-2-phenylindole (DAPI)[26]. Mutant BRCA2 expression constructs were generated in pcDNA3.1. Assessment of HR was performed with a BRCA2-deficient VC8 hamster cell line harbouring a single stable integration of the DR-GFP HR reporter construct[18]. For patient material, pathology samples were frozen and stored in liquid nitrogen. Tumour cells were dissected from sectioned tissue by laser capture microdissection and DNA extracted by standard methods[27].

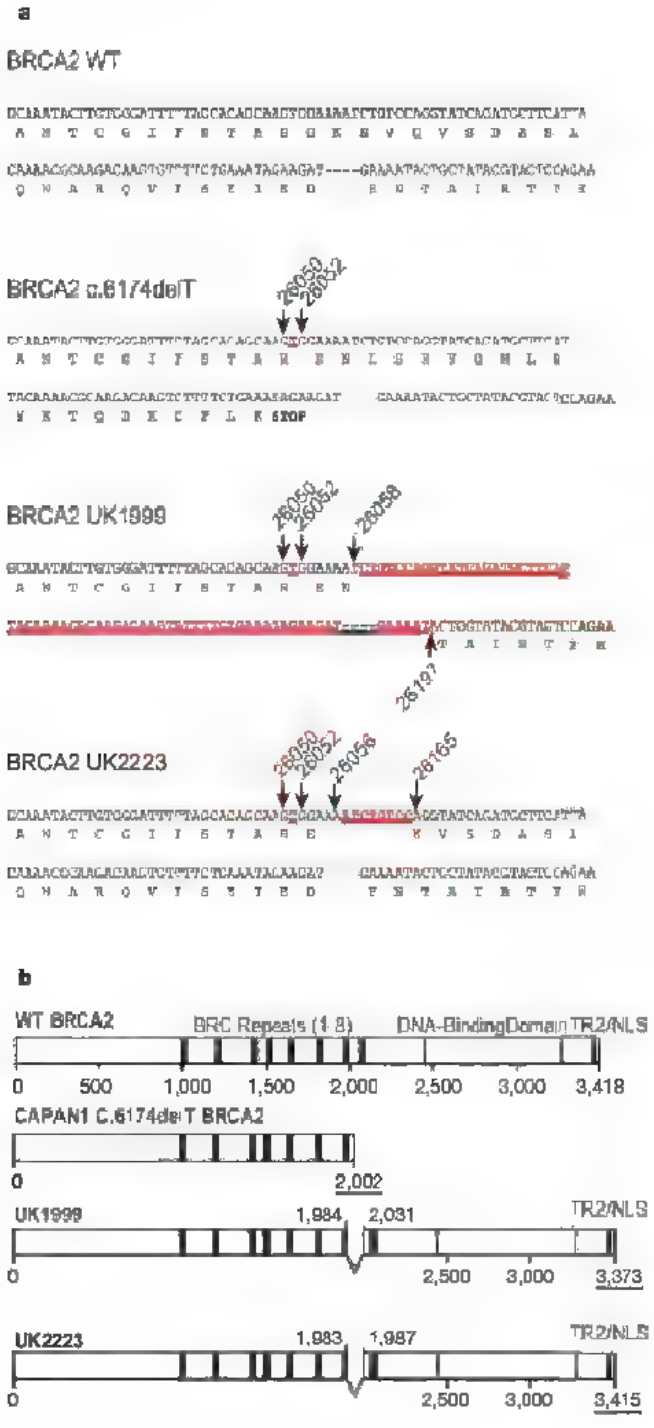

Figure 4 | Identification of BRCA2 ORF-restoring mutations in carboplatin-resistant tumours in BRCA2 c.6174delT mutation carriers. **a**, Part of the *BRCA2* exon 11 sequence from UK1999 and UK2223. Nucleotide sequences are shown above predicted amino acid sequences. For brevity, some of the intervening sequences are noted by dashes. Deletions are shown in red underlined type and flanking nucleotide sequences, based on GenBank accession no. AY436640, are shown. The deletion flanked by nucleotides 26050 and 26052 is c.6174delT. The 137-bp deletion in UK1999 was flanked by two identical 6-bp sequences. **b**, Diagram of new BRCA2 proteins in UK1999 and UK2223, predicted from genomic sequencing of *BRCA2*. The predicted number of amino acids for each new isoform is in bold and underlined. WT, wild type.

Full Methods and any associated references are available in the online version of the paper at www.nature.com/nature.

Received 5 July; accepted 10 December 2007.
Published online 10 February 2008.

1. Farmer, H. *et al.* Targeting the DNA repair defect in *BRCA* mutant cells as a therapeutic strategy. *Nature* 434, 917–921 (2005).
2. Bryant, H. E. *et al.* Specific killing of BRCA2-deficient tumours with inhibitors of poly(ADP-ribose) polymerase. *Nature* 434, 913–917 (2005).
3. Tutt, A. *et al.* Mutation in *Brca2* stimulates error-prone homology-directed repair of DNA double-strand breaks occurring between repeated sequences. *EMBO J.* 20, 4704–4716 (2001).
4. Moynahan, M. E., Pierce, A. J. & Jasin, M. BRCA2 is required for homology-directed repair of chromosomal breaks. *Mol. Cell* 7, 263–272 (2001).
5. Domchek, S. M. & Weber, B. L. Clinical management of *BRCA1* and *BRCA2* mutation carriers. *Oncogene* 25, 5825–5831 (2006).
6. Gudmundsdottir, K. & Ashworth, A. The roles of BRCA1 and BRCA2 and associated proteins in the maintenance of genomic stability. *Oncogene* 25, 5864–5874 (2006).
7. Davies, O. R. & Pellegrini, L. Interaction with the BRCA2 C terminus protects RAD51-DNA filaments from disassembly by BRC repeats. *Nat. Struct. Mol. Biol.* 14, 475–483 (2007).
8. Esashi, F., Galkin, V. E., Yu, X., Egelman, E. H. & West, S. C. Stabilization of RAD51 nucleoprotein filaments by the C-terminal region of BRCA2. *Nat. Struct. Mol. Biol.* 14, 468–474 (2007).
9. Ratnam, K. & Low, J. A. Current development of clinical inhibitors of poly(ADP-ribose) polymerase in oncology. *Clin. Cancer Res.* 13, 1383–1388 (2007).
10. Goggins, M. *et al.* Germline *BRCA2* gene mutations in patients with apparently sporadic pancreatic carcinomas. *Cancer Res.* 56, 5360–5364 (1996).
11. Yang, H. *et al.* BRCA2 function in DNA binding and recombination from a BRCA2–DSS1–ssDNA structure. *Science* 297, 1837–1848 (2002).
12. Spain, B. H., Larson, C. J., Shihabuddin, L. S., Gage, F. H. & Verma, I. M. Truncated BRCA2 is cytoplasmic: implications for cancer-linked mutations. *Proc. Natl Acad. Sci. USA* 96, 13920–13925 (1999).
13. Abaji, C., Cousineau, I. & Belmaaza, A. BRCA2 regulates homologous recombination in response to DNA damage: implications for genome stability and carcinogenesis. *Cancer Res.* 65, 4117–4125 (2005).
14. McCabe, N. *et al.* BRCA2-deficient CAPAN-1 cells are extremely sensitive to the inhibition of poly(ADP-ribose) polymerase: an issue of potency. *Cancer Biol. Ther.* 4, 934–936 (2005).
15. Tutt, A. N. *et al.* Exploiting the DNA repair defect in BRCA mutant cells in the design of new therapeutic strategies for cancer. *Cold Spring Harb. Symp. Quant. Biol.* 70, 139–148 (2005).
16. Furuta, T. *et al.* Phosphorylation of histone H2AX and activation of Mre11, Rad50, and Nbs1 in response to replication-dependent DNA double-strand breaks induced by mammalian DNA topoisomerase I cleavage complexes. *J. Biol. Chem.* 278, 20303–20312 (2003).
17. Weinstock, D. M., Elliott, B. & Jasin, M. A model of oncogenic rearrangements: differences between chromosomal translocation mechanisms and simple double-strand break repair. *Blood* 107, 777–780 (2006).
18. Saeki, H. *et al.* Suppression of the DNA repair defects of BRCA2-deficient cells with heterologous protein fusions. *Proc. Natl Acad. Sci. USA* 103, 8768–8773 (2006).
19. Cass, I. *et al.* Improved survival in women with BRCA-associated ovarian carcinoma. *Cancer* 97, 2187–2195 (2003).
20. Pal, T., Permuth-Wey, J., Kapoor, R., Cantor, A. & Sutphen, R. Improved survival in *BRCA2* carriers with ovarian cancer. *Fam. Cancer* 6, 113–119 (2007).
21. Wang, D. & Lippard, S. J. Cellular processing of platinum anticancer drugs. *Nature Rev. Drug Discov.* 4, 307–320 (2005).
22. Hirschhorn, R. *In vivo* reversion to normal of inherited mutations in humans. *J. Med. Genet.* 40, 721–728 (2003).
23. Xia, B. *et al.* Fanconi anemia is associated with a defect in the BRCA2 partner PALB2. *Nature Genet.* 39, 159–161 (2007).
24. Daniels, M. J., Wang, Y., Lee, M. & Venkitaraman, A. R. Abnormal cytokinesis in cells deficient in the breast cancer susceptibility protein BRCA2. *Science* 306, 876–879 (2004).
25. Vichai, V. & Kirtikara, K. Sulforhodamine B colorimetric assay for cytotoxicity screening. *Nature Protocols* 1, 1112–1116 (2006).
26. Gudmundsdottir, K., Lord, C. J., Witt, E., Tutt, A. N. & Ashworth, A. DSS1 is required for RAD51 focus formation and genomic stability in mammalian cells. *EMBO Rep.* 5, 989–993 (2004).
27. Reis-Filho, J. S. *et al.* Pleomorphic lobular carcinoma of the breast: role of comprehensive molecular pathology in characterization of an entity. *J. Pathol.* 207, 1–13 (2005).

Supplementary Information is linked to the online version of the paper at www.nature.com/nature.

Acknowledgements We thank M. Jasin and N. Staud for providing the VC8-DR-GFP cell line, G. Smith and N. Martin for the provision of KU0058948, and S. Swift, A. Smith and K. Savage for technical support. This work was funded by Breakthrough Breast Cancer and Cancer Research UK. S.-E. is a C. J. Martin Fellow and is supported by the National Health and Medical Research Council of Australia.

Author Information Reprints and permissions information is available at www.nature.com/reprints. The authors declare competing financial interests: details accompany the full-text HTML version of the paper at www.nature.com/nature. Correspondence and requests for materials should be addressed to A.A. (alan.ashworth@icr.ac.uk).

LETTERS

Secondary mutations as a mechanism of cisplatin resistance in *BRCA2*-mutated cancers

Wataru Sakai[1,2], Elizabeth M. Swisher[3,4], Beth Y. Karlan[5], Mukesh K. Agarwal[6], Jake Higgins[4,7], Cynthia Friedman[1], Emily Villegas[1,2], Céline Jacquemont[1,2], Daniel J. Farrugia[6], Fergus J. Couch[6], Nicole Urban[2] & Toshiyasu Taniguchi[1,2]

Ovarian carcinomas with mutations in the tumour suppressor *BRCA2* are particularly sensitive to platinum compounds[1]. However, such carcinomas ultimately develop cisplatin resistance. The mechanism of that resistance is largely unknown[2]. Here we show that acquired resistance to cisplatin can be mediated by secondary intragenic mutations in *BRCA2* that restore the wild-type *BRCA2* reading frame. First, in a cisplatin-resistant *BRCA2*-mutated breast-cancer cell line, HCC1428, a secondary genetic change in *BRCA2* rescued BRCA2 function. Second, cisplatin selection of a *BRCA2*-mutated pancreatic cancer cell line, Capan-1 (refs 3, 4), led to five different secondary mutations that restored the wild-type *BRCA2* reading frame. All clones with secondary mutations were resistant both to cisplatin and to a poly(ADP-ribose) polymerase (PARP) inhibitor (AG14361). Finally, we evaluated recurrent cancers from patients whose primary *BRCA2*-mutated ovarian carcinomas were treated with cisplatin. The recurrent tumour that acquired cisplatin resistance had undergone reversion of its *BRCA2* mutation. Our results suggest that secondary mutations that restore the wild-type *BRCA2* reading frame may be a major clinical mediator of acquired resistance to platinum-based chemotherapy.

Women with ovarian cancer generally have a high initial response to platinum-based chemotherapy, but over time most ovarian carcinomas become refractory, and most patients die with progressive chemoresistant disease[2]. The molecular basis of initial platinum sensitivity and acquired resistance remains largely unknown. Individuals with germline mutations in *BRCA1* or *BRCA2* (*BRCA1/2*) have an increased risk of developing cancer in the breast and ovary[5] as well as in some other organs including the pancreas and prostate[6]. *BRCA2* is identical to the Fanconi anaemia gene *FANCD1*[7]. The BRCA2 protein directly binds to and regulates RAD51, an essential protein for DNA repair through homologous recombination[8]. Tumours from *BRCA1/2* mutation carriers usually have deletion of the wild-type allele at the *BRCA1/2* locus and are BRCA1/2-deficient[9–11]. BRCA1/2-deficient cancer cells are hypersensitive to DNA-crosslinking agents including cisplatin[1,12]. Therefore, cisplatin or its derivative, carboplatin, is a logical choice for the treatment of *BRCA1/2*-mutated tumours[13], and women with *BRCA1/2*-mutated ovarian carcinoma have a better prognosis than those without *BRCA1/2* mutation if they receive platinum-based therapy[4,13]. However, even *BRCA1/2*-mutated tumours eventually develop platinum resistance.

In several genetic disorders such as Fanconi anaemia, spontaneous genetic alterations compensating for inherited disease-causing mutations have been described[16]. These alterations in Fanconi anaemia include secondary genetic changes of one of the mutated Fanconi anaemia alleles, such as back-mutations to wild type, compensatory mutations in *cis*, intragenic crossovers and gene conversion[16–18]. We speculated that secondary mutations in *BRCA2*-mutated alleles might also occur in cancer cells during chemotherapy.

To study the mechanism of acquired cisplatin resistance of *BRCA2*-mutated cancer, first we screened 12 human breast-cancer cell lines for alterations in BRCA2 protein expression (Fig. 1a). A pancreatic cancer cell line, Capan-1 (refs 3, 4), with a truncated BRCA2 protein, was used as a control.

From breast-cancer cell line HCC1428[19], BRCA2 protein was undetectable by western blotting using anti-BRCA2 (Ab-1), which recognizes the middle part of BRCA2 (Fig. 1a); however, it was detectable with anti-BRCA2 (Ab-2), which recognizes the BRCA2 C terminus. The small size of HCC1428 BRCA2 identified by Ab-2 suggested that the protein might have an internal in-frame deletion. Constitutional DNA from a lymphoblast cell line (HCC1428BL) from the same patient had one wild-type *BRCA2* allele and one mutant allele with a frameshift mutation, 6174delT, which is common in the Ashkenazi Jewish population (Fig. 1b and Supplementary Fig. 1)[20].

Sequence of genomic DNA from HCC1428 cancer cells revealed no wild-type allele and a mutant allele with a 2,135-base-pair (bp) deletion surrounding the original 6174delT mutation and the exon 11/intron 11 junction (Fig. 1c and Supplementary Fig. 1). Sequence of complementary DNA (cDNA) indicated that this deletion activated two cryptic splice donor sites in exon 11, resulting in expression of two transcripts with in-frame deletions (Fig. 1d and Supplementary Fig. 1). HCC1428 transcript 1 had a 2,640-bp deletion and encoded a protein lacking amino acids 1401–2281. Transcript 2 had a 2,187-bp deletion and encoded a protein lacking amino acids 1552–2281 (Fig. 1d, e and Supplementary Fig. 1). Both HCC1428 BRCA2 proteins retain the single-strand DNA (ssDNA)-binding domain and the carboxy (C)-terminus nuclear localization signals (NLSs), whereas these domains are lost in *BRCA2.6174delT* (Fig. 1e). A recent report that only one BRC repeat plus ssDNA-binding domain and NLSs are sufficient for BRCA2 function[21] suggests that the novel BRCA2 proteins in HCC1428 might be functional. Indeed, HCC1428 cells were resistant to cisplatin (Fig. 1g). Furthermore, depletion of these novel BRCA2 proteins with short interfering RNA (siRNA) restored sensitivity of HCC1428 cells to cisplatin (Fig. 1f, g).

HCC1428 was derived after chemotherapy from the pleural effusion of a 49-year-old woman with stage IV breast carcinoma who died six months later[19]. We speculate that the patient's chemotherapy selected *in vivo* for secondary mutations in *BRCA2*-mutated breast tumour cells.

To test this hypothesis, we selected *in vitro* for cisplatin-resistant clones from the cisplatin-sensitive *BRCA2*-mutated pancreatic

[1]Division of Human Biology, [2]Division of Public Health Sciences, Fred Hutchinson Cancer Research Center, Seattle, Washington 98109-1024, USA. [3]Department of Obstetrics and Gynecology, [4]Department of Medicine, University of Washington, Seattle, Washington 98195-7720, USA. [5]Cedars-Sinai Medical Center, Women's Cancer Research Institute, Los Angeles, California 90048-1865, USA. [6]Department of Laboratory Medicine and Pathology, Mayo Clinic, Rochester, Minnesota 55905, USA. [7]Department of Genome Sciences, University of Washington, Seattle, Washington 98195-7720, USA

cancer cell line Capan-1. Capan-1 has the mutant allele *BRCA2.6174delT*, but no wild-type allele (Supplementary Fig. 5a)[3,4]. Fluorescence *in situ* hybridization (FISH) revealed that Capan-1 harbours at least two copies of the *BRCA2* gene, indicating duplication of the chromosome 13 with the mutant *BRCA2* gene (Supplementary Fig. 2).

After selection in cisplatin, we obtained 14 cisplatin-resistant Capan-1 clones from twelve million cells (Supplementary Fig. 3 and Supplementary Table 1). Importantly, in 7 of these 14 clones, BRCA2 expression, at close to the length of the wild-type protein, was now detectable (Fig. 2). The other seven cisplatin-resistant clones still lacked BRCA2 protein expression.

In all seven cisplatin-resistant clones with restored, nearly full-length BRCA2 protein expression, we identified additional *BRCA2* mutations that corrected the frameshift caused by the 6174delT mutation (Fig. 2b, Supplementary Figs 4 and 5, and Supplementary Table 1). These secondary genetic changes included a small deletion, insertion and deletion/insertion at sites close to the original mutation, and in-frame deletions surrounding the original mutation site. Interestingly, in each clone we observed both the original mutant *BRCA2.6174delT* sequence and the 6174delT sequence with additional mutations (Supplementary Figs 4 and 5), indicating that the secondary mutations occurred on only one of the duplicated mutant *BRCA2* copies (Supplementary Fig. 5g). None of the seven cisplatin-resistant clones lacking BRCA2 protein expression harboured additional mutations in *BRCA2*.

Next, we assessed the function of the restored BRCA2 proteins in the 14 cisplatin-resistant Capan-1 clones by evaluating RAD51 foci

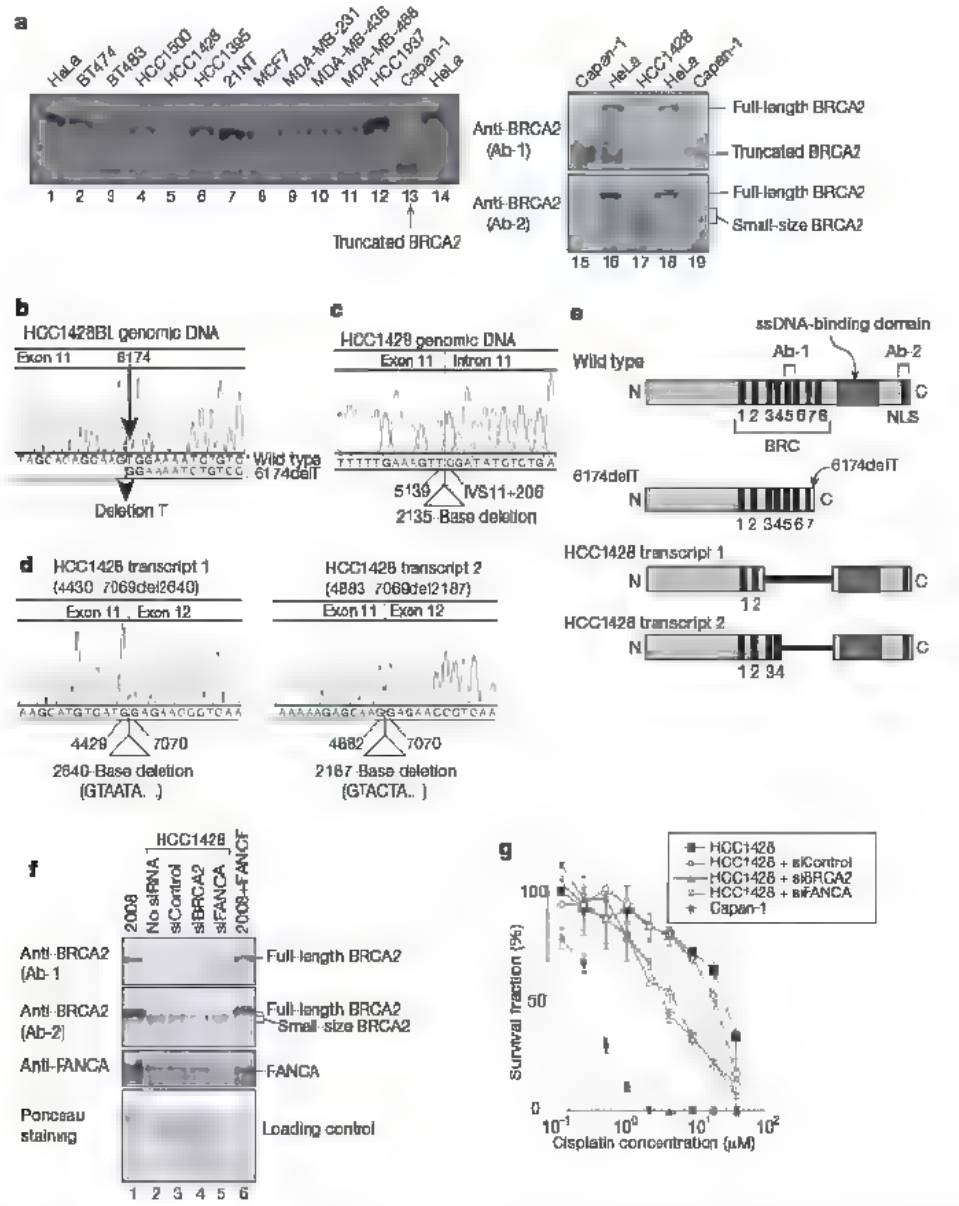

Figure 1 | HCC1428 is a cisplatin-resistant breast-cancer cell line with a secondary *BRCA2* mutation. (Full-length blots are presented in Supplementary Fig. 9.) **a**, Cell lysates from HeLa, Capan-1 and indicated breast-cancer cell lines were immunoblotted with BRCA2 antibodies. **b**, Genomic DNA sequence of *BRCA2* in HCC1428BI lymphoblast. A heterozygous mutation (6174delT) was identified. **c**, Genomic DNA sequence of *BRCA2* in HCC1428 breast-cancer cell line. A homozygous 2,135-bp deletion from nt5140 (in exon 11) to IVS11 + 205 (in intron 11) was identified. **d**, Sequences of the two *BRCA2* transcripts in HCC1428 breast-cancer cell line. The two products of polymerase chain reaction with reverse transcription (RT–PCR) shown in Supplementary Fig. 1b were purified from the gel and sequenced separately. HCC1428 transcripts 1 and 2 had a 2,640-bp deletion (nucleotides 4430–7069) and a 2,187-bp deletion (nucleotides 4883–7069), respectively, suggesting activation of the cryptic splice donor sites in exon11. **e**, Schematic presentation of BRCA2 proteins. The regions that the BRCA2 antibodies (Ab-1 and Ab-2) recognize are also depicted. HCC1428 transcripts 1 and 2 encode BRCA2 lacking 881 amino acids and 730 amino acids, respectively, both of which have ssDNA-binding domains, NLSs and some of the BRC repeats. **f**, Cell lysates from HCC1428 cells treated with indicated siRNA were immunoblotted with BRCA2 and FANCA antibodies. 2008 and 2008 + FANCF were used as controls. **g**, Cisplatin sensitivity assessed by XTT assay. HCC1428 was resistant to cisplatin, and depletion of BRCA2 or FANCA sensitized HCC1428 to cisplatin (mean ± s.e.m., $n = 3$)

formation after exposure to ionizing radiation (Fig. 3a). Ionizing-radiation-induced RAD51 foci formation was impaired in parental Capan-1 (ref. 1). In contrast, in six of the seven cisplatin-resistant Capan-1 clones with restored BRCA2 expression, ionizing-radiation-induced RAD51 foci formation was significantly improved, suggesting that these novel BRCA2 isoforms are functional.

In most of the cisplatin-resistant Capan-1 clones without secondary mutations, ionizing-radiation-induced RAD51 foci formation remained impaired (Fig. 3a), suggesting that these clones acquired cisplatin resistance through mechanisms other than the restoration of the BRCA2-RAD51 pathway.

Next, we analysed the homologous-recombination-based DNA double-strand-break (DSB) repair function of some of the novel BRCA2 proteins by using an I-SceI-dependent DR-GFP reporter assay in BRCA2-deficient V-C8 Chinese hamster cells[22]. The proportions of GFP-positive cells arising through the repair of I-SceI-induced DSB by homologous recombination after transfection of various mutant *BRCA2* constructs were compared (Fig. 3b, Supplementary Fig. 6 and Supplementary Table 2). Transfection of a wild-type *BRCA2* construct resulted in about fivefold more GFP-positive cells compared with transfection of vector control or the *BRCA2.6174delT* mutant. Transfection of constructs with any of the secondary *BRCA2* mutations resulted in GFP-positive frequencies equal to or greater than that of the construct with wild-type *BRCA2*. These results indicate that the novel BRCA2 proteins efficiently promote homologous recombination.

PARP inhibitors selectively kill BRCA1/2-deficient tumour cells[23,24] and are expected to become a therapeutic option for patients with *BRCA1/2*-mutated cancers[13]. However, it remains unclear whether *BRCA1/2*-mutated tumours with acquired cisplatin resistance are sensitive to PARP inhibitors. We tested the sensitivity of cisplatin-resistant Capan-1 clones to a PARP inhibitor (AG14361) (Fig. 3c). Both parental Capan-1 and cisplatin-resistant clones without secondary mutations were sensitive to the PARP inhibitor. In contrast, Capan-1 clones with secondary *BRCA2* mutations were resistant, consistent with the restoration of functional BRCA2 in these clones, although the differences in the sensitivity between parental Capan-1 and these clones were relatively small.

Finally, we analysed tissues of five patients with *BRCA2* mutations and recurrent ovarian carcinomas previously treated with platinum. Three recurrent tumours were clinically refractory to platinum and two were sensitive (Supplementary Table 3). Platinum-refractory tumour UW3548 revealed genetic reversion of *BRCA2.6174delT* (Fig. 4). Evidence for genetic reversion is as follows. Constitutional DNA of this patient was heterozygous for *BRCA2.6174delT* and at two single nucleotide polymorphisms (SNPs). As expected, the microdissected specimen of the recurrent tumour was hemizygous at each SNP reflecting loss of heterozygosity of *BRCA2* in the tumour. However, in the same tumour sample, sequences of both *BRCA2.6174delT* and wild-type *BRCA2* were detected, suggesting that the recurrent tumour had acquired wild-type *BRCA2* by genetic reversion, or back mutation to wild type. We speculate that the appearance of both mutant and wild-type sequences resulted from duplication of the mutant *BRCA2* followed by genetic reversion of one of the duplicates, similar to the situation occurring in Capan-1 clones with secondary mutations (Supplementary Figs 4 and 5). A larger clinical study is warranted to determine the prevalence and clinical significance of *in vivo* secondary mutations in *BRCA2* in human tumours.

The second platinum-refractory relapsed tumour (CS2) presented a complex profile. This patient carried germline mutations in both *BRCA1* and *BRCA2* (Supplementary Fig. 7). The primary ovarian tumour was sensitive to platinum and showed loss of the wild-type *BRCA1* allele and heterozygosity of *BRCA2*, indicating that carcinogenesis was primarily driven by the *BRCA1* mutation. Importantly, the recurrent platinum-refractory tumour had lost the mutant *BRCA2* allele. We speculate that loss of the mutant *BRCA2* allele was the result of selection by chemotherapy and contributed to platinum resistance.

The tumour of a third patient (UW174) recurred five months after her primary chemotherapy, so her tumour is defined as clinically refractory to platinum. No secondary mutation in *BRCA2* was detectable in the tumour specimen of this patient. Recurrent tumours of two other patients (CS9 and CS15) were sensitive to cisplatin. No secondary genetic alterations in *BRCA2* were identified in either of these tumours.

Taken together, our data demonstrate that secondary mutations that correct the frameshift caused by mutated *BRCA2* alleles are a mechanism of acquired resistance to cisplatin (Supplementary Fig. 8). Testing for secondary mutations in platinum-treated *BRCA2*-mutated cancers may be clinically important, because tumours with secondary mutations are likely to be resistant both to cisplatin and PARP inhibitors. Theoretically, it might be possible to re-sensitize these tumours to cisplatin and to PARP inhibitors by treatment with drugs such as proteasome inhibitors that inhibit RAD51 recruitment to sites of DNA repair[25]. In contrast, platinum-resistant *BRCA2*-mutated tumours without secondary *BRCA2* mutations may remain sensitive to PARP inhibitors

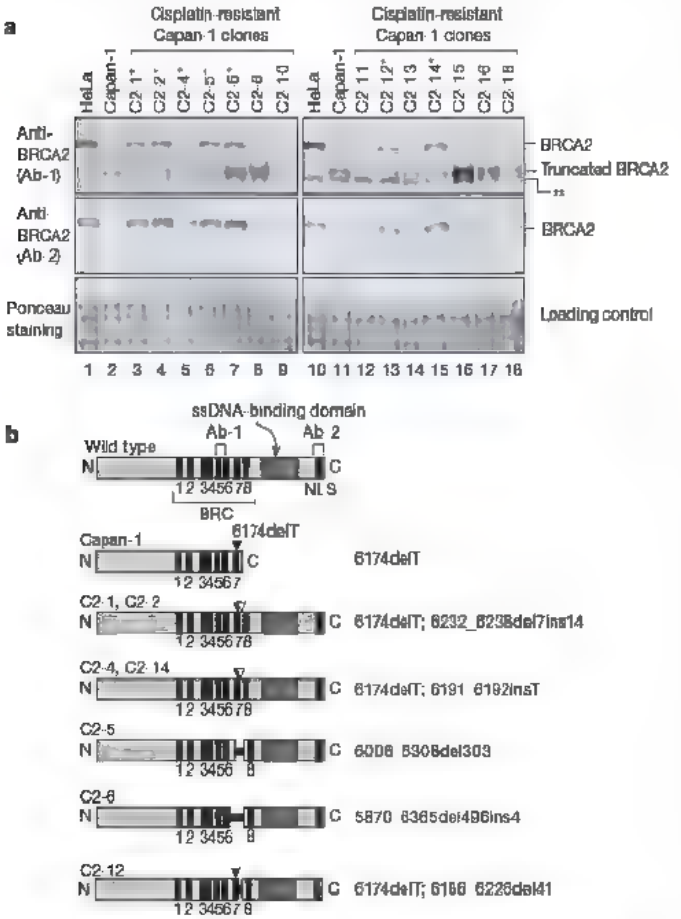

Figure 2 | Secondary genetic changes in mutated *BRCA2* in cisplatin-resistant clones of a pancreatic cancer cell line, Capan-1. (Full-length blots are presented in Supplementary Fig. 9.) **a**, Seven Capan-1 clones indicated with a single asterisk restored apparently full-length BRCA2 protein expression. Cell lysates from indicated cells were immunoblotted with BRCA2 antibodies (Ab-1 and Ab-2). A double asterisk indicates a band presumed to be non-specific. **b**, Schematic presentation of BRCA2 proteins encoded by transcripts in Capan-1 clones. In all of the BRCA2-restored Capan-1 clones, additional genetic changes in exon 11 of *BRCA2* were detected (Supplementary Table 1, and Supplementary Figs 4 and 5). All of these secondary genetic changes (shown as white arrowheads or black horizontal bars) cancel the frameshift caused by the original mutation (6174delT, black arrowheads), and the encoded BRCA2 proteins have intact C-terminal regions containing an ssDNA-binding domain and NLSs.

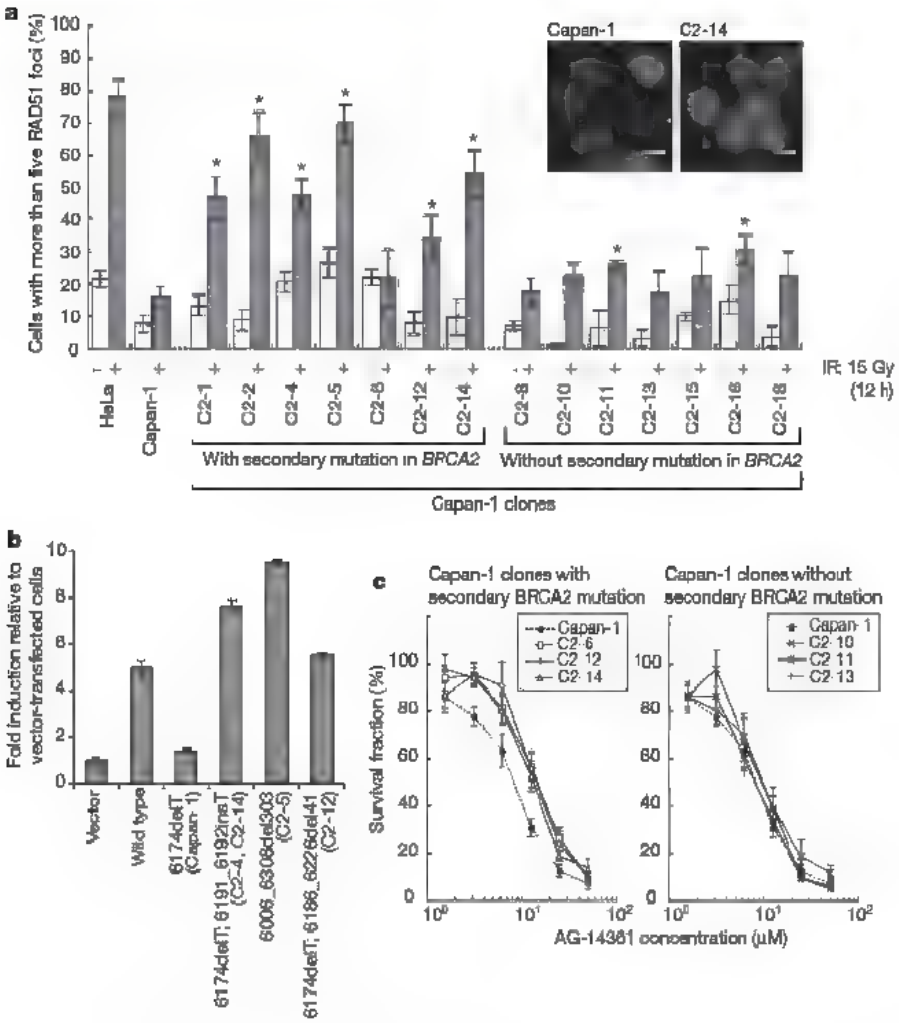

Figure 3 | Functional analyses of the restored BRCA2 proteins. **a**, Ionizing-radiation-induced RAD51 foci formation is restored in most of BRCA2-restored Capan-1 clones. Indicated cells were irradiated (15 Gy) and fixed 12 h after ionizing radiation. Cells were immunostained with RAD51 antibody. Representative pictures of immunostained cells after ionizing radiation are shown, with quantification of the cells with at least five RAD51 foci before (−, white bars) and 12 h after ionizing radiation (+, grey bars) (mean values of at least three independent experiments ± s.e.m.). Asterisks indicate significant difference with irradiated parental Capan-1 cells ($P < 0.05$, unpaired *t*-test). Scale bar, 40 μm. **b**, Quantification of homologous recombination induced by I-SceI in V-C8-DR-GFP cells transiently transfected with wild-type and mutant forms of FLAG-tagged human *BRCA2* cDNA. The proportion of GFP-positive cells for each construct relative to vector control is shown (mean ± s.e.m., $n = 3$). **c**, BRCA2-restored Capan-1 clones are resistant to a PARP inhibitor. Capan-1, its clones with secondary *BRCA2* mutation (C2-6, C2-12 and C2-14) and clones without secondary *BRCA2* mutation (C2-10, C2-11 and C2-13) were treated with a PARP inhibitor (AG-14361) at the indicated concentrations for six days, and survival fraction was measured by XTT assay (mean ± s.e.m., $n = 6$).

Treatment with cisplatin could facilitate secondary mutations by increasing the mutation rate through DNA damaging effects. Alternatively, because BRCA2 is involved in error-free DNA repair, homologous recombination, it is possible that BRCA2 deficiency itself promotes secondary mutations through compensatory use of more error-prone DNA repair processes[26].

Secondary mutations are relevant as a mechanism of resistance only in those tumours that contain frameshift mutations in *BRCA2*, which occurs in only 5% of ovarian carcinomas. However, *BRCA2* mRNA expression is undetectable in 13% of ovarian carcinoma[27]. We speculate that other mechanisms yet to be identified could restore BRCA2 in acquired cisplatin resistance in these sporadic cases.

Our findings may be applicable to cancers other than ovarian. Secondary mutations in *BRCA2* occurred in a mitomycin-C-resistant human acute myeloid leukaemia cell line with bi-allelic *BRCA2* mutations derived from a patient with Fanconi anaemia (D1 subtype)[28] and *BRCA2*-mutated Chinese hamster fibroblast lines[29], suggesting that secondary mutations in *BRCA2* may have a general role in resistance to DNA-crosslinking agents in cells derived from various organs.

Secondary mutation of mutated *BRCA2* is reminiscent of mechanisms of acquired resistance of Philadelphia-chromosome-positive leukaemia to imatinib[30], such as BCR-ABL point mutations that prevent imatinib binding. In both cases, the disease-causing mutations increase tumour sensitivity to specific agents, but development

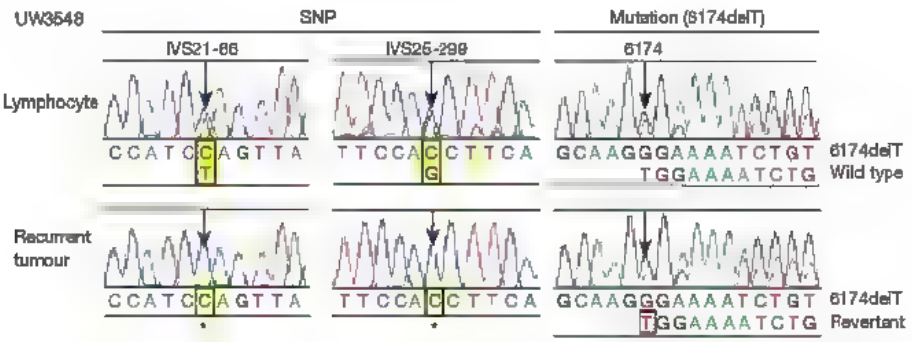

Figure 4 | Genetic reversion of *BRCA2* in platinum-resistant recurrent *BRCA2*-mutated ovarian cancer. DNA sequences of *BRCA2* in peripheral blood lymphocytes and a microdissected specimen of the recurrent tumour from a patient (UW3548) with *BRCA2*-mutated ovarian cancer previously treated with cisplatin. In the lymphocytes, heterozygous SNPs of the *BRCA2* locus (IVS21-66C/T and IVS25-299C/G) were detected, in addition to a heterozygous mutation (6174delT). In the microdissected recurrent tumour specimen, loss of heterozygosity of the SNPs was confirmed, but mixed sequences of 6174delT and wild-type *BRCA2* were detected.

of further mutations in the disease-causing genes during targeted drug treatment leads to drug resistance. It will be important to explore mechanisms for restoring drug sensitivity.

METHODS SUMMARY

HCC1428, Capan-1 and a lymphoblast cell line (HCC1428BL) were purchased from the American Type Culture Collections. Cisplatin-resistant Capan-1 clones were generated by long-term culture in cisplatin (2 μM)-containing medium. Polymerase chain reaction (PCR)-amplified *BRCA2* gene fragments were analysed for sequence alterations with BigDye Terminator version 3.1 Cycle Sequencing Kit (Applied Biosystems). All nucleotide numbers refer to the wild-type cDNA human sequence of *BRCA2* (accession number U43746, version U43746.1 GI, 1161383) and *BRCA1* (U14680.1).

For western blot analysis, anti-BRCA2 Ab-1 (1:100; OP95, EMD Biosciences), anti-BRCA2 Ab-2 (1:100, PC146, EMD Biosciences), and anti-FANCA (1:1000, (#7488) (a gift from M. Hoatlin)) were used. For immunofluorescence microscopy, cells were fixed with 4% paraformaldehyde in PBS for 10 min, followed by permeabilization with 0.25% Triton X-100 in PBS (10 min). A primary antibody (anti-RAD51 (Ab-1) (1:1000, PC130, EMD Biosciences)) and a secondary antibody (Alexa Fluor 488 goat anti-rabbit IgG (H+L) antibody (A-11034, Invitrogen)) were used. Cisplatin sensitivity and PARP inhibitor sensitivity of cells were determined either by crystal violet or XTT (3′-1-phenylaminocarbonyl-3,4-tetrazolium-bis(4-methoxy-6-nitrobenzenesulfonic acid)) assays. A PARP inhibitor, AG14361, was a gift of Pfizer. Expression of targeted genes was knocked down by transient transfection of siRNA directed against *FANCA* (5′-AAGGGTCAAGAGGGAAAAATA-3′), *BRCA2* (5′-AACAACAATTACGAAC-CAAAC-3′) and negative control (5′-AATTCTCCGAACGTGTCACGT-3′). Homologous recombination assay was done as previously described[24]. A BAC clone, RP11-37E23, was used as a probe for FISH on metaphase chromosome preparations of Capan-1 cells. Three DNA samples from patients with ovarian cancer with the *BRCA2* mutation were obtained from Cedars-Sinai Medical Center through the Pacific Ovarian Cancer Research Consortium and two from the tissue bank of the University of Washington. The study was approved by institutional review boards of the Fred Hutchinson Cancer Research Center and the University of Washington.

Full Methods and any associated references are available in the online version of the paper at www.nature.com/nature.

Received 12 July 2007; accepted 3 January 2008.
Published online 10 February 2008.

1. Yuan, S. S. *et al.* BRCA2 is required for ionizing radiation-induced assembly of Rad51 complex *in vivo*. *Cancer Res.* 59, 3547–3551 (1999).
2. Agarwal, R. & Kaye, S. B. Ovarian cancer: strategies for overcoming resistance to chemotherapy. *Nature Rev. Cancer* 3, 502–516 (2003).
3. Goggins, M. *et al.* Germline BRCA2 gene mutations in patients with apparently sporadic pancreatic carcinomas. *Cancer Res.* 56, 5360–5364 (1996).
4. Abbott, D. W., Freeman, M. L. & Holt, J. T. Double-strand break repair deficiency and radiation sensitivity in BRCA2 mutant cancer cells. *J. Natl Cancer Inst.* 90, 978–985 (1998).
5. Li, A. J. & Karlan, B. Y. Genetic factors in ovarian carcinoma. *Curr. Oncol. Rep.* 3, 27–32 (2001).
6. van Asperen, C. J. *et al.* Cancer risks in BRCA2 families: estimates for sites other than breast and ovary. *J. Med. Genet.* 42, 711–719 (2005).
7. Howlett, N. G. *et al.* Biallelic inactivation of BRCA2 in Fanconi anemia. *Science* 297, 606–609 (2002).
8. Moynahan, M. E., Pierce, A. J. & Jasin, M. BRCA2 is required for homology-directed repair of chromosomal breaks. *Mol. Cell* 7, 263–272 (2001).
9. Neuhausen, S. L. & Marshall, C. J. Loss of heterozygosity in familial tumors from three BRCA1-linked kindreds. *Cancer Res.* 54, 6069–6072 (1994).
10. Collins, N. *et al.* Consistent loss of the wild type allele in breast cancers from a family linked to the BRCA2 gene on chromosome 13q12–13. *Oncogene* 10, 1673–1675 (1995).
11. Gudmundsson, J. *et al.* Different tumor types from BRCA2 carriers show wild-type chromosome deletions on 13q12–q13. *Cancer Res.* 55, 4830–4832 (1995).
12. Bhattacharyya, A., Ear, U. S., Koller, B. H., Weichselbaum, R. R. & Bishop, D. K. The breast cancer susceptibility gene BRCA1 is required for subnuclear assembly of Rad51 and survival following treatment with the DNA cross-linking agent cisplatin. *J. Biol. Chem.* 275, 23899–23903 (2000).
13. Tutt, A. N. *et al.* Exploiting the DNA repair defect in BRCA mutant cells in the design of new therapeutic strategies for cancer. *Cold Spring Harb. Symp. Quant. Biol.* 70, 139–148 (2005).
14. Foulkes, W. D. BRCA1 and BRCA2: chemosensitivity, treatment outcomes and prognosis. *Fam. Cancer* 5, 135–142 (2006).
15. Boyd, J. *et al.* Clinicopathologic features of BRCA-linked and sporadic ovarian cancer. *J. Am. Med. Assoc.* 283, 2260–2265 (2000).
16. Hirschhorn, R. *In vivo* reversion to normal of inherited mutations in humans. *J. Med. Genet.* 40, 721–728 (2003).
17. Hamanoue, S. *et al.* Myeloid lineage-selective growth of revertant cells in Fanconi anaemia. *Br. J. Haematol.* 132, 630–635 (2006).
18. Xia, B. *et al.* Fanconi anaemia is associated with a defect in the BRCA2 partner PALB2. *Nature Genet.* 39, 159–161 (2007).
19. Gazdar, A. F. *et al.* Characterization of paired tumor and non-tumor cell lines established from patients with breast cancer. *Int. J. Cancer* 78, 766–774 (1998).
20. Neuhausen, S. *et al.* Recurrent BRCA2 6174delT mutations in Ashkenazi Jewish women affected by breast cancer. *Nature Genet.* 13, 126–128 (1996).
21. Saeki, H. *et al.* Suppression of the DNA repair defects of BRCA2-deficient cells with heterologous protein fusions. *Proc. Natl Acad. Sci. USA* 103, 8768–8773 (2006).
22. Wu, K. *et al.* Functional evaluation and cancer risk assessment of BRCA2 unclassified variants. *Cancer Res.* 65, 417–426 (2005).
23. Farmer, H. *et al.* Targeting the DNA repair defect in BRCA mutant cells as a therapeutic strategy. *Nature* 434, 917–921 (2005).
24. Bryant, H. E. *et al.* Specific killing of BRCA2-deficient tumours with inhibitors of poly(ADP-ribose) polymerase. *Nature* 434, 913–917 (2005).
25. Jacquemont, C. & Taniguchi, T. Proteasome function is required for DNA damage response and fanconi anemia pathway activation. *Cancer Res.* 67, 7395–7405 (2007).
26. Tutt, A. *et al.* Mutation in Brca2 stimulates error-prone homology-directed repair of DNA double-strand breaks occurring between repeated sequences. *EMBO J.* 20, 4704–4716 (2001).
27. Hilton, J. L. *et al.* Inactivation of BRCA1 and BRCA2 in ovarian cancer. *J. Natl. Cancer Inst.* 94, 1396–1406 (2002).
28. Ikeda, H. *et al.* Genetic reversion in an acute myelogenous leukemia cell line from a Fanconi anemia patient with biallelic mutations in BRCA2. *Cancer Res.* 63, 2688–2694 (2003).
29. Wiegant, W. W., Overmeer, R. M., Godthelp, B. C., van Buul, P. P. & Zdzienicka, M. Z. Chinese hamster cell mutant, V-C8, a model for analysis of Brca2 function. *Mutat. Res.* 600, 79–88 (2006).
30. Gorre, M. E. *et al.* Clinical resistance to STI-571 cancer therapy caused by BCR-ABL gene mutation or amplification. *Science* 293, 876–880 (2001).

Supplementary Information is linked to the online version of the paper at www.nature.com/nature.

Acknowledgements We thank M.C. King and C. W. Drescher for discussions, B. Trask for overseeing the FISH analyses in her laboratory and for comments on the manuscript, J. W. Huang for comments on the manuscript, and M. Hoatlin and K. Polyak for reagents. We thank Pfizer for AG14361. We thank the Pacific Ovarian Cancer Research Consortium (supported by a Specialized Program of Research Excellence in Ovarian Cancer) for clinical specimens. This work was supported by grants from the National Institutes of Health/National Cancer Institute (to T.T. and E.M.S.), the Searle Scholars Program, the V Foundation and the Hartwell Innovation Fund (to T.T.), the L&S Milken Foundation (to B.Y.K.), the American Cancer Society California Division-Early Detection Professorship (to B.Y.K.), start-up funds from the Fred Hutchinson Cancer Research Center (to T.T.) and a gift from the Yvonne Betson Trust (to E.M.S.).

Author Contributions W.S. performed most of the experiments. E.M.S., B.Y.K. and N.U. provided clinical samples and expertise on ovarian cancer. E.M.S. performed laser capture microdissection and DNA extractions. M.K.A., D.J.F. and F.J.C. performed homologous recombination assays. J.H. sequenced *BRCA2* in HCC1428. C.F. performed FISH analysis. E.V. performed the siRNA experiments shown in Fig. 1f, g. C.J. performed the PARP inhibitor sensitivity assays in Fig. 3c. T.T., W.S. and E.M.S. wrote the manuscript.

Author Information Reprints and permissions information is available at www.nature.com/reprints. Correspondence and requests for materials should be addressed to T.T. (ttaniguc@fhcrc.org).

LETTERS

Gamete formation without meiosis in *Arabidopsis*

Maruthachalam Ravi[1], Mohan P. A. Marimuthu[1] & Imran Siddiqi[1]

Apomixis, the formation of asexual seeds in plants, leads to populations that are genetically uniform maternal clones. The transfer of apomixis to crop plants holds great promise in plant breeding for fixation of heterozygosity and hybrid vigour because it would allow the propagation of hybrids over successive generations[1,2]. Apomixis involves the production of unreduced (diploid) female gametes that retain the genotype of the parent plant (apomeiosis), followed by parthenogenetic development of the egg cell into an embryo and the formation of functional endosperm[3]. The molecular mechanisms underlying apomixis are unknown. Here we show that mutation of the *Arabidopsis* gene *DYAD/SWITCH1* (*SWI1*)[4,5], a regulator of meiotic chromosome organization, leads to apomeiosis. We found that most fertile ovules in *dyad* plants form seeds that are triploid and that arise from the fertilization of an unreduced female gamete by a haploid male gamete. The unreduced female gametes fully retain parental heterozygosity across the genome, which is characteristic of apomeiosis. Our results show that the alteration of a single gene in a sexual plant can bring about functional apomeiosis, a major component of apomixis.

Apomixis is found in more than 400 species of flowering plants and occurs by three distinct developmental routes[2]. It has been suggested that apomixis results from deregulated expression of the sexual programme[3]; however, the molecular mechanisms controlling apomixis remain undeciphered. One hypothesis is that genes controlling apomixis may be variant alleles of genes that act during normal sexual development[6]. Such genes may be revealed by an analysis of model sexual plants. In *Arabidopsis*, the female gametophyte containing the egg and associated cells develops from one of four haploid megaspores formed by meiotic divisions of a single cell within the ovule, the megasporocyte. *SWI1* is required for sister chromatid cohesion and centromere organization during meiosis. Mutations in *swi1* (Supplementary Fig. 1) cause a single equational division in place of normal female meiosis, followed by arrest in further progression[4,5] (Fig. 1a–d). These defects lead to the production of two diploid cells in place of four haploid megaspores, and failure to form a female gametophyte. The *dyad* allele of *SWI1* causes female specific sterility without affecting pollen development[7]. Although *dyad* plants show sterility, there is variable expressivity and only a few seeds are

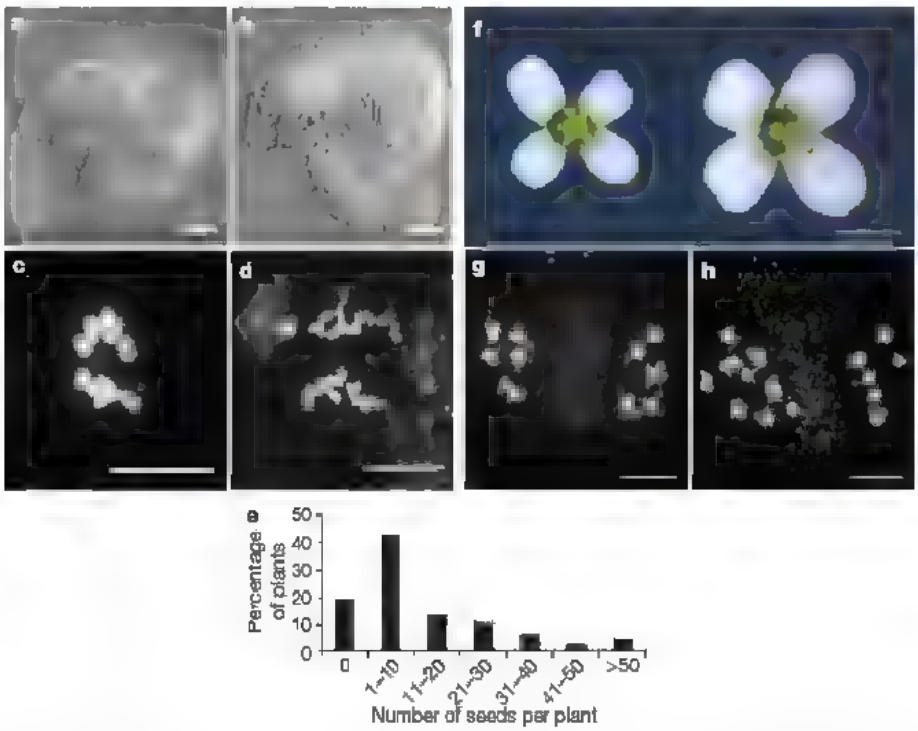

Figure 1 | The *dyad* mutant produces triploid progeny. **a**, Wild-type ovule containing a female gametophyte. **b**, *dyad* ovule showing two arrested cells in place of a female gametophyte. **c**, Wild-type female meiosis anaphase I reductional (5–5) segregation of chromosomes. **d**, *dyad* female meiosis anaphase I equational (10–10) separation of chromosomes. **e**, Reduced seed set in *dyad* plants the mode is 1–10 seeds per plant, whereas wild-type plants produce more than 2,000 seeds. The frequency of functional female gamete formation in *dyad* is about 0.24% (Supplementary Notes). **f**, A flower from progeny of a self-fertilized *dyad* plant (right) is larger than a flower from a *dyad* F_2 segregant (left) **g**, **h**, Male meiocyte at the end of meiosis I from a diploid *dyad* plant showing 5–5 segregation of chromosomes (**g**), and a triploid *dyad* plant showing 9–6 segregation (**h**) Scale bars, 20 μm (**a**, **b**), 10 μm (**c**, **d**, **g**, **h**); 2 mm (**f**)

[1]Centre for Cellular and Molecular Biology Uppal Road, Hyderabad 500007, India.

produced, the modal range being one to ten seeds per plant (Fig. 1e). We found that seeds obtained from a pool of *dyad* plants germinated efficiently (89%; $n = 296$) and grew into plants that showed normal vegetative growth. However, a majority of plants examined (80%; $n = 52$) showed large flowers compared with both the wild type and the *dyad* parent (Fig. 1f). A possible reason for greater floral size was higher ploidy, which results in an increased size of floral structures including pollen grains[8]. Pollen from progeny of *dyad* plants was heterogeneous in size, indicative of differences in ploidy (Supplementary Fig. 2). To determine the ploidy of *dyad* progeny, we performed chromosome counts on 19 randomly chosen plants and found that 17 were triploid (Fig. 1h) and 2 were diploid. Diploid *dyad* plants therefore produce triploid progeny with incomplete penetrance. The formation of triploids in *dyad* does not reflect a background level that is present in the wild type, because we did not detect any triploids among more than 7,000 wild-type plants (Supplementary Notes). We therefore examined the mechanism by which triploids arise.

Triploids can form by fusion of an unreduced ($2n$) gamete with a haploid gamete or by polyspermy. Equational division of the female meiocyte in *dyad*[8] indicated the likelihood of fertilization of unreduced female gametes by haploid male gametes. In this case, the triploid seeds would carry an excess contribution from the maternal genome. Experiments that alter the relative dosage of the maternal and paternal genomes by crosses between diploid and tetraploid plants have shown that an excess maternal genome reduces seed size, whereas an excess paternal genome causes increase in seed size. These findings have been interpreted according to theories of parental conflict or differential dosage[9,10]. To address the origin of triploid seeds in *dyad* we examined seed size (Fig. 2). Seeds produced by *dyad* fell into three categories: shrunken (44%), normal (27%) and large (29%) ($n = 1{,}131$; Fig. 2e). To determine the ploidy of seeds in each category, we performed chromosome counts on all the progeny ($n = 119$) from a set of *dyad* plants. Most shrunken and normal seeds were triploid, whereas most large seeds were diploid (Fig. 2f). To compare seeds from *dyad* with maternal and paternal excess triploid seeds, we performed reciprocal crosses between wild-type diploid and tetraploid *Arabidopsis* and measured seed weight. The seed weight of shrunken seeds from *dyad* (13.7 μg) was similar to that for the maternal excess triploids (13.0 μg) and less than that for the paternal excess triploids, which weighed more than twice as much (32.0 μg). Because the largest class of seeds from *dyad* is shrunken and triploid, our observations suggest that these seeds arise from an excess maternal genome contribution.

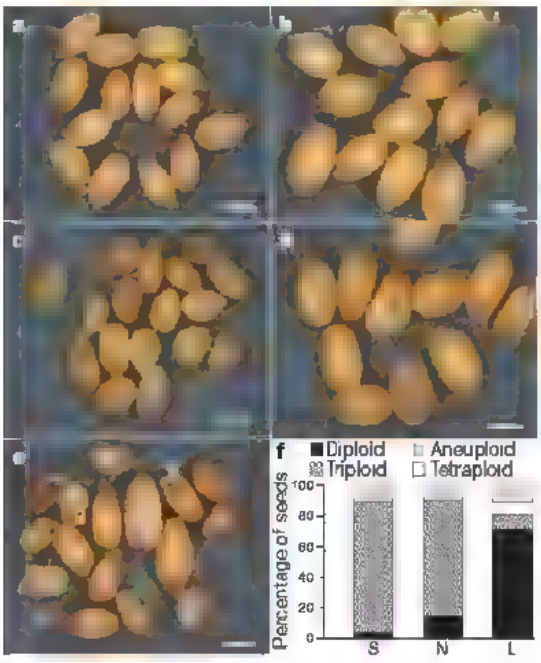

Figure 2 | Triploids arise from a maternal excess contribution. **a**, Wild-type diploid seeds (21.3 μg) **b**, Tetraploid seeds (33 μg) **c**, Maternal excess seeds from a tetraploid female × diploid male cross (13 μg) **d**, Paternal excess seeds from a wild-type diploid female × tetraploid male cross (32 μg) **e**, Heterogeneous seeds obtained from a diploid *dyad* mutant plant: L, large (33.5 μg); N, normal (20.2 μg); S, shrunken (13.7 μg) **f**, Proportion of different ploidy types in progeny of *dyad* mutant plants from each category of seeds. Shrunken (S), $n = 48$, normal (N), $n = 35$; large (L), $n = 36$. Values in parentheses for **a**–**e** indicate single-seed weights. Scale bars, 0.3 mm.

To determine parental contributions in the triploids directly, we performed a three-way cross between *dyad*, a marker line ET60 carrying a single copy of a kanamycin resistance gene (Kan^R), and a wild-type strain. We first crossed *dyad* as a female parent with ET60 and obtained five seeds from 360 crosses. The five F_1 plants were analysed for ploidy and also crossed to the wild type. Segregation of Kan^R:Kan^S in the second cross followed a 1:1 ratio diagnostic of a simplex condition (K– –) for the Kan^R marker in the parent, demonstrating that the plants arose from fertilization of an unreduced female gametophyte by a haploid pollen and did not occur as a result of an unreduced male gametophyte or polyspermy (Table 1).

Several mechanisms can give rise to unreduced gametes in sexual plants, but most do not result in the full retention of parental heterozygosity[11]. Complete retention of parental heterozygosity in the unreduced female gametes defines apomeiosis. *dyad*, like other mutants that show unreduced female gamete formation[12–14], is incompletely penetrant and produces both reduced and unreduced gametes. In all mutants that have been examined, loss of parental alleles in the unreduced gametes occurs, to different extents[12,15–17]. To determine whether unreduced female gametes in *dyad* retain parental genotype we examined progeny from *dyad* for loss of parental heterozygosity. We crossed *dyad* in the Columbia genetic background to a wild-type Nossen strain and genotyped F_2 mutant plants for five polymorphic microsatellite markers distributed over four chromosomes. Seeds collected from 52 F_2 plants were grown to give F_3 plants, and each F_3 plant was genotyped for those markers for which the F_2 parent was heterozygous. Out of 262 plants, 52 had lost heterozygosity for at least one marker (Table 2). The ploidy of 41 of these 52 plants was determined; 40/41 were diploid, whereas 1 was hyperdiploid with 13 chromosomes. Loss of heterozygosity therefore occurred almost exclusively in diploids. A marker unlinked to the centromere would be expected to show loss of heterozygosity in 16.7% of triploid plants at normal levels of recombination. Failure to detect loss of heterozygosity in triploids indicates the complete absence of recombination in unreduced gametes and further rules out polyspermy and post-meiotic doubling as mechanisms for their formation. These results clearly show that triploids arise from the fertilization of an apomeiotic female gamete. The proportion of *dyad* progeny arising from apomeiosis is 63%.

Loss of heterozygosity in diploid progeny of *dyad* shows that they form by the sexual union of haploid gametes rather than by the parthenogenesis of a diploid egg cell. Thus, both reduced and

Table 1 | Triploids arise from an unreduced female gamete

Plant no.	Ploidy of ♀ parent	Kan^R:Kan^S	χ^2 (1:1)
1	$3n$	254:236	0.660
2	$3n + 1$	61:52	0.717
3	$3n$	121:132	0.478
4	$3n + 2$	112:94	1.573
5	$3n + 1$	107:86	2.285

Segregation of kanamycin resistance after germination of seeds obtained from the three-way cross (*dyad* ♀ × ET60 (Kan^R)♂) ♀ × wild-type (Kan^S)♂. Five seeds from a cross of *dyad* ♀ × ET60 (Kan^R)♂ were obtained. Two were triploid ($2n = 15$) and three were hypertriploid (16–17 chromosomes). The five plants were crossed to the wild type. A 1:1 segregation for Kan^R:Kan^S indicates that the Kan^R determinant is present in the simplex condition (K– –) in the ♀ parent, which would be the case only if the triploid parent were formed from an unreduced female gamete in the first cross. In each case, $P(\chi^2) > 0.1$ for a 1:1 model and $P(\chi^2) < 0.005$ for a 5:1 model predicted for a duplex condition (KK–). The duplex control cross (KK ♀ × wild-type (Kan^S)♂ segregated 126:31 Kan^R:Kan^S, for which $P(\chi^2) > 0.25$ for a 5:1 model and $P(\chi^2) < 0.005$ for a 1:1 model.

Table 2 | Retention of marker heterozygosity in triploid progenies of *dyad*

Marker	Chromosome number	Centromere distance (cM)	No. of plants	No. of homozygotes*
nga168	2	58	185	22 (12)
nga6	3	37	108	7 (6.5)
nga162	3	29	74	8 (11)
nga1107	4	76	107	11 (10)
nga225	5	56	169	20 (12)

* Numbers in parentheses show the percentage homozygosity observed for a given marker. No homozygous triploids were obtained. A subset of plants ($n = 65$) that had not lost heterozygosity for any of the five markers were analysed and found to be 78% triploids, 11% diploids and 11% aneuploids.

unreduced embryo sacs coexist in the same plant (in two F_3 families analysed, comprising 44 and 22 sibs, there were 17 and 6 diploids, and 23 and 13 triploids, respectively), a feature that is characteristic of facultative apomicts. Apart from producing apomictic and sexual seeds, apomicts are capable of giving rare 3*n* and 4*n* seeds, as well as aneuploids arising from the mis-segregation of chromosomes[18,19]. The range of ploidy in *dyad* progeny (Fig. 2f) therefore resembles that observed in natural apomictic species.

A likely origin of the apomeiotic embryo sac in *dyad* is one of the diploid cells formed after equational division of the megasporocyte. To assess the developmental potential of the division products of the megasporocyte, we examined expression of the FM1 marker, which is expressed first in the functional megaspore (but not in degenerating megaspores) as well as in the developing female gametophyte[20]. FM1 expression was detected in *dyad* ovules after megasporocyte division, at a frequency that was comparable to that in the wild type (67% ($n = 106$) and 93% ($n = 150$), respectively). Expression was restricted to the lower (chalazal) cell of the dyad, as is observed for the functional megaspore in the wild type (Fig. 3). It is therefore likely that the apomeiotic embryo sacs arise from this cell, as occurs in diplospory[3]. However, because the frequency of seed formation is low, we cannot exclude alternative mechanisms. The low frequency of functional female gamete formation in *dyad* is likely to be at least partly due to the triggering of checkpoint mechanisms that block progression through the meiotic cell cycle[5].

The discovery of apomeiotic female gamete formation in the *dyad* mutant of *Arabidopsis* demonstrates that alteration of a gene that is directly involved in meiotic chromosome organization can confer apomeiosis. Mapping experiments in the apomictic species *Tripsacum dactyloides* indicate that a marker that is linked to apomixis is syntenic to a region in maize that contains the *AMEIOTIC1* (*AM1*) gene[21]. *AM1* has recently been proposed to be a functional homologue of *SWI1* (ref. 22). Thus, *SWI1* homologues may have a function in apomixis in nature. Whereas a strong *swi1* allele causes both male and female sterility[4], the *dyad* allele, which is predicted to form a truncated protein[5], is of intermediate strength. The phenotype of *dyad* most closely resembles natural apomicts, in that the alteration in sporogenesis leading to apomeiosis is biased towards the female side. Hence, female specificity in this case is due to a partial reduction in activity and not to a complete loss of function. Quantitative rather than binary changes in gene activity may be a wider feature of genetic mechanisms controlling apomixis, as has recently been found for the evolution of autogamy in tomato[23].

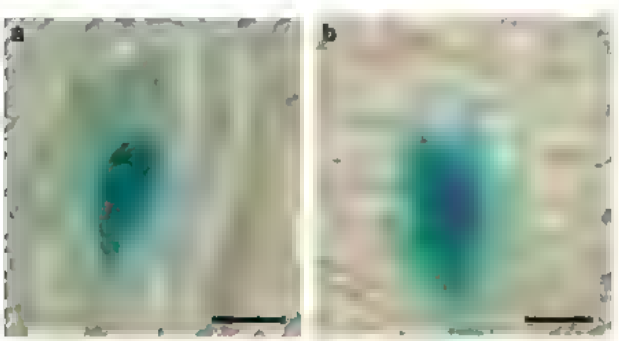

Figure 3 | *dyad* ovules express a functional megaspore marker. **a**, Functional-megaspore-specific GUS expression driven by the FM1 promoter in a wild-type ovule. **b**, FM1-promoter-driven GUS expression specific to the chalazal (lower) cell of the dyad in a *dyad* ovule. Black dots outline the two cells of the dyad for clarity. Scale bars, 10 μm

Attempts to introgress apomixis from natural apomicts into crop species have failed[2], and efforts to identify apomixis genes in natural apomicts by map-based cloning have been hampered by the finding that apomixis is associated with large genomic regions that are repressed for recombination[24–27]. The difficulties involved in the genetic analysis of natural apomicts have motivated alternative approaches towards understanding and ultimately engineering apomixis by the analysis of genes that control meiosis, gametogenesis and seed development in sexual plants[2]. The *fertilization independent seed* (*FIS*) class genes act as regulators of cell division and proliferation in the female gametophyte and the developing seed, and encode members of the Polycomb group of proteins[3]. *fis* class mutants show spontaneous initiation of endosperm development, and, in *msi1*, spontaneous division of the egg cell[3,28]. However, these structures abort early in development and do not lead to the formation of viable seeds. Here we have shown that mutation of *SWI1* leads to the formation of functional apomeiotic female gametes. Our results demonstrate the occurrence of apomeiosis, a major component of apomixis, by mutation of a single gene whose molecular identity is known. The findings represent a significant step towards the synthesis of apomixis by the manipulation of genes that function in normal sexual development.

METHODS SUMMARY

Plant material and growth conditions. Wild-type *Arabidopsis* strains were Col-0 and No-0. The *dyad* mutant was maintained as an F_2 segregating population in the Col-0 background. The tetraploid *Arabidopsis* strain CS3900, which is quadruplex for Kan^R (KKKK), was obtained from the Arabidopsis Biological Resource Centre (ABRC). The ET60 enhancer trap line contains a single-copy *Ds* transposon[29] in the gene At1g73160. Plants were grown at 21 °C in a growth chamber under a 16-h/8-h light/dark cycle. For growth under sterile conditions, seeds were surface sterilized with ethanol and plated on MS medium supplemented with the appropriate antibiotic.

Analysis of ovule and seed phenotypes. Whole-mount analysis of cleared ovules was as described previously[7]. Ploidy was determined by the analysis of male meiotic chromosomes[30]. Female meiosis was analysed as described previously[5]. Seeds were classified and sorted according to size by observation under a stereomicroscope. Seed weight was estimated by weighing two sets of 100 seeds in a fine microbalance (Sartorius) and calculating the average weight of a single seed.

Microsatellite marker analysis. DNA isolation and simple sequence length polymorphism (SSLP) marker analysis was performed as described previously[5]. The *dyad* (Col-0) and No-0 parental strains were screened for polymorphisms on the basis of known differences between the two ecotypes (www.arabidopsis.org) and a set of five markers was selected.

Generation and analysis of transgenic plants. The *proFM1::uidA* fusion was constructed as described in an earlier study[20]. The construct was introduced into heterozygous *dyad*/+ plants by *Agrobacterium*-mediated transformation *in planta*[5]. Wild-type and *dyad* mutant plants were identified among primary transformants. Staining of ovules in GUS staining solution was as described previously[20], using an incubation time of two days. Images were observed on a Zeiss Axioplan 2 microscope equipped with differential interference contrast optics using 40× or 100× Apochromat objectives, and captured on an Axiocam HRC charge-coupled device camera.

Full Methods and any associated references are available in the online version of the paper at www.nature.com/nature.

Received 15 October; accepted 20 December 2007
Published online 13 February 2008.

1. Koltunow, A. M., Bicknell, R. A. & Chaudhury, A. M. Apomixis: molecular strategies for the generation of genetically identical seeds without fertilization. *Plant Physiol.* 108, 1345–1352 (1995).
2. Spillane, C., Steimer, A. & Grossniklaus, U. Apomixis in agriculture: the quest for clonal seeds. *Sex. Plant Reprod.* 14, 179–187 (2001).
3. Koltunow, A. M. & Grossniklaus, U. Apomixis: a developmental perspective. *Annu. Rev. Plant Biol.* 54, 547–574 (2003).

4. Mercier, R. *et al.* SWITCH1 (SWI1): a novel protein required for the establishment of sister chromatid cohesion and for bivalent formation at meiosis. *Genes Dev.* 15, 1859–1871 (2001).
5. Agashe, B., Prasad, C. K. & Siddiqi, I. Identification and analysis of *DYAD*: a gene required for meiotic chromosome organisation and female meiotic progression in *Arabidopsis*. *Development* 129, 3935–3943 (2002).
6. Mogie, M. A model for the evolution and control of generative apomixis. *Biol. J. Linn. Soc.* 35, 127–154 (1988).
7. Siddiqi, I., Ganesh, G., Grossniklaus, U. & Subbiah, V. The *dyad* gene is required for progression through female meiosis in *Arabidopsis*. *Development* 127, 197–207 (2000).
8. Altmann, T. *et al.* Easy determination of ploidy level in *Arabidopsis thaliana* plants by means of pollen size measurement. *Plant Cell Rep.* 13, 652–656 (1994).
9. Dilkes, B. P. & Comai, L. A. Differential dosage hypothesis for parental effects in seed development. *Plant Cell* 16, 3174–3180 (2004).
10. Spielman, M., Vinkenoog, R., Dickinson, H. G. & Scott, R. J. The epigenetic basis of gender in flowering plants and mammals. *Trends Genet.* 17, 705–711 (2001).
11. Bretagnolle, F. & Thompson, J. D. Gametes with the somatic chromosome number: mechanisms of their formation and role in the evolution of autopolyploid plants. *New Phytol.* 129, 1–22 (1995).
12. Rhoades, M. M. & Dempsey, E. Induction of chromosome doubling at meiosis by the *elongate* gene in maize. *Genetics* 54, 505–522 (1966).
13. Finch, R. A. & Bennet, M. D. Action of *triploid inducer* (*tri*) on meiosis in barley (*Hordeum vulgare* L.). *Hereditas* 43, 87–93 (1979).
14. Curtis, C. A. & Doyle, D. G. Production of aneuploid and diploid eggs by meiotic mutants of maize. *J. Hered.* 83, 335–341 (1992).
15. Douches, D. S. & Quiros, C. F. Genetic strategies to determine the mode of *2n* egg formation in diploid potatoes. *Euphytica* 38, 247–260 (1988).
16. Barone, A., Gebhardt, C. & Frusciante, L. Heterozygosity in *2n* gametes of potato evaluated by RFLP markers. *Theor. Appl. Genet.* 91, 98–104 (1995).
17. Vorsa, L. & Rowland, L. J. Estimation of *2n* megagametophyte heterozygosity in a diploid blueberry (*Vaccinium darrowi* Camp) clone using RAPDs. *J. Hered.* 8, 423–426 (1997).
18. Noyes, R. D. Inheritance of apomeiosis (diplospory) in fleabanes (*Erigeron*, *Asteraceae*). *Heredity* 94, 193–198 (2005).
19. Savidan, Y. H. Apomixis: genetics and breeding. *Plant Breed. Rev.* 18, 13–86 (2000).
20. Huanca-Mamani, W., Garcia-Aguilar, M., Leon-Martinez, G., Grossniklaus, U. & Vielle-Calzada, J. P. CHR11, a chromatin-remodeling factor essential for nuclear proliferation during female gametogenesis in *Arabidopsis thaliana*. *Proc. Natl Acad. Sci. USA* 102, 17231–17236 (2005).
21. Blakey, C. A., Goldman, S. L. & Dewald, C. L. Apomixis in *Tripsacum*: Comparative mapping of a multigene phenomenon. *Genome* 44, 222–230 (2001).
22. Hamant, O., Ma, H. & Cande, W. Z. Genetics of meiotic prophase I in plants. *Annu. Rev. Plant Biol.* 57, 267–302 (2006).
23. Chen, K. Y., Cong, B., Wing, R., Vrebalov, J. & Tanksley, S. D. Changes in regulation of a transcription factor lead to autogamy in cultivated tomatoes. *Science* 318, 643–645 (2007).
24. Ozias-Akins, P., Roche, D. & Hanna, W. W. Tight clustering and hemizygosity of apomixis-linked molecular markers in *Pennisetum squamulatum* implies genetic control of apospory by a divergent locus that may have no allelic form in sexual genotypes. *Proc. Natl Acad. Sci. USA* 95, 5127–5132 (1998).
25. Pessino, S. C. *et al.* A genetic map of the apospory-region in *Brachiaria* hybrids: Identification of two markers closely associated with the trait. *Hereditas* 128, 153–158 (1998).
26. Grimanelli, D. *et al.* Mapping diplosporous apomixis in tetraploid *Tripsacum*: one gene or several genes? *Heredity* 80, 33–39 (1998).
27. Pupilli, F. *et al.* Comparative mapping reveals partial conservation of synteny at the apomixis locus in *Paspalum spp.* *Mol. Genet. Genomics* 270, 539–548 (2004).
28. Guitton, A. E. & Berger, F. Loss of function *MULTICOPY SUPPRESSOR OF IRA1* produces nonviable parthenogenetic embryos in *Arabidopsis*. *Curr. Biol.* 15, 750–754 (2005).
29. Sundaresan, V. *et al.* Patterns of gene action in plant development revealed by enhancer trap and gene trap transposable elements. *Genes Dev.* 9, 1797–1810 (1995).
30. Ross, K. J., Fransz, P. & Jones, G. H. A light microscopic atlas of meiosis in *Arabidopsis thaliana*. *Chromosome Res.* 4, 507–516 (1996).

Supplementary Information is linked to the online version of the paper at www.nature.com/nature.

Acknowledgements We thank V. Vijaybhaskar and V. Subbiah for characterization of the ET60 transposon line, S. Andreuzza, J. Dhawan, S. Mayor, B. Nishal, M. Ramaswami, A. Ray and O. Siddiqi for comments on the manuscript; and the ABRC for seeds. This work was supported by the Council for Scientific and Industrial Research (CSIR, Government of India), and a Centre of Excellence grant from the Department of Biotechnology (to I.S.). M.R. and M.M. were supported by fellowships from the University Grants Commission and the CSIR, respectively.

Author Contributions M.P.M. conducted the experiments on marker gene expression and interpreted the results. M.R. and I.S. planned, and M.R. performed, the remaining experiments and interpreted the results. I.S. wrote the paper with input from M.R.

Author Information Reprints and permissions information is available at www.nature.com/reprints. Correspondence and requests for materials should be addressed to I.S. (imran@ccmb.res.in).

LETTERS

Regulation of progenitor cell proliferation and granulocyte function by microRNA-223

Jonathan B. Johnnidis[1], Marian H. Harris[2], Robert T. Wheeler[1], Sandra Stehling-Sun[1], Michael H. Lam[1], Oktay Kirak[1], Thijn R. Brummelkamp[1], Mark D. Fleming[2] & Fernando D. Camargo[1]

MicroRNAs are abundant in animal genomes and have been predicted to have important roles in a broad range of gene expression programmes[1,2]. Despite this prominence, there is a dearth of functional knowledge regarding individual mammalian microRNAs. Using a loss-of-function allele in mice, we report here that the myeloid-specific microRNA-223 (miR-223) negatively regulates progenitor proliferation and granulocyte differentiation and activation. *miR-223* (also called *Mirn223*) mutant mice have an expanded granulocytic compartment resulting from a cell-autonomous increase in the number of granulocyte progenitors. We show that *Mef2c*, a transcription factor that promotes myeloid progenitor proliferation, is a target of miR-223, and that genetic ablation of *Mef2c* suppresses progenitor expansion and corrects the neutrophilic phenotype in *miR-223* null mice. In addition, granulocytes lacking miR-223 are hypermature, hypersensitive to activating stimuli and display increased fungicidal activity. As a consequence of this neutrophil hyperactivity, *miR-223* mutant mice spontaneously develop inflammatory lung pathology and exhibit exaggerated tissue destruction after endotoxin challenge. Our data support a model in which miR-223 acts as a fine-tuner of granulocyte production and the inflammatory response.

MicroRNA-223 (miR-223) was first identified bioinformatically and subsequently characterized in the haematopoietic system, where it is specifically expressed in the myeloid compartment[3,4]. To dissect fully the role of miR-223 in haematopoietic differentiation, we first evaluated its expression throughout myeloid development in highly purified cell populations from bone marrow and peripheral blood. Expression of mature miR-223 was detected at low levels in pluripotent haematopoietic stem cells and common myeloid progenitors (Fig. 1a). As granulocytic differentiation proceeds through granulocyte–monocyte progenitors, immature bone-marrow neutrophils and subsequently mature peripheral blood granulocytes, expression of miR-223 steadily increases. Conversely, as granulocyte–monocyte progenitors adopt the alternative monocytic fate, miR-223 levels are repressed (Fig. 1a). These data demonstrate a highly lineage-specific pattern of expression for miR-223,

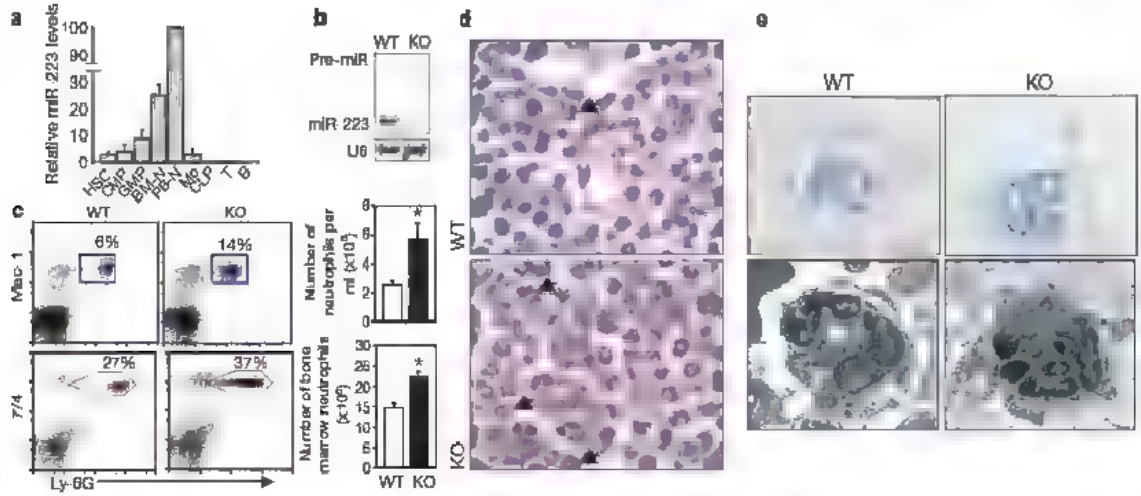

Figure 1 | Phenotypic characterization of *miR-223*$^{-/Y}$ mice. a, Quantitative PCR analysis of miR-223 expression during haematopoietic development (mean ± s.d., $n = 3$). B, B cells; BM-N, bone marrow neutrophils; CLP, common lymphoid progenitor; CMP, common myeloid progenitors; GMP, granulocyte–monocyte progenitors; HSC, haematopoietic stem cells; Mo, monocytes; PB-N, peripheral blood neutrophils; T, T cells. **b,** Northern blot analysis for the detection of miR-223 transcripts in bone marrow neutrophils from wild type (WT) and *miR-223* mutant mice (*miR-223* $^{-/Y}$, KO). **c,** Representative FACS analysis of peripheral blood (upper panel) and bone marrow (lower panel). Neutrophils are Mac1$^+$ Ly-6G$^+$ or 7/4$^+$ Ly-6G$^+$. Note the relative decrease in Ly-6G and Mac-1 expression in peripheral blood granulocytes and increase in 7/4 expression in mutant bone marrow cells. Total numbers of neutrophils are represented in bar graphs. Values represent mean ± s.e.m., $n = 11$ mice of each genotype. Asterisk, $P < 0.001$ (Student's *t*-test). **d,** Control and mutant bone marrow stained with haematoxylin and eosin. Note the marked neutrophil hyperplasia (some neutrophils are denoted with arrows) in the mutant section (original magnification, ×40). **e,** Morphological analysis of peripheral blood neutrophils. May–Grünwald Giemsa stain (top panel; original magnification, ×100) and transmission electron micrograph (bottom panel, original magnification, ×890). Note the marked nuclear hypersegmentation of *miR-223*-deficient neutrophils.

[1]Whitehead Institute for Biomedical Research, Cambridge, Massachusetts 02142, USA. [2]Department of Pathology, Children's Hospital, Harvard Medical School, Boston, Massachusetts 02115, USA

the expression of which continuously increases with differentiation, and suggested to us that miR-223 might be important for both granulocyte development and mature homeostasis.

To test this hypothesis, and to assess further the function of miR-223 in an *in vivo* context, we engineered a loss-of-function allele by excising the *miR-223* gene (Supplementary Fig. 1). The *miR-223* locus is located on the X chromosome and is transcribed independently of any known genes[5,6]. Northern blot analysis of granulocyte RNA revealed a complete absence of miR-223 in the granulocytes of hemizygous *miR-223*$^{-/Y}$ mice (Fig. 1b). *miR-223*-deficient mice were born at normal mendelian ratios, were fertile and displayed no gross abnormalities. Unexpectedly, complete and differential blood counts revealed a significant increase in the number of circulating neutrophils in mutant mice: $5.7 \pm 1.1 \times 10^5$ cells ml^{-1} versus $2.5 \pm 0.3 \times 10^5$ cells ml^{-1} in controls ($P < 0.001$) (Fig. 1c and Supplementary Fig. 2). Flow cytometric analysis of peripheral blood confirmed the neutrophilia in *miR-223*$^{-/Y}$ mice (Fig. 1c). Morphological and fluorescence-activated cell sorting (FACS) analyses also revealed marked granulocyte hyperplasia in the bone marrow of mutant mice (Fig. 1c, d). *miR-223*-deficient neutrophils also exhibited an unusual hypermature morphology characterized by nuclear hypersegmentation and blebbing, reminiscent of the granulocytes observed in human myelokathexis[7] (Fig. 1e). Additionally, mutant neutrophils displayed an aberrant pattern of lineage-specific marker expression (Fig. 1c and Supplementary Fig. 3). Altogether, these results demonstrate that although miR-223 is dispensable for granulocyte cell fate specification, it is essential for normal neutrophil maturation and regulation of the granulocyte compartment size.

The marked neutrophilia in *miR-223* null mice could be explained by either a decrease in the rate of neutrophil clearance or, alternatively, an increase in the number of granulocyte progenitors. To study the first possibility, we performed 5-bromodeoxyuridine (BrdU) pulse–chase studies as a way of measuring the kinetics of neutrophil turnover. We found no difference in the lifespan of mutant and control peripheral neutrophils (Supplementary Fig. 4). Moreover, granulocytes from *miR-223*$^{-/Y}$ mice exhibited normal rates of apoptosis as assessed by annexin V staining (Supplementary Fig. 5). The pulse–chase studies did reveal that the absolute number of BrdU-labelled granulocytes was increased approximately twofold in *miR-223*$^{-/Y}$ mice, thereby suggesting an expanded mitotically active progenitor population (Supplementary Fig. 4). Indeed, mutant bone marrow cells generated 2.3-fold more colonies than wild-type bone marrow in methylcellulose cultures with granulocyte colony-stimulating factor (G-CSF) (Fig. 2a). Additionally, we found an approximately 1.6-fold increase in the absolute number of phenotypically defined granulocyte–monocyte progenitors in the bone marrow of *miR-223*$^{-/Y}$ mice, numbers of common myeloid progenitors were unchanged, and megakaryocyte–erythroid progenitors were slightly reduced (Fig. 2b). Methylcellulose assays in the presence of myelo-erythroid cytokines revealed increased granulocytic differentiation from haematopoietic stem cells and common myeloid progenitors from mutant mice (Supplementary Fig. 6). Furthermore, *in vivo* BrdU-incorporation assays demonstrated that mutant granulocyte–monocyte progenitors had a significantly higher proliferative index (Supplementary Fig. 6). Altogether, these data suggest that the neutrophilia observed in *miR-223* null mice probably results from enhanced differentiation and proliferation of the granulocyte progenitor pool.

We next sought to determine whether the phenotypes described above were cell autonomous. To do so, we generated haematopoietic chimaeras by performing competitive repopulation assays in which 1×10^6 bone marrow cells isolated from wild-type C57BL/6 mice

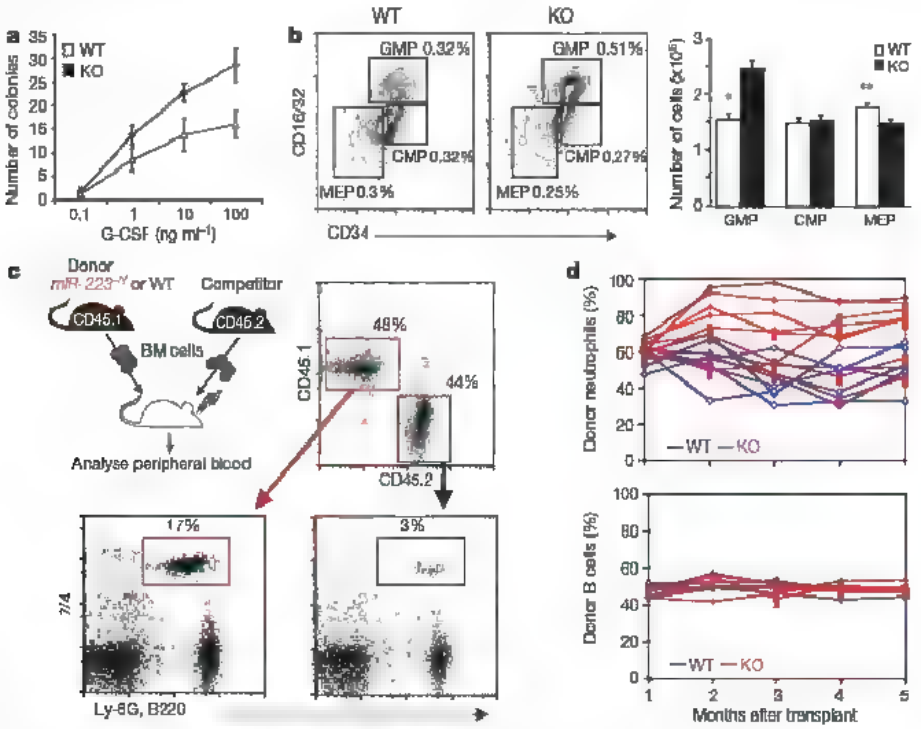

Figure 2 | Regulation of progenitor cell proliferation by miR-223. **a**, Colony formation by 4×10^4 bone marrow cells from wild type (WT) or *miR-223* mutant mice (KO) in methylcellulose containing varying concentrations of G-CSF (mean ± s.d., $n = 5$). Colony counts were performed at day 10. **b**, FACS analysis of myeloid progenitor cell populations of 8-week-old mice. Plots shown were previously gated on Lin$^-$ Sca1$^-$ c-Kit$^+$ cells. The right panel shows the overall number of progenitors per bone marrow sample isolated from femurs and tibiae (mean ± s.e.m., $n = 7$ mice of each genotype). CMP, common myeloid progenitors; GMP, granulocyte–monocyte progenitors; MEP, megakaryocyte–erythroid progenitors. Single asterisk, $P < 0.001$, double asterisk, $P < 0.01$ (Student's *t*-test). **c**, Experimental design for competitive transplant assays (top left) and representative FACS analysis of peripheral blood from a mouse transplanted with 1×10^6 bone marrow cells each from a *miR-223*$^{-/Y}$ CD45.1 donor and C57BL/6 CD45.2 competitor mouse. Analysis shown is 3 months after transplant. Granulocytes are 7/4$^+$Ly-6G$^+$ and are highlighted in the two bottom panels. **d**, Representative time-course analysis of haematopoietic engraftment in distinct blood lineages. Each line represents the 'donor' chimaerism in individual mice transplanted with either wild type (blue) or *miR-223* mutant (red) bone marrow cells along with competitor cells. Representative results are shown from one of three independent experiments performed.

carrying the CD45.2 antigen (subsequently referred to as 'competitor') were co-transplanted with 1×10^6 cells from either *miR-223*$^{-/Y}$ or wild-type littermate controls carrying the CD45.1 antigen (henceforth referred to as 'donor') (Fig. 2c). Notably, we found that most of the circulating neutrophils in mice receiving the mutant plus competitor grafts were of donor origin (82 ± 13% *miR-223*$^{-/Y}$ versus 18 ± 9% competitor neutrophils), whereas recipients of wild-type plus competitor transplants had the expected 1:1 ratio of peripheral granulocytes (42 ± 10% wild-type versus 58 ± 7% competitor neutrophils) (Fig. 2d, top panel). The competitive advantage observed in the mutant neutrophils is lineage specific, as *miR-223*$^{-/Y}$ donor cell contribution was approximately 50% in the B- and T-cell lineages (Fig. 2d, and data not shown). FACS analysis also revealed that the aberrant marker expression profile and increased nuclear complexity remained present in mutant neutrophils of chimaeric mice (Fig. 2c, and data not shown). From these results, we conclude that the hyperproliferative and abnormal differentiation phenotypes caused by loss of *miR-223* are cell autonomous.

Among the more than 100 computationally predicted targets of miR-223 we noticed that the transcription factor *Mef2c* was the only gene that contained two conserved miR-223 complementary 'seed' sites in its 3′ untranslated region (UTR), making it the target predicted with highest confidence[8]. Notably, a recent study reported that *Mef2c* messenger RNA levels are upregulated in highly proliferative leukaemic granulocyte–monocyte progenitors and that its ectopic expression enhanced their proliferation[9]. Given this evidence and the observed phenotype in *miR-223*$^{-/Y}$ mice, we sought to test whether *Mef2c* was a target of miR-223. Luciferase reporter assays using the 3′ UTR of *Mef2c* demonstrated a miR-223-specific regulation of reporter gene expression (Fig. 3a, b). This downregulation was specific to the predicted miR-223 target sites, as mutation of the 3′ UTR seed match sequences relieved the inhibitory activity of miR-223 (Fig. 3a, b). Given that microRNAs can also promote target mRNA degradation[10], we also tested whether *Mef2c* mRNA levels were increased in granulocyte–monocyte progenitors from *miR-223*$^{-/Y}$ mice. Real-time polymerase chain reaction with reverse transcription (RT–PCR) analysis revealed a 1.9 ± 0.2-fold increase in *Mef2c* mRNA levels in mutant granulocyte–monocyte progenitors (Fig. 3c). As a control for the specificity of Mef2c dysregulation in granulocyte–monocyte progenitors, we also evaluated the levels of this transcript in B cells (which do not express miR-223), where we observed unchanged *Mef2c* expression (Fig. 3c).

To examine functionally the importance of Mef2c upregulation as part of the miR-223 circuitry *in vivo*, we bred a *Mef2c* loss-of-function allele onto the *miR-223*-deficient background[11]. As mice with a germline mutation in *Mef2c* are embryonic lethal, we chose to study the effects of a myeloid-specific deletion of a floxed (f) allele of *Mef2c* in *miR-223*-deficient mice. Conditional deletion of *Mef2c* within the myeloid lineage using the lysozyme M-Cre (L-Cre) strain resulted in no haematopoietic abnormalities, indicating that Mef2c is dispensable for steady-state myelopoiesis (Supplementary Fig. 7). Interestingly, when the *Mef2c* mutation was combined with the *miR-223* deletion, the increased number of peripheral neutrophils in *miR-223*$^{-/Y}$ mutants was corrected (Fig. 3d). Furthermore, methylcellulose assays revealed a rescue in the number of G-CSF-responsive colony-forming progenitors in the bone marrow of *miR-223*$^{-/Y}$ *L-Cre Mef2c*$^{f/f}$ mice (Fig. 3e). In spite of this, mature *miR-223*$^{-/Y}$ *L-Cre Mef2c*$^{f/f}$ neutrophils still exhibited morphological and immunophenotypical abnormalities typical of *miR-223* deficiency (Fig. 3f and Supplementary Fig. 8). Therefore, our results provide compelling genetic evidence that Mef2c is a critical target of miR-223 in early myeloid progenitors.

Neutrophils are an essential part of the innate immune response as they are critical for the first line of defence against bacteria and fungi. Given the range of anomalies observed in mature *miR-223*$^{-/Y}$ granulocytes, we sought to evaluate whether their immunological function was impaired. We found no difference in the ability of mutant neutrophils to extravasate, migrate or to phagocytose *Escherichia coli* (data not shown). We next measured the production of reactive oxygen metabolites, which are generated after neutrophil activation and are critical for the killing of microorganisms. After stimulation with phorbol myristate acetate (PMA), *miR-223*$^{-/Y}$ neutrophils exhibited an enhanced oxidative burst compared to wild-type

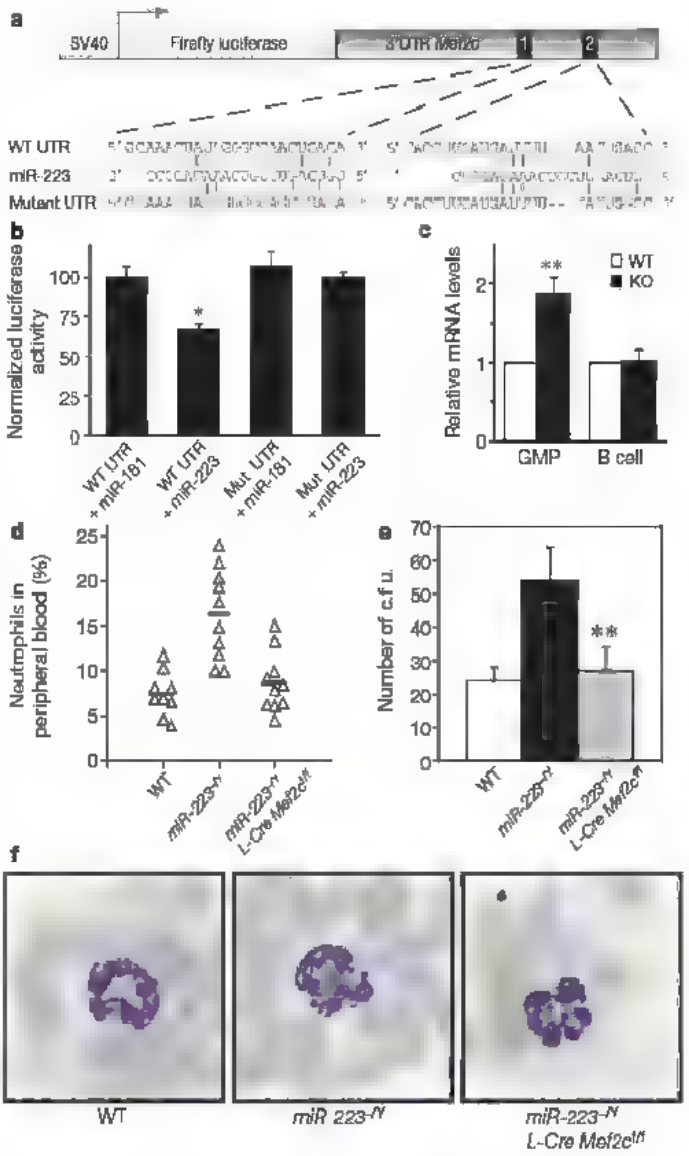

Figure 3 | Mef2c is a functional miR-223 target in myeloid progenitors. **a**, Schematic representation of luciferase constructs used for reporter assays. The two miR-223 target sites within the 3′ UTR of *Mef2c* are shown as black boxes. Sequences below indicate putative miR-223 target sites on the wild-type 3′ UTR, its mutated derivative and the pairing regions of miR-223. **b**, Luciferase reporter assays performed on 293T cells transfected with constructs shown in **a**. Values are normalized to the wild-type reporter (mean ± s.e.m., $n = 3$). Asterisk, $P < 0.02$. **c**, Granulocyte–monocyte progenitors or mature B cells were isolated from wild type or *miR-223*$^{-/Y}$ (KO) mice and levels of *Mef2c* mRNA expression were evaluated by Taqman quantitative PCR. Values are relative to the expression in wild-type cells (± s.e.m., $n = 4$). Double asterisk, $P < 0.001$. **d**, Percentage of circulating neutrophils in 2-month-old control, *miR-223* mutant and *miR-223*$^{-/Y}$ *L-Cre Mef2c*$^{f/f}$ compound mutant mice. The horizontal bar represents the mean value for each genotype. **e**, Colony formation by 4×10^4 bone marrow cells from control and single or double mutant mice in methylcellulose containing 50 ng ml^{-1} G-CSF (mean ± s.e.m., $n = 3$). Colony counts were performed at day 10. c.f.u., colony-forming units. Double asterisk, $P < 0.001$. **f**, Morphological analysis of circulating neutrophils (May–Grünwald Giemsa) from control, *miR-223*$^{-/Y}$ and *miR-223*$^{-/Y}$ *L-Cre Mef2c*$^{f/f}$ mutant mice. Note that the hypersegmented morphology typical of *miR-223*$^{-/Y}$ granulocytes is still present in animals also carrying the *Mef2c* mutation.

granulocytes (Fig. 4a). These differences became more prominent with lower concentrations of the stimulant, where we observed an almost 70% increase in superoxide production. Additionally, at the lowest concentration of PMA, where less than 10% of wild-type granulocytes underwent a respiratory burst, approximately 30–40% of mutant neutrophils produced superoxide, indicating that knockout neutrophils were hypersensitive to activating stimuli (Fig. 4b). Consistent with these observations, *miR-223*$^{-/Y}$ neutrophils displayed enhanced killing when co-cultured with *Candida albicans* (Fig. 4c). Taken together, our results indicate that miR-223 acts as a negative modulator of neutrophil activation and killing.

These *in vitro* data predict that granulocyte hyperactivation in the absence of miR-223 could, in certain contexts, lead to neutrophil-mediated disease. On histological examination, the lungs of adult *miR-223*$^{-/Y}$ animals (>1.2 yr) consistently displayed inflammatory lung pathology characterized by areas of atelectasis, increased cellularity within the parenchyma, and inflammatory infiltration into the interstitium (Fig. 4d). As predicted, neutrophils represented the most prominent cell type within the infiltrates (Supplementary Fig. 9). These observations are highly reminiscent of the pulmonary pathology observed in mice with hyperactive innate immune responses[12,13]. To test the response of *miR-223*-deficient neutrophils in a more acute inflammatory setting, experimental endotoxaemia was induced by the systemic administration of a sub-lethal dose of bacterial lipopolysaccharide (LPS). Under these conditions, control mice developed mild symptoms that disappeared within 24 h. In contrast, *miR-223*$^{-/Y}$ mice showed evidence of clinical distress and exhibited delayed recovery from endotoxaemia. To quantify the extent of inflammation-induced tissue damage in LPS-treated mice, we examined the serum levels of proteins that reflect liver necrosis, renal function and muscle damage 48 h after endotoxin challenge. As shown in Fig. 4e, mutant mice had significantly higher levels of aspartate aminotransferase (ALT), blood urea nitrogen (BUN) and creatine kinase (CK), indicative of considerable widespread tissue damage. Additionally, histological examination of the livers of LPS-treated *miR-223*$^{-/Y}$ mice showed an exaggerated inflammatory cell presence and distinct areas of hepatocyte necrosis and intralobular haemorrhage (Fig. 4f).

We next tested whether Mef2c could also be implicated in the regulation of neutrophil activation in *miR-223*$^{-/Y}$ mice. Our results show that *miR-223*$^{-/Y}$ *L-Cre Mef2c*$^{f/f}$ neutrophils displayed the same hyperactive responses as *miR-223* mutant mice, indicating that other potential targets might explain these phenotypes (Supplementary Fig. 8). One compelling candidate target is insulin-like growth factor receptor 1 (Igf1r), the activation of which leads to neutrophil priming and activation[14–16]. We thus tested whether this gene transcript could be regulated by miR-223. Luciferase reporter assays using the 3′ UTR of *Igf1r* demonstrated a miR-223-specific regulation of Igf1r expression (Supplementary Fig. 10). Additionally, western blot analysis demonstrated significantly upregulated levels of Igf1r protein in purified mutant neutrophils (Supplementary Fig. 10). Although regulation of the Igf1–Igf1r axis represents a potential mechanism by which miR-223 might control granulocyte function, given that some phenotypes present in *miR-223* mutant mice (that is, neutrophil hypersegmentation and lung pathology) have not been linked to Igf1 signalling, it is likely that other targets will also be an important part of the miR-223 network in mature granulocytes.

Our findings seem to contradict the previous conclusion indicating that miR-223 is a positive regulator of granulocytic differentiation[5].

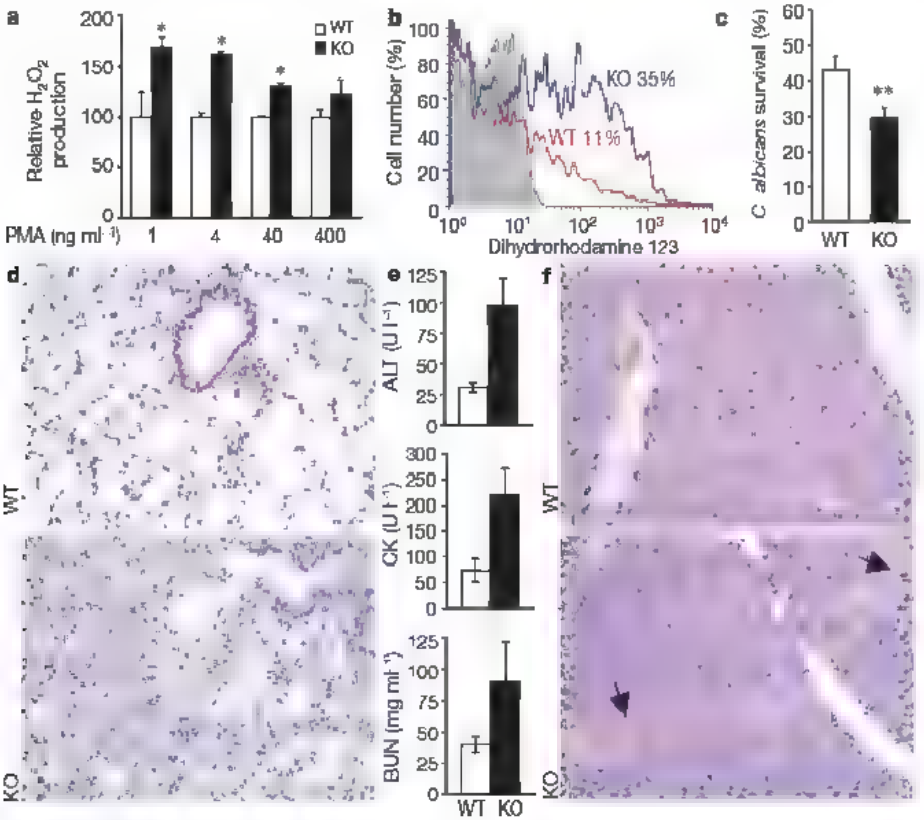

Figure 4 | Regulation of neutrophil activity and inflammation by miR-223. **a**, Respiratory burst by peritoneal neutrophils as measured by oxidation of dihydrorhodamine 123 after activation with different concentrations of PMA. Data represent the mean fluorescent intensity of all cells with a signal above background and are normalized for wild-type values (mean ± s.d., $n = 5$). Asterisk, $P < 0.01$ (Student's *t*-test). **b**, Representative histogram showing the percentage of dihydrorhodamine-positive cells after incubation of peripheral blood neutrophils with 4 ng ml^{-1} PMA for 15 min. The grey histogram shows the baseline fluorescence of unstimulated granulocytes. **c**, *In vitro* killing activity of control and *miR-223*$^{-/Y}$ (KO) bone-marrow-derived neutrophils incubated with *C. albicans*. Data represent the mean (±s.d.) of 12 replicates from one representative experiment out of four performed. Double asterisk, $P < 1 \times 10^{-7}$ (Student's *t*-test). **d**, Haematoxylin-and-eosin-stained sections of lung tissue from aged wild type and *miR-223*$^{-/Y}$ mice. **e**, Serum levels of aspartate aminotransferase (ALT), blood urea nitrogen (BUN) and creatine kinase (CK) in control and mutant mice 48 h after the injection of 15 mg kg^{-1} LPS (mean ± s.d., $n = 7$ mice of each genotype). **f**, Representative haematoxylin-and-eosin-stained section of livers of control and mutant mice 48 h after endotoxin injection. Note the large areas of haemorrhage and hepatocyte necrosis (arrows) in the mutant liver

Several reasons could explain these discrepancies: for instance, it is possible that the overexpression strategies used by ref. 5 could have distinct consequences compared with those that are extrapolated from our deletion studies. Additionally, in our work, miR-223 is absent in the entire granulocytic lineage in a mouse, whereas ref. 5 manipulated expression of miR-223 in a leukaemic cell line resembling an early granulocyte progenitor. This issue is more relevant given that our data provide evidence for distinct functions of miR-223 during different stages of myeloid cell development, during which microRNA concentrations change dynamically. Future experiments aimed at manipulating miR-223 expression at defined granulocyte differentiation stages will be useful in determining the multiple roles of this microRNA.

Our results indicate that miR-223 is an intrinsic modulator of neutrophil sensitivity, similar to the role proposed for miR-181, which acts as a 'rheostat' controlling T-cell activation[17]. Our data support a model in which miR-223 physiologically fine tunes both the generation and function of granulocytic cells, thereby delimiting their production and dampening their activation. As misregulation of neutrophil activation is associated with autoimmune and inflammatory disease[18–20], further work will determine whether pharmacological manipulation of this microRNA could be useful in a clinical setting.

METHODS SUMMARY

A vector was constructed to replace the endogenous *miR 223* locus on the X chromosome by means of homologous recombination in embryonic stem (ES) cells. Resulting chimaeric offspring were crossed to C57BL/6 mice, and male offspring were further backcrossed for five generations to C57BL/6 mice congenic for CD45.1. Femur bones from 6–8-week-old mice were fixed in Bouin's fixative until fully decalcified and embedded in paraffin. Bone marrow sections were stained with haematoxylin and eosin. Peripheral blood smears were stained with a May–Grunwald Giemsa protocol. Complete blood counts were determined from blood obtained by retro-orbital puncture on an ADVIA 120 hematology analyser. Bone marrow neutrophils were purified using MACS columns (Myltenyi Biotech) on the basis of Gr-1 surface antigen expression. *Candida albicans* strain SC5314 (CA) was grown overnight in YPD media at 37 °C, washed in phosphate buffered saline and counted. A total of 2.5×10^5 CA were incubated with or without 5×10^5 bone marrow neutrophils in flat-bottom 96-well plates for 2.75 h. Surviving CA were incubated with Alamar blue (Biosource) and fluorescence was measured using a SafireII plate reader (Tecan).

Full Methods and any associated references are available in the online version of the paper at www.nature.com/nature.

Received 30 October; accepted 21 December 2007.
Published online 17 February 2008.

1. Bartel, D. P. MicroRNAs: genomics, biogenesis, mechanism, and function. *Cell* 116, 281–297 (2004)
2. Taganov, K. D., Boldin, M. P. & Baltimore, D. MicroRNAs and immunity: tiny players in a big field. *Immunity* 26, 133–137 (2007)
3. Lim, L. P., Glasner, M. E., Yekta, S., Burge, C. B. & Bartel, D. P. Vertebrate microRNA genes. *Science* 299, 1540 (2003)
4. Chen, C. Z., Li, L., Lodish, H. F. & Bartel, D. P. MicroRNAs modulate hematopoietic lineage differentiation. *Science* 303, 83–86 (2004)
5. Fazi, F. *et al.* A minicircuitry comprised of microRNA-223 and transcription factors NFI-A and C/EBPα regulates human granulopoiesis. *Cell* 123, 819–831 (2005)
6. Fukao, T. *et al.* An evolutionarily conserved mechanism for microRNA-223 expression revealed by microRNA gene profiling. *Cell* 129, 617–631 (2007)
7. Bohinjec, J. Myelokathexis: chronic neutropenia with hyperplastic bone marrow and hypersegmented neutrophils in two siblings. *Blut* 42, 191–196 (1981)
8. Lewis, B. P., Burge, C. B. & Bartel, D. P. Conserved seed pairing, often flanked by adenosines, indicates that thousands of human genes are microRNA targets. *Cell* 120, 15–20 (2005).
9. Krivtsov, A. V. *et al.* Transformation from committed progenitor to leukaemia stem cell initiated by MLL-AF9. *Nature* 442, 818–822 (2006)
10. Jackson, R. J. & Standart, N. How do microRNAs regulate gene expression? *Sci. STKE* 2007, re1 (2007)
11. Vong, L. H., Ragusa, M. J. & Schwarz, J. J. Generation of conditional *Mef2c*$^{lox P/lox P}$ mice for temporal- and tissue-specific analyses. *Genesis* 43, 43–48 (2005)
12. Ernst, M. *et al.* Constitutive activation of the SRC family kinase Hck results in spontaneous pulmonary inflammation and an enhanced innate immune response. *J. Exp. Med.* 196, 589–604 (2002)
13. Yu, C. C. *et al.* B and T cells are not required for the viable motheaten phenotype. *J. Exp. Med.* 183, 371–380 (1996)
14. Bjerknes, R. & Aarskog, D. Priming of human polymorphonuclear neutrophilic leukocytes by insulin-like growth factor I: increased phagocytic capacity, complement receptor expression, degranulation, and oxidative burst. *J. Clin. Endocrinol. Metab.* 80, 1948–1955 (1995).
15. Fu, Y. K., Arkins, S., Wang, B. S. & Kelley, K. W. A novel role of growth hormone and insulin-like growth factor-I: Priming neutrophils for superoxide anion secretion. *J. Immunol.* 146, 1602–1608 (1991).
16. Inoue, T. *et al.* Growth hormone and insulin-like growth factor I augment bactericidal capacity of human polymorphonuclear neutrophils. *Shock* 10, 278–284 (1998)
17. Li, Q. J. *et al.* miR-181a is an intrinsic modulator of T cell sensitivity and selection. *Cell* 129, 147–161 (2007)
18. Vorcken, J. W. *et al.* Increased neutrophil respiratory burst in bcr-null mutants. *Cell* 80, 719–728 (1995)
19. Smith, J. A. Neutrophils, host defense, and inflammation: a double-edged sword. *J. Leukoc. Biol.* 56, 672–686 (1994)
20. Malech, H. L. & Gallin, J. I. Current concepts: immunology. Neutrophils in human diseases. *N. Engl. J. Med.* 317, 687–694 (1987)

Supplementary Information is linked to the online version of the paper at www.nature.com/nature.

Acknowledgements We thank D. Bartel and M. Goodell for critical reading of the manuscript, and members of the Bartel and Jaenisch laboratories for discussions. We also thank H. Mulhern, D. Campagna and S. Gokhale for assistance with morphological analysis, and D. Kombe for mouse handling. We are grateful to J. Schwarz for the gift of *Mef2c* mutant mice. This work was supported by grants from the Whitehead Institute Fellows program.

Author Information Reprints and permissions information is available at www.nature.com/reprints. Correspondence and requests for materials should be addressed to F.D.C. (camargo@wi.mit.edu)

LETTERS

Backbone structure of the infectious ε15 virus capsid revealed by electron cryomicroscopy

Wen Jiang[1]*, Matthew L. Baker[2]*, Joanita Jakana[2], Peter R. Weigele[3], Jonathan King[3] & Wah Chiu[2]

A half-century after the determination of the first three-dimensional crystal structure of a protein[1], more than 40,000 structures ranging from single polypeptides to large assemblies have been reported[2]. The challenge for crystallographers, however, remains the growing of a diffracting crystal. Here we report the 4.5-Å resolution structure of a 22-MDa macromolecular assembly, the capsid of the infectious epsilon15 (ε15) particle, by single-particle electron cryomicroscopy. From this density map we constructed a complete backbone trace of its major capsid protein, gene product 7 (gp7). The structure reveals a similar protein architecture to that of other tailed double-stranded DNA viruses, even in the absence of detectable sequence similarity[3,4]. However, the connectivity of the secondary structure elements (topology) in gp7 is unique. Protruding densities are observed around the two-fold axes that cannot be accounted for by gp7. A subsequent proteomic analysis of the whole virus identifies these densities as gp10, a 12-kDa protein. Its structure, location and high binding affinity to the capsid indicate that the gp10 dimer functions as a molecular staple between neighbouring capsomeres to ensure the particle's stability. Beyond ε15, this method potentially offers a new approach for modelling the backbone conformations of the protein subunits in other macromolecular assemblies at near-native solution states.

Bacteriophages have been valuable model systems for studying virus structures and assembly[5–8] as well as protein folding and maturation[9,10]. These viruses also have a critical function in transferring genes between bacterial host cells, influencing host pathogenicity[11] and the population ecology of environmental microorganisms[12]. With an estimated 10^{31} particles, tailed double-stranded DNA (dsDNA) bacteriophages are likely to be the most abundant life forms in the biosphere[13]. Despite repeated efforts, no infectious tailed dsDNA phage has been crystallized, although the crystal structure of a recombinant empty capsid of HK97 has been determined[8]. The great variation and diversity in the amino acid sequences among these tailed dsDNA bacteriophages has prevented the prediction of the structural organization of the capsid from the genome sequence alone

Single-particle electron cryomicroscopy (cryo-EM) was used about ten years ago to determine the first structures of icosahedral viruses to subnanometre resolutions (7.4–9 Å), revealing long α-helices[14,15]. Here we report a 4.5-Å resolution icosahedral capsid structure of the infectious tailed dsDNA bacteriophage ε15 of *Salmonella anatum*[6] with the use of single-particle cryo-EM.

Purified infectious ε15 particles were imaged with a liquid-helium 300-kV electron cryomicroscope[16,17]. Typical images (Fig. 1a) clearly demonstrated signals beyond 5 Å in their power spectra (Supplementary Fig. 1a, b). From about 20,000 individual particle images, the density map of ε15 was reconstructed to a resolution of 4.5 Å (Fig. 1b, Supplementary Fig. 1c and Supplementary Movie 1). This resolution is the result of advances and accumulated experience in instrumentation, the collection of large data sets, and image processing, and also in the availability of large-scale distributed computing (see Methods). The map clearly shows protruding densities around all the icosahedral and local two-fold positions (Fig. 1b and Supplementary Movie 1) that connect the underlying masses, forming the capsid shell. The density map was sufficiently well resolved to allow each of the seven subunits in the asymmetric unit of the $T = 7laevo$ icosahedron to be computationally extracted (Fig. 1c and Supplementary Movie 1). At this resolution it was evident that each subunit consists of two distinct lobes connected by weak densities. Each of the lobes was segmented individually, yielding a small protruding, mainly hollow, globular density and a larger, more extended density

In the larger of the two density lobes, eight α-helices and two β-sheets were identified with the feature recognition program SSEHunter[18] (Supplementary Fig. 2a). The spatial dispositions of these secondary structure elements seemed to be similar to those of the major capsid proteins of other tailed dsDNA phages and herpesviruses[3,6]. The large density lobe was therefore assigned to the major capsid protein, gp7 (335 amino-acid residues).

Using computational modelling methods (Supplementary Information) together with sequence analysis, we constructed the Cα backbone models (residues 1–335) for each of the seven gp7 monomers (Fig. 2a, Supplementary Fig. 2 and Supplementary Movie 2). The pitch of the α-helices, the separation of the β-strands, and several bulky side-chains were visible in the density and corresponding models (Fig. 2b). The gp7 model could be roughly divided into four domains: an extended amino terminus (N-arm), a central, triangular domain (A-domain), an elongated protrusion domain (P-domain) and a long, extended loop (E-loop) (Fig. 2c). As noted previously[6], the architecture of gp7, including the overall shape and the arrangement of its domains and secondary structure elements, was similar to that of the HK97 capsid protein[8], although no sequence similarity was evident. However, the connectivity of the secondary structure elements (that is, their topology) was different because of the permutation of the order of the two carboxy-terminal sequence segments (residues 158–250 and 251–335) of ε15 gp7 (Supplementary Information and Supplementary Fig. 8a). Further sequence analysis indicates that this type of sequence permutation might be a general feature of the major capsid proteins of tailed dsDNA phages (Supplementary Information). Similar types of structural conservation in the presence of sequence and topology permutation have been reported in several protein families[19–21].

This model building was possible primarily because of the ability to distinguish unique secondary structure elements accurately in

[1]Markey Center for Structural Biology, Department of Biological Sciences, Purdue University, West Lafayette, Indiana 47907, USA. [2]National Center for Macromolecular Imaging, Verna and Marrs McLean Department of Biochemistry and Molecular Biology, Baylor College of Medicine, Houston, Texas 77030, USA. [3]Department of Biology, Massachusetts Institute of Technology, Cambridge, Massachusetts 02139, USA.
*These authors contributed equally to this work.

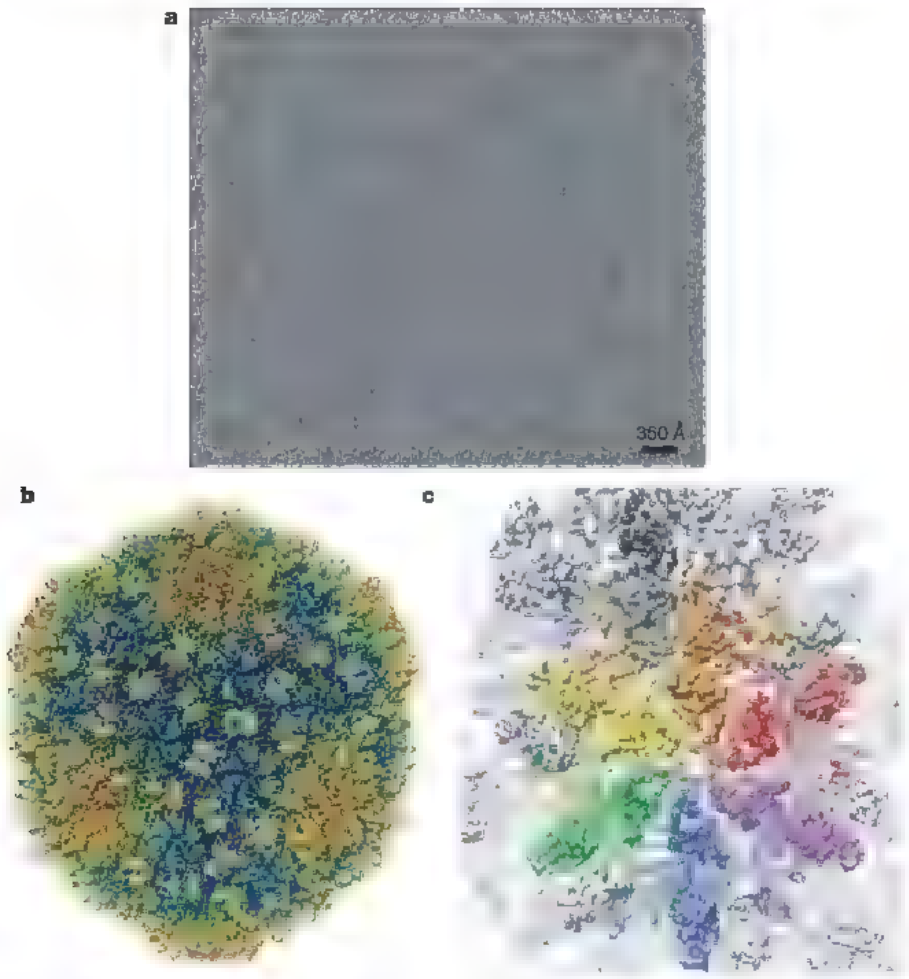

Figure 1 | Cryo-EM image and three-dimensional map of bacteriophage ε15. a, Typical 300-kV image of ice-embedded ε15 kept at 4.2 K, recorded in a JEM3000SFF electron cryomicroscope. Fingerprint signature features of viral DNA are clearly seen in the projection images. **b,** The 4.5-Å resolution three-dimensional reconstruction of ε15 phage, about 700 Å in diameter, radially coloured. **c,** The seven subunits in an asymmetric unit, annotated in different colours. Each subunit contains one copy of gp7 and one copy of gp10.

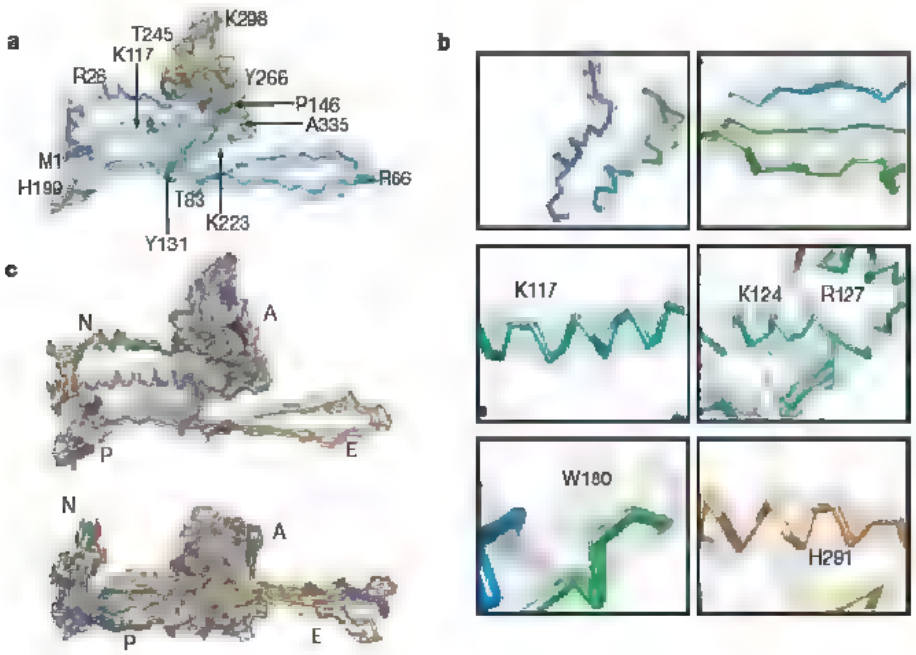

Figure 2 | Model of gp7 monomer. a, A gp7 model superimposed on the corresponding segmented density map. The model is coloured from the N terminus (blue, to the C terminus (red) and several landmark residues are annotated. **b,** Regions of the density map and model of gp7, illustrating model features such as the 5.4-Å pitch in a helix (top left, middle left and bottom right), the roughly 4.8-Å β-strand separation (top right) and bulky side chains **c,** Two views of the seven gp7 models and an average density map from the asymmetric unit, illustrating the conformational variations among the seven gp7 monomers. The seven models are coloured with the colour scheme in Fig. 1c. The four domains of a gp7 monomer are also annotated. N, N-arm, P, P-domain, A, A-domain, E, E-loop.

both the sequence and the cryo-EM map (Supplementary Information). Failure to correlate these structural elements accurately may limit model accuracy and the general applicability of this approach to other data at a similar resolution. As a result of low sequence identity, neither the HK97 nor the T4 capsid proteins was used explicitly as a structural template during the model building process (Supplementary Information). However, the quality of the map and our method of modelling were adequate for a backbone trace of gp7. The accuracy of our backbone trace was subsequently verified by a root mean squared deviation of 3.765 Å of the 198 structurally conserved residues throughout the structures of ε15 gp7 and HK97 gp5 (Supplementary Information and Supplementary Fig. 8b, c).

Although mostly similar, the seven individual gp7 subunit models within the asymmetric unit do contain some structural variations as expected for the quasi-equivalent packing of chemically identical subunits in an icosahedral lattice[22] (Fig. 2c and Supplementary Fig. 3). On average, the models have a root mean squared deviation of about 2.3 Å (2.1–3.5 Å), with the major differences occurring at the N terminus and the E-loop. In particular, the E-loops of the gp7 subunits in the pentameric capsomere (penton) and the hexameric capsomere (hexon) most proximal to the penton show a significant bend (about 20°) towards the interior of the capsid (Fig. 2c). This bending is needed to pack the subunits into a five-fold vertex and to form the icosahedral lattice structure.

Applying icosahedral symmetry to the seven gp7 models of an asymmetric unit, a model of the $T = 7l$ capsid containing 420 copies of gp7 was constructed (Fig. 3a and Supplementary Movie 3). Although our Cα models lack side-chain conformations and are therefore not sufficient for inferences to be made about the exact nature of inner surface charge and its influences on the packing of the encapsulated dsDNA genome, the capsid model clearly shows the arrangement and interaction sites of gp7 throughout the capsid (Supplementary Fig. 4a, b). The triangular A-domain interacts laterally around the centre of the penton/hexon ring (Fig. 3a) through interactions between two nearly parallel helices (residues 256–269 and 284–296, respectively), one from each of the two adjacent subunits (Supplementary Fig. 4a). In contrast, the N-arm, P-domain and E-loop are located at the periphery of the penton/hexon capsomeres. In particular, the extended E-loop crosses over the middle region of the P-domain of the adjacent subunit in the same capsomere (Supplementary Fig. 4b) and contacts the distal end 'hook' of a P-domain from a neighbouring capsomere (Fig. 3b). Two sequential positively charged arginine residues (R66, R67) at the end of the E-loop of one subunit are proximal to the highly negatively charged hook (E200, D201, D204, D205) of a subunit in an adjacent capsomere at the icosahedral and local three-fold axes. These interactions across capsomeres probably stabilize the E-loop and the entire capsid. These interactions occur at the equivalent locations in HK97 where two subunits are covalently crosslinked to stabilize the capsid[8].

In this 4.5-Å map it became clear that gp7 could not account for the entire capsid shell as had previously been assumed[6]. We re-examined the protein composition of the phage particles with a polyacrylamide gel at a higher percentage, which resolved a second, small, high-copy-number capsid protein (Fig. 4a). Mass spectrometry analysis identified this protein as gp10 (about 12 kDa; 111 residues) and it was therefore assigned to the small protruding density lobe.

Feature detection with SSEHunter[18] revealed that the relatively hollow gp10 consists mainly of β-sheets, although two short α-helices (about three turns each) were observed; a similar set of secondary structure elements was predicted computationally from the sequence (Supplementary Fig. 5a, b). Sequence searches revealed no known homologues. However, several structure-based searches did consistently return PDZ domains as potential structural templates. Unlike gp7, constructing a reliable model for gp10 from the density map was not possible owing to the relatively high percentage of β-sheet and only two short, similar-sized α-helices. Nevertheless, the PDZ-like domain model seems to have a size and shape similar to those of the small-lobe density of the subunit (Supplementary Fig. 5c).

Despite the lack of a high-resolution model for gp10, a potential role for this protein can be derived from its relative position on the capsid. A back-to-back dimer of gp10 sits on the surface of the virus at the two-fold axes and makes contact with six gp7 subunits (Fig. 4b and Supplementary Movies 1 and 3). Each gp10 molecule contacts four gp7 subunits, namely two subunits contributed from each of the two neighbouring capsomeres (Fig. 4c and Supplementary Fig. 4a). In the gp10 dimer, the two N-arms of gp7 buttress the gp10 dimer laterally (Fig. 4d), and the insertion loop and the E-loop line the groove in which the dimer rests. These interactions not only join neighbouring gp7 subunits, but they also link the neighbouring capsomeres. Thus, gp10 'staples' the underlying gp7 capsomeres into a robust cage that can withstand the pressure from the densely packed dsDNA genome in the infectious phage particles.

In support of this potential role, a significant amount of gp10 was subsequently found to remain bound to the capsid in the presence of 5 M guanidinium chloride (GuHCl) (Fig. 4a and Supplementary Fig. 6), far beyond the concentration of denaturant needed to remove the tail and portal proteins in infectious phage particles. Capsids are disrupted by 6 M GuHCl, indicating that the gp7–gp10 interactions are of the same order of magnitude as those of gp7–gp7 interactions.

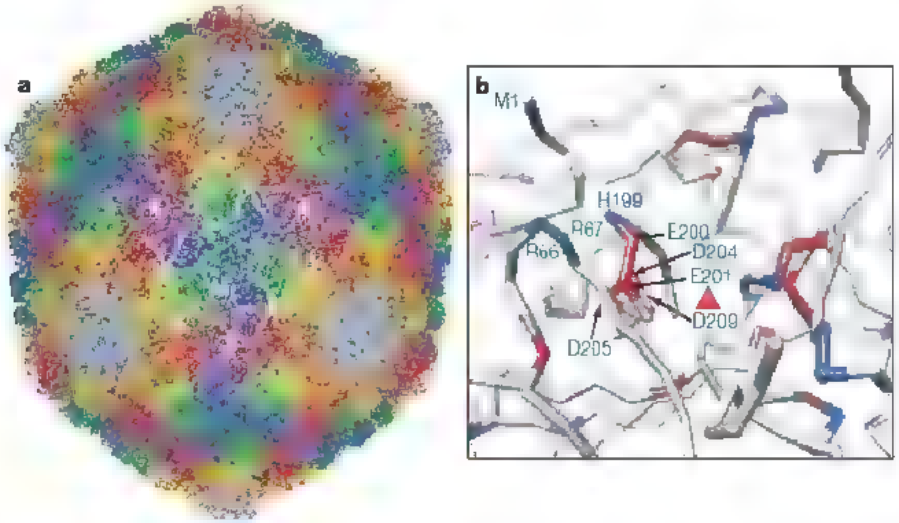

Figure 3 | Capsid model and interactions of gp7. a, A full capsid model of gp7, with the same colour scheme as in Fig. 1c. **b**, The charged amino acids of gp7, viewed slightly offset from the three-fold axis. The residue labels are shown in blue and green, corresponding to the gp7 monomer colour scheme in **a**

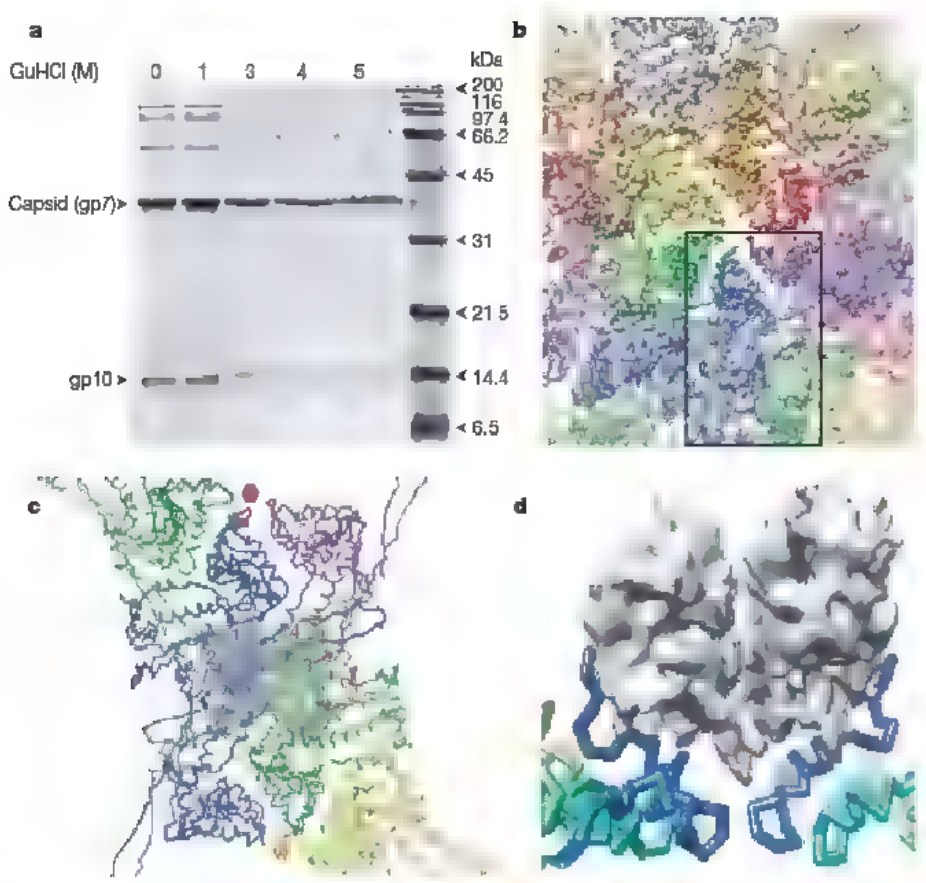

Figure 4 | Gp10, a molecular staple. a, SDS gel of GuHCl-treated virions, showing the retention of gp10. Virion particles were incubated in GuHCl at the indicated concentrations and sedimented onto a cushion of high-density CsCl. Virion particles were harvested, dialysed and resolved by SDS–PAGE. Note the loss of other structural proteins from gp7–gp10. **b,** The density of gp10 coloured similarly to that of gp7 with the most extensive contacts. **c,** gp7 and gp10 subunits corresponding to the boxed region in **b**. The centres of the two adjacent hexameric capsomeres are labelled with red and orange hexagons, respectively. Gp7–gp10 (left) interactions are labelled 1 and 2 in red and 3 and 4 in yellow to indicate the two sets of sites from two different capsomeres. Sites 1 and 2 contact the two adjacent gp7 subunits in one capsomere at the insertion loop on the end of the helix that is about 40 Å long (top blue gp7) and the distal end of the E-loop (top green gp7), respectively. The same gp10 subunit also makes contacts with the N-arm (bottom blue gp7, site 3) and the proximal portion of the E-loop (bottom green gp7, site 4) of two gp7 subunits in the adjacent capsomere. **d,** The two N-arms from two gp7 subunits clearly buttressing the gp10 dimer laterally at site 3. Gp7 is coloured from N terminus (blue) to C terminus (red).

Similar stabilizing roles have been ascribed to other phage decorating proteins[23,24], as well as being consistent with the role of PDZ domains in mediating protein interactions in large protein complexes[25]. The ε15 gp10 dimer interacts with the underlying gp7 shell around two-fold axes, whereas the decorating proteins in phage λ (ref. 24) and L (ref. 26) are located at the three-fold axes. However, in bacteriophage HK97, another tailed dsDNA bacteriophage with a similar structure, no accessory protein is needed because interactions between capsomeres are mediated through a covalently crosslinked chain-mail network[8]. As such, the 'molecular staple' role of gp10 is probably an alternative strategy taken by ε15 to maintain capsid stability and indicates the evolution of additional surface proteins in maintaining capsid stability in tailed dsDNA bacteriophages. Taken together, gp7 and gp10 form a complex network of interactions to protect the viral genome while maintaining an intact viral capsid in the face of various stressful conditions present in natural environments.

Beyond the insight into the structure and function of the ε15 bacteriophage capsid shell afforded by these models, this work signifies a new stage in the structural research of complex biological nanomachines. These biological nanomachines can now be studied in near-native solution conditions by cryo-EM without crystals, at a level of detail close to X-ray crystallography and nuclear magnetic resonance.

METHODS SUMMARY

Infectious bacteriophage ε15 was purified from cultures of *Salmonella anatum*[6]. The purified phage particles were rapidly plunge-frozen and imaged on a JEM3000SFF electron cryo-microscope operating at liquid-helium specimen temperature[16,17]. Of about 3,000 digitized photographic film images, about 40% preserved clear signals beyond a resolution of 6 Å and were used for further image processing and three-dimensional reconstruction. Individual particles (36,259) were manually selected from these micrographs and were then processed with EMAN[27]. These particle images were refined iteratively and reconstructed with a large-scale distributed Condor computing resource at Purdue University (http://web.rcac.purdue.edu/condorview). Icosahedral symmetry was imposed during refinement and reconstruction, resulting in the final 4.5-Å resolution structure of the icosahedral shell as assessed by the 0.5 Fourier shell correlation criteria[28]. Individual subunits were segmented from the reconstruction with Amira (http://www.amira.com) and Chimera[29] and then analysed with SSEHunter[30]. Coupling the cryo-EM densities with secondary structure elements predicted from the sequence, the Cα backbone models for each of the seven gp7 subunits were constructed individually. A full capsid model for gp7 was then generated by applying icosahedral symmetry to the gp7-based asymmetric unit. Analysis of the gp10 sequence was performed with a meta-prediction server (http://meta.bioinfo.pl), ALIGN[30] (http://workbench.sdsc.edu) and the NCBI psi-blast server (http://www.ncbi.nlm.nih.gov/blast). Structural alignments were calculated with MinRMS[31] and displayed with Chimera[29].

Full Methods and any associated references are available in the online version of the paper at www.nature.com/nature.

Received 23 September 2007; accepted 3 January 2008.

1. Kendrew, J. C. *et al.* A three-dimensional model of the myoglobin molecule obtained by x-ray analysis. *Nature* 181, 662–666 (1958)
2. Berman, H. M. *et al.* The Protein Data Bank. *Nucleic Acids Res.* 28, 235–242 (2000)
3. Baker, M. L., Jiang, W., Rixon, F. J. & Chiu, W. Common ancestry of herpesviruses and tailed DNA bacteriophages. *J. Virol.* 79, 14967–14970 (2005)

4 Bamford, D. H., Grimes, J. M. & Stuart, D. I. What does structure tell us about virus evolution? *Curr. Opin. Struct. Biol.* 15, 655–663 (2005)
5 Hendrix, R. W. & Duda, R. L. Bacteriophage HK97 head assembly: a protein ballet. *Adv. Virus Res.* 50, 235–288 (1998)
6 Jiang, W. *et al.* Structure of epsilon15 phage reveals organization of genome and DNA packaging/injection apparatus. *Nature* 439, 612–616 (2006)
7 Prevelige, P. E. Jr & King, J. Assembly of bacteriophage P22: a model for ds-DNA virus assembly. *Prog. Med. Virol.* 40, 206–221 (1993)
8 Wikoff, W. R. *et al.* Topologically linked protein rings in the bacteriophage HK97 capsid. *Science* 289, 2129–2133 (2000).
9 King, J., Haase-Pettingell, C., Robinson, A. S., Speed, M. & Mitraki, A. Thermolabile folding intermediates: inclusion body precursors and chaperonin substrates. *FASEB J.* 10, 57–66 (1996).
10 Sumkovsky, R. & King, J. An elongated spine of buried core residues necessary for *in vivo* folding of the parallel β-helix of P22 tailspike adhesin. *Proc. Natl Acad. Sci. USA* 103, 3575–3580 (2006)
11 Breitbart, M. & Rohwer, F. Method for discovering novel DNA viruses in blood using viral particle selection and shotgun sequencing. *Biotechniques* 39, 729–736 (2005)
12 Hendrix, R. W. Bacteriophages: evolution of the majority. *Theor. Popul. Biol.* 61, 471–480 (2002).
13 Wommack, K. E. & Colwell, R. R. Virioplankton: viruses in aquatic ecosystems. *Microbiol. Mol. Biol. Rev.* 64, 69–114 (2000)
14 Bottcher, B., Wynne, S. A. & Crowther, R. A. Determination of the fold of the core protein of hepatitis B virus by electron cryomicroscopy. *Nature* 386, 88–91 (1997).
15 Conway, J. F. *et al.* Visualization of a 4-helix bundle in the hepatitis B virus capsid by cryo-electron microscopy. *Nature* 386, 91–94 (1997)
16 Fujiyoshi, Y. *et al.* Development of a superfluid helium stage for high-resolution electron microscopy. *Ultramicroscopy* 38, 241–251 (1991).
17 Chen, D. H., Jakana, J. & Chiu, W. Single-particle cryo-EM data collected on a 300-kV liquid helium-cooled electron cryomicroscope. *J. Chinese Electron Microscopy Soc.* 26, 473–479 (2007)
18 Baker, M. L., Ju, T. & Chiu, W. Identification of secondary structure elements in intermediate-resolution density maps. *Structure* 15, 7–19 (2007).
19 Pan, J., Vakharia, V. N. & Tao, Y. J. The structure of a birnavirus polymerase reveals a distinct active site topology. *Proc. Natl Acad. Sci. USA* 104, 7385–7390 (2007)
20 Yuan, X. & Bystroff, C. Non-sequential structure-based alignments reveal topology-independent core packing arrangements in proteins. *Bioinformatics* 21, 1010–1019 (2005)
21 Agrawal, V. & Kishan, R. K. Functional evolution of two subtly different (similar) folds. *BMC Struct. Biol.* 1, 5 (2001).
22 Caspar, D. L. D. & Klug, A. Physical principles in the construction of regular viruses. *Cold Spring Harb. Symp. Quant. Biol.* 27, 1–24 (1962)
23 Iwasaki, K. *et al.* Molecular architecture of bacteriophage T4 capsid: vertex structure and bimodal binding of the stabilizing accessory protein. *Soc. Virology* 271, 321–333 (2000)
24 Yang, F. *et al.* Novel fold and capsid-binding properties of the lambda-phage display platform protein gpD. *Nature Struct. Biol.* 7, 230–237 (2000).
25 Nourry, C., Grant, S. G. & Borg, J. P. PDZ domain proteins: plug and play! *Sci. STKE* 2003, RE7 (2003).
26 Tang, L., Gilcrease, E. B., Casjens, S. R. & Johnson, J. E. Highly discriminatory binding of capsid-cementing proteins in bacteriophage L. *Structure* 14, 837–845 (2006).
27 Ludtke, S. J., Baldwin, P. R. & Chiu, W. EMAN: semiautomated software for high-resolution single-particle reconstructions. *J. Struct. Biol.* 128, 82–97 (1999).
28 Harauz, G. & van Heel, M. Exact filters for general geometry three dimensional reconstruction. *Optik* 73, 146–156 (1986).
29 Goddard, T. D., Huang, C. C. & Ferrin, T. E. Visualizing density maps with UCSF Chimera. *J. Struct. Biol.* 157, 281–287 (2007).
30 Pearson, W. R. Rapid and sensitive sequence comparison with FASTP and FASTA. *Methods Enzymol.* 183, 63–98 (1990)
31 Jewett, A. I., Huang, C. C. & Ferrin, T. E. MINRMS: an efficient algorithm for determining protein structure similarity using root-mean-squared-distance. *Bioinformatics* 19, 625–634 (2003).

Supplementary Information is linked to the online version of the paper at www.nature.com/nature.

Acknowledgements We thank D. Braun, P. Smith and B. Loftis; D. Sierkowski, P. Mikeal and S. Wilson for their support with the Condor computing system; and R. H. Goradia and M. Dougherty for digitizing the image data and preparing the Supplementary Movies respectively. This work was supported by grants from the National Institutes of Health and the National Science Foundation.

Author Contributions M.L.B. and W.J. conducted the structural analysis and contributed equally to this work. W.J. performed the image processing and reconstructions. J.J. collected the cryo-EM image data. P.R.W. performed the biochemical purification and characterization of ε15. M.L.B., W.J., P.R.W., J.K. and W.C. interpreted the results and wrote the manuscript.

Author Information The three-dimensional density map has been deposited into the EBI–MSD EMD database with accession number EMD-5003. The backbone model has also been deposited in the Protein Data Bank with accession number 3C58. Reprints and permissions information is available at www.nature.com/reprints. Correspondence and requests for materials should be addressed to W.C. (wah@bcm.edu) or W.J. (jiang12@purdue.edu).

Tools to Make Genotyping a SN(a)P

Image courtesy of Transgenomic

Single nucleotide polymorphisms (SNPs) are one of the most common types of genetic variation. Genetic Association studies utilizing SNPs are considered key to identifying the causes of many complex diseases as well as understanding the basis of variable response to drugs (pharmacogenetics). Researchers have an ever-increasing range of products and services for discovering and validating SNPs as genetic markers and for using them in large-scale genotyping efforts.

SNP Arrays

With a single SNP-specific or gene-specific qPCR, TissueScan Disease Panels from **OriGene** can reveal SNPs or expression changes of individual genes in a large number of tissues, providing a quick and comprehensive SNP analysis or expression profile. These arrays are panels of normalized cDNA prepared from pathologist-certified disease and normal samples. As the samples on each TissueScan Disease Panel are derived from 48 individuals, they can be used to study the frequency of a particular SNP. Comparing the diseased with the normal tissues may reveal a potential association of genotypes with disease. Currently available panels include lymphoma, sarcoma, melanoma, breast, prostate, lung, colon, ovarian, liver, bladder, endometrial, and kidney cancer, as well as Crohn's disease and colitis.

Affymetrix, Inc. recently announced the launch of its Genome Wide Human SNP Array 6.0, a single microarray that measures more than 1.8 million markers for genetic variation. The array enables researchers to perform powerful whole-genome association studies by genotyping more markers from more individuals at a lower cost per sample. This increases the probability of discovering genes associated with adverse drug response or complex diseases such as Alzheimer's, diabetes, heart disease, and Parkinson's. The Affymetrix® SNP Array 6.0 contains more than 900,000 SNPs and more than 946,000 non-polymorphic probes for the detection of copy number variation. Researchers can use the same array to test multiple study or disease hypotheses simultaneously, and the same meta analysis can be used across multiple cohorts. The Affymetrix® SNP Array 6.0 was developed in collaboration with the Broad Institute of Harvard University and the Massachusetts Institute of Technology.

The Infinium BovineSNP50 BeadChip, a 12-sample genotyping array, is now available from **Illumina, Inc.** for detecting genetic variation in any breed of cattle. Developed in collaboration with leading bovine researchers from the United States Department of Agriculture-Agricultural Research Service (USDA-ARS), the University of Missouri-Columbia, the University of Alberta, and other industry partners, the BovineSNP50 BeadChip features more than 54,000 SNPs evenly spaced across the entire bovine genome, 24,000 of which are not available on any other commercial array or in any public database. Illumina also recently released the Infinium CanineSNP20 BeadChip, a 22,000-SNP panel developed in collaboration with the Broad Institute and the University of California, Davis. To date, Illumina has developed customized genotyping solutions for 15 nonhuman species using both the GoldenGate® and Infinium Assays.

Applied Biosystems has signed a licensing and collaboration agreement with **BioTrove, Inc.** to commercialize an analysis platform for high-throughput genotyping applications. Applied Biosystems will develop and market custom-built arrays of TaqMan® SNP Genotyping Assays pre-loaded on BioTrove's OpenArray™ platform,

Figure 1. The Affymetrix® Genome-Wide Human SNP Array 6.0 contains more than 900,000 single nucleotide polymorphisms (SNPs) and more than 946,000 non-polymorphic probes for the detection of copy number variation on one chip.

Figure 2. Tissue Scan Disease Panels from OriGene provide for quick and comprehensive SNP analysis on a large number of tissues from a single PCR reaction.

which will enable researchers to perform genotyping studies that investigate tens to hundreds of SNPs across hundreds to thousands of samples.

SNP Services

SNP detection and validation services are offered on several different platforms at **SeqWright**, based upon users' needs. As a GLP-compliant, Affymetrix Authorized Service Provider, SeqWright offers the latest in SNP detecting microarray technology. For large-scale screening and *de novo* SNP discovery, SeqWright offers SNP detection as an official SOLiD™ Service Provider on ABI's next generation SOLiD™ platform, which interrogates each base twice, thereby minimizing false SNP calls. Once SNPs have been discovered, they can be confirmed through SeqWright's Sanger-based SNP validation services.

Genotyping on both the BovineSNP50 and CanineSNP20 products is available as a service through the **Illumina** FastTrack Genotyping Services group. Researchers can also take advantage of the iSelect™ Infinium Custom product process to design powerful multisample BeadChips with specific disease-related or pathway-related SNPs for their organisms.

Other Products for SNP Analysis

PrimeSTAR™ HS DNA Polymerase from **Takara Bio** is a novel PCR enzyme that provides maximum fidelity as well as extended product length (8.5 kb for human genomic DNA; 22 kb for λ DNA). It offers extremely high accuracy (10x higher fidelity than *Taq*, 5x higher than *Pfu*) and is the only enzyme whose fidelity is calculated by sequence analysis. The antibody-mediated hot start formulation prevents false initiation events during reaction assembly due to mispriming or primer digestion, thus lowering background. PrimeSTAR™ HS offers the high fidelity, high sensitivity, and high specificity required for demanding SNP genotyping applications.

A wide variety of oligonucleotides to support most SNP detection platforms is available from **Integrated DNA Technologies** (IDT), ranging from unmodified PCR or sequencing primers to dual-labeled probes. IDT's Molecular Beacons and Dual Labeled Locked Nucleic Acid (LNA) Probes are ideal for investigating single nucleotide polymorphisms. Since the hairpins in probes containing Molecular Beacons result in enhanced specificity for their targets, they are often better able to discriminate SNPs than simple linear probes. Selective incorporation of LNA bases correctly positioned within the oligonucleotide sequence also improves SNP assay discrimination by conferring increased sensitivity to base mismatch. Quality control of all oligonucleotides is performed with mass spectrometry, and purified oligonucleotides also receive capillary electrophoresis (CE) QC.

The combination of **Invitrogen's** Platinum® Taq Polymerase and PCR mixes with SYTO® 9 Dye is ideal for use in High Resolution Melt (HRM) analysis. Following PCR the dsDNA binding SYTO® 9 dye is bound to the amplicons, which are then slowly heated to determine their exact melting temperature in order to distinguish homozygosity from heterozygosity of the SNP in question. Invitrogen also provides amplification enzymes and detection reagents for genotyping platforms such as Affymetrix and Illumina.

Transgenomic now provides a high-throughput SURVEYOR® Mutation Detection Kit for Universal Primer Fluorescent Capillary Electrophoresis. The new mutation detection system is designed to digest target DNA, amplified with two Universal Fluorescent Primers included in the kit, for subsequent analysis by fluorescent capillary electrophoresis. SURVEYOR nuclease is an endonuclease that recognizes mismatches in heteroduplex dsDNA and cleaves both DNA strands on the 3' side of the mismatch site. SURVEYOR nuclease cleaves all types of mismatches arising from the presence of single nucleotide polymorphisms, small insertions, or deletions in normal/mutant heteroduplexes. Subsequent size determination of the resulting fragments by capillary electrophoresis pinpoints the location of the mutation. Kits are also available for standard gel electrophoresis and DHPLC/Wave® system analysis.

"Researchers are increasingly using next-generation sequencing platforms to identify novel SNPs in the genome. We've also seen this methodology applied to nonhuman genomes, and as a result, customized microarrays are being developed for focused research."

Carsten Rosenow, Ph.D.
Senior Marketing Manager, DNA Analysis Products
Illumina, Inc.

Companies listed in editorial:

Affymetrix
www.affymetrix.com
Applied Biosystems
www.appliedbiosystems.com
Illumina
www.illumina.com
Integrated DNA Technologies
www.idtdna.com
Invitrogen
www.invitrogen.com
OriGene
www.origene.com
SeqWright
www.seqwright.com
Takara Bio
www.takara-bio.com
Transgenomic
www.transgenomic.com

NATURE|Vol 451|28 February 2008

THE CAREERS MAGAZINE FOR SCIENTISTS

- FOCUS
- SPOTLIGHT
- RECRUITMENT
- ANNOUNCEMENTS
- EVENTS

nature jobs

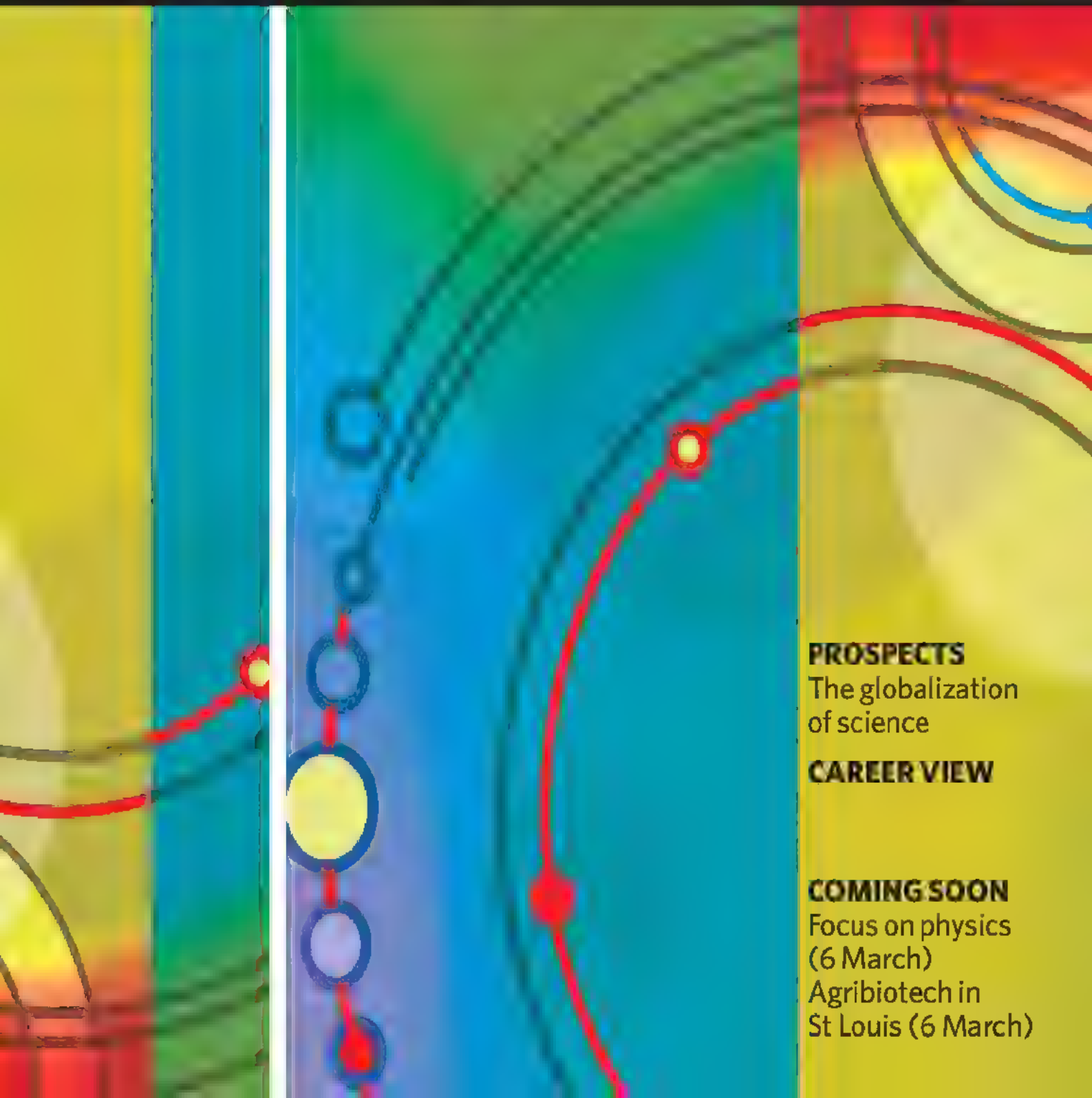

PROSPECTS
The globalization of science

CAREER VIEW

COMING SOON
Focus on physics (6 March)
Agribiotech in St Louis (6 March)

L'Oréal UK and Ireland Fellowships for Women in Science

in partnership with the United Kingdom National Commission for UNESCO, the Irish National Commission for UNESCO, the Royal Institution of Great Britain and the UK Resource Centre for Women in Science, Engineering and Technology

CALL FOR APPLICATIONS 2008

Dr Anna Git
Cancer Research UK
Cambridge Research Institute

Dr Araxi Urrutia Odabachian
University of Bath

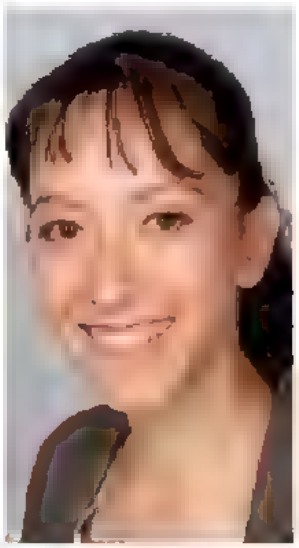

Dr Theresa Burt de Perera
University of Oxford

Dr Selrian Sumner
Zoological Society of London

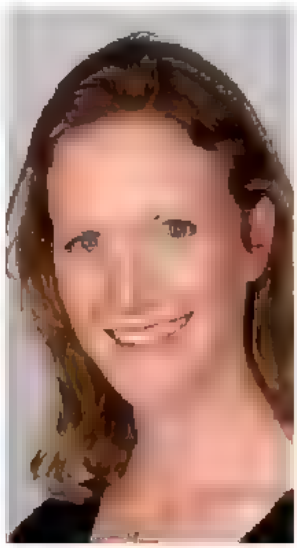

In July 2007, four exceptional women scientists were awarded with For Women in Science national fellowships to encourage the advancement of their research.

In 2008, four fellowships of £15,000 (equivalent € for Irish candidates) will be offered to outstanding female scientists. They are tenable at any UK or Irish university or research institution to support 12 months of postdoctoral research in the life or physical sciences.

The prize money can be spent in any number of innovative ways to enable women scientists to further their careers and facilitate world class research.

For further information, and to apply, please visit:

www.unesco.org.uk/For_Women_In_Science.htm

The deadline for applications is Wednesday 2 April 2008

FOR WOMEN IN SCIENCE

United Nations Educational, Scientific and Cultural Organization

L'ORÉAL UK & IRELAND

The Royal Institution of Great Britain

UK Resource Centre for Women

United Kingdom National Commission for UNESCO Irish National Commission for UNESCO

U125568A

naturejobs

JOBS OF THE WEEK

Globalization implies increased information sharing, capital investment and communication among the countries of the world. In other words, it's a greater integration of economies and labour markets. But when it comes to science, globalization's reach has been less than global.

At the meeting of the American Association for the Advancement of Science in Boston earlier this month, several sessions examined the effects of globalization. For instance, Mark Fishman, president of the Novartis Institutes for BioMedical Research, explained why the Swiss company seeks scientists in India and China and why it has moved its research headquarters to Boston: it follows the talent. In the case of Boston, it wanted an entrepreneurial talent base that was not too risk averse, which is harder to find in Switzerland, said Fishman.

Several speakers noted the rising prevalence of branches of US universities overseas where funds are plentiful and nations are looking to diversify their economies. In the Qatari desert, for example, Cornell University has set up a medical school, Texas A&M teaches engineering and Georgetown University holds classes on foreign services.

But from Nigeria to Mexico, and Indonesia to Chile, globalization is less obvious. One potentially disappointing, even damaging, trend in these nations is an increased prevalence of private universities — schools that are often unaccredited and that tend to favour more profitable business-administration classes over a basic-science curriculum. This was the thesis of Wayne Patterson, a programme manager for developing countries at the US National Science Foundation. Patterson canvassed representatives from 19 countries and found that most shared his concerns, citing a lack of money, a shift in students' careers away from science, and a continued loss of scientific talent to regions such as Europe and the United States.

So far, science's spread is more of a regionalization or a concentration than a globalization. This is quite a shame, as developing nations could stand to benefit most from research talent and innovation.

Gene Russo, acting editor of *Naturejobs*

CONTACTS
Acting Editor: Gene Russo

US Head Office
New York
75 Varick Street, 9th Floor
New York, New York 10013-1917
Tel: +1 800 989 7718
Fax: +1 800 989 7103
e-mail: naturejobs@natureny.com

US Sales Manager/Corporations:
Peter Bless
Tel: +1 800 989 7718

San Francisco Office
Classified Sales Representative:
Michaela Bjorkman
West USA/West Corp. Canada
225 Bush Street, Suite 1453
San Francisco,
California 94104
Tel: +1 415 781 3803
Fax: +1 415 781 3805
e-mail: m.bjorkman@nature.com

India
Vikas Chawla
Tel: +91 124 2881057
e-mail: v.chawla@nature.com

European Head Office, London
The Macmillan Building,
4 Crinan Street,
London N1 9XW, UK
Tel: +44 (0) 20 7843 4961
Fax: +44 (0) 20 7843 4996
e-mail: naturejobs@nature.com

European Sales Manager:
Andy Douglas (4975)
Advertising Production Manager:
Stephen Russell
To send materials use London address above.
Tel: +44 (0) 20 7843 4816
Fax: +44 (0) 20 7843 4996
e-mail: naturejobs@nature.com
***Naturejobs* web development:** Tom Hancock
***Naturejobs* online production:** Dennis Chu

Japan Head Office, Tokyo
Chiyoda Building, 2-37
Ichigayatamachi,
Shinjuku-ku, Tokyo 162-0843
Tel: +81 3 3267 8751
Fax: +81 3 3267 8746

Asia-Pacific Sales Manager:
Ayako Watanabe
Tel: +81-3-3267-8765
e-mail: a.watanabe@natureasia.com
Business Development Manager, Greater China/Singapore:
Gloria To
Tel: +852 2811 7191
e-mail: g.to@natureasia.com

MOVERS

Felipe Pereira, distinguished professor, School of Energy Resources and Department of Mathematics, University of Wyoming, Laramie

1999–2007: Professor, computational and applied mathematics, State University of Rio de Janeiro, Brazil
1997–99: Visiting professor, State University of Rio de Janeiro, Brazil
1997–99: Associate researcher National Laboratory for Scientific Computing, Petrópolis, Brazil

Felipe Pereira made his mark in the world of applied mathematics by modelling the flow of oil in underground reservoirs — information needed for the efficient extraction of this precious resource. Although he will continue working on such models, his latest research challenge is a sign of changing times. As one of the distinguished faculty members at the new School of Energy Resources at the University of Wyoming in Laramie, Pereira will apply those same skills to determine how best to inject and sequester carbon dioxide beneath Earth's surface and so help reduce its contribution to climate change.

Pereira studied physics at the Federal University of Minas Gerais in his native Brazil. As a graduate student under Michael O'Carroll, a US mathematician working at the interface of quantum field theory and statistical mechanics, Pereira became increasingly interested in applied mathematics. Impressed when Pereira quickly solved a problem that had stumped him, O'Carroll directed his student to James Glimm and the maths PhD programme at New York University.

There in 1985, with funding from the Brazilian government, Pereira began working on simulations relating to gas dynamics and oil reservoirs. Until this time Pereira had never used a computer, so when he followed Glimm to the State University of New York at Stony Brook, he set about honing his computing skills.

Moving to Purdue University in West Lafayette, Indiana, in 1994, Pereira worked with Jim Douglas, the top oil-reservoir modelling and simulation mathematician of the time. Douglas says that Pereira provided key information about underground flows of oil despite a lack of detailed data from studies probing beneath Earth's surface, which often were not feasible. After three years, Pereira returned to Brazil, first at the National Laboratory for Scientific Computing in Petrópolis and then as a faculty member at State University of Rio de Janeiro.

As he takes on his new position in Wyoming, Pereira says that applied mathematics has a critical role to play in the energy field because oil will still be needed to supply our immediate energy needs, and sequestering carbon is one way to mitigate the effects of greenhouse-gas emissions. Douglas agrees, noting that applied mathematics remains a very active field as it offers a way to solve such real-world problems. ■

Virginia Gewin

NETWORKS

Neuroscience in the developing world

How do you teach neuroscience techniques in countries bereft of funding and infrastructure? In Argentina, the education programme of the International Brain Research Organization (IBRO) found a creative answer: crabs.

John Hildebrand, one of the founders of the IBRO's international schools, chose Buenos Aires for a class on neuroethology, the neural basis of natural behaviour. Crabs, which provide good nervous-system models, were abundant. "Students work with little crabs they collect in mud flats near the seashore," says Hildebrand, a neuroscience professor at the University of Arizona, Tucson. "They have no animal-rearing costs. They can work in shirtsleeves and do very beautiful work."

But the three-week course — which attracted students from several Latin American countries — was no seaside outing. During a week each of lectures, fieldwork and experiments, work started early and discussions continued late into the evenings.

The IBRO offers courses in developing countries at four levels — from basic lectures introducing neuroscience concepts to courses teaching the latest brain-science techniques and analysis of complex data sets. Students can start on the introductory rung and work on up.

The IBRO uses visiting teams of six or seven scientists. They hold classes in places that have had little interaction with the West, including the Andes, Iran and remote parts of Africa. One challenge is deciding what technology to take with them and use in the host countries. Picking the right model organism, such as the crabs in Argentina, provides a way to bridge the resources gap. They have used insects in Africa and frogs in China.

The course has informed and even altered career paths. It inspired one medical student from Uruguay to switch to neuroscience: a bold move because medicine is a more stable, lucrative profession in Latin America. "Doing what she did was a very, very risky decision," says instructor Martín Giurfa, an Argentinian neuroscience professor now at the University of Toulouse, France. He was gratified when she told him later that she had made the right decision.

In Argentina, the course included discussions of career concerns. Drawing on his own experience (see *Nature* **451**, 494–496; 2008), Giurfa said that pursuing a scientific career in a developing country is challenging, but can be done: "You just have to fight and fight and fight." ■

Paul Smaglik

POSTDOC JOURNAL

Role models

Having postdocs rather than professors as 'role models' may seem a bit odd, but I am fortunate to have several postdoc friends who have been exactly that. They enrich my life by the diversity of their expertise and personalities. One is a cell biologist who plays a Renaissance-era trombone and runs marathons, showing that scientists can maintain a healthy work–life balance. Another is a structural biologist who taught me much about biophysics and pushed me to run farther and faster. Yet another is a virologist who combines motherhood with good science, thanks to efficiency and a positive attitude.

They may not be deans or directors, but nor are they like statues on pedestals. I can relate to them. Their dedication and rigour inspire me more than their awards. Knowing their struggles increases my respect for them, and I hope that I can similarly overcome adversity. Most importantly, they take the time to mentor and to be friends, sharing joys and disappointments alike.

In young labs such as my current one, where most of us are first-time postdocs, peer support is a substitute, to some extent, for mentorship. We are like first-time kayakers navigating expert-level class V whitewater. I'm cold and drenched but still paddling. And now it's my turn to serve as a role model as best I can, to try to help others navigate those waters. ■

Amanda Goh is a postdoctoral fellow in cell biology under the Agency of Science, Technology and Research in Singapore.

EMBL

The European Molecular Biology Laboratory is an international research organisation offering a highly collaborative, uniquely international culture. It fosters top quality, interdisciplinary research by promoting a vibrant environment consisting of young independent research groups with access to outstanding graduate students and post-doctoral fellows. The Scientific Programme of EMBL emphasises experimental analysis at multiple levels of biological organisation, from the molecule to the organism, as well as Computational Biology, Bioinformatics and Systems Biology. In addition to exciting colleagues, the laboratory provides excellent shared facilities for a variety of advanced experimental approaches. High-level expertise is also available in Computational Biology, diverse aspects of experimental Molecular Biology as well as Physics, Biophysics, Chemical Biology and instrument development.

Group Leaders Heidelberg, Germany

Structural and Computational Biology Unit

The vision of the Structural and Computational Biology Unit is to provide a detailed spatial and temporal description of various biological systems across different scales of resolution (from molecules to cells) by combining different structure determination techniques (X-ray, NMR, cryo-EM, EM tomography) with computational, chemical and systems biology. We would like to recruit one Group Leader for each of the two areas:

Electron Microscopy/X-ray Crystallography

Ref. no. N/08/14

The successful candidate should work with one or more of the major structure determination techniques, electron microscopy (single particle EM and/or tomography) or X-ray crystallography, and apply these techniques to address fundamental questions in molecular or cellular biology. Particular interests of the unit are dynamics and architecture of protein assemblies and protein-protein interaction networks.

Structural Systems Biology/Chemical Biology/ Biochemistry

Ref. no. N/08/13

The successful candidate is expected to pursue a strong experimental research program at the intersection of cellular, molecular, structural and computational biology. (S)he should integrate various experimental approaches complementary to those already existing in the unit to tackle fundamental biological questions. Example research areas are the in vitro and in vivo characterisation of macromolecular assemblies, protein or small molecule interaction mapping, innovative molecule labelling, dynamics of molecular machines or metabolome research.

An initial contract of 5 years will be offered to the successful candidates. This can be renewed, depending on circumstances at the time of review.

EMBL is an inclusive, equal opportunity employer offering attractive conditions, benefits and child care facilities appropriate to an international research organisation.

Closing date: 6 April 2008

To apply, please email a CV, a concise description of research interests and future research plans and three letters of recommendation, quoting the corresponding reference number in the subject line, to:
application@embl.de

www.embl.org

W126403R

UNIS

UNIS provides education and perform science with basis in the geographical location of Svalbard within a high Arctic area, and the excellent advantage this gives. Approximately half of the staff and students are from abroad, and all teaching are done in English. UNIS is located in new and modern locations in Longyearbyen, Svalbard, with very good access to modern laboratories and equipment. UNIS is a state-owned limited company

Full/Associate Professor in Arctic Terrestrial Ecology

More information about the position can be found at **www.unis.no**

Contact: Associate Professor Steve Coulson, phone +47 79 02 33 34, email steve.coulson@unis.no
Please apply online on www.unis.no – vacant positions

Deadline for application is 31st of March

W126245R

The newly founded Interdisciplinary Center for Molecular Materials (ICMM) offers the position of

W2-Professur für Molecular Nanostructures

at the earliest possible date. The position is located in the Department of Chemistry and Pharmacy in the Faculty of Natural Sciences.

The successful applicant is expected to fulfil teaching and research obligations in the field of Chemistry with particular emphasis on Molecular Materials, Supramolecular Chemistry and Nanochemistry. The active participation in other collaborative research initiatives, such as the cluster of excellence "Engineering of advanced materials" is highly appreciated.

Qualifications include university undergraduate and doctoral degrees, good teaching skills, and a habilitation or equivalent other qualification, which may have been gained outside the University or within a "Juniorprofessur".

At the time of appointment the candidate must not be older than 52 years of age. The Ministry for Science, Research and Art may allow an exception in special cases, which has to be approved by the Ministry of Finance.

The University of Erlangen-Nuremberg actively encourages applications from female candidates in an effort to increase female representation in research and teaching.

Applications from the severly disabled having the same suitability for appointment as other candidates will be given priority.

Application documents (curriculum vitae, photograph, list of publications and teaching activities, certified copies of degree certificates but no publications) must be sent by the latest **March 31, 2008**, to: Dekan der Naturwissenschaftlichen Fakultät der Universität Erlangen-Nürnberg, Universitätsstr. 40, D-91054 Erlangen.

Friedrich-Alexander-Universität Erlangen-Nürnberg

www.uni-erlangen.de

W126373R

UCL

UCL Institute of Nuclear Medicine

Esperança Chair of Molecular Imaging

This is a new Chair at the Institute of Nuclear Medicine (INM) of UCL (University College London), established for the development of a molecular imaging programme based on radiolabelled ligands. A novel initiative aims to develop interfaculty links between Medicine and Chemical Biology at UCL in a programme of translational research. The Chair will be housed within the Centre for Chemical Biology and will develop technologies for the investigation of the phenotype expression of disease, from the laboratory to man, using advanced PETCT and SPETCT imaging technologies.

Significant opportunities have also arisen with the successful award of a Comprehensive Biomedical Research Centre arising from a collaborative partnership between University College London Hospitals (UCLH) and UCL, resulting in a new radiochemistry facility being developed and a Senior Lecturer post established.

The Chair will conceptually lead and develop the infrastructure and a team for the above programme, spanning the areas of oncology, cardiovascular and neurological applications. The ideal candidate will have an international reputation in radiopharmaceutical research, spanning the area from basic science to clinical applications, a proven record in obtaining grant support, and experience and/or potential in running a multidisciplinary team. Salary will be negotiable on the professorial scale.

Informal enquiries may be made to Professor Peter Ell, Director, Institute of Nuclear Medicine, tel: +44 (0)207 631 1066, email: peter.ell@uclh.nhs.uk, or to Professor Stephen Caddick, Professor of Organic Chemistry and Chemical Biology, Department of Chemistry, tel: +44 (0)207 679 2071, email: s.caddick@ucl.ac.uk. Further particulars and application details for the post can be obtained from Professor Ell.

We particularly welcome female applicants and those from an ethnic minority, as they are currently under-represented within UCL at this level.

Closing date: 30th April 2008.

U126123R

University of Oxford

Department of Earth Sciences
(In Collaboration with Plant Sciences and Zoology)

Postdoctoral Research Associate and PhD Student for ERC-funded Project "GRACE"

Applications are invited for a Research Associate and a PhD student to work as part of a new ERC (European Research Council) funded interdisciplinary team at the University of Oxford. The GRACE (Genetic Record of Atmospheric Carbon dioxidE) project aims to investigate the climate signals harboured within the "living geological record", the genes encoding photosynthetic proteins. The prime motivation is the reconstruction of history of atmospheric gases from adaptive signals within the genetic make-up of extant photosynthesizing organisms, but the project will yield additional insight into the interactive feedback between vegetation and climate and carbon isotopic signatures found in the geological record. You will ideally have experience in one or more areas of molecular biology, biochemical assays and plant or algal physiology and photosynthesis. For informal enquiries about the project, please contact Ros Rickaby by e-mail: ros@earth.ox.ac.uk

Postdoctoral Research Associate

£26,666 - £32,796 p.a.

You will have a PhD (or equivalent) in Zoology, Plant Sciences, Earth Sciences, Molecular Biology, Marine Sciences, Biochemistry or similar, have current and relevant analytical experience and a demonstrated record of research and innovation.

The deadline for applications is 25 April 2008. Further Particulars and details on how to apply are available from www.earth.ox.ac.uk/department/vacancies.htm or e-mail: caroline.hutchings@earth.ox.ac.uk quoting reference DQ/08/02.

PhD Student

You will have a Master's or Bachelor's (or equivalent) in Zoology, Plant Sciences, Earth Sciences, Molecular Biology, Marine Sciences, Biochemistry or similar and a track record for academic excellence.

For details on how to apply please e-mail: emma.brown@earth.ox.ac.uk or tel. (01865) 272043. The deadline for applications is 11 April 2008.

As an Equal Opportunity employer, we positively encourage applications from people of all backgrounds

U126384RM

www.ox.ac.uk/jobs

Faculty Position - Viral Genome Analysis Initiative

The Wellcome Trust Sanger Institute announces a strategically important initiative in Virus Genome Analysis, employing state-of-the-art sequencing power and informatics expertise at the Institute to analyse the genomes of several classes of virus implicated in human and animal disease. The aim is to link sequence variation to phenotype/pathogenicity and also to identify new viral pathogens The project will be in collaboration with clinical virologists, infectious disease physicians, epidemiologists and scientific collaborators from around the world.

We are searching for an independent Faculty level individual to lead in this new area. Applicants should ideally be experienced both in the study of viruses involved in human and animal disease and in the generation and analysis of genomic information, and should have a PhD and/or MD. The project will be core supported by dedicated staff and the Sanger sequencing pipelines, but the successful candidate will also be expected to seek external funding.

Applicants may contact Julian Parkhill (Director of Sequencing) email: parkhill @sanger.ac.uk, Gordon Dougan (Head of Pathogens) email: gd1@sanger.ac.uk or Michael Stratton (WTSI Deputy Director) email: mrs@sanger.ac.uk for further information.

Applicants should send curriculum vitae, complete list of publications and details of 3 referees accompanied by:

- A summary of scientific achievements (approx 1-2 pages)
- An outline of research plans (approx 2-3 pages) indicating how these would link in with other Sanger programmes and infrastructure.

Please email to facultysearch@sanger.ac.uk or post to
Sancha Martin
Faculty Search Committee,
The Wellcome Trust Sanger Institute,
Wellcome Trust Genome Campus,
Hinxton, Cambridgeshire,
CB10 1SA, UK

Application deadline: 14th March 2008

www.sanger.ac.uk

Working towards equality through diversity

wellcome trust sanger institute

Genome Research Limited is a Registered Charity No. 10211457

J126146R

Principal Investigator

International Center for Materials Nanoarchitectonics
National Institute for Materials Science, JAPAN

The National Institute for Materials Science (NIMS) invites applications for principal investigators of the International Center for Materials Nanoarchitectonics (MANA). The ultimate research goal of MANA is to develop novel materials that support "sustainable development." MANA will contribute to solving various serious problems confronting humankind in the 21st century concerning environment, energy, resources and others, from the direction of materials, which is one of Japan's greatest strengths. Additional information about MANA is available at http://www.nims.go.jp/mana.

The candidate should be a world's top-caliber researcher in any aspect of Materials Science with a strong record of outstanding research performance. The candidate must also be able to demonstrate his/her potential for attracting external research funding The base salary ranges from 15,000,000 JPY to 20,000,000 JPY, depending on qualifications and experience. We offer enough start-up funds, a high degree of work autonomy, and a highly international research environment with new state-of-the-art equipments and facilities.

Candidates should send a curriculum vitae, bibliography, statement of research interests and a list of references to mana@nims.go.jp by May 30, 2008. Only electronic submission will be accepted.

JP125910R

MANCHESTER 1824

The University of Manchester

www.manchester.ac.uk/vacancies

Faculty of Life Sciences

Manchester Interdisciplinary Biocentre

Postdoctoral Research Associate

£26,666 - £29,139 p.a. **Ref: LS/028/08**

You will work on a BBSRC funded project that will apply methods of genetics, biophysics, biochemistry and structural biology to the study of proteins involved in mRNA metabolism and its regulation. The project will examine interdependent structure-function relationships the role of these proteins in gene expression and their subcellular localisation.

The above project will be based in the McCarthy group, housed in the Manchester Interdisciplinary Biocentre (www.manchester.ac.uk/mib) which, with support from the Wellcome Trust and the Wolfson Foundation, has been constructed to accommodate a range of research at the interface between the physical sciences and biology

You should hold a PhD or equivalent and have some experience of biochemical work on a eukaryotic system.

This position is available until 31 December 2009.

Informal enquiries should be made to Professor John McCarthy, Email: john.mccarthy@manchester.ac.uk Tel: +44 (0) 161 306 8916.

Application forms and further particulars are available from our website or by contacting +44 (0) 161 275 8836 or Lifesciences-hr@manchester.ac.uk quoting the reference number.

Closing date: 21 March 2008.

Faculty of Engineering and Physical Sciences

School of Chemical Engineering and Analytical Sciences

Manchester Interdisciplinary Biocentre

Postdoctoral Research Associate – Systems Analysis of Translation

£26,666 - £29,139 p.a. **Ref: EPS/80016**

A BBSRC funded Postdoctoral position is available in the Manchester Interdisciplinary Biocentre to work with Professor John McCarthy and Professor Hans Westerhoff. The position involves experimental rate control analysis of the eukaryotic translation initiation pathway, both *in vivo* and *in vitro*.

We seek an enthusiastic and highly capable researcher with appropriate experience in computational data handling and/or experimental lab experience in molecular biology. You should have an interest in systems biology approaches, and have a keen interest in computational analysis and/or model building, ideally in relation to gene expression systems. However, candidates with other relevant experience in quantitative bioscience are also welcome to apply.

The position will be for two years. Funding is available to support a candidate with three years' postdoctoral experience

The work will be carried out in the newly opened Manchester Interdisciplinary Biocentre (www.mib.ac.uk) which, with support from the Wellcome Trust and the Wolfson Foundation has been constructed to accommodate a range of research at the interface between physical sciences and biology

This project will be supported by a full time technician.

Informal enquiries should be made to Professor John McCarthy. Email: john.mccarthy@manchester.ac.uk Tel: +44 (0) 161 306 8916.

Application forms and further particulars are available from our website or by contacting +44 (0) 161 275 8837 or eps-hr@manchester.ac.uk quoting the reference number.

Closing date: 21 March 2008.

Faculty of Medical and Human Sciences

School of Clinical and Laboratory Sciences

Research Assistant

£22,332 - £25,889 p.a. **Ref: MHS/073/08**

This project, conducted at the Maternal and Fetal Health Research Centre at St Mary's Hospital, Manchester will investigate the effects of growth factors on trophoblast invasion. Our general aim is to improve understanding of early placental development in the human. These studies will involve collection and analysis of human placentas, using cell culture and trophoblast isolation techniques, immunohistochemistry, western blotting and quantitative PCR.

You will have a BSc in Biological Science, or equivalent, together with postgraduate laboratory experience. A PhD is preferable but not essential. Experience in one or more of the techniques (cell culture, Western Blotting, Quantitative PCR) is also required. Work on the placenta would be an advantage but is not essential.

The project will be for one year in the first instance

Informal enquiries may be made to Dr Clare Tower, Clinical Lecturer, email: clare.tower@manchester.ac.uk

Application forms and further particulars are available from our website or by contacting +44 (0) 161 275 1197 or julie.heydon@manchester.ac.uk quoting the reference number.

Closing date: 14 March 2008.

The University will actively foster a culture of inclusion and diversity and will seek to achieve true equality of opportunity for all members of its community.

C126410R

Umeå University

announces...

Umeå University in Northern Sweden is a dynamic university with appr. 3 800 employees and more than 29 000 students of which 1 300 are in PhD programs. **The Chemistry and Biology Center, KBC,** at Umeå University comprises five departments with almost 600 employees and about 200 PhD students. For a general presentation of Umeå and the university, see the homepage of the International office: <www.umu.se/international office>

A number of post-doctoral fellowships at the Chemistry and Biology Center

The Chemistry and Biology Center, KBC, at Umeå University hereby advertises nine two-year post-doctoral fellowships for collaborative projects within the center. The fellowships have been made possible through a generous contribution from The Kempe Foundation.

Titles of the nine projects are as follows:

Structural and functional studies of the plant Mediator in transcriptional regulation
Ref no 315-769-08

Protein-mediated remodeling of biological membranes
Ref no 315-771-08

Structure of the eukaryotic leading strand DNA polymerase
Ref no 315-772-08

NMR structural studies of transient protein states critical for human amyloid diseases
Ref no 315-773-08

A systems biology approach to elucidate mechanism underlying enhanced growth in hybrid aspen
Ref no 315-774-08

Speciation and dynamics of organic phosphorus in terrestrial and aquatic ecosystems
Ref no 315-775-08

Molecular design for organic electronics
Ref no 315-776-08

Are plants cultivated in growth chamber actually the same as plants grown outdoor? – A study using comparative proteomics, metabolomics and transcriptomics
Ref no 315-777-08

Metabolomics and chemometric bioinformatics to find markers for tumor detection, prognosis, progression and therapy prediction: prostate, ovarian and brain malignancies
Ref no 315-778-08

A detailed description of the various projects can be found on the following address: <www.chemistry.umu.se>.

Union information is available from SACO, +46-(0)90-786 53 65, SEKO civil, +46-(0)90-786 52 96 and ST, +46-(0)90-786 54 31.

Successful candidates should have earned a PhD degree in fields relevant for the positions.

A complete application should include:

- Introductory letter with a statement of research interest
- CV
- A list of publications
- Names and contacts of three persons willing to act as references

Your application should be marked with the appropriate Ref no for the postdoc position. If You apply to several fellowships You have to send an application for each position. Documents sent electronically should be in MS Word or PDF format.

Your complete application (state the reference number as subject, when You submit the electronic application), should be sent to <jobb@umu.se> the Registrar, Umeå University, SE-901 87 Umeå, Sweden to arrive no later than **28 March, 2008.**

We look forward to
receive your application!

UMEÅ UNIVERSITET

W126187A

Creighton
UNIVERSITY
Medical Center
School of Medicine

Department of Biomedical Sciences
Chair, Professor-Tenure Track

Creighton University School of Medicine invites applications and nominations for Chair of the Department of Biomedical Sciences. Information about the department can be found at http://www2.creighton.edu/medschool/medicine/departments/biomedicalsciences/. The school is seeking an individual with leadership ability and administrative experience who will work with faculty, other chairs, students, and senior administration to promote excellence in meeting all missions of the department, school, and university. The major responsibilities of the Chair are to promote high quality scholarship by faculty and trainees, provide leadership in creating and implementing a vision to enhance existing programs and develop new initiatives, and to oversee research and teaching in the department.

The successful candidate should have a Ph.D. and should preferably be at or qualified for the rank of Professor. He/she should also have a record of distinguished research accomplishments highlighted by publications in peer-reviewed journals, and a research program supported by ongoing extramural funding. A strong commitment to mentoring in order to promote professional growth and development of faculty in the department and to establishing collaboration with faculty in other basic and clinical science departments is essential.

The School of Medicine is one of nine schools or colleges at Creighton University including professional schools of Business, Law, Nursing, Dentistry, Pharmacy and Health Professions, and a Graduate School. Founded in 1878, Creighton University is a Catholic, Jesuit institution with an enrollment of approximately 6725 students. It is consistently ranked as one of the finest comprehensive universities in the nation by U. S. News and World Report and regularly appears in Best Buys in American Colleges.

Applications will be accepted until the position is filled.

A Curriculum Vitae and letter of application that includes a description of administrative and teaching experiences, current and future research activities and funding sources, and the names and contact information of three references may be submitted by mail or e-mail to:

Richard V. Goering, Ph.D.
Chair, Biomedical Sciences Search Committee
Chair, Department of Medical Microbiology and Immunology
Creighton University School of Medicine
2500 California Plaza
Omaha, NE 68178
rgoeri@creighton.edu
(402) 280-4091

Women and minority candidates are encouraged to apply.
Creighton University is an Equal Opportunity, Affirmative Action employer.

NW126111R

WE MAKE LIVES BETTER
UT HEALTH SCIENCE CENTER

The University of Texas Health Science Center

San Antonio, Texas

Dean, Graduate School of Biomedical Sciences

The University of Texas Health Science Center at San Antonio is looking for a dynamic leader who will assume the position of Dean, Graduate School of Biomedical Sciences. This individual is the chief advocate and spokesperson for the Graduate School which includes seven departments. The position reports to the President of the University.

This individual will be a high caliber leader whose responsibilities will be to advance the quality of graduate education and research endeavors in the biomedical sciences and foster interdisciplinary graduate education and collaboration between the Graduate School of Biomedical Sciences and internal and external partners. The successful candidate will also provide strong administrative leadership of graduate degree programs, admissions, student support programs, and postdoctoral scholars. He/she will be required to keenly review programs currently in place and be a bridge builder who understands and embraces accountability and stewardship of graduate school resources. He/she will work with the leadership of four other Health Science Center professional schools (Medical, Dental, Nursing and Allied Health Sciences) in creating and successfully implementing programs to enhance graduate student and postdoctoral scholar life, and improve academic enrichment and translational science programs. In addition, the successful candidate will oversee a variety of outreach and diversity programs aimed to increase the participation of underrepresented persons in the graduate health sciences.

The successful candidate will hold a PhD or MD/PhD, be a highly competitive scientist or clinical scientist with national and/or international recognition and reputation. The candidate should have experience leading MD/PhD programs and familiarity with preclinical medical and dental education. He/she will be a scholar who has strong research experience and who is, or who has been, actively engaged in educating students and appreciates and professes the value of education. In addition, this individual should have a track record of success in recruiting high caliber individuals to institutions to which he/she has been affiliated and a track record of success in seeking funds from external sources.

Nominations and CV's may be sent to The UT Health Science Center at San Antonio's search consultants, Marvene Eastham and Ryan Hubbs, at JTBioMed@wittkieffer.com. Items that cannot be emailed may be sent to 10375 Richmond Ave, Suite 1625, Houston, TX 77042. We may be reached confidentially at 713/266.6779 (p) or 713/266.8133 (f).

The University of Texas Health Science Center at San Antonio is an Equal Employment Opportunity/Affirmative Action Employer. All faculty appointments are designated as Security-sensitive positions.

NW126316R

WITT / KIEFFER

NIAID

NATIONAL INSTITUTE OF ALLERGY AND INFECTIOUS DISEASES

Help Us Help Millions

Clinical Tenure-Track Position

The National Institute of Allergy & Infectious Diseases (NIAID), Division of Intramural Research (DIR), is seeking an outstanding tenure-track investigator to develop a clinical research program to better understand, treat, and ultimately prevent infectious, immunologic, and/or allergic diseases. The scope of the NIAID research portfolio has expanded considerably in recent years in response to new challenges such as bioterrorism; emerging and reemerging infectious diseases, including acquired immunodeficiency syndrome (AIDS), influenza, severe acute respiratory syndrome (SARS), West Nile virus, malaria, and tuberculosis; immunologic diseases and the increase in asthma prevalence among children in this country.

The successful candidate will implement and direct an independent clinical research program with research emphasis on clinical research but may include translational or basic research. The incumbent will have the opportunity to choose the Laboratory in which he/she would like to be affiliated. It is expected that clinical protocols developed will complement the research goals of the Laboratory selected. In addition, the candidate will be paired with a Senior Investigator who will serve as a clinical mentor.

An outstanding postdoctoral record of research accomplishment and M.D., M.D./Ph.D. or equivalent degree is required for this position; board eligibility/board certification is also required. The incumbent will be expected to be qualified for credentialing by the NIH Clinical Center.

Candidates will be assigned independent resources to include clinical and/or laboratory support personnel, equipment, space, and an allocated annual budget for services, supplies, and salaries to ensure success. This is a tenure-track appointment under Title 42. Salary is dependent on experience and qualifications.

Interested candidates may contact Dr. Karyl Barron, Deputy Director, DIR, NIAID at 301/402-2208 or email (kbarron@nih.gov) for additional information about the position.

To apply for the position, send your curriculum vitae, bibliography, and an outline of your proposed research program (no more than two pages), by **March 14, 2008** via email to Ms. Wanda Jackson at jacksonwa@niaid.nih.gov. In addition, three letters of recommendation must be sent to Chair, NIAID DIR Clinical Tenure Track Search Committee, c/o Ms. Wanda Jackson at jacksonwa@niaid.nih.gov or 10 Center Drive MSC 1356, Building 10, Rm. 4A-26, Bethesda, Maryland 20892-1356. E-mail is preferred. Please note search #018 when sending materials.

Further information regarding the DIR laboratories is available at: http://www3.niaid.nih.gov/about/organization/dir/default.htm and information on working at NIAID is available on our website at: http://healthresearch.niaid.nih.gov/tdir

Department of Health and Human Services
National Institutes of Health
National Institute of Allergy and Infectious Diseases

Proud to be Equal Opportunity Employers

NW125126R

UNLV
CELEBRATING FIFTY YEARS

Dean of the College of Sciences

The University of Nevada, Las Vegas (UNLV), seeks an innovative and energetic individual for the position of Dean of the College of Sciences. The successful candidate will have the experience and demonstrated skills to advance the College in step with the University's rapid progress toward achieving research extensive status while maintaining our historic commitment to teaching excellence.

The Dean reports to the Executive Vice President and Provost. Candidates must possess a terminal degree from an accredited institution in a discipline appropriate to the College, along with a record of accomplishment meriting a tenured appointment at the rank of Professor in one of the College's academic units. Experience in administration at or above the department chair level is strongly preferred.

The Search Committee will accept applications until the position is filled. To guarantee full consideration applications should be completed by March 17, 2008 and include a curriculum vitae as well as contact information for five professional references. A cover letter should describe the applicant's past accomplishments with specific reference to program development, resource acquisition, fostering a collaborative environment and promoting transparency in decision making. Materials should be addressed to Dr. Paul Jarley, Dean of the College of Business, Search Committee Chair, and must be submitted online at **https://hrsearch.unlv.edu/** For assistance with UNLV's online applicant portal, please contact Jen Martens at (702) 895-3886 or hrsearch@unlv.edu.

UNLV is an Affirmative Action/Equal Opportunity educator and employer committed to excellence through diversity.

NW128325R

Brown BioMed
DIVISION OF BIOLOGY AND MEDICINE

Faculty Position in Tissue Engineering and Regenerative Medicine

Assistant Professor

The Department of Molecular Pharmacology, Physiology & Biotechnology at Brown University invites applications for a tenure-track position in the general area of tissue engineering and regenerative medicine. The preferred start date is July 1, 2008. Research space will be provided in a renovated laboratory with access to modern core facilities.

Applicants will be expected to develop an independent, externally funded research program in tissue engineering and regenerative medicine with expertise in cellular technology, tissue engineering, drug and gene delivery, and/or biomaterials with an eye towards translational applications. Research programs of potential interest include stem cell growth/differentiation, tissue engineering of the major organ systems and models of disease, as well as applications in cancer therapy.

Collaborations with affiliated hospitals of the Warren Alpert School of Medicine at Brown University and Brown University's Center for Biomedical Engineering are encouraged. Candidates should have a PhD and/or MD degree and relevant postdoctoral research training. Successful candidates must be committed to excellence in teaching at the undergraduate, graduate, and/or medical school levels.

Review of applications will commence on March 1, 2008, and will continue until the position is filled. Candidates should submit a curriculum vitae, three recent representative publications, a description of career objectives and future research plans, a teaching statement, and three letters of recommendation either electronically to: MPPB@brown.edu, or by mail to: **Search Committee-2, Department of Molecular Pharmacology, Physiology & Biotechnology, Box G-B3, Brown University, Providence, RI 02912.** Electronic submission in pdf format is encouraged.

Brown University is an Equal Opportunity/Affirmative Action employer and welcomes applications from women and minorities

NW128186RM

Pioneering Achieving Caring Enduring

The Abbott Neuroscience Discovery Research Unit in Ludwigshafen, Germany offers a fulltime, permanent position as:

Lab Head Molecular Histology (m/f)

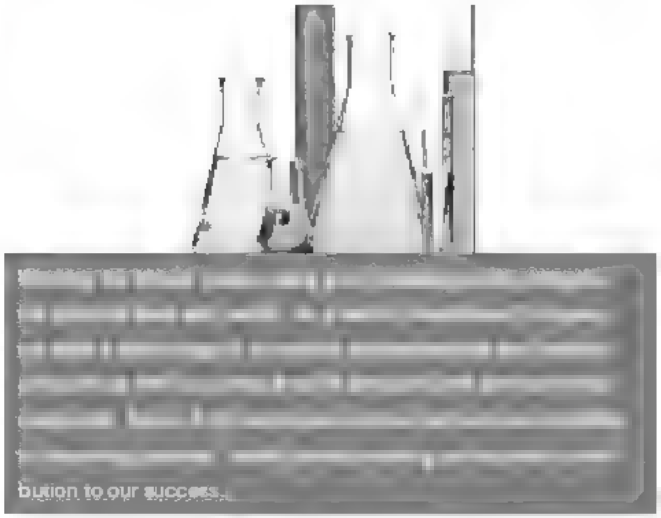

The position:

- Leader of a molecular neurohistology lab
- Conducting studies in the areas of psychosis and neurodegereneration/-regeneration
- Establishing and validating molecular markers in project-relevant neurohistological models with emphasis on radioactive labeling
- Establishing and validating in vivo and in vitro models for target validation and drug optimization in preclinical drug development

Your skills and experiences:

- Qualified Ph.D. in neuroscience or relevant [illegible]
- Several years of Post-Doc experience in pharmacology/histology, preferably in a pharmaceutical company
- ..ong experience in animal research
- Knowledge of standard scientific software, including statistical and imaging analysis
- Sound publication record
- Experience in project management would be an advantage
- Excellent communication skills in English and German
- Highly motivated team player with leadership abilities

Does the above appeal to you as a personal challenge? If so, we are looking forward to getting in touch with you. Please visit our homepage to apply online via our career portal. We will get back to you right away.

TOP ARBEITGEBER DEUTSCHLAND '07 AWARDED BY crf.com karriere

Abbott GmbH & Co. KG
67061 Ludwigshafen
www.abbott.de

Abbott
A Promise for Life

W126378R

Imperial College London

Anatomy Section

Department of Biosurgery and Surgical Technology

Division of Surgery, Oncology, Reproductive Biology and Anaesthetics

Professor of Anatomy

Salary negotiable (minimum starting salary £63,000)

Lecturer in Anatomy

Salary £38,880 - £43,420 per annum

Imperial College is ranked Fifth best University in the world (Times Higher QS World University Rankings 2007).

We are seeking to appoint a Professor of Anatomy who has the leadership ability to promote inspirational teaching and research. Additionally a Lecturer in Anatomy is sought to support the Chair appointment.

Both appointees will join the Department of Biosurgery and Surgical Technology based at the Charing Cross campus, with responsibilities in the following key areas:

- Lead teaching of anatomy in the medical and biomedical science courses, including a large teaching commitment to undergraduate entry anatomy
- Responsibility for teaching of anatomy on the Graduate Entry course
- Managing the resources for anatomy teaching
- Responsibility for examinations and assessments for both UG courses and Graduate Entry course
- Organising and leading external short courses
- Providing support for academic and NHS staff wishing to carry out research projects on anatomical topics

It is anticipated that the successful candidates will, within the constraints of the teaching requirements, develop a research programme.

Informal enquiries are very much welcomed and should be to Mr Barry Paraskevas, Deputy Head of Division (Teaching), SORA (p.paraskevas@imperial.ac.uk 020 7886 1461, or Professor Jenny Higham (email: jenny.higham@imperial.ac.uk tel: 020 7594 3005).

An application form and job description, along with further details may be obtained from the following link: www.imperial.ac.uk/employment

For the Lecturer position, you can send your complete application to the Human Resources Assistant, Faculty of Medicine, Imperial College London, St Mary's campus, Medical School Building, London W2 1PG or by email to: smrecr@imperial.ac.uk quoting reference SM030/08.

Alternatively, for the position of Professor, please contact Maria Monteiro, Senior Appointments Co-ordinator (Professors and Readers), Human Resources Division, Level 3 Faculty Building, Imperial College London, London SW7 2AZ. Email: m.monteiro@imperial.ac.uk quoting reference SM031/08.

Closing date: 26 March 2008.

Valuing diversity and committed to equality of opportunity

U128386BM

MRC | Medical Research Council

MRC Laboratory of Molecular Biology, Cambridge

Postdoctoral Scientists

£25,368 – £26,953 pa

The MRC Laboratory of Molecular Biology is a world famous institution with a strong track record in training postdoctoral fellows who have gone on to become leading scientists.

We are looking for four Postdoctoral Scientists to join Dr Jason Chin's pioneering research programme, which focuses on innovative approaches to engineering cellular translation (see Nature Biotech. (2007), 25, 770 & Nature Chem. Bio. (2008), 4, in press). Dr Chin's cutting-edge work has gained international recognition and has been selected for funding by the prestigious European Research Council, which supports investigator-driven frontier research.

You will join our strong inter-disciplinary team at the LMB's Protein and Nucleic Acid Chemistry Division. We have broad expertise extending from x-ray crystallography and chemical biology through to transgenic animals. We also have an excellent record of innovative basic research leading to applications in medicine.

Postdoctoral Synthetic Chemist **Ref: LMB08/096**

You will make a significant contribution to a project to perform chemical synthesis of creatively designed small molecules as part of the overall programme. You will have a PhD degree in chemistry with demonstrated expertise in chemical synthesis and may have an interest in learning biological techniques. You will enjoy interacting closely with synthetic biologists as part of a dynamic interdisciplinary team.

Postdoctoral Molecular Biologists (3 posts) **Ref: LMB08/097**

You will make a significant contribution to a project, which will evolve the macromolecular machinery of cells to perform new functions, to characterize the evolved machinery, and to develop applications of the evolved machinery. You will have a PhD degree in molecular biology and significant experience with biological methods, which may include directed evolution, cell biology, biochemistry, synthetic biology, protein purification methods or biophysical methods.

Successful applicants will be awarded a 2.5 year MRC Career Development Fellowship, which is a training and development position for a postdoctoral scientist who has recently completed their doctoral studies or is moving into a new research discipline.

Informal enquiries may be directed to Dr Jason Chin email: chin@mrc-lmb.cam.ac.uk

The starting salary will be in the range of £25,368 – £26,953 per annum and is supported by a flexible pay award policy, 6 weeks annual leave and public holidays, optional MRC final salary pension scheme and excellent onsite sports and social facilities.

This position is subject to pre-employment screening.

Applications for this post must be made online at http://jobs.mrc.ac.uk inputting the reference number above. Please include a CV and covering letter with your application. If you do not have access to the internet or experience technical difficulties please contact 01793 301280.

Closing date: 28 March 2008.

For further information about the MRC visit www.mrc.ac.uk

The MRC is an Equal Opportunities Employer

'Leading science for better health'

U128401B

UNIVERSITÄTSMEDIZIN GÖTTINGEN : UMG

The Universitätsmedizin (University Hospital and Faculty of Medicine) of the Georg-August-Universität Gottingen invites applications for a

PROFESSORSHIP "ADULT STEM CELLS"
(SALARY LEVEL W2 TENURE TRACK)

The position will first be filled for 5 years, with the possibility of extension to a life time position (tenure track).

The applicant should be an internationally recognized expert on the pathobiology of adult stem cells of the gastrointestinal tract including pancreas and liver. The applicant is expected to strengthen the clinical research in this field by establishing cellular and molecular methods to study animal as well as human material. The participation in existing local collaborative research centers (Forschergruppe, SFB) and the engagement in initiatives to acquire additional funding is expected.

The formal requirements for the recruitment follow § 25 NHG. Details can be given upon inquiry. Candidates need to hold an MD or PhD degree and should have prior experience as independent group leaders.

The University of Gottingen is determined to increase the percentage of female professors. Therefore, we strongly encourage qualified female scientists to apply.

Handicapped candidates are given priority, if equally qualified. A part time appointment can eventually be given.

Applications with the standard documents (CV, list of publications, outline of research focus, teaching record, diplomas, reprints of three selected publications) should be sent within 3 weeks to

Dekan und Vorstand für Forschung und Lehre der Universitätsmedizin Göttingen, Georg-August-Universität, Robert-Koch-Str. 42, D-37075 Göttingen

Please provide also the CV questionaire that can be downloaded from the following URL:
www.universitaetsmedizin-goettingen.de/content/berufungen.html

W126275R

GENERALITAT VALENCIANA

60 Santiago Grisolia PhD/Postdoctoral Grants
European Region of Valencia (Spain) Research Centres

Valencian Regional Government offers sixty Santiago Grisolia grants for foreign fellow investigators interested in participating in specific research programmes in several Valencian Region's research centres. Santiago Grisolia Program seeks international scientific cooperation through young researchers' exchange

Applicants must be:
- Foreign citizen or Spanish citizen permanent resident in a foreign country,
- University graduate or PhD, having completed these degrees after January 1st 2006,
- Fluent in either Spanish or English

Research Areas: Plant genetics, plant infectious pathology, Crop science and technology, Psychology and human behaviour, Neurophysiology and Neuropathology, Cell physiology and cell pathology, Stem cell science, Cytomics and Proteomics, Molecular biology and virology, Chemistry and biochemistry, Microprobes and array technology, Materials science, Nanotechnology, Imaging and image transmission, Digital music, Earth science and disasters preventive technology, Environment science and regulations, Space technology, Quantic physics, Particle science, Alternative energy sources, Electronic Engineering, Human rights protection and regulations, Prospective methods in Economy.

Duration of the grant: Up to 24 months

Grant endowment
Wages: 14,400 € (Euros, per year before taxes.
Travel and moving expenses: up to 1.600 €
Full health insurance provided by the Spanish National Health System.

Applications, list of offered projects, and additional information are available at http://www.edu.gva.es/poci/va/GRISOLIA_e.htm Candidates are allowed to apply for up to three projects. Only one will be awarded.

U126280R

---

welcome trust sanger institute

U128144RL

Wellcome Trust Sanger Institute
Mouse Genetics
Scientific Team Leader

The mouse genetics group plans an extensive sequence/phenotype driven mutagenesis programme and we are seeking scientific team leaders to provide the hands on expertise to drive and develop the phenotyping of mice. Experience of supervising research technicians, analyzing and presenting data at scientific meetings and PhD or equivalent experience essential.

Contact
Human Resources
Email: recruit@sanger.ac.uk
www.sanger.ac.uk

---

the Beatson
institute for cancer research

Postdoctoral Scientist

Studies on autophagic and apoptotic regulators of programmed cell death

Starting salary from £25.5k - £33k (Depending on experience)
Three year fixed term contract

The Beatson Institute is one of Europe's leading cancer research centres. It is core funded by Cancer Research UK and supports cutting edge research into the molecular mechanisms of cancer development. The institute recently moved to a new state-of-the-art building in Parkland on the north-western edge of Glasgow and provides a dynamic, supportive and well-resourced environment for its scientists.

The Tumour Cell Death Laboratory is interested in factors that regulate autophagy, apoptosis and how the pathways these factors engage integrate to determine cell fate (Crighton et al. (2006) Cell 126:121. Crighton et al. (2007) Autophagy 3:72. Bell et al. (2007) JCI 17:1008. Crighton et al. (2007) Cell Death Differ. 14:1071).

We are seeking a highly-motivated and dedicated postdoctoral researcher to study the role of autophagy and apoptosis in the regulation of cell death during tumour development and cancer therapy. We have recently identified a number of novel factors that control cell death and the successful candidate will study the molecular basis behind the role of these factors in controlling autophagy, apoptosis or both in vitro and in vivo. Studies will involve RNAi studies, confocal microscopy, proteomics and mutational and biochemical analysis of protein function.

Applications with CV and names of two referees should be sent to Prof Kevin Ryan, The Beatson Institute for Cancer Research, Garscube Estate, Switchback Road, Bearsden, Glasgow G61 1BD, Scotland.
(Fax: +44 141-942 6521) or by Email to k.ryan@beatson.gla.ac.uk

Charity no: SC006106

CANCER RESEARCH UK

U126280RM

www.cam.ac.uk/jobs/
A world of opportunities

UNIVERSITY OF CAMBRIDGE

Genetic and Molecular Mechanisms in Human Obesity

We are seeking experienced and highly-motivated postdoctoral research associates who would like to develop their scientific skills in a multidisciplinary research group with a focus on mechanisms of human obesity. You will be based within the new purpose built Institute of Metabolic Science at Addenbrooke's Hospital, Cambridge which is host to several internationally recognised groups undertaking research in the genetic, molecular and physiological determinants of Obesity and Diabetes http://www.mrl.ims.cam.ac.uk/

Institute of Metabolic Science – Metabolic Research Laboratories

Postdoctoral Research Associate

£25,134 - £32,796 pa
Limit of tenure: 30th September 2009

The aim of our research programme funded by an MRC Programme Grant to Professor Stephen O'Rahilly is to identify novel pathways and molecular and physiological mechanisms involved in human obesity and its complications. You will be involved in the characterization of the function of novel genes that are emerging from our programme of gene discovery and in the functional characterisation of novel mutations in genes that are associated with the pathogenesis of severe human obesity.

You will hold a PhD in molecular biology, biochemistry or a related discipline, with substantial experience in a broad range of techniques including cell culture, cell signalling and protein biochemistry.

Please quote reference: RG03075.

Postdoctoral Research Associate

£25,134 - £32,796 pa
The funds for this post are available for up to 56 months in the first instance

The aim of the research programme funded by a Wellcome Trust Senior Fellowship to Dr Sadaf Farooqi is to identify novel pathways and molecular and physiological mechanisms involved in human obesity and its complications. We are complementing our continuing candidate gene approach with high-density SNP-array based approaches to gene discovery. These include autozygosity mapping in consanguineous pedigrees and assessment of Copy Number Variation in patients with obesity and additional syndromic features.

You will hold a PhD in genetics or a relevant discipline, with substantial molecular biology experience. Experience in statistical methods and the analysis of microarray data from major platforms would be an advantage.

Please quote reference: RG03074.

Applications, including CV, covering letter, names and addresses of three referees and a completed PD1B form (available on http://www.mrl.ims.cam.ac.uk) should be sent to: Dr Sadaf Farooqi, Metabolic Research Laboratories, Institute of Metabolic Science, Box 289, Addenbrooke's Hospital, Hills Road, Cambridge, CB2 0QQ, UK from whom further information can be obtained, email: sf20@cam.ac.uk

Closing date for both posts: 18 March 2008

The University is committed to Equality of Opportunity.

U126374A

University of Erlangen-Nuremberg, Germany
Faculty of Medicine

1. The Department of Urology at the Faculty of Medicine offers the position of

Professor (W2-Professor) for Molecular Urology

A fixed-term professorship with the status of a civil servant is available for a total of six years. The permanent appointment to professor following this term is possible in principle subject to the existence of the legal prerequisites.

The successful candidate will represent the discipline in research and teaching. The applicant should have a recognizable profile in basic research in the field of uro-oncology. Experiences in the approach to biological samples of greater cohorts and their analysis by means of modern high throughput techniques (genome, transcriptome, proteome) are desirable. We expect the applicant to be ready for cooperations in joint research projects within the Faculty of Medicine and to translate results from research into clinic. The Faculty of Medicine offers programs in medicine and dentistry as well as in molecular medicine.

The candidate must have a Ph.D. or M.D. degree, teaching skills, and professional experience, preferably, but not necessarily in a junior faculty position. Moreover, experience as a group-leader, excellent publications, and above-average fund-raising are expected.

2. The Institute of Anatomical Pathology at the Faculty of Medicine offers a

Professorship (W2-Professor) for Experimental Tumorpathology

A fixed-term professorship with the status of a civil servant is available for a total of six years. The permanent appointment to professor following this term is possible in principle subject to the existence of the legal prerequisites.

The successful candidate will represent the discipline in research and teaching. There will be teaching responsibilities in the Bachelor program in Molecular Medicine. The applicant should have a recognizable profile in basic research in the field of experimental and molecular tumor pathology and should closely cooperate with the existing research groups at the Institute of Pathology with special focus on molecular pathology of gastrointestinal, urogenital and head and neck malignancies. We expect the applicant to be ready for cooperations in joint research projects within the Faculty of Medicine and to translate results from research into clinic. The Faculty of Medicine offers teaching programs in Medicine and Dentistry and in Molecular Medicine.

The candidate must have a university education in medicine or natural sciences and hold a M.D. or Ph.D. degree. Furthermore, excellent teaching skills, professional experience as a group-leader, high-ranking publications, and above-average research funds are required. These additional academic qualifications have been either obtained in a previous junior faculty position or during equivalent appointments outside the university.

Applicants must not be older than 52 years at the time of appointment. In urgent cases exceptions are possible but require the consent of the Bavarian Ministry of Science, Research, and Art and the Bavarian Ministry of Finances (Art. 10 Abs. 3 Satz 2 BayHSchPG).

The University of Erlangen-Nuremberg intends to increase the number of women in research and teaching positions and, therefore, strongly encourages female researchers to apply.

Disabled applicants will be preferentially considered in case of equivalent qualification.

Please send a letter of application, a resume (picture required), a structured list of publications and teaching activities (one copy in written form, one copy on data CD) as well as officially certified copies of credentials and certificates to the Office of the Dean of the Medical Faculty of the University of Erlangen-Nuremberg, Oestliche Stadtmauerstrasse 30a, D-91054 Erlangen. The deadline for application is **4th April 2008**.

Friedrich-Alexander-Universität Erlangen-Nürnberg

www.uni-erlangen.de

W 26375A

UNIVERSITY OF BATH

Department of Pharmacy & Pharmacology

Professor or Reader in Medicinal Chemistry & Drug Design

Ref: 08H061A

This top-rated, internationally renowned Department (see: http://www.bath.ac.uk/pharmacy/home/index.shtml) has significant research strengths in Medicinal and Biological Chemistry, particularly in molecular signal transduction, carbohydrate chemistry, anti-cancer, anti-viral and anti-infective drug design and a developing reputation in Chemical Biology. The development of interdisciplinary collaborations within the Department and across the Faculty of Science is encouraged and supported

We seek an outstanding senior researcher with interests in the application of chemistry to biological problems (such as drug design, discovery and/or mechanistic enzymology) and a focus in the use of biophysical techniques involving, for example, NMR spectroscopy, protein crystallography or computational chemistry/ molecular modelling. The appointee will be expected to maintain a vigorous, externally-funded research programme at an international level, complementary to existing strengths of the Department and to be committed to excellence in teaching

Informal enquiries are welcome and should be directed to the Head of Department, Prof. Richard Guy, on +44 (0)1225 384901 or email: r.h.guy@bath.ac.uk

Further details of the post can be found at http://www.bath.ac.uk/jobs or from the Department of Human Resources, University of Bath, Claverton Down, Bath BA2 7AY email: jobs@bath.ac.uk tel +44 (0)1225 386026 or the 24-hour answerphone service on +44 (0)1225 386924 quoting the reference.

Closing date: 15 April 2008.

U126385A

www.bath.ac.uk/jobs

ECCPS

JOHANN WOLFGANG GOETHE UNIVERSITÄT FRANKFURT AM MAIN

The **Excellence Cluster Cardio-Pulmonary System** (www.ECCPS.de) of the universities of Frankfurt and Giessen and the Max-Planck-Institute (MPI) for Heart and Lung Research in Bad Nauheim constitutes a unique translational research center, dedicated to combine cutting edge basic sciences with predinical and clinical studies in the field of vascular and parenchymal heart and lung diseases.

Within the frame work of the ECCPS it is planned to install a

Chair for Vascular Signalling (W3)

The chair at the University of **Frankfurt** is expected to develop close collaborations with other members of the ECCPS at both universities and the MPI. Applicants should have expertise in adipose tissue, adipokines and (preferably) lipidomics as well as a vascular biology and vascular signalling background. The chair comprises a W3 position (Chair), two post-doctoral positions, three PhD students, two technicians, and a secretarial assistant as well as fixed budget for consumables and specific laboratory equipment (€ 130.000 per year). The host university will provide appropriate laboratory facilities and basic laboratory equipment. Moreover, the group will also take part in the excellence-based ECCPS-internal competition for project support. Funding is initially for five years, thereafter, continuous financing will be provided for the ECCPS positions for at least a further 5 year period.

According to § 71 of the Hessisches Hochschulgesetz (HHG) the following qualifications are required: Full university education in a biomedical or related discipline; a doctorate with merit; outstanding scientific achievements and academic teaching references. Applicants are expected to participate in the teaching of cardiac, pulmonary and vascular medicine, e. g. in graduate school programs.

Frankfurt University is an equal opportunity employer. For further information regarding the general conditions for professorship appointments, please see http://www.uni-frankfurt.de/aktuelles/ausschreibung/professuren/index.html

Applications including a full CV, publication list, reprints of 5 key publications, as well as a proposal for a cutting edge research program to be integrated into the ECCPS framework should be sent no later then **4 weeks** after publication of this advertisement to: **The Dean of the Medical Faculty, Prof. Dr. Josef Pfeilschifter, Theodor-Stern-Kai 7, D-60590 Frankfurt/Main, E-Mail: Pfeilschifter@em.uni-frankfurt.de**

W125688A

www.uni-frankfurt.de

UNIVERSITÄTSKLINIKUM GREIFSWALD DER ERNST MORITZ ARNDT UNIVERSITÄT GREIFSWALD ANSTALT ÖFFENTLICHEN RECHTS

Department of Diagnostic Radiology and Neuroradiology
School of Medicine
University of Greifswald, Germany

At the School of Medicine, University of Greifswald, the research program "Validation of magnetic resonance imaging (MRI) for the reduction of numbers of laboratory animals and refinement of experimental methods in medical basic research" is supported by the Federal Ministry of Research and Education (BMBF). The supported projects cover a broad range of animal research in the fields of cardiology, gastroenterology, medical microbiology, molecular neurobiology, pharmacology, physiology, and surgery. Within this program, the Department of Diagnostic Radiology and Neuroradiology is currently seeking a highly qualified candidate for a **research associate position**.

Responsibilities will include coordination of the MRI studies within the research program at the new Animal Imaging Centre, which is supplied with a Bruker 7T high field system (ClinScan).

We offer a three-year full-time position for an experimental radiologist or medical physicist starting on April 1st, 2008. Salary is according to the German TV-L (Entgeltgruppe 14) with benefits.

Applicants must have an MD or PhD or MD/PhD degree. They must have demonstrated excellent qualifications in research and education, preferably in medical imaging. Radiologists with a second degree in physics or chemistry will be preferred. The appointment will be in the Department of Diagnostic Radiology and Neuroradiology, School of Medicine, University of Greifswald.

The University and Hanseatic City of Greifswald is located near the Bay of Greifswald, which is a part of the Baltic Sea between the islands of Rügen and Usedom, and offers great recreational possibilities.

Please submit a cover letter, curriculum vitae, publication list, a statement of research interests and three letters of reference to:

Prof. Dr. N. Hosten
Department of Diagnostic Radiology and Neuroradiology
School of Medicine, University of Greifswald, Ferdinand-Sauerbruch-Strasse, 17475 Greifswald, Germany
hosten@uni-greifswald.de
www.medizin.uni-greifswald.de

The University of Greifswald is an equal opportunity employer and particularly encourages applications from female candidates. We welcome applications from suitably qualified people from all sections of the community regardless of race, religion, gender or disability.

W126120RM

CHARITÉ

UNIVERSITÄTSMEDIZIN BERLIN
Gliedkörperschaft der Freien Universität und der Humboldt-Universität zu Berlin

The Charité - Universitätsmedizin Berlin, Centrum für Grundlagenmedizin (CC2), Institut für Zell- und Neurobiologie is offering the following position:

University Professorship for Anatomy with focus on Neuroanatomy

Salary group W2 BBesG

(reference number 03.08)

- ***Tasks:***
  The professor will represent the subject anatomy in research and education. In detail, in the neuroscientific environment in Berlin the professor will build up in close interaction with the other groups of the institute a new research team with focus on cellular and molecular neurobiology.
- ***Prerequisites and qualifications:***
  According to § 100 BerlHG junior professorship or *Habilitation*, or equivalent scientific achievements and teaching competence, or similar qualification.
- ***Additionally:***
  We expect outstanding scientific achievements in the field of anatomy, especially in cell and neurobiology, successfully acquired third-party funding, and a concept paper outlining the applicant's specific plans for her/his proactive collaboration with Charité's research partners (www.charite.de). Required are broad, verified experiences and strong commitment to teaching anatomy and excellent teaching skills. Experience in innovative teaching methods are a plus.

The Charité is an equal opportunity employer committed to excellence through diversity. As women are under-represented in scientific work, we explicitly encourage women to send in their application.

Please see (**http://www.charite.de/jobs/prof.html**) for application instructions before sending your written application (listing the relevant position reference number) within **four weeks** to **Charité - Universitätsmedizin Berlin, Der Dekan, Prof. Dr. Martin Paul, Charitéplatz 1, 10117 Berlin.**

W1258835

IGF DEPARTEMENT D'ENDOCRINOLOGIE

Post-doctoral research scientists

(2 two-year posts)

1. A highly motivated scientist to investigate the functioning of pituitary-scale endocrine cell networks, using a newly-developed cellular in vivo imaging technique (Bonnefont et al., 2005 PNAS 102(46) 16880-5)
2. An electrophysiologist to explore the functioning of hypothalamic TIDA neurons using acute slice preparations.

Research engineer

(1 three-year post)

The successful candidate will be responsible for the development of new cellular in vivo techniques within the National Biophotonics Imaging Platform (NBIPI, http://www.nbipireland.ie/) at the Institute of Functional Genomics (IGF)

Please visit the IGF website for further information – http://www.igf.cnrs.fr/ or alternatively contact address below

Applications should include a covering letter, CV, summary of current and past research experience, and two professional references. Salaries will be determined following CNRS guidelines. Positions will be available starting from April 1st, 2008

Contact:
Patrice Mollard
Institut de Génomique Fonctionnelle
CNRS UMR 5203 & INSERM U661
Universités de Montpellier 1 & 2
141 rue de la Cardonille
34094 MONTPELLIER CEDEX 5, FRANCE
tel. +33(0)4 67 14 29 25, fax: +33(0)4 67 54 24 32
e-mail: Patrice.Mollard@igf.cnrs.fr

W1260654R

CHIEF EXECUTIVE

CSIRO

The Commonwealth Scientific and Industrial Research Organisation (CSIRO), is Australia's premier national science agency and one of the largest and most diverse public sector research agencies in the world. The organisation employs close to 6,500 staff on 55 sites across Australia and is involved in a wide range of projects with other major research organisations in Australia and around the world. The CSIRO's annual budget, derived from both government and industry, exceeds A$1 billion.

CSIRO, through the development, maintenance and deployment of a strong capability in scientific research and development, provides science and technology aimed at assisting Australian industry and furthering the interests of the Australian community. Its major focus is on delivering solutions to current and emerging national challenges and opportunities that impact the economic, environmental and social well being of Australia.

CSIRO is seeking a new Chief Executive to succeed Dr Geoff Garrett, who will successfully conclude his term at the end of 2008. He or she will continue to drive CSIRO's position and success as a world-class scientific research organisation. They will have outstanding leadership, strategic and management skills.

Experience in applied scientific research, technology transfer and business management at a senior level is essential as are proven skills dealing with a broad diversity of stakeholders

Applicants are invited to submit a cover letter accompanied by a detailed resume attention to Dr John Stocker AO, Chairman CSIRO via mel.search@ezi.net.A detailed position specification is available from www.csiro.au/careers or by contacting Dean Ireland on +613 9629 7203. Applications close Monday 31 March 2008

JP125812R

nature

News editor (online), *Nature*

Nature needs a skilled and experienced editor to run its online news operation. Online news is the most immediate and time sensitive of Nature's journalistic enterprises, and requires an exceptional leader.

The job requires energy, excellent news judgement, some technological acumen and an unflappable temperament. The successful candidate will delight in deadlines, edit with flair, feel comfortable with all kinds of scientific subject matter and be able to lead and motivate a highly capable team. At the same time, she or he will be diligent in the details of online production. She or he will have imaginative ideas about how further to expand Nature's online news operation, and be fascinated by the possibilities of online journalism in general.

Candidates must meet these requirements and have significant experience that demonstrates these skills

To apply, please send your CV, covering letter quoting reference number NPG/LON/833, To Geetika Juneja Personnel Assistant at londonpersonnel@macmillan.co.uk

Closing date: 7th March 2008

nature publishing group npg

JN125837R

Open positions

Two post doctoral positions open

LUND UNIVERSITY

The research at Neurona, Survival Unit, Lund University, Sweden is focused on pathogenetic mechanisms and pharmacological treatment in cell and animal models of Parkinson's and Huntington's diseases. We also study cell replacement therapy with stem cells in attempts to repair brains in animal models of Parkinson's and Huntington's diseases. The group's mission is to understand neurodegenerative diseases and develop new therapies that are of benefit to patients and their caregivers. For more information please visit http://www.med.lu.se/expmed/nesu

1. Neuroprotection

This position is a part of a Nordic Center of Excellence Neurodegeneration. The post doctoral project will focus on studying the neuroprotective effects exerted by N-terminal fragments of mutant huntingtin so as to protect against neurological diseases.

The applicant should have a relevant background in neuroscience and neurodegenerative disease, preferably with an emphasis on cell culture and protein chemistry. The start date should be as soon as possible. The duration is 2 years.

2. Stems

This postdoc position is a part of an international collaboration called "STEMS-Preclinical evaluation of Stem Cell Therapy in Stroke" financed by the EU. The project will focus on characterization of human adult stem cells and human embryonic stem cells for the purpose of transplantation in stroke. The applicant should have a relevant background in neuroscience or stem cell research, preferably with emphasis on methods such cell culture, immunocytochemistry, Western blotting and PCR. The start date should be as soon as possible. The duration is 2 years.

Requirements

A PhD degree in neuroscience or closely related subject. All applicants should also be fluent in spoken and written English. Three references required.

Application

If you are interested in any of these positions email your application, CV and the name and email addresses to three persons that can function as references for you to Birgitta.Larsson@med.lu.se. Clearly mark your application with the number and name of the position you are interested in. Please note that only complete applications will be considered!

W1283826R

For our new, state-of-the-art Research Facilities in Düsseldorf/Germany we are seeking a highly motivated

Ph. D. Chemist

Nucleic Acid Chemistry

Your expertise covers automated synthesis of chemically modified RNA. You have been trained in organic synthetic chemistry with a major focus on nucleoside and oligonucleotide synthesis. You are well versed in the design and synthesis of complex nucleic acid structures as well as modified oligonucleotides derivatives. You are familiar with the basics of analytical tools, such as HPLC, mass spectrometry and LC-MS. Experience with state-of-the-art literature and patent search systems is of advantage. You enjoy working independently and as part of a scientific network, you communicate well and you have good social skills.

Pfizer

If you want to be part of a totally dedicated team in an international environment, and if you strive to translate cutting edge science into new drugs, please forward your CV and a brief summery of relevant experience via e-mail to sfaehndrich@coleypharma.com

COLEY

Coley Pharmaceutical GmbH
Merowingerplatz 1a
40225 Düsseldorf
www.coleypharma.com

W1282734R

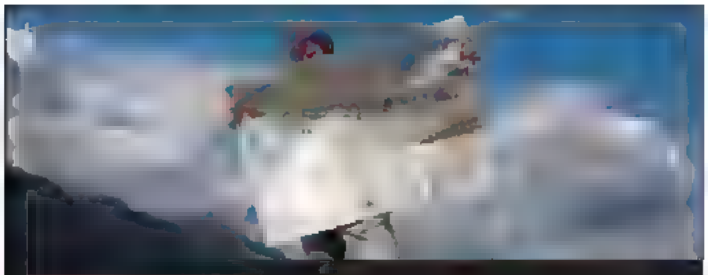

Lost in today's ever-changing biosciences environment?

...get your bearings with these Stanford School of Medicine Career Center (SoMCC) seminars presented by *Naturejobs*.

Naturejobs and the Stanford School of Medicine have collaborated to bring you this video series featuring SoMCC "Industry Insights" and "Careers in Science" programs. This monthly series, delivered by top experts within the biomedical sciences and healthcare industries, will allow you to:

- OBTAIN OF THE LATEST TRENDS AND FORCES SHAPING THE BIOSCIENCES
- GAIN VISIBILITY INTO THE DIVERSE SETTINGS WHERE BIOMEDICAL PROFESSIONALS ENGAGE
- LEARN FROM FIRST-HAND PERSPECTIVES OF THE FOREMOST LEADERS IN BUSINESS AND ACADEMIA

Visit www.naturejobs.com/magazine/video to stream or download the following presentations:

- *Convergence of Science, Banking, and Finance with MDS Capital*, Nandini Tandon, Ph.D, MDS Capital
- *How Should We Be Developing Drugs in the 21st Century?*, Hal Barron, MD, Genentech

And stay tuned for these seminars coming soon:

Intellectual Property Management & Technology Transfer, Panel of Experts
Science & the Media, Donald Kennedy, PhD, Emeritus Professor, Stanford
The Future of Personalized Medicine, with Agilent Technologies

If you are interested to learn more about the SoMCC, please contact Suzanne Frasca, Program Coordinator, at (650) 725-7687 or somcareers@stanford.edu.

naturejobs

---

nature REVIEWS MICROBIOLOGY

Associate Editor

Nature Reviews Microbiology has a vacancy for an Associate Editor. This exciting position involves working closely with the Chief Editor and other members of the journal team on all aspects of the editorial process, including commissioning and editing reviews, organizing peer-review, writing for the journal, and developing the content of the journal, both in print and online.

To meet these challenging tasks, the ideal candidate will have a broad knowledge of microbiology and hold a PhD in a relevant field. We are particularly interested in applicants with at least 2 years of postdoctoral experience, but we would welcome applications from outstanding candidates who have recently completed their Ph.D. A key aspect of the job is liaising with the scientific community and attending international conferences, so the successful candidate must be dynamic and outgoing with good interpersonal skills. Previous editorial experience would be an advantage, but is not essential.

The position will be based in the London office of Nature Publishing Group, and the terms and conditions are highly competitive, reflecting the importance and responsibilities of the role. For further information about *Nature Reviews Microbiology* series visit http://www.nature.com/nrmicro

Contact Details

To apply please send your CV, a summary of relevant experience, and current salary, quoting reference number NPG/LON/835 to: Denise Pitter, Personnel Assistant, at londonrecruitment@macmillan.co.uk

All candidates must demonstrate the right to live and work in the UK to be considered for the vacancy.

nature publishing group npg

Closing date: Friday 14th March 2008

IN1281181R

St George's University of London

Medicine, Biomedical Sciences, Health and Social Care Sciences

Division of Basic Medical Sciences
Centre for Molecular & Metabolic Signalling

Research Assistant

(2 years fixed-term in the first instance) **Ref: 103/08**

Applications are invited for a postdoctoral Research Assistant to join a research group with an international reputation, for research on novel technologies for screening of cancer therapeutic agents, with emphases on melanoma, cell senescence and specific signalling pathways as targets.

This project funded by the CR-UK Discovery program, is a collaboration with 4 other leading British research groups and may involve some short periods working at collaborating centres. Activities will include establishment of melanoma and melanocyte lines genetically modified as screening and investigative tools. Experience in cellular and molecular techniques and a PhD in a relevant topic are essential

Anticipated start date is between 1 April 2008 and 1 June 2008.

Starting salary in the range £30,030 to £35,360 (inclusive of London Allowance)

For further information and application forms, visit www.sgul.ac.uk/jobs or contact the Recruitment Team on 020 8725 5020 (24 hour answerphone) or email recruitment@sgul.ac.uk.

Please quote reference number 103/08

Closing date: 20 March 2008.

St George's is an Equal Opportunities Employer

U126464R

University of Oxford

Department of Plant Sciences

Two Departmental Lecturerships

Two posts are available from 1 October 2008, or earlier by agreement, to teach and provide tutorial support for the u/g degree course in Biological Sciences in the area *either* Plant Ecology and Population Biology (reference AP08005) *or* Evolution, Systematics and Biodiversity (reference AP08004).

Further particulars and how to apply are available from http://www.plants.ox.ac.uk/ Closing date is noon on 3 April 2008.

As an Equal Opportunity employer, we positively encourage applications from people of all backgrounds

J126386BM

www.ox.ac.uk/jobs

Associate and Assistant Professors in Protein Science at Aalborg University, Denmark

Expertise in the chemistry, function, structure determination, production, purification or biophysical characterization of proteins is required. The two positions are available from 1 August 2008. See

www.bio.aau.dk/en/biotechnology/vacant_positions/

W126013R

The **CNIC** *www.cnic.es (Spanish National Cardiovascular Research Center)* is a public Foundation established by the Spanish Ministry of Health and Consumer Affairs through the Carlos III Institute of Health located in Madrid, Spain

The newly established **Cardiovascular Developmental Biology Department** (CDBD) seeks to appoint one **Senior Group Leader** and two **Junior Group Leaders**

The CDBD seeks to recruit scientists interested in the development of the cardiovascular system who are either looking for their first independent position (junior) or who would like to consolidate their career as a senior scientist. The CDBD has established facilities for the use of the mouse, chicken and zebrafish as model systems. The CNIC places a special emphasis on Advanced Imaging applications, which will be accessible as core services and include multiphoton spectroscopy, optical projection tomography, intravital microscopy and non-invasive whole animal imaging

The CNIC offers:

- **an internationally competitive salary**
- **state-of-the-art core facilities**
- **start-up research funding commensurate with track record**
- **a dynamic career development program**
- **minimal administrative responsibilities**
- **an opportunity to work in a dynamic, growing Center which combines basic and translational research**

Informal enquiries may be addressed to the Director of the CDB Department, Dr Miguel Torres – mtorres@cnic.es.

Formal applications should be sent, together with a CV, the contact details of three referees and a two-page account of your proposed research, by e-mail to rrhh@cnic.es, quoting the reference CDBD/2008.

The CNIC is committed to equal opportunities.

Details of our employment policy and further information about the CDBD and the CNIC can be obtained at http://www.cnic.es

Applications will be considered until the posts are filled.

cnic

W126263RM

nesci North East England Stem Cell Institute

Professor of Stem Cell Research and Institute Co-Director (two posts)

The North East England Stem Cell Institute (NESCI) is a collaboration between Durham and Newcastle Universities. Each University wishes to appoint a Professor who will also assume, on a three-yearly alternate basis, the Directorship of the institute. This represents an outstanding opportunity to develop your career, building upon world leading facilities and backed by high quality resources, in terms of both equipment and staff. You will also have access to excellent clinical facilities via the third NESCI partner, the Newcastle upon Tyne Hospitals NHS Foundation Trust. You will have an exceptional record of scientific achievement and an international research profile in the field, as well as proven leadership abilities. In addition, you will have an interest in basic mechanisms in stem cell biology, tissue engineering or clinical translation of stem cell science, as well as commercial development and/or public engagement activities. You will have the credibility to influence key decision-makers at regional and national level and will, crucially, work in close collaboration with your equivalent Co-Director of NESCI at Newcastle or Durham University.

For informal enquiries in strict confidence, contact the interim joint Directors: Professor Chris Hutchison (0191) 334 1270, c.j.hutchison@dur.ac.uk or Professor Michael Whitaker (0191) 222 5264, michael.whitaker@ncl.ac.uk

Further details and an application form are available on our website: http://jobs.dur.ac.uk or tel. +44 (0)191 334 6499, fax +44 (0)191 334 6495. Please quote job reference 2071 Closing date: 25/04/08.

Durham University NHS Newcastle University

U126383R

FOOD STANDARDS AGENCY

Research Requirements

Applications are invited from UK and international organisations for research/surveys in the following areas

Research Requirement Document Issue 27, February 2008

- Food additives
- Food contact materials
- Food irradiation
- Nitrate monitoring
- Methods of analysis
- Chemical risk assessment
- Food intolerance
- Food authenticity

Details of the requirements together with an application form and guidance on submitting proposals can be obtained from the Agency website at: http://www.food.gov.uk/science/researchpolicy/researchfunding/rrd/requirements/

Procurement & Contracts Team, tel: +44 (0) 20 7276 8219, email: procurement@foodstandards.gsi.gov.uk

The Food Standards Agency – putting the consumer first.

J128154A

VU RESEARCH SCORES!

VU University Amsterdam congratulates Rick, Bas, Arianna,

www.vuamsterdam.com

VU University Amsterdam

W125861A

NW125513A

ANGLOBIOTECH NORDIC CONFERENCE V

Ezenze

The Nordic region continues to be one of the fastest growing biotech regions in the world. In its fifth year, the Anglonordic Biotech Conference provides the ideal one-stop opportunity to discover and invest in this success. By invitation only, the select audience is restricted to drug discovery, pharmaceuticals and venture capital firms (more than 85% of the delegates are at CEO, CFO, VP or Investment Manager level). The conference also includes opportunities for companies to do 15 minutes investment and Partnering pitches.

For more information about elevator pitches and sponsorship please contact: Mattias Johansson on tel: +44 (0 207795 81132 or email: mattias@anglonordicbiotech.com

Venue: DBERR Conference Centre, 1 Victoria Street, SW1H 0ET, London
Date: 15 May, 2008
Website: www.anglonordicbiotech.com

Co-organisers:

U125853E

Fighting Cancer's biggest killer: CHILDREN with LEUKAEMIA

UCL

Childhood Leukaemia Causes & Prevention

29th - 30th April 2008

The second 'Causes and Prevention of Childhood Leukaemia Conference' will focus on environmental risk factors in the development of leukaemia and the interplay of these with genetic factors. It will include talks across a range of scientific disciplines, exploring the latest thinking on possible causes of leukaemia, and aims to stimulate further debate and discussion across the traditional boundaries of these disciplines.

Abstracts for poster presentations, on no more than four A4 pages including tables and figures, are invited for submission by 29th February 2008.

Speakers to include: Mel Greaves (Institute of Cancer Research), Mike Murphy (University of Oxford), Tim Eden (Teenage Cancer Trust), Pat Buffler (University of California), Liz Milne (Telethon Institute for Child Health Research), Joachim Schuz (Institute of Cancer Epidemiology), Louise Parker (Dalhousie University), Anne Cooke (University of Cambridge), Malcolm Taylor (University of Manchester), Caroline Fox (Children's Hospital of Philadelphia), Julie Ross (University of Minnesota), Richard Houlston (Institute of Cancer Research), Denis Henshaw (University of Bristol), Rob Mairs (Cancer Research UK) & Eric Wright (University of Dundee).

Molecular Basis of Childhood Leukaemia

1st - 2nd May 2008

This conference will discuss the latest and most cutting edge research related to childhood leukaemia. There will be a focus on haematopoietic stem cells and leukaemic stem cells, the central role of the MLL gene in infant leukaemia and congenital syndromes related to childhood leukaemia.

Speakers to include: Jay Hess (University of Michigan), Yali Dou (University of Michigan), Patricia Ernst (Dartmouth Medical School), Scott Armstrong (Dana Farber Cancer Institute), Michael Cleary (Stanford University Medical School), Kevin Shannon (University of California), Charlotte Niemeyer (University of Freiburg), Inderjeet Dokal (Queen Mary's London), Alan D'Andrea (Dana Farber Cancer Institute), Mel Greaves (Institute of Cancer Research), Tsvee Lapidot (Weizmann Institute of Science), Stuart Orkin (Children's Hospital, Boston), Yair Reisner (Weizmann Institute of Science), Frederic Barabe (CHUL, Quebec), Sten Erik Jacobsen (University of Oxford), Stephen Hunger (University of Florida), Jacques van Dongen (Erasmus University), Kjeld Schmiegelow (University of Copenhagen) & Kimberley Stegmaier (Dana Farber Cancer Institute)

Great Ormond Street Hospital for Children NHS

For further details about these events, or to download a brochure or registration form, please see the following website: http://conferenceleukaemia.org/

U120454E

5th International Kloster Seeon Meeting

Angiogenesis: Molecular Mechanisms and Functional Interactions

Sept. 20-23, 2008, Kloster Seeon, Germany

W126378E

Chair: Christer Betsholtz (Stockholm) Co-Chair: Lena Claesson-Welsh (Uppsala)

Confirmed Speakers: Ralf Adams (Münster/London) • Kari Alitalo (Helsinki) • Hellmut Augustin (Heidelberg/Mannheim) • Victoria Bautch (Chapel Hill) • Georg Breier (Dresden) • Lisa Coussens (San Francisco) • George Davis (Columbia) • Michele de Palma (Milano) • Elisabetta Dejana (Milano) • Anne Eichmann (Paris) • Ulf Eriksson (Uppsala) • Holger Gerhardt (London) • Karen Hirschi (Houston) • Timothy Hla (Farmington) • Kairbaan Hodivala-Dilke (London) • Luisa Iruela-Arispe (Los Angeles) • Eli Keshet (Jerusalem) • Michael Klagsbrun (Boston) • Eckhard Lammert (Dresden) • Nathan Lawson (Worcester) • Julian Lewis (London) • Dean Li (Salt Lake City) • Donald McDonald (San Francisco) • Lieve Moons (Leuven) • Christiana Ruhrberg (London) • Michael Simons (Lebanon) • Dietmar Vestweber (Münster) • Ryan Watts (San Francisco)

www.vwfb.de

4th International Conference on Trace Element Speciation in Biomedical, Nutritional and Environmental Sciences

May 25th – 29th 2008

GSF - National Research Center for Environment and Health
Institute of Ecological Chemistry
Munich-Neuherberg, Germany

http://www.gsf.de/spec

W125964E

REPROGRAPHICS: CTT, London E17 6BU UK and **Alden Multimedia**, Northampton UK.
PRINTED BY: St. Ives Plymouth Ltd. UK; **Publishers Press**, Lebanon Junction, Ky, USA and **Obun Printing Co. Inc**, Tokyo, Japan

Meeting with Max

It's all about control.

John Gilbey

It was inevitable that Emma would find out about phase two of the project, but I really didn't think she would react the way she did. She called me a bastard, then a devious bastard and lastly an unethical bastard — that last one really hurt. Finally she switched approach, and waves of perfume-enhanced empathy sluiced towards me.

"You don't have to do this you know," she said quietly. "If we both leave, then the project is finished — they'd have to abandon it." Trying not to lose myself again in the ocean-blue trap of her eyes, I shook my head slowly. "I really can't afford to walk away." I didn't mention the obvious — that she was brilliant and beautiful enough to get whatever job she wanted, but one more failure would put me straight into the world of fast-food facilitation.

JACEY

When she had gone, escorted home to her smallholding by an armed, leather-clad security man, I stared at the photo on the wall and wondered how it could all have gone so wrong. It showed Emma and me kneeling in a summer meadow and grinning into the camera. Between us a fine specimen of European lynx sat on its haunches and examined the middle distance with feline hauteur. It was a stunt lynx of course, hired for the day. Ours are much bigger and never socialize.

The psychology was explained to me when we did the publicity shoot.

They needed a reason why a chunk of the Black Mountains was being set aside as a research preserve, and a project to deliver a technology-assisted rescue lynx — that could search out lost children and other worthy targets — was just right. This was bullshit, of course. The main deliverable of the programme was a new line in assassination tools.

Think about it: a lynx is resourceful, almost silent, preys on things up to the size of deer and can disappear without trace for weeks at a time. Implant some symbiotic bioactive technology that grows to form part of the nervous system and you can control its actions by satellite from anywhere. It is politically safe too: "Murder? Surely not, people get killed by wild animals all the time…"

Emma and I were teamed up to do the training. She would lounge in the office using the command-system headset to read the sensory inputs from the animal and send it subliminal hints on where food and shelter might be found, using her undoubted powers of persuasion to build its reliance on the alien thoughts. Once it accepted them, Emma turned the animal over to me for phase two — which only I knew was based on negative reinforcement. I used the system to show it what happened when it ignored me: bad dreams, pain, sensations of fear and panic. If it wanted to avoid these things it must obey me. Specifically, it had to attack on command the figure whose pictures I put in its head — a foreign concept to an animal that killed only when hungry.

Her resignation came just at the wrong time. We had an important target coming up — some tribal warlord in a mountain stronghold — but we didn't have a good candidate available. Emma had been only halfway through training Max, but I took him over anyway and gave him a crash-course in obeying orders — he fought back, refusing to attack the test targets. I guess I must have pushed him too hard — he broke out of the preserve and went on the run.

If the satellite downlink hadn't failed I could have tracked him easily, but instead I had to crunch across country by Land Rover until I picked up his signal. He had reverted to instinct and was trying to lose himself in a pine forest — I chased him on foot, cursing satellite technology and feeling his mind through the portable kit. As the day wore on we got increasingly hungry and tired: in the dusk, snow began to fall.

Shaking with cold and exertion, I struggled down the hillside. At the edge of the trees was a field of sheep, beyond it a farmhouse. Hunger had grown to a nauseating physical pain — like a bad migraine. Max was close now and I could sense him coldly planning the attack. I felt the slow, silent feline approach — head close to the ground — then the adrenaline rush and the dash to the target. The neck bite brought the lamb down cleanly; tearing at its throat splashed steaming blood onto the snow — it felt hot running down my face as I ripped at the flesh with greedy satisfaction.

I heard a yell close by, then something heavy hit me on the side of the head. I struck out wildly and connected with something — a body sprawled backwards onto the snow. Pouncing on it, I wrenched the head back and my jaws went down for the killing bite.

It was her perfume that saved her. As if waking from a nightmare I saw Emma's eyes looking up at me. There was no fear in her face — just loathing, hatred and profound revulsion. Horrified beyond words at what I had done, I backed away and stumbled into the trees.

I should have guessed that I would lose if I challenged Max on his own ground — but I had no idea that the command interface could work in both directions. Just before I tore off the headset I caught a snatch of cold contentment, so perhaps I have taught him to enjoy revenge. Far away I can hear the security team crashing through the undergrowth towards me, but I'm too tired to run any further. So I'm sitting here in the snow — remembering Emma's face, feeling the caked blood in my beard and considering my future. Part of me hopes that Max will find me before they do. ■

John Gilbey insists that this is a work of fiction. His nightmares are his own.

25,000 Tagged ORF Clones

including the ones you want

TrueORF™

for tagged protein expression

TrueORF enables the expression of the encoded transcript as a C-terminally tagged protein with Myc and FLAG® epitopes, facilitating multiple applications that utilize an anti-tag antibody, such as protein detection, protein purification, subcellular localization, etc.

- Genome-wide coverage
- Sequence verified and guaranteed
- The C-terminal dual tag of Myc and FLAG®
- Transfection-ready: Provided as 10 ug of purified plasmid
- Easy shuttling into 20 tagged vectors using PrecisionShuttle™ system

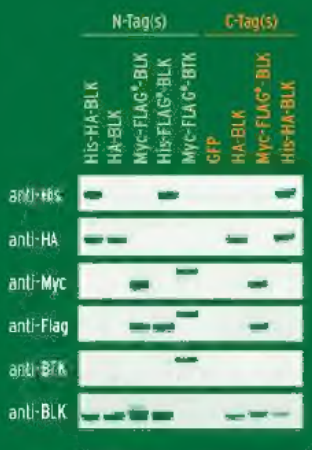

The Western blot analysis of HEK293 cell lysate over-expressing BLK or BTK tagged with indicated epitopes.

FLAG® is a registered trade mark of Sigma-Aldrich

ORIGENE
Your Gene Company

1-888-267-4436 • origene.com

R&D Systems NEW PlusCellect™ Kits

Positively the BEST in Cell Selection.

✓ Positive selection for the isolation of rare cell populations ✓ Flexible – compatible with several magnetic systems
✓ Selection and detection antibodies included ✓ Fast – enrichment in about 1 hour ✓ Specific & simple

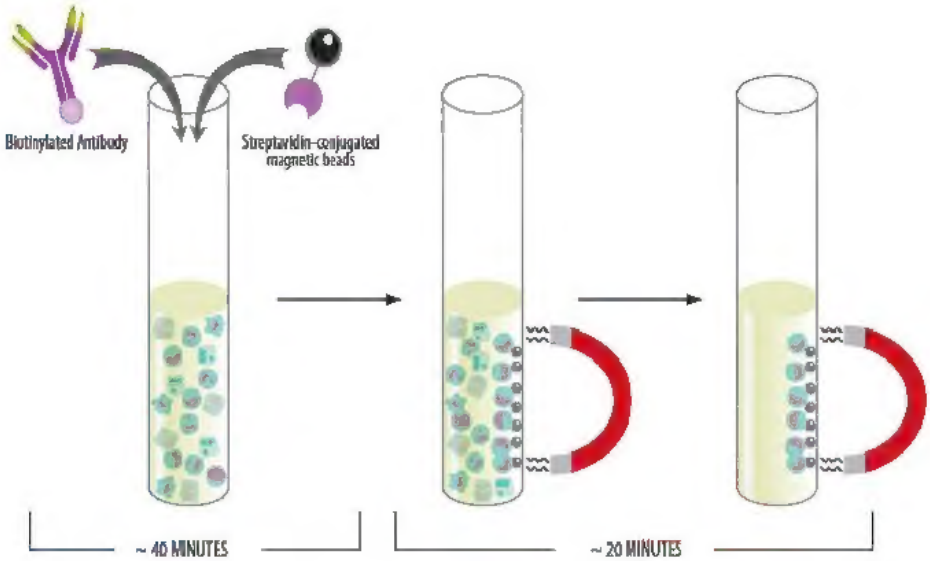

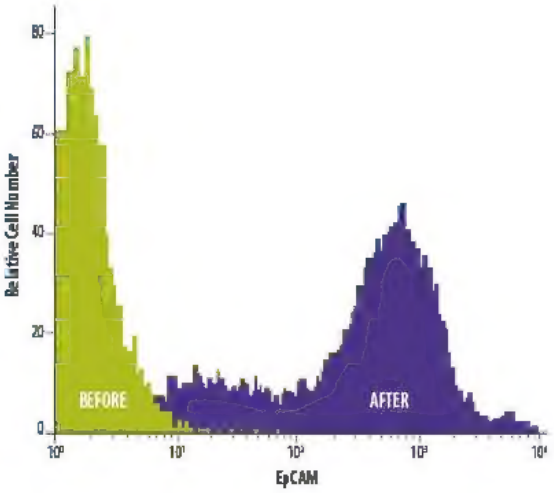

The human EpCAM PlusCellect Kit (Catalog # PLS960) was used to enrich for EpCAM+ cells in a culture containing human whole blood cells spiked with MCF-7 human breast cancer cells. Cells were stained with PE-conjugated anti-human EpCAM detection antibody both before (green) and after (purple) selection.

Kits for these markers are currently available:

- ACE/CD143
- CCR5
- CD3
- CD4
- CD45
- E-Selectin/CD62E
- CXCR4
- E-Cadherin
- Endoglin/CD105
- EpCAM
- IntegrinαV/CD51
- MCAM/CD146
- NCAM-1/CD56
- PECAM-1/CD31
- VE-Cadherin/CD144
- VCAM-1/CD106
- VEGF R2

For more information visit our website at www.RnDSystems.com/go/PlusCellect

For research use only. Not for use in diagnostic procedures.

R&D Systems Tools for Cell Biology Research™

USA & Canada **R&D Systems, Inc.** Tel: (800) 343-7475 info@RnDSystems.com
Europe **R&D Systems Europe, Ltd.** Tel: +44 (0)1235 529449 info@RnDSystems.co.uk

Selection expanding weekly—visit www.RnDSystems.com to sign up for weekly new product updates.

R&D SYSTEMS®